Biosensor imaging of dopamine and glutamate signaling in striatal projection neurons in a mouse model of dopamine depletion

Louise-Laure Mariani

Sorbonne Université

Ecole doctorale Cerveau-Cognition-Comportement

Laboratoire Institut du Fer à Moulin, UMR S-839 / Equipe Neurotransmission et Signalisation

Biosensor imaging of dopamine and glutamate signaling in striatal projection neurons in a mouse model of dopamine denervation

Par **Louise-Laure MARIANI**

Thèse de doctorat de Neurosciences

Dirigée par Jean-Antoine GIRAULT et Denis HERVE

Présentée et soutenue publiquement le 14/12/2018

Devant un jury composé de :

Pr. Angela CENCI, Professeur des universités	Rapportrice
Pr. Avrama BLACKWELL, Professeur des universités	Rapportrice
Dr Peter VANHOUTTE, Directeur de recherche	Examinateur
Pr. Emmanuel ROZE, PU-PH	Membre invité
Dr. Denis HERVE, Directeur de recherche	Directeur de thèse

Table of contents

List of Figures and Tables

Figures

Results

Article:

Discussion

Tables

Acknowledgments

In the final version of the manuscript.

Abbreviations

6-OHDA : 6-hydroxydopamine
α-syn: α-synuclein
AAV: adeno-associated virus
AC: adenylate cyclase
ACh: Acetylcholine
AKAR: A kinase activity reporter
AMP: Adenosine monophosphate
AMPA: α-amino-3-hydroxy-5-methyl-4-isoxazolepropionic acid
AMPAR: AMPA receptor
ATP: Adenosine triphosphate
Ca^{2+} : Calcium
CaM: Ca^{2+}/calmodulin
CaMK: Ca^{2+}/calmodulin-dependent protein kinase
cAMP: cyclic AMP
CFP: blue variant of GFP
CICR: Ca^{2+}-induced Ca^{2+}-release
CREB: cAMP-response element binding protein D1R: Dopamine D1 receptor
D2R: Dopamine D2 receptor
DA: Dopamine
DAG: diacylglycerol
DARPP-32: 32-kDa DA and cAMP-regulated phosphoprotein
dSPN: SPN of the direct pathway
EGFP: enhanced green fluorescent protein
EKAR: ERK activity reporter
ER: endoplasmic reticulum
ERK: Extracellular signal-Regulated Kinases
FRET: fluorescence resonance energy transfer
GABA: γ-aminobutyric acid
GECIs: genetically encoded calcium indicator
GFP: green fluorescent protein
GluA: subunit of AMPAR
GluN: subunit of NMDAR
GPCR: guanine nucleotide binding protein-coupled receptors
GPe: globus pallidus pars externa
GPi: globus pallidus pars interna
IBMX: Broad spectrum PDE inhibitor, 3-isobutyl-1-methylxanthine

IF: Immunofluorescence
iGluR: ionotropic glutamate receptors
IHC: Immunohistochemistry
IP3: inositol trisphosphate
IP3R: inositol trisphosphate receptor
iSPN: SPN of the indirect pathway
KO: knockout
LIDs: Levodopa-induced dyskinesia
LTD: Long-term depression
LTP: Long-term potentiation
MEK: MAP-kinase and ERK-kinase
mGluR: metabotropic glutamate receptors
MSK1: mitogen- and stress-activated kinase 1
NHP: Non-human primates
NMDA: N-methyl-d-aspartate
NMDAR: NMDA receptor
MPTP: 1-methyl-4-phenyl-1,2,3,6-tetrahydropyridine
PD: Parkinson's Disease
PDE: phosphodiesterase
PET: positron emission tomography
PFA: paraformaldehyde
PIP2: phosphatidylinositol-4,5-bisphosphate
PKA: cAMP-dependent protein kinase
PKC: protein kinase C
PLA: proximity ligation assay
PLC: phospholipase C
PMCA: Plasma membrane Ca^{2+}-ATPase
PP1: protein phosphatase 1
PSD: post-synaptic density
RyRs: ryanodine receptors
SERCA: Sarco/endoplasmic reticulum Ca^{2+}-ATPase
SNr: Substantia Nigra pars reticulate
SNc: Substantia Nigra pars compacta
SOCE: store-operated Ca^{2+} entry
SPN: striatal projection neurons
STEP: striatal enriched tyrosine phosphatase
STN: subthalamic nucleus
VGCC: Voltage gated calcium channels

VTA: ventral tegmental area
WB: Western Blot
YFP: Yellow variant of GFP

Summary/Context of the study

Parkinson's disease (PD) is the second most common neurodegenerative disorder after Alzheimer's disease. There is currently no cure for this disease. Symptomatic drug therapy essentially relies on dopamine (DA) replacement therapy. The spectacular antiparkinsonian effect of L-DOPA in PD is however hampered by long-term complications. One of the most difficult complications to treat is dyskinesia, which occurs in virtually all patients during the course of the disease. L-DOPA-induced dyskinesia (LID) results from maladaptive striatal plasticity whose mechanisms are not fully understood yet. The aim of this project is to address a question of therapeutic importance: what are the dysregulations of signaling pathways in striatal projection neurons (SPNs) that will ultimately lead to the development of LID?

To address this question, we explored in striatal neurons the changes of various signaling pathways produced by DA depletion, using genetically encoded protein sensors for two-photon imaging in identified living neurons in mouse striatal slices. We tracked the activity of neuronal populations with genetically encoded Ca^{2+} indicator GCaMP6S. We used fluorescence resonance energy transfer (FRET)-based biosensors to monitor protein kinase activities with a high temporal resolution in living neurons to address signaling integration. We monitored protein kinase A (PKA) activity with AKAR-3 and extracellular signal-regulated kinase (ERK) activity with EKAR-EV. We compared the effects of various pharmacological manipulations of glutamate, DA and adenosine receptors as well as phosphodiesterase and kinase activities in striatal slices of intact and 6-hydroxydopamine (6-OHDA)-lesioned mice. These latter mice correspond to a model of striatal DA depletion occurring in PD. Using Cre-Lox system we targeted biosensor expression specifically in striatal projection neurons of the direct pathway (dSPNs) bearing D1 DA receptors and/or striatal projection neurons of the indirect pathway (iSPNs) bearing DA D2 receptors and adenosine $A2_A$ receptors.

We first demonstrate that two-photon imaging with various biosensors allows monitoring the signaling pathway dynamics in specific populations of SPN in DA-intact and depleted striatum. We show increased spontaneous activity of SPNs and up-regulation of Ca^{2+}, cAMP/PKA and ERK signaling in SPNs following DA depletion. In the 6-OHDA-lesioned striatum, cAMP/PKA and ERK responses to D1 receptor stimulation are increased in dSPNs whereas cAMP/PKA signaling downstream of adenosine A2A receptors is not affected in iSPNs. Interestingly, the upregulation of cAMP/PKA signaling is associated with an apparent loss of phosphodiesterase activity in the dSPNs of DA-depleted striatum, an effect not observed in the iSPNs. Upregulation of Ca^{2+} and ERK signaling is observed in response to stimulation of AMPA-type glutamate ionotropic receptors (AMPAR) selectively in the iSPNs. DA depletion also amplifies the activation of Ca^{2+} signaling downstream metabotropic glutamate receptor stimulation in SPNs.

Our results studying the DA- or glutamate-dependent pathways in different subpopulations of SPNs suggest that the increased ERK activation following DA D1R activation relies at least partly on the upregulation of PKA signaling in dSPNs and not iSPNs. Glutamate released from corticostriatal afferent also participate in the upregulation of ERK signaling but Ca^{2+} entry induced by cell depolarization after AMPAR stimulation is only increased in iSPN and not dSPNs. Hence DA/D1R and glutamate/AMPAR signaling pathways seem to be affected differentially in the two populations of SPNs rather than being jointly modified to enhance ERK activation in the same population.

Introduction

Introduction

Parkinson's disease (PD) is the second most common neurodegenerative disorder after Alzheimer's disease. The number of PD patients will increase by ~65% between 2010 (n=155,000) and 2030 (n~260,000) (Wanneveich *et al.*, 2018). There is currently no cure for PD, which means that there is no therapeutic possibility to reverse the neurodegenerative processes of dopamine (DA) neurons and other types of neurons. Symptomatic dopaminergic replacement therapy does not prevent debilitating complications occurring during disease course. Development of new disease modifying drugs remains a major challenge in PD.

Symptomatic drug therapy essentially relies on DA replacement therapy. The characteristic triad of motor symptoms of PD—akinesia, rigidity and tremor (Hughes *et al.*, 1992) — related to the loss of dopaminergic neurons is indeed spectacularly improved by DA replacement therapy. The gold standard remains the DA precursor, levodopa, whose efficacy was demonstrated more than 50 years ago (Hornykiewicz, 1966; Cotzias *et al.*, 1967; Rascol *et al.*, 2011; Fahn, 2015, 2018; Lees *et al.*, 2015). This spectacular antiparkinsonian effect of levodopa in PD is however balanced by major limitations. The dopatherapy is hampered by long-term complications, motor fluctuations and dyskinesia (You, Mariani *et al.*, 2018). Apart from the classical dopa-responsive motor symptom triad, PD course is also characterized by the occurrence of motor symptoms resistant to levodopa like postural instability, falls, freezing of gait and non-motor features affecting cognition, sleep, mood, behavior, and autonomic functions (Mariani et al submitted 2018 under review). L-DOPA causes motor fluctuations and L-DOPA-induced dyskinesia (LIDs) in 40% of the patients after 4–6 years and up to 90% after 10 years (Ahlskog and Muenter, 2001; Manson *et al.*, 2012). Thus, due to the high frequency of LID, and L-DOPA remaining the gold standard for PD symptomatic treatment, understanding the molecular processes leading to LID occurrence is of major importance.

The majority of movement alterations observed in PD is linked to the lack of DA in the dorsal striatum (DS) (Bernheimer *et al.*, 1973; Price *et al.*, 1978; Dauer and Przedborski, 2003) and LID are induced by altered synaptic plasticity in the DS challenged by intermittent sharp variations of DA (Carta *et al.*, 2006; Cenci and Lundblad, 2006; Lindgren *et al.*, 2007; Iravani and Jenner, 2011; Iravani *et al.*, 2012; Antonini and Jenner, 2018). To progress in the understanding of PD pathophysiology and find new ways to decrease the incidence or severity of DOPA-therapy negative effects, it is critical to identify signaling alterations in DS neurons in the absence of DA. This thesis work aims at addressing this question using for the first time live biosensor imaging in striatal neurons in a mouse model of DA deficiency. In the bibliographic introduction we will review the organization and function of the DS and basal ganglia, the signaling pathways in striatal neurons, the pathophysiology of PD and LID, and the bases of biosensor imaging.

1- The dorsal striatum and the basal ganglia-thalamo-cortical motor circuit

1.1 General organization of the striatum

The basal ganglia have a key role in action selection; it has been proposed that the basal ganglia carry out the task of devoting most brain resources to a single movement or behavior at a time, adapted to the context (Mink, 1996; Redgrave *et al.*, 1999; Grillner *et al.*, 2005).

The striatum is the main input structure of the basal ganglia (Kincaid *et al.*, 1998; Bolam *et al.*, 2000) (**Figure Intro 1**). The striatum is a convergence point for glutamatergic inputs from cortex and thalamus into specific downstream pathways (Alexander *et al.*, 1986; Alexander and Crutcher, 1990; Berendse and Groenewegen, 1990; Gerfen, 1992; Smith *et al.*, 2011; Kress *et al.*, 2013; Huerta-Ocampo *et al.*, 2014), as well as dopaminergic afferents from the midbrain (Smith and Bolam, 1990; Bolam *et al.*, 2000; Björklund and Dunnett, 2007; Surmeier *et al.*, 2010; Gerfen and Surmeier, 2011a). The striatal projection neurons (SPNs) integrate these convergent glutamatergic inputs predominantly on their spines (Kemp and Powell, 1971; Kincaid *et al.*, 1998; Carter *et al.*, 2007; Huerta-Ocampo *et al.*, 2014; Hunnicutt *et al.*, 2016).

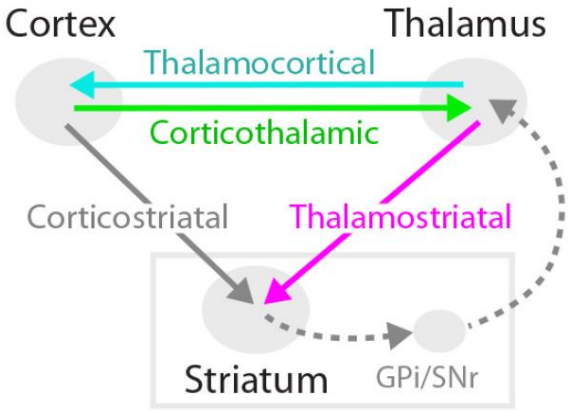

*[**Figure intro 1: Schematic of the connections between the cortex, thalamus, and basal ganglia.** The indicated output nuclei of the basal ganglia are the globus pallidus internal segment (GPi) and the substantia nigra pars reticulata (SNr) (gray box indicates the basal ganglia). **adapted from Hunnicutt et al 2016**]*

The striatum is classically divided into three functionally and anatomically distinct circuits: the dorsolateral, dorsomedial, and ventral striatum respectively accounting for the sensorimotor, associative, and limbic domains (Yin and Knowlton, 2006; Balleine *et al.*, 2009; Belin *et al.*, 2009; Kreitzer, 2009; Thorn *et al.*, 2010; Gruber and McDonald, 2012) (**Figure intro 2**). In rodents, motor descending axonal bundles perforate the striatum. In primates and carnivores, the dorsal striatum is divided by the internal capsule into: on the medial side the caudate nucleus and on the lateral side, the putamen. In both rodents and primates, even if there is no clear division between dorsomedial and dorsolateral striatum, these striatal regions are anatomically and functionally distinct (Joel and Weiner, 1994; Parent and Hazrati, 1995; Yin and Knowlton, 2006). The dorsolateral striatum receives inputs from sensorimotor cortex (Künzle, 1975; Liles and Updyke, 1985; McGeorge and Faull, 1989). The dorsomedial striatum receives inputs from associative cortices (Goldman and Nauta, 1977; Ragsdale and Graybiel, 1981; McGeorge and Faull, 1989). The ventral striatum, the nucleus accumbens subdivided into core and shell, has distinct properties from the dorsal striatal regions (Nicola, 2007; Taha *et al.*, 2007). It receives glutamatergic inputs from the frontal cortex and limbic regions (Brog *et al.*, 1993). The dopaminergic

innervation of the ventral striatum comes from a midbrain nucleus adjacent to the SNc, the ventral tegmental area (VTA), which is less affected in PD and explains why denervation predominates in the dorsal striatum in PD (Price *et al.*, 1978; Joel and Weiner, 2000; Dauer and Przedborski, 2003).

The dorsal striatum seems more involved in action selection, goal-directed behaviour and the emergence of habits (Yager *et al.*, 2015; Howard *et al.*, 2017; Volkow *et al.*, 2017). The nucleus accumbens is more likely an interface between the limbic and motor systems implicated in reward processing and motivation (Bolam *et al.*, 2000; Joel and Weiner, 2000; Morgane *et al.*, 2005; Wise, 2009; Volkow *et al.*, 2011).

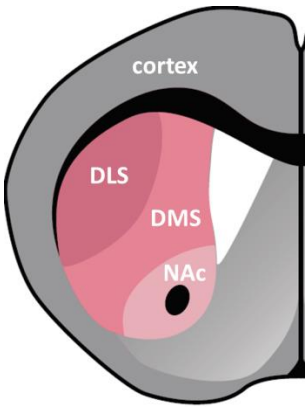

[***Figure intro 2: Striatal regions. Coronal schematic hemi-section of the mouse forebrain****. The dorsolateral (DLS), dorsomedial (DMS), and ventral divisions (nucleus accumbens, NAc) of the striatum are schematically illustrated in the left hemisphere.* ***adapted from Kreitzer et al 2009.***]

In addition to these regional differences, the dorsal striatum is divided in two intermingled compartments, the matrix and the striosomes (or patches) (Joel and Weiner, 2000; Crittenden and Graybiel, 2011). These two compartments are distinguished by neurochemical markers and have a different organization of inputs and outputs (Prensa and Parent, 2001; Fujiyama *et al.*, 2006; Matsuda *et al.*, 2009). The proper balance between their activities appears to be critical for the function of the dorsal striatum (Crittenden and Graybiel, 2011), although their exact respective role in the overall function is still not fully clarified.

1.2 Striatal projection neurons and main efferent pathways of the dorsal striatum

The striatum is mainly composed by GABAergic medium-sized spiny neurons also known as striatal spiny projection neurons (SPN), which represent 95% (in rodents) of the neurons of the striatum. SPN are characterized by the presence of spines on their dendrites. These spines are absent from the most proximal dendrites. Their peak density (1–2 per µm) is 50–60 µm away from the soma. Then their density gradually decreases down to the tips of the sparsely branching dendrites (250–400 µm). SPNs form the main or sole output to downstream basal ganglia nuclei. Activation of GABAergic SPNs inhibits their primary targets (Chevalier *et al.*, 1985; Deniau and Chevalier, 1985; Chevalier and Deniau, 1990).

The role of the striatum in the control of many aspects of movement and motivation depends on the balance between two trans-striatal circuits, involving pathways called the direct and indirect pathways (**Figure intro 3**). The striatonigral SPNs (dSPN), of the **direct pathway** facilitating movement execution, directly project to the GABAergic output nuclei of the basal ganglia, the *globus pallidus pars interna* (GPi) and the *substantia nigra pars reticulata* (SNr). They modulate the thalamus and brainstem outputs (**Figure intro 3**), with the GPi involved in axial and limb movements and the SNr involved in head and eye movements. The substantia nigra pars reticulata (SNr) neurons are tonically active and maintain

a strong inhibition of their targets including the thalamus. Thus they inhibit action. Activation of the direct pathway inhibits SNr neurons (Chevalier *et al.*, 1985; Deniau and Chevalier, 1985) and thus facilitates action (e.g., a movement due to the selective activation of appropriate muscle groups).

The striatopallidal SPNs (iSPN) of the **indirect pathway,** a multisynaptic circuit between the striatum and basal ganglia output nuclei inhibiting movement, project to and inhibit the GABAergic neurons of the *globus pallidus pars externa* (GPe). The latter in turn project to and modulate the glutamatergic neurons of the *subthalamic nucleus* (STN) that project to the GPi/SNr, resulting in the inhibition of thalamocortical projection neurons thus inhibiting movement (Bateup *et al.*, 2010; Kravitz *et al.*, 2010; Gerfen and Surmeier, 2011b; Cui *et al.*, 2013). Activation of the indirect pathway results in increased activity of subthalamic neurons and further activates SNr neurons, thereby reinforcing action inhibition (**Figure intro 3 left panel**).

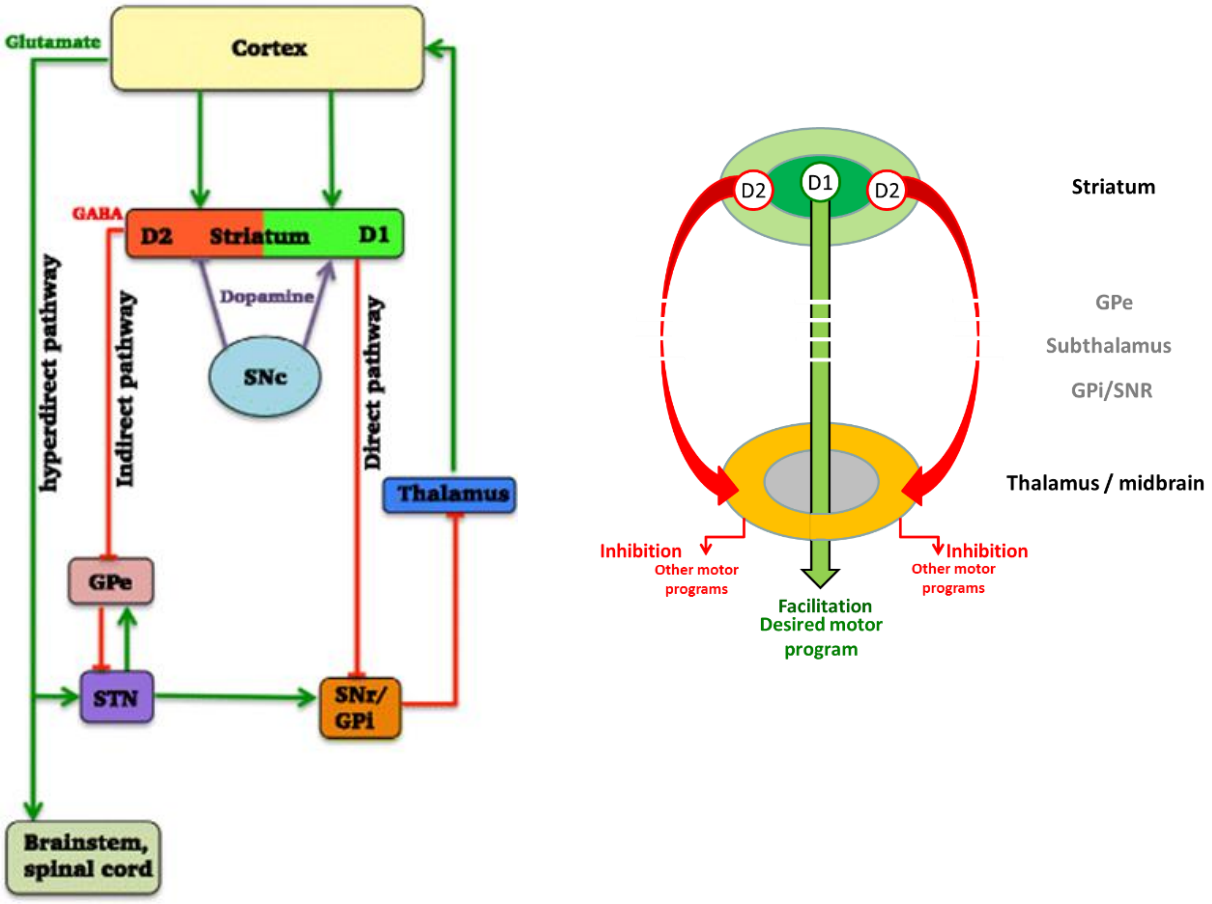

[Figure intro 3:

Left Panel. Model of the basal ganglia-thalamo-cortical motor circuit. *Arrows represent excitatory projections; «T» represent inhibitory projections. The striatum receives excitatory cortical and thalamic inputs. Dopaminergic nigrostriatal projections to dSPN activate the direct pathway and those to iSPN inhibit the indirect pathway. Outputs of the basal ganglia from GPi and SNr are directed to the thalamus, superior colliculus, and pedunculopontine nucleus (PPN).* **from You, Mariani et al 2017**

Right Panel. Schematic illustration of putative action selection mechanism. *D1 : DA receptors of D1 type situated on the dSPN, D2: D2 receptors of the D2 type situated on the iSPN***. *Adapted by Girault after Mink, Prog Neurobiol, 1996.]***

The function of the basal ganglia depends on the balance between the two pathways exerting opposing influences on motor function (Alexander *et al.*, 1986; Albin *et al.*, 1989; DeLong, 1990; Kravitz *et al.*, 2010). These two pathways are oppositely modulated by DA. Tonic release of DA inhibits the indirect pathway. Phasic release of DA activates the direct pathway. Recent models propose coordinated activation of both pathways during action selection (Cui *et al.*, 2013; Alcacer *et al.*, 2017). Activation of the direct pathway could facilitate output of the desired motor programs but activation of the indirect pathway would inhibit competing motor programs (Hikosaka *et al.*, 2000; Mink, 2003; Nambu, 2008; Alcacer *et al.*, 2017) (**Figure 3 right panel**).

Histochemically, striatonigral dSPNs express high levels of DA D1 (D1R) and muscarinic M4 receptors, as well as dynorphin and substance P (Gerfen *et al.*, 1990; Gerfen, 1992; Yung *et al.*, 1995; Ince *et al.*, 1997). Striatopallidal iSPNs have a high expression of D2R and adenosine $A2_A$ receptors, and immunoreactivity for enkephalin (Gerfen *et al.*, 1990; Schiffmann *et al.*, 1991; Fink *et al.*, 1992; Gerfen, 1992; Yung *et al.*, 1995; Bertran-Gonzalez *et al.*, 2009). Morphologically, striatopallidal iSPNs seem to have more primary dendrites than striatonigral dSPNs (Gertler *et al.*, 2008) but it is not always the case in other studies (Huerta-Ocampo *et al.*, 2014). Physiologically, dSPNs and iSPNs exhibit similar properties, characterized by their hyperpolarized resting membrane potential at ~ –90mV (Wilson and Kawaguchi, 1996; Kawaguchi, 1997; Stern *et al.*, 1997; Blackwell *et al.*, 2003), low input resistance, inward rectification, and a long delay to initial spiking (Kreitzer, 2009). Although iSPNs exhibit increased excitability with an action potential discharge rate twice bigger (Kreitzer and Malenka, 2007; Cepeda *et al.*, 2008; Gertler *et al.*, 2008; Valjent *et al.*, 2009). Conditional expression of fluorescent proteins under the control of D1R or D2R gene promoter (**Figure intro 4**) allowed further characterization of the differences between direct- and indirect-pathway SPNs (Lobo *et al.*, 2006; Heiman *et al.*, 2008, 2014b; Matamales *et al.*, 2009). Some of these differences are summarized in **Table 1** and intracellular signaling aspects are further detailed below.

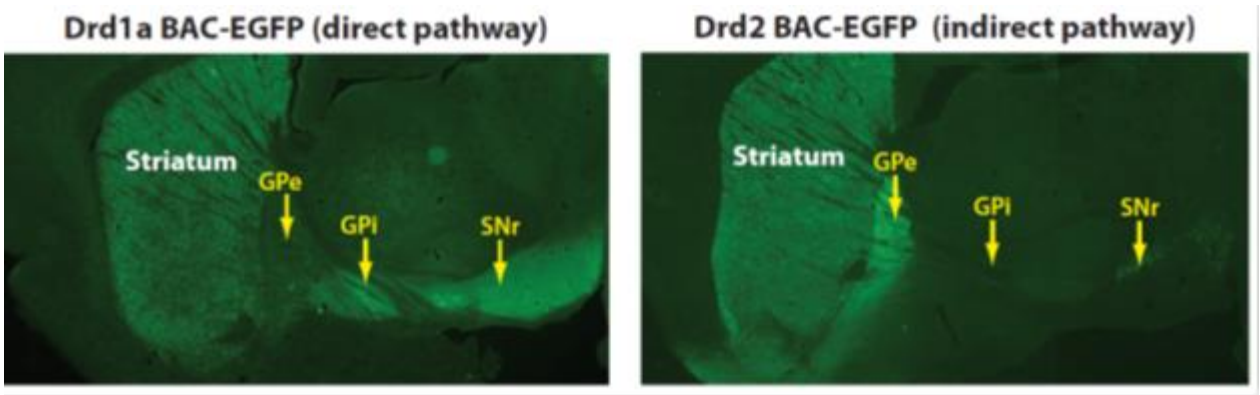

Figure Intro 4: Fluorescence imaging of D1-SPN and D2-SPN in the dorsal striatum, corresponding to the direct and indirect pathway neurons. Left panel: *Brain section from a BAC-transgenic mouse expressing enhanced green fluorescent protein (EGFP) under regulation of the Drd1a promoter (Drd1a BAC-EGFP) shows D1-expressing SPNs in the striatum that project axons which terminate in the GPi and GPe.* ***Right panel.*** *Fluorescent imaging of a Drd2-EGFP mouse (BAC-transgenic mouse expressing EGFP under regulation of the Drd2 promoter) shows that D2-expressing SPNs project to the GPe but not to the GPi or SNr.* ***From Gerfen and Surmeier 2011]***

	Striatonigral (D1R) MSNs	Striatopallidal (D2R) MSNs
Morphology	More primary dendrites	Less primary dendrites
Intra-striatal projections	To D1R–MSNs	To D1R–MSNs and D2R–MSNs
Intrinsic properties		
- Excitability	- Lower	- Higher
- Action potential back propagation (APBP)	- Less distal APBP	- More distal APBP
Corticostriatal synapses		
- Presynaptic activation	- Lower	- Higher
- GABAA tone	- Weaker	- Stronger
- LTD	- mGluR, Cav1.3, D2-dependent	- mGluR, Cav1.3, eCB, D2-dependent
- LTP	- D1/NMDA-dependent	- A2a/NMDA-dependent

*[**Table 1:** Major differences between the two types of SPNs found with BAC transgenic mice. **From Valjent et al 2009**]*

In addition to the SPNs, the dorsal striatum contains several types of interneurons which represent the remaining 5% of the total number of neurons in rodents (Kawaguchi, 1997; Tepper and Bolam, 2004; Tepper *et al.*, 2004, 2010; Ibáñez-Sandoval *et al.*, 2011; Gittis and Kreitzer, 2012; Assous and Tepper, 2018). They include the large size cholinergic interneurons and several types of GABAergic interneurons like the parvalbumin Fast-spiking interneurons (FSIs) inhibiting both dSPNs and iSPNs, persistent and low-threshold spike (PLTS) interneurons which release neuropeptides such as neuropeptide Y (NPY) and somatostatin (SOM) and the neuromodulator nitric oxide (NO), Neuropeptide Y-neurogliaform interneurons and TH positive interneurons.

1.3 Cortical and thalamic inputs to the dorsal striatum

The corticostriatal input is overall topographically organized. Corticostriatal pyramidal cells have multiple projections sites including ipsi- but also contralateral striatum (Shepherd, 2013). Recent studies have focused on systematically mapping the precise excitatory projection patterns to the entire striatum (Hunnicutt *et al.*, 2016), revealing striatal subregions and their boundaries by systematic analysis of these input patterns from individual cortical and thalamic subregions (Oh *et al.*, 2014; Hunnicutt *et al.*, 2016). They found clear boundaries separating the three traditional striatal domains and uncovered a fourth subdivision in the posterior striatum. Interestingly, the posterior striatum has also been reported to be innervated by a specific dopamine neurons population (Menegas *et al.*, 2015). The dorsomedial striatum seem to show the highest degree of cortical input heterogeneity, suggesting it serves as an information hub. In addition, thalamic subregions receiving basal ganglia outputs are preferentially interconnected with motor-related cortical subregions.

Thalamic subregions are defined by cytoarchitectural boundaries to delineate ~40 nuclei. The organization of thalamostriatal inputs, which provide ~1/3 of all glutamatergic synapses in the striatum (Huerta-Ocampo *et al.*, 2014), particularly originating from the intralaminar thalamic nuclei (Smith *et al.*, 2004; Doig *et al.*, 2010), has been less studied than corticostriatal inputs.

Cortical and thalamic neurons regulate the activity of SPNs in the striatum through long-range glutamatergic excitatory projections (Landry *et al.*, 1984; Wilson, 1987; Graybiel *et al.*, 1994; Lovinger and Tyler, 1996; Reiner *et al.*, 2003; Kress *et al.*, 2013; Hunnicutt *et al.*, 2016), while inhibition is mediated by feed-forward and feed-back circuits (Tepper *et al.*, 2008). The main feed-forward circuit is characterized by GABAergic striatal interneurons receiving excitatory inputs from the cortex and monosynaptically inhibiting SPNs. The feed-back circuit comprises SPNs interconnections via local axon collaterals (Calabresi *et al.*, 1991; Kawaguchi, 1993; Kita, 1993, 1996; Kawaguchi *et al.*, 1995; Tunstall *et*

al., 2002; Planert *et al.*, 2010). SPN to SPN synapses are typically unidirectional, predominantly localized onto distal dendrites of other SPNs (Tunstall *et al.*, 2002; Plenz, 2003; Koos *et al.*, 2004; Taverna *et al.*, 2004, 2005). dSPNs preferentially innervate other dSPNs, whereas iSPNs innervate both subtypes equally (Taverna *et al.*, 2008). More recent work using optogenetic and electrophysiology approaches to activate SPNs has inferred an even higher degree of connectivity (Chuhma *et al.*, 2011; Wei *et al.*, 2017).

Each SPN receives several thousands of corticostriatal synapses on its dendrites, but each individual corticostriatal axon makes only a few contacts with each SPN, typically making one or two en passant synapses (Kincaid *et al.*, 1998; Parent and Parent, 2006). Corticostriatal and thalamostriatal glutamatergic synapses are similar morphologically and intermingled along the dendrites of SPNs (Smith *et al.*, 2004; Raju *et al.*, 2006). The synapses they form on SPNs are nearly equal in number, corticostriatal synapses being slightly more numerous (Smith *et al.*, 2004). The vast majority of synapses target spines rather than dendritic shafts and the proportion seems more elevated in corticostriatal than thalamostriatal synapses (Fujiyama *et al.*, 2006; Raju *et al.*, 2006, 2008; Moss and Bolam, 2008; Doig *et al.*, 2010; Lei *et al.*, 2013; Zhang *et al.*, 2013; Huerta-Ocampo *et al.*, 2014) (**Figure Intro 5).**

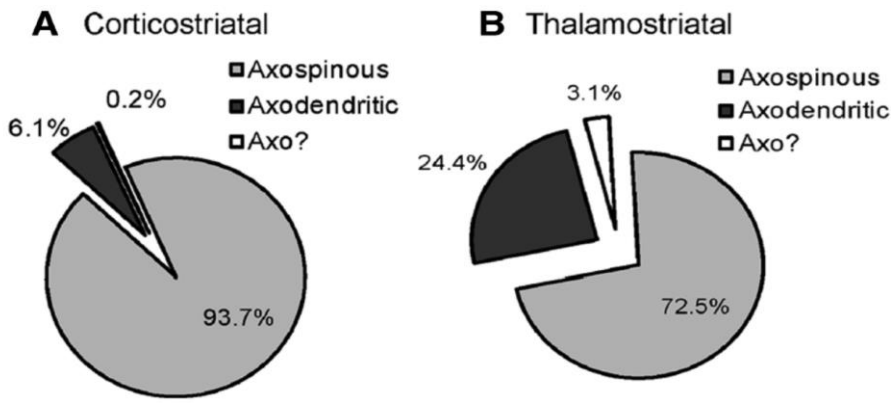

*[**Figure Intro 5**: **Pie charts illustrate the proportions of targets for corticostriatal (A) and thalamostriatal (B) synapses in mice**. Axospinous, synapses onto spines; Axodendritic, contacts onto dendrites; Axo?, contacts onto undetermined targets. **From Zhang et al 2013**].*

A study from Wall et al 2013, using a monosynaptic rabies virus system, also showed that innervation of D1-SPN and D2-SPN seems anatomically biased towards specific brain regions (Wall *et al.*, 2013). They found that thalamostriatal input and dopaminergic input seem similar onto both pathways. Motor cortex preferentially targets the indirect pathway while sensory cortical and limbic structures preferentially innervate the direct pathway. Others find that pyramidal tract axons innervate both type of SPN (Kress *et al.*, 2013).

1.4 Striatal dopamine inputs

There are ten DA-producing nuclei in the mammalian brain (Björklund and Dunnett, 2007; Tritsch and Sabatini, 2012) designated A8 to A17 (**Figure intro 6**). Projections from a given subset of DA neurons target one region of the brain (Yetnikoff *et al.*, 2014), but projections to a given subset of DA neurons arise from many different regions as shown by studies using combinations of techniques using CLARITY and Rabies virus injections (Watabe-Uchida *et al.*, 2012; Menegas *et al.*, 2015). The substantia nigra pars compacta (SNc; field A9) and VTA (field A10), which project to the dorsal and ventral striatum, and form the nigrostriatal and mesocorticolimbic pathways respectively; each contain in the rodent ≈20,000 – 30,000 neurons bilaterally (German and Manaye, 1993; Zaborszky and Vadasz, 2001), and a total of neurons between 160 000–320 000 in monkeys and 400 000–600 000 in humans, with >70% of the neurons located in the SN (Björklund and Dunnett, 2007). These neurons form widely spread highly

dense axonal arborizations in the striatum (Prensa and Parent, 2001; Matsuda *et al.*, 2009). Individual SNc neurons extend highly branched axons of half a meter in total length that densely ramify throughout up to 1 mm^3 of tissue (Matsuda *et al.*, 2009). Dopaminergic synaptic boutons represent ≈10% of all synapses in the striatum (Groves *et al.*, 1994). The closest distance in between each dopaminergic bouton is only ∼1.18 µm (Arbuthnott and Wickens, 2007). Some of these terminals are found at spine necks abutting cortical synapses (Smith *et al.*, 1994; Moss and Bolam, 2008), but many dopaminergic terminals have been found against dendritic shafts with no detectable electron-dense postsynaptic structure (Groves *et al.*, 1994; Hanley and Bolam, 1997).

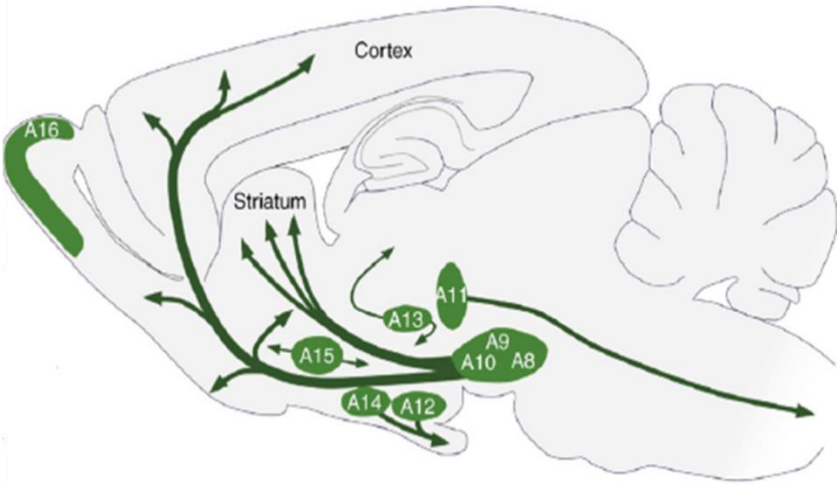

*[**Figure intro 6: Distribution of DA neuron cell groups in the adult rodent brain** as illustrated schematically on a sagittal view. The numbering of cell groups, from A8 to A16, was introduced in the classic study of Dahlström and Fuxe in 1964. A17 Retinal dopaminergic neurons are not shown on this drawing. The principal projections of the DA cell groups are illustrated by arrows. **Adapted from Bjorklund and Dunnett 2007]***

Midbrain DA neurons are autonomous pacemakers spontaneously active at low frequencies (1–8 Hz) in vivo (Guzman *et al.*, 2009; Kreitzer, 2009), suggesting that each neuron provides a basal DA tone to many target neurons, adjusted by either phasic bursts or transient pauses of activity, critical for normal striatal function (Schultz, 2007a). This basal DA tone most likely activates high-affinity DA receptors of the D2-type (D2–D4) (Richfield *et al.*, 1989). Bursts of action potentials that briefly elevate striatal extracellular DA are fired by DA neurons in response to behaviorally relevant stimuli (Schultz, 2007b). These phasic spikes of DA are activating both the high-affinity D2 type receptors and the lower-affinity DA receptors of the D1 type (D1, D5) (Richfield *et al.*, 1989). The phasic and tonic firings of DA neurons allow encoding transient responses, for instance to reward prediction error, or longer timescale responses like uncertainty (Fiorillo *et al.*, 2003; Schultz, 2007b). Dopamine thus plays a crucial role in the control of motor, cognitive and emotional behaviors and their adaptation by learning in response to reward.

2- Neurotransmitter receptors and signaling pathways in the dorsal striatum

2.1 DA receptors

DA receptors belong to the large superfamily of guanine nucleotide binding protein-coupled receptors (GPCRs). These metabotropic receptors share interaction with G-proteins, structure with seven alpha-helices transmembrane domains that are interconnected by alternating intracellular and extracellular loops. The heterotrimeric G-proteins are formed by a combination of an α-subunit and a βγ dimer that can each lead to activation of signaling effectors. These receptors do not signal exclusively through heterotrimeric G proteins and may also engage in G protein-independent signaling events (Luttrell, 2014; Peterson and Luttrell, 2017; Luttrell *et al.*, 2018; Pack *et al.*, 2018).

DA binds and activates two families of GPCRs (Kebabian and Calne, 1979; Andersen *et al.*, 1990; Sibley and Monsma, 1992; Greengard *et al.*, 1999; Beaulieu and Gainetdinov, 2011; Tritsch and Sabatini, 2012): the D1 family (D1 and D5 subtypes) (Tiberi *et al.*, 1991) and the D2 family (D2, D3 and D4 subtypes) with different affinities for DA ranging from nanomolar to micromolar range, but less different between individual subtypes within a family. The affinity of D2-like receptors for DA is generally reported to be 10- to 100-fold greater than that of D1-like receptors, with D3 and D4 receptors displaying the highest sensitivity for DA and D1 receptors the lowest (Beaulieu and Gainetdinov, 2011) (**Table 2**). But D1 and D2 receptors can exist in both high and low affinity states.

	D1-like Family		D2-like Family		
DA receptor subtype	D1	D5	D2	D3	D4
Gene name	*Drd1a*	*Drd5*	*Drd2*	*Drd3*	*Drd4*
Number of introns	0	0	6	5	3
Splice variants	No	No	Yes (D2S, D2L)	Yes	Yes
Affinity for DA (μM)*	1.0–5.0	0.2–2.0	0.2–2.0	0.02–0.2	0.01–0.1
G protein coupling	$G\alpha_s$, $G\alpha_{olf}$	$G\alpha_s$, $G\alpha_q$	$G\alpha_i$, $G\alpha_0$	$G\alpha_i$, $G\alpha_0$	$G\alpha_i$, $G\alpha_0$
Common family-specific agonists	SKF-38393, SKF-81297		(–) Quinpirole, Cabergoline		
Common family-specific antagonists	SCH-23390, SKF-83566		(–) Sulpiride, Spiperone, Nemonapride		

*RKi ranges for cloned human DA receptors obtained from the NIMH Psychoactive Drug Screening Program database (http://pdsp.med.unc.edu) and the International Union of Basic and Clinical Pharmacology.

*[**Table 2: Basic characteristics of DA receptors.** from **Tritsch and Sabatini 2012**]*

The organization of the genes of D1- and D2-class DA receptors is also different. The D1 and D5 DA receptor genes do not contain introns in their coding regions, so do not generate splice variants. The genes encoding the D2-class receptors have several introns, with six introns in the gene that encodes the D2R receptor, five in the gene for the D3R, and three in the gene for the D4R (Gingrich and Caron, 1993). The alternative splicing of an 87-base-pair exon between introns 4 and 5 lead to different isoforms. The two main isoforms are the short and long variants of D2 receptors (D2S and D2L, respectively mediating pre- and post- synaptic signaling (De Mei *et al.*, 2009). D2S and D2L isoforms differ in the presence of an additional 29 amino acids in the third intracellular loop. Variants of D3 and D4 receptors have also been described (Callier *et al.*, 2003). The D3 splice variants encode proteins essentially nonfunctional (Giros *et al.*, 1991). The D4 polymorphic variants have a 48 bp repeat sequence in the third cytoplasmic loop, with up to 11 repeats reported (Van Tol *et al.*, 1992).

The D1 and D5 DA receptors are 80% identical in their transmembrane domains, whereas the D3 and D4 DA receptors are 75% and 53% identical, respectively, with the D2R. Whereas the NH2-terminal domain has a similar number of amino acids in all of the DA receptors, the COOH-terminal for the D1-class receptors is seven times longer than for the D2-class receptors (Gingrich and Caron, 1993).

DA receptors are broadly expressed in the CNS, their distribution matching the density of innervation by DA fibers. D1- and D2-like receptors are expressed in both SPNs and interneurons in the striatum, and in subpopulations of pyramidal neurons, interneurons, and glial cells in cortex (Tritsch and Sabatini, 2012) (**Table 2**). DA receptors are located both synaptically and extrasynaptically (Gerfen and Surmeier, 2011b).

As mentioned above, D1 receptors (D1R) are expressed by striatonigral neurons of the direct pathway (D1-dSPNs), whereas D2 receptors (D2R) are expressed by striatopallidal neurons of the indirect pathway (D2-iSPNs) (**Figure intro 3**). The segregation in two distinct populations is high but not complete (Le Moine and Bloch, 1996; Bertran-Gonzalez *et al.*, 2008, 2010; Matamales *et al.*, 2009) and changes in technical approaches have allowed to further detail these repartitions (Valjent *et al.*, 2009; Ade *et al.*, 2011; Durieux *et al.*, 2011). In the dorsal striatum, only 5% of the striato-pallidal iSPN express D1R and 5% of the striato-nigral dSPN express D2R (Le Moine and Bloch, 1995; Ince *et al.*, 1997; Valjent *et al.*, 2009) (**Table 3**). In the nucleus accumbens (Le Moine and Bloch, 1995), a higher proportion of iSPN, mainly originating from the shell of the nucleus accumbens rather than from the core, express D1-like receptors (Robertson and Jian, 1995; Bertran-Gonzalez *et al.*, 2010; Gangarossa *et al.*, 2013a). The D3R are also mostly present in the ventral regions of the striatum. Along the rostro-caudal axis of the mouse dorsal striatum, D1R- and D2R-expressing SPNs are randomly distributed in most of the dorsal striatum, except a specific region in the caudal striatum, adjacent to the GPe. This region exclusively comprises D1R-expressing dSPNs and lacks neurons expressing markers for iSPN, and especially D2R (Gangarossa *et al.*, 2013b).

	D1	D2	D3	D4	D5
Striatum					
dSPNs	+++ (>90%)	–	+ (50%)	+ (<10%)	–
iSPNs	+ (<10%)	+++ (>90%)	+ (<10%)	+ (<10%)	+ (<10%)
Cholinergic interneurons	+ (<20%)	++ (>80%)	–	–	++ (>80%)
PV^+ interneurons					+ (>70%)
$NPY/SOM/NO^+$ interneurons	+ (<10%)				+ (>70%)
CR^+ interneurons					+ (50%)
Cortex					
L2/3 pyramidal neurons	++ (<20%)	+ (<10%)		+	+
L5/6 pyramidal neurons	++ (20%–40%)	+ (25%)		+	+
L2–L6 interneurons	++ (30%–60%)*	+ (20%)*	+	+	+

*[**Table 3: Cellular distribution of DA receptors in the cortex and striatum of rodents.** This table reports semiquantitative expression levels of various DA receptor subtypes (+++, highest expression; +, low expression; -, mRNA not detected) and their relative cellular distribution (in parentheses) within defined cortical and striatal neuronal populations. *For the most part, PV+ interneurons. from **Tritsch and Sabatini 2012**]*

As mentioned above, D2R are also expressed at the presynaptic level, on dopaminergic neurons where they act as autoreceptors. D2R have also been reported on non-dopaminergic afferent fibers to the striatum among which the glutamatergic cortical and thalamic afferents and that innervate SPNs and interneurons (Sesack *et al.*, 1994; Wang and Pickel, 2002). D1R have also been observed in a small

number of presynaptic glutamatergic terminals in the striatum (Huang *et al.*, 1992; Dumartin *et al.*, 2007). Some interneurons have also been reported to bare DA receptors: D2 and D5 receptors on cholinergic interneurons, D5 receptors on somatostatin/neuropeptide Y interneurons, on parvalbumin and on calretinin GABAergic interneurons (Yan and Surmeier, 1997; Rivera *et al.*, 2002) (**Table 3**).

2.2 Glutamate receptors

Glutamate is the major excitatory neurotransmitter in the vertebrate central nervous system responsible for the fast excitatory transmission. Glutamate acts on two types of glutamate receptors: the ionotropic (iGluR), which are ligand-gated ion channels, and the metabotropic glutamate receptors (mGluR).

2.2.1 Striatal ionotropic glutamate receptors (iGluRs)

The iGluRs comprise two major groups termed after their selective synthetic ligands: the N-methyl-d-aspartate (NMDA) receptors (NMDAR) and the α-amino-3-hydroxy-5-methyl-4-isoxazolepropionic acid (AMPA)/kainate receptors (AMPAR) (Dingledine *et al.*, 1999). NMDAR and AMPAR are heterotetramers and their subunit composition controls their properties (Seeburg and Hartner, 2003; Traynelis *et al.*, 2010; Paoletti *et al.*, 2013).

Localization

NMDA- and AMPA/kainate iGluR are expressed presynaptically in dopaminergic and glutamatergic terminals, but also postsynaptically in SPNs where they produce postsynaptic excitatory currents (Bernard *et al.*, 1997; Bernard and Bolam, 1998; Tarazi *et al.*, 1998; Tarazi and Baldessarini, 1999; Gardoni and Bellone, 2015). A study has shown that AMPAR, but not NMDAR, are located on glutamatergic corticostriatal and thalamostriatal terminals (Fujiyama *et al.*, 2004). AMPA, NMDA and kainate receptors are also expressed on cholinergic and GABAergic striatal interneurons (Tallaksen-Greene and Albin, 1994; Deng *et al.*, 2007, 2010).

Function

AMPARs, heteromers composed of GluA1-4 subunits, are the main type of glutamate receptor mediating the fast excitatory response of neurons to glutamate (Traynelis *et al.*, 2010). They are permeable to cations and, at normal resting membrane potential, depolarize the cell by letting Na^+ flow in and K^+ flow out. AMPAR lacking the GluA2 subunit can also let Ca^{2+} enter the cell. GluA2 subunits impair Ca^{2+} permeability of AMPAR. RNA editing and alternative splicing generate sequence variants, and those variants, as in GluA2-4 AMPA receptor subunits, generally show different properties (Seeburg and Hartner, 2003; Penn *et al.*, 2012; Wright and Vissel, 2012; La Via *et al.*, 2013; Wen *et al.*, 2017).

NMDAR are heterotetramers composed of GluN1 subunits and GluN2 (A-D) and/or GluN3 (A-B) subunits encoded by 7 different genes (Stroebel *et al.*, 2018). Subunit composition determines receptor properties. The GluN2 regulatory subunits are responsible for glutamate binding (Laube *et al.*, 1997) and exist as four different isoforms, mostly GluN2A and GluN2B in the striatum (formerly known as NR2A and NR2B, respectively). To open NMDAR requires binding not only of glutamate but also a coagonist, namely glycine (Johnson and Ascher, 1987; Kleckner and Dingledine, 1988) or D-serine (Mothet *et al.*, 2000) at GluN1 or GluN3, the obligatory subunit to form the ion channel. Importantly, at negative membrane potential (i.e., resting potential or partial depolarization), NMDA channels are blocked by extracellular Mg^{2+} ions (Nowak *et al.*, 1984). This obstruction is lifted at positive membrane potential (Mayer *et al.*, 1984) and the channels then become permeable to Na^+, K^+ and Ca^{2+} ions; providing a major entry point for Ca^{2+}-dependent intracellular pathways. NMDA channels are coincidence detectors that

are activated when the presynaptic terminal releases glutamate and when the postsynaptic element is depolarized.

Regarding synaptic plasticity, long term potentiation (LTP) usually corresponds to an increased function of AMPAR,with first an increased permeability of existing channels followed by an increased number of channels at the postsynaptic side, with possible changes in subunit composition. LTP is usually triggered by a massive postsynaptic Ca^{2+} influx resulting from the opening of NMDAR. Long-term depression (LTD), in contrast, often results from a decreased permeability and mostly a decreased number of AMPAR in the synaptic region and is triggered by a small increase in postsynaptic Ca^{2+}.

2.2.2 Striatal metabotropopic glutamate receptor (mGluRs)

The mGluR are GPCR. Eight mGluRs are classified into three groups, namely the group I mGlu receptors (that includes the mGlu1 and mGlu5 receptors), the group II mGlu receptors (that includes the mGluR2 and mGluR3 receptors) and the group III mGlu receptors (that includes the mGluR4, mGluR6, mGluR7, and mGluR8 receptors)(David *et al.*, 2005; Ferraguti and Shigemoto, 2006).

Localization

Histological studies have revealed that mGlu receptors are densely distributed within the striatum (Ferraguti and Shigemoto, 2006). Although the vast majority (90%) of mGlu receptors is thought to be preferentially located postsynaptically and less in presynaptic level, it has been discussed wether mGluR, notably group I, were located at the presynaptic level which seems to be the case (Pittaluga, 2016). Postsynaptic mGluR group I receptors appear to be concentrated in perisynaptic and extrasynaptic area (Nicoletti *et al.*, 2011). Main localizations of mGluR in the basal ganglia circuits are summarized in **Figure intro 7** (Conn *et al.*, 2005).

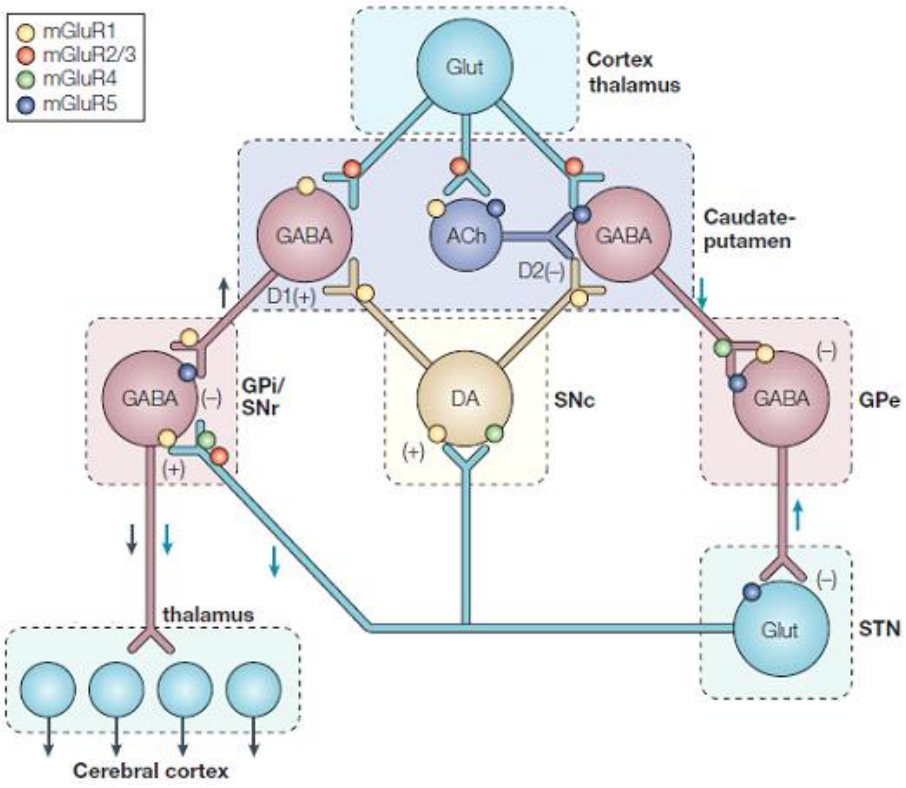

[Figure intro 7: Localization of mGluR in the basal ganglia. adapted from Conn et al 2005.]

Function

mGluR1 and mGluR5 are Gq protein-coupled and stimulate phosphoinositide hydrolysis. Their activation induces mobilization of intracellular Ca^{2+} stores and activation of phospholipase C (PLC)(Conn *et al.*, 2005). Activation of PLC catalyzes the cleavage of phosphatidylinositol-4,5-bisphosphate to inositol trisphosphate (IP3) and diacylglycerol (DAG). The latter activates protein kinase C (PKC) in the presence of Ca^{2+}. mGluR5 regulates IP3-induced and indirectly Ca^{2+}-induced Ca^{2+}-release (CICR) from the endoplasmic reticulum (ER) via IP3 and ensuing stimulation of IP3 receptors. mGluR5 also modulates L-type VGCC in a PLC/PKC dependent way (Fieblinger *et al.*, 2014b). The activation of the presynaptic Group II mGluRs inhibits cyclic AMP (cAMP) and cAMP-dependent protein kinase A (PKA) signaling since they are coupled to Gi/o proteins. Group III, similarly to Group II mGluRs, are negatively coupled to adenylate cyclase (AC) activity and found presynaptically in the glutamatergic terminals of the striatum.

mGluR exist as either homo or heterodimers (Nicoletti *et al.*, 2011). When they are presynaptic, they regulate the release of glutamate and of various transmitters, including GABA, dopamine, noradrenaline, and acetylcholine (Musante *et al.*, 2008; Vergassola *et al.*, 2018).

2.3 cAMP production and actions

In the intact striatum, DA regulates the cAMP pathway in opposite directions in dSPN and iSPN. In D1-dSPNs, DA activates D1R, which increase cAMP production by activating the AC. In D2-iSPNs, DA activates D2R, which decrease cAMP production by inhibiting the AC (Greengard *et al.*, 1999). D1R in dSPNs and $A2_AR$ in iSPNs are coupled to Golf proteins, whereas D2R to Go and Gi proteins (Neve *et al.*, 2004; Beaulieu and Gainetdinov, 2011). Gs and Golf proteins stimulate AC. Golf is a heterotrimeric G protein involved in olfaction, very closely related to Gs (88% amino acid homology) (Jones and Reed, 1989). In the neostriatum, expression of Gαs is very low, whereas Gαolf is abundantly expressed (Hervé *et al.*, 1993). The heterotrimeric olfactory type G-protein Golf comprising the Gαolf, Gβ2 and Gγ7 subunits is required for DA-activated AC in the striatum, expressed in the two types of SPNs. Its alpha subunit, Gαolf, is necessary to couple D1 receptors in D1R expressing-SPNs but also $A2_A$ receptors in D2R expressing-SPNs, to the AC (Zhuang *et al.*, 2000; Corvol *et al.*, 2001). The G-protein γ subunit, Gγ7, associates with Gαolf to couple the receptors to the AC (Wang *et al.*, 2001). In mutant KO mice for Gαolf or Gγ7, the activation of AC by DA or adenosine is severely impaired (Zhuang *et al.*, 2000; Corvol *et al.*, 2001; Hervé *et al.*, 2001; Schwindinger *et al.*, 2003). The main AC isoform in SPNs is AC5 (Visel *et al.*, 2006; Hervé, 2011), whose deletion has severe functional consequences (Kheirbek *et al.*, 2009). AC5 is inhibited by Ca^{2+} at concentration < 1 µM (Hanoune and Defer, 2001).

The major target of cAMP in neurons is the regulatory subunit (R) of PKA, a heterotetramer kinase containing two regulatory and two catalytic (C) subunits (Girault, 2012). The binding releases the C subunits, which become fully active, phosphorylate membrane-bound and cytosolic substrates, and can penetrate the nucleus to phosphorylate nuclear targets. R subunits interact with a family of partners called A-kinase-associated proteins (AKAPs), which enrich PKA at specific subcellular locations such as postsynaptic sites or perinuclear region (Logue and Scott, 2010). cAMP can also activate directly guanine nucleotide exchange factors (cAMP-GEF or EPACs) highly enriched in the striatum (Gloerich and Bos, 2010). The importance of these targets is increasing but not fully understood yet.

In the striatum, several protein substrates of PKA were identified as highly enriched in DA-innervated regions including 32-kDa DA and cAMP-regulated phosphoprotein (DARPP-32) (Walaas *et al.*,

1983), and a number of other PKA substrates (Girault *et al.*, 1990; Girault, 2012). Recent approaches using phosphoproteomics have extended the early work of Greengard and colleagues and identified numerous proteins phosphorylated in response to stimulation of D1R (Nagai *et al.*, 2016b).

2.4 Phosphodiesterases

In SPN, cAMP is degraded by several phosphodiesterases (PDE) highly enriched in SPNs (Polli and Kincaid, 1994; Fujishige *et al.*, 1999; Coskran *et al.*, 2006; Xie *et al.*, 2006) where they play a key role in regulating cAMP signaling (Reed *et al.*, 2002; Menniti *et al.*, 2006; Siuciak *et al.*, 2006; Nishi *et al.*, 2008; Sharma *et al.*, 2013). PDEs are enzymes cleaving the phosphodiester bond in the second messenger molecules cAMP and/or cGMP. PDEs are encoded by 21 genes and subdivided into 11 families according to structural and functional properties (Conti and Beavo, 2007; Heckman *et al.*, 2018), each gene containing several splice variants and isoforms making up to more than one hundred specific PDEs in human (Bender and Beavo, 2006). PDE isoforms share a common structural organization, with a conserved catalytic domain (250–300 amino acids) in the C-terminal portion, followed by a short hydrophilic C-terminal tail and preceded by an N-terminal regulatory region (Sharma *et al.*, 2013). Catalytic domains contain family-specific sequences that determine differences in substrate affinities, catalytic properties, and sensitivities to specific effectors and inhibitors, as well as common structural determinants involved in cleavage of cyclic phosphate bonds. N-terminal portions of PDEs contain domains involved in selective responses of individual PDEs to specific signals that regulate catalytic activity, protein–protein interactions, or targeting to specific subcellular locations. These regulatory domains contain autoinhibitory modules, dimerization domains, GAF domains, sites for phosphorylation by PKA, protein kinase G (PKG), Ca^{2+}/calmodulin-dependent protein kinases (CaMK), protein kinase B (PKB/Akt), protein kinase C, etc (Sharma et al 2013). PDE10A (Fujishige *et al.*, 1999; Coskran *et al.*, 2006; Xie *et al.*, 2006), PDE1B (Polli and Kincaid, 1994; Lakics *et al.*, 2010), and PDE7A and B (Miró *et al.*, 2001; Sasaki *et al.*, 2002; Reyes-Irisarri *et al.*, 2005) are enriched in the striatum. PDE4 (A, B and D isoforms) (Conti *et al.*, 2003), PDE2A and PDE9A, which are widely distributed in the brain, are also expressed in the striatum (Menniti *et al.*, 2006; Lakics *et al.*, 2010; Sharma *et al.*, 2013; Nthenge-Ngumbau and Mohanakumar, 2018). PDE4B and to a lesser extent PDE4A and PDE4D have been reported in the caudate–putamen expression level being higher in iSPNs than in dSPNs (Pérez-Torres *et al.*, 2000; Ramirez and Smith, 2014).

PDE1B. PDE1B may have a predominant role in dSPN. Mice lacking PDE1B exhibit increased phosphorylation of DARPP-32 at Thr34 and GluR1 at PKA sites, indicating that PDE1B normally downregulates cAMP/PKA signaling in striatal neurons. These mice exhibited increased spontaneous locomotor activity (Reed *et al.*, 2002). PDE1B expression correlates with D1R regional expression (Polli and Kincaid, 1994).

PDE7B1. In the D1-dSPNs, the expression of PDE7B1 is reported to increase with D1R activation (Sasaki and Omori, 2004).

PDE4. PDE4 is a cAMP-specific PDE with high affinity for cAMP. Interestingly, Extracellular signal-Regulated Kinase (ERK) signaling can modulate PDE activity. Dopamine-induced ERK activation phosphorylates at the C-terminus at Ser579 and inhibits PDE4 basal activity by 80% (Hoffmann *et al.*, 1999). This effect is enhanced by increased cAMP levels and PKA-mediated phosphorylation of DARPP-32 (Song *et al.*, 2013). PDE4 inhibitors predominantly regulate TH phosphorylation and stimulate dopamine

synthesis at dopaminergic terminals. PDE4 inhibitors also facilitate adenosine $A2_AR$-activated cAMP/PKA signaling in iSPN (Nishi *et al.*, 2008; Nishi and Snyder, 2010).

PDE10A. PDE10A is the major cAMP-hydrolyzing enzyme in striatum, abundant in the SPNs across all their cellular compartments, including cell body, axon terminals and dendrites. Inhibition of PDE10 produces the greatest effect on cAMP hydrolysis (60 to 70%) as compared to inhibition of other PDEs. Electron microscopy studies further support that PDE10A is located close to the post-synaptic density (PSD) in synaptic spines (Xie *et al.*, 2006). More recently, PDE10A has been reported to be targeted into a signaling complex containing the scaffolding proteins AKAP150 and PSD95, as well as the NMDAR (Russwurm *et al.*, 2015) (Russwurm et al 2015). The complex to which PDE10A is targeted might put PDE10A into the position of a "gate keeper" that limits cAMP accumulation at postsynaptic sites, prevents spreading of synaptic signals into the cell body, and ensures precisely timed phosphorylation and thereby regulation of NMDAR for instance.

Nishi et al reported distinct predominant roles of PDE4 and PDE10A in striatal dopamine neurotransmission in relation to their predominant cellular localization: in dopaminergic terminals (PDE4) and SPNs (PDE10A). PDE10A inhibitors counteract D2R signaling in iSPNs. They potentiate D1R signaling in dSPNs mainly via cAMP-mediated effects, increasing for instance phosphorylation of DARPP-32 at Thr34, GluR1 at Ser845 and CREB at PKA sites (Nishi *et al.*, 2008; Grauer *et al.*, 2009)(**Figure Intro 8**). PDE10A inhibitors have a predominant action in D2-iSPN. They regulate DARPP-32 phosphorylation and induction of c-Fos in iSPNs (Nishi *et al.*, 2008; Wilson *et al.*, 2015). They increase PKA activity only in $A2_A$-R SPN (Polito *et al.*, 2015). Their effect on behavior and cAMP increase can be reversed via $A2_A$ antagonism (Bleickardt *et al.*, 2014). The phosphorylation of ERK1/2 that they induce is potentiated when combined with a D2R-antagonist and to a lesser degree with a D1R-agonist (Hsu *et al.*, 2011). It was hypothesized that PDE10A and PDE1B have complementary functions in striatal neurons, since knockout (KO) mice for each of these phosphodiesterases show opposing phenotypes: PDE10A KO mice show decreased exploratory activity whereas PDE1B KO mice show a hyperlocomotor phenotype (Reed *et al.*, 2002; Siuciak *et al.*, 2006).

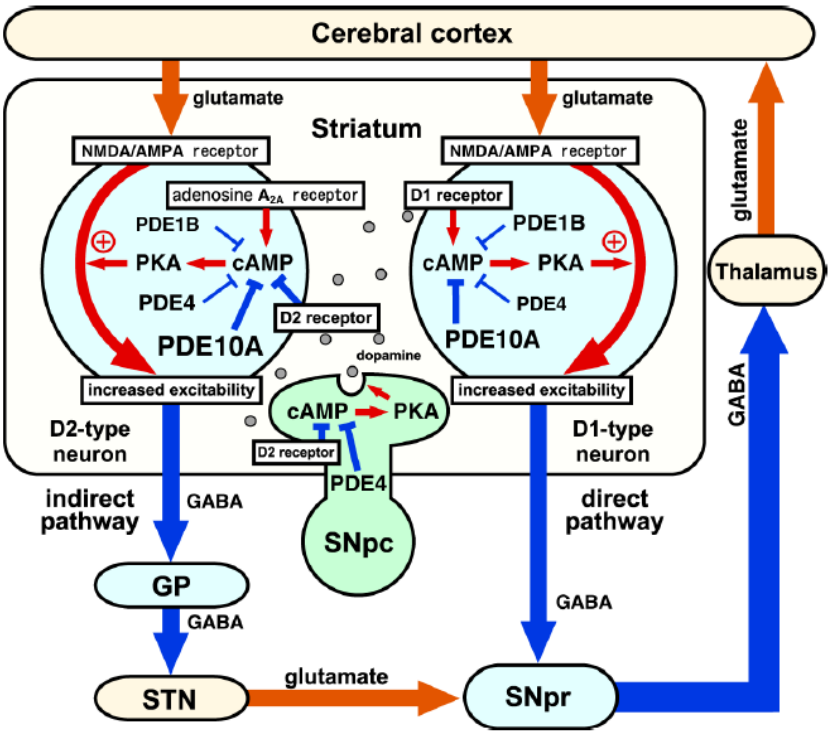

*[**Figure Intro 8: Roles of PDEs in the control of basal ganglia–thalamocortical circuitry.** The inhibition of PDEs increases cAMP/PKA signaling in both dSPNs and iSPNs. PDE inhibitors predominantly acting in dSPNs work like D1R agonists and activate motor function. PDE inhibitors predominantly acting in iSPNs work like D2R antagonists and inhibit motor function. Relative size of each PDE in different SPNs subtypes reflects its predominant action. **from Nishi and Snyder 2010, Nishi et al 2011**]*

2.5 DARPP-32

DARPP-32 (dopamine- and cAMP-regulated phosphoprotein, Mr 32 000) is the most studied striatal-enriched PKA-regulated phosphoproteins. DARPP-32 is a small unstructured protein of about 202 amino acids (Yger and Girault, 2011)(**Figure Intro 9**). The phosphorylation levels of DARPP-32 are low at Thr34 and high at Thr75, Ser97, and Ser130 under basal conditions. Activation of PKA induces the phosphorylation of DARPP-32 at Thr34 and the dephosphorylation of DARPP-32 at Thr75 and Ser97 by PP-2A/B56δ complex. When Thr-34 is phosphorylated by PKA or PKG, DARPP-32 becomes a powerful inhibitor of PP1 (IC50 in the nM range). Thus, a major function of DARPP-32 is to provide a feed-forward amplification of PKA signaling by inhibiting dephosphorylation of substrates of this kinase that are dephosphorylated by PP1 (**Figure Intro 10**). It is also a potential source of cross talk with other signaling pathways by preventing dephosphorylation by PP1 of substrates of other kinases. pThr-34 is dephosphorylated by two phosphatases, Ca^{2+}/calmodulin-activated calcineurin (also known as PP2B or PPP3) and PP2A (or PPP2) thereby allowing PP1 activity (Nishi *et al.*, 1999).

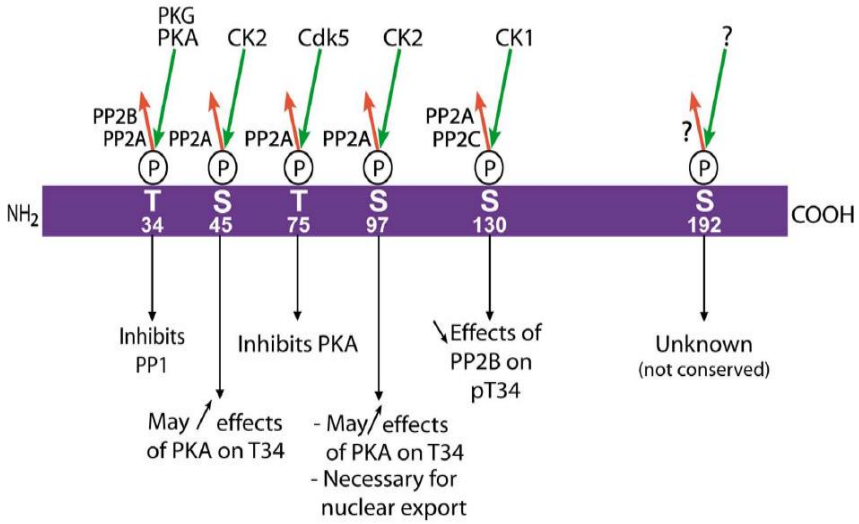

[Figure Intro 9: Multisite phosphorylation of DARPP-32. *Schematic representation of mouse DARPP-32 with the residues found phosphor-rylated in vivo (Thr-34, Ser-45, Thr-75, Ser-97, Ser-130, Ser-192). The identified kinases are indicated with green arrows (phosphorylation), and protein phosphatases by the red arrows (dephosphorylation). The role of the phosphorylation is given for each residue. P, phosphate.* ***From Yger et Girault 2011]***

DARPP-32 is also phosphorylated by cyclin-dependent protein kinase 5 (CDK5) on Thr-75. When DARPP-32 is phosphorylated on Thr-75, it becomes a powerful inhibitor of PKA (Bibb *et al.*, 1999). DARPP-32 is both a PKA-regulated inhibitor of PP1 and a CDK5-regulated inhibitor of PKA, providing the theoretical possibility to switch on and switch off the PKA pathway in striatal neurons.

DARPP-32 is expressed in both dSPNs and iSPNs (Bertran-Gonzalez *et al.*, 2008). In BAC transgenic mice where tagged DARPP-32 is expressed under the control of the D1R and D2R promoters, respectively, D1R stimulation results in an increased phosphorylation of DARPP-32 at Thr34 in response to PKA activation in dSPNs, whereas D2R stimulation reduces this phosphorylation, presumably as a consequence of a reduction in PKA activaty (Bateup *et al.*, 2008) and/or activation of the calmodulin-dependent PP2B-calcineurin resulting from the increased intracellular Ca^{2+} after activation of D2R (Nishi *et al.*, 1997). DARPP-32 plays an important role in the regulation of ion channels activity by controlling directly or indirectly their phosphorylation state through inhibition of PP1. Thus, the D1R–cAMP–PKA–DARPP-32 pathway is strongly involved in DA-enhanced function of AMPAR, NMDAR, voltage-gated Na, and L-type Ca^{2+} channels, as well as in DA-decreased function of GABA-A channels and Ca^{2+} channels

(Surmeier *et al.*, 1995; Fienberg *et al.*, 1998; Schiffmann *et al.*, 1998; Snyder *et al.*, 1998, 2000; Flores-Hernandez *et al.*, 2000; Onn *et al.*, 2003).

2.6 The ERK Cascade

Mitogen-activated protein kinases (MAP kinases) are regulated by two upstream kinases, a MAP-kinase-kinase and a MAP-kinase-kinase-kinase, which form a highly conserved 3-kinase signaling module. One type of MAP kinases, namely, the extracellular signal-regulated kinases 1/2 (ERK1/2), has been shown to play an important role in striatal signaling. ERK signaling could be critically involved in molecular adaptations that are necessary for long-term behavioral changes (Girault *et al.*, 2007).

2.7.1 ERK functional importance

Several reports have shown that ERK is necessary for LTP, including at corticostriatal synapses (Pascoli *et al.*, 2011a, b). The activation of ERK1/2 by drugs of abuse in SPNs involves a crosstalk between D1R and NMDAR, which are both necessary for this response (Valjent *et al.*, 2000, 2005). It provides a mechanism by which SPNs can detect the simultaneous occurrence of a raise in DA, for example due to an unexpected reward, and the activity of specific cortico and thalamo-striatal glutamatergic inputs, linked to the external and internal context (Girault *et al.*, 2007). As ERK is important for long-term changes in behavior, this mechanism that could be considered as coincidence detector or logical AND gate, has a potential to play an important functional role in learning specific behaviors (Girault *et al.*, 2007). As in other neurons, a strong stimulation of NMDAR is sufficient to activate ERK in striatal neurons in culture (Pascoli *et al.*, 2011a). In hippocampal neurons, it has also been shown, using two-photon fluorescence lifetime imaging microscopy (2pFLIM) and two-photon glutamate uncaging, that ERK is activated NMDAR-dependently in both the stimulated spine and adjacent dendrite spreading along the shaft over 12 µm, reaching a plateau within 5 min and returning back to baseline at around 20 min (Tang and Yasuda, 2017). This ERK activation is associated with a sustained phase of spine volume increase lasting more than 30 min. ERK activation can also be induced in vivo or ex vivo by electrical stimulation of the corticostriatal pathway (Sgambato *et al.*, 1998; Quiroz *et al.*, 2009). D1R stimulation potentiates this effect in vivo. Moreover, ERK phosphorylation has also been shown to increase in response to elevated DA levels in the striatum of freely moving mice in D1-SPNs using FRET imaging in vivo (Goto *et al.*, 2015).

2.7.2 Regulation of ERK in SPNs

ERK1/2 are activated by phosphorylation of their activation loop by MAP-kinase and ERK-kinase (MEK1 and 2). Upstream from MEK, ERK activation involves the MAP-kinase-kinase-kinase, RAF, Ras and calcium-activated guanine nucleotide exchange factor Ras-GRF1 (Fasano *et al.*, 2009; Fasano and Brambilla, 2011), and possibly other guanine nucleotide exchange factors. DARPP-32 plays a critical role in ERK phosphorylation in vivo. PKA-mediated phosphorylation of DARPP-32 promotes ERK activation through an indirect inhibition of striatal enriched tyrosine phosphatase (STEP), a tyrosine phosphatase that dephosphorylates the Tyr residue of ERK activation loop (Pulido *et al.*, 1998; Nishi *et al.*, 2011) (**Figure Intro 10**). DARPP-32 phosphorylation thus prevents ERK dephosphorylation and contributes to enhanced glutamate mediated-ERK activation. In DARPP-32 KO or Thr-34-Ala knock-in mutant mice, the phosphorylation of ERK was blocked in the striatum (Valjent *et al.*, 2005). STEP is phosphorylated by PKA and dephosphorylated by PP1. This phosphorylation inactivates the enzyme. In the dSPNs, DA enhances STEP phosphorylation directly through PKA activation and indirectly by blocking PP1 through pThr34–DARPP-32. DARPP-32 also seems active upstream from MEK. After administration of cocaine, the cAMP-

dependent phosphorylation of ERK and DARPP-32 peaks and returns to baseline within the first 30 min (Valjent *et al.*, 2000, 2005).

Mechanisms of ERK activation by NMDAR stimulation in the striatum have been investigated. Experiments in neurons in culture show that it is a Ca^{2+}-mediated response (Pascoli *et al.*, 2011a). NMDAR associates with Ca^{2+}-activated Ras-GRF1 to activate Ras, Raf, MEK and then ERK (Krapivinsky *et al.*, 2003; Fasano *et al.*, 2009; Fasano and Brambilla, 2011). The group I mGluR can modulate NMDAR signaling onto ERK activation via PKC (Niswender and Conn, 2010) and also via direct physical interactions (Perroy *et al.*, 2008). Overall, activation of D1R and subsequent PKA/DARRP-32 signaling cascade leads to the inactivation of PP1 and the consequent inactivation of STEP, modifying the equilibrium and enabling NMDAR-induced activation of ERK. More recently, intracellular signaling mechanism of ERK activation through other guanine nucleotide exchange factors like Rap1 GEF in D1R-SPN has been described in a novel DA-PKA-Rap1-ERK pathway (Nagai *et al.*, 2016a, b). Rap1 GEF is activated by cAMP dependent phosphorylation and contributes to D1R- or cocaine-induced ERK activation (Nagai *et al.*, 2016a). These various observations show that ERK being activated by both cAMP- and Ca^{2+}-dependent mechanisms, some of them being synergistic, might act as a signal integrator for DA and glutamate neurotransmission.

2.7.3 Actions of ERK in SPNs

ERK can phosphorylate proteins in the cytoplasm of neurons that are important for plasticity, including ion channels (Sweatt, 2004; Thomas and Huganir, 2004; Patterson *et al.*, 2010). In the context of striatal signaling, the nuclear targets of ERK have been more thoroughly investigated. Under basal conditions, the unphosphorylated form of ERK1/2 is detected in the cytoplasm of neurons. The active di-phosphorylated ERKs translocate to the nucleus where they control both epigenetic and genetic responses.

In dSPNs, the actions of ERK in the nucleus include direct phosphorylation of the transcription factor Elk1 (Vanhoutte *et al.*, 1999; Brami-Cherrier *et al.*, 2005, 2007; Lavaur *et al.*, 2007; Trifilieff *et al.*, 2009) leading to the transcription of immediate early genes such as Zif268 (also known as NGFI-A or Krox24. ERK also activate protein kinases, among which mitogen- and stress-activated protein kinase 1 (MSK1) which play a critical role in the phosphorylation of cAMP-response element binding protein (CREB) and histone H3 as well as induction of cFos (Soloaga *et al.*, 2003; Brami-Cherrier *et al.*, 2005; Chwang *et al.*, 2007; Santini *et al.*, 2007, 2009) (**Figure Intro 10**). The induction of these nuclear targets is critical for long lasting behaviors.

ERK activation, as well as the phosphorylation of MSK1 and histone H3, occurs in D1R-expressing neurons of the direct pathway after D1R stimulation. ERK can be activated in D2R-SPNs of the indirect pathway in response to other types of stimuli. The simple blockade of D2R by haloperidol or raclopride triggers ERK phosphorylation, at least in part by removing the brake exerted by D2R on $A2_AR$ (Pozzi *et al.*, 2003; Bertran-Gonzalez *et al.*, 2008). However, in D2R-expressing iSPN, ERK activation remains limited and the phosphorylation of numerous proteins that are targets of ERK appears to occur through other mechanisms, including direct phosphorylation by PKA (Bertran-Gonzalez *et al.*, 2009)(Bertran-Gonzalez et al 2009). In addition, a powerful synergistic interaction of $A2_AR$ with the fibroblast growth factor receptor to activate ERK has been reported and may have a significant role in the physiology of the striatum (Flajolet *et al.*, 2008).

The origin of this difference between the two populations of striatal neurons is not clear. Thus, the ERK pathway appears to be an important player in the striatum, with different regulations in dSPNs and iSPNs.

2.7 Integration of multiple signaling pathways activated by DA, roles of D1R and D2R

As discussed above there is no one-to-one correspondence between any neurotransmitter receptor in SPNs and signaling pathways. Instead stimulation of one type of receptor triggers a combination of signaling responses whose combination is also modulated by the previous "history" of the cell and the simultaneous activation of other receptors. As an example of multiple pathways **Figure Intro 10** summarizes a few of the signaling responses extensively studied following D1R activation.

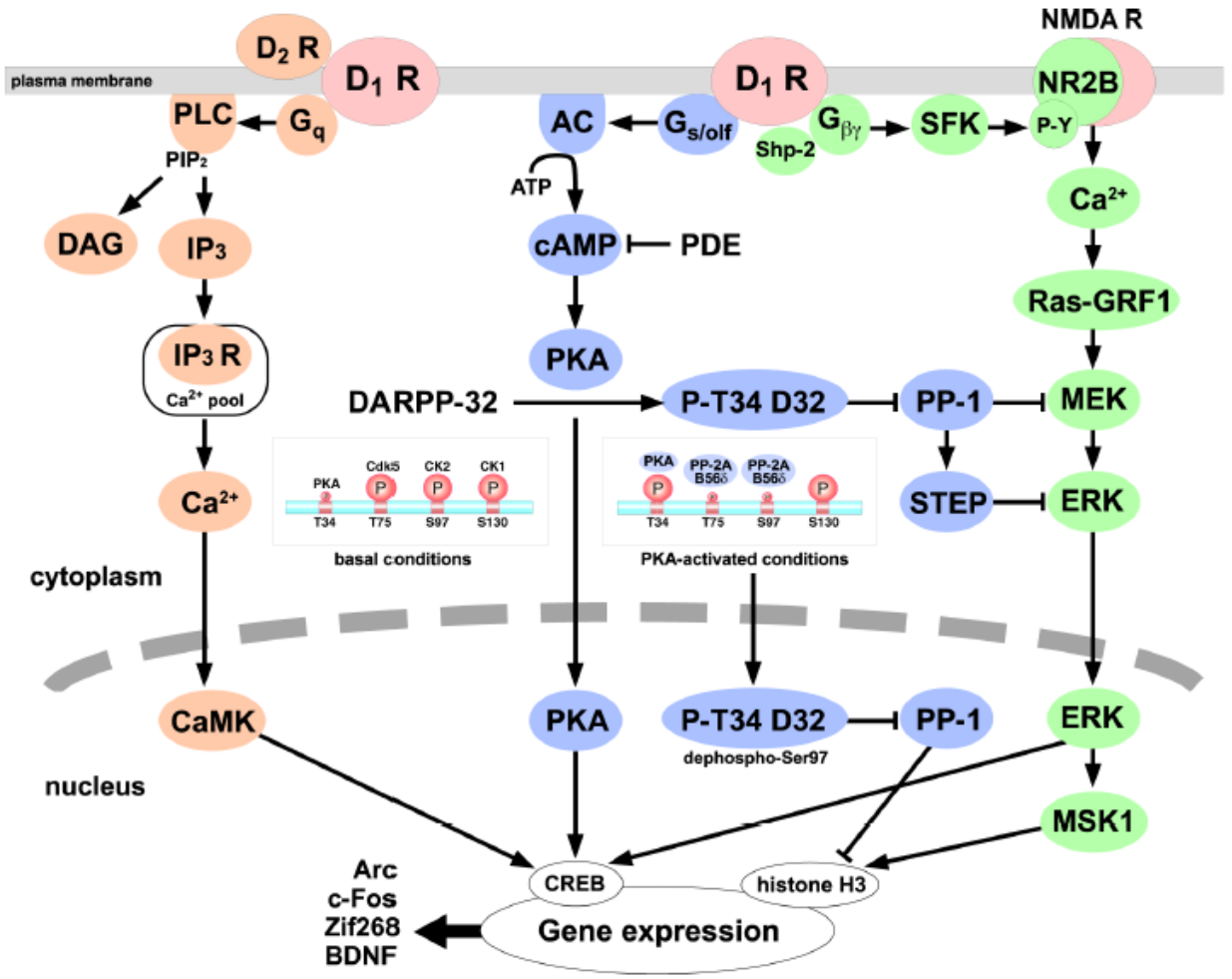

[Figure Intro 10: The D1 receptor signaling cascades in striatonigral/direct pathway SPNs. *D1R couple to at least three distinct signaling cascades: (1) Golf/adenylate cyclase (AC)/cAMP/PKA/DARPP-32/protein phosphatase-1 (PP-1) signaling (blue), (3) Gβγ/Src family kinase (SFK)/NMDAR NR2B subunit/Ca2+/Ras-GRF) mitogen-activated protein kinase/ERK kinase (MEK)/ERK signaling (green). ERK, activated by two D1R pathways, induces MSK1 activation and histone H3 and CREB phosphorylation in the nucleus. Thus, D1R-mediated activation of PKA, intracellular Ca^{2+}, and ERK signaling induces the changes in downstream signaling cascades and the transcriptional activation of many genes. CaMK: Ca^{2+}/calmodulin-dependent protein kinase.* ***From Nishi et al 2011]***

D2R are coupled to Gi/o heterotrimeric G proteins. Gi/o inhibits AC, opposing the effects of adenosine in iSPN. The main isoform of AC in SPNs, AC5, is directly inhibited by Gαi and is insensitive to Gβγ (Taussig *et al.*, 1994; Visel *et al.*, 2006). D2-class receptors modulate intracellular Ca^{2+} levels through various mechanisms (Nishi *et al.*, 1997; Beaulieu and Gainetdinov, 2011) (**Figure Intro 11 A and B**). Activation of Gi/o are able to target voltage-dependent ion channels through a membrane-delimited mechanism (Gβγ), inhibiting L-type Ca^{2+} channels (Hernandez-Lopez *et al.*, 2000). Gβγ subunits released following D2R activation bind and activate PLCβ increasing the cytoplasmic Ca^{2+} concentration (Hernandez-Lopez *et al.*, 2000; Kreitzer and Malenka, 2007). Gi/o can also activate K^+ channels such as GIRKs (Lavine *et al.*, 2002; Hamasaki *et al.*, 2013; Kramer and Williams, 2016), resulting in inhibition of neurons (**Figure Intro 11 B**). After endocytosis, D2R is also able to activate a number of signaling pathways through the recruitment of β-arrestins (Beaulieu and Gainetdinov, 2011).

DA receptor heteromerization with ion channels (D1R and NMDAR, D5R and GABAAR), tyrosine kinase receptor (D2R/D4R and the epidermal growth factor and platelet-derived growth factor receptors), other DA receptor subtypes (D1, D2 and D3) or other GPCRs (such as $A2_AR$ and mGluR) have been reported and may have functional consequences. D1R/D2R heteromers are coupled with Gαq and activating PLC and IP3 and diacylglycerol (DAG)-dependent signaling (Rashid *et al.*, 2007; Hasbi *et al.*, 2009; Perreault *et al.*, 2010; Nishi *et al.*, 2011) (**Figure intro 10**). This is probably very marginal in the dorsal striatum since it would be restricted to the small number of neurons expressing significant levels of both receptors.

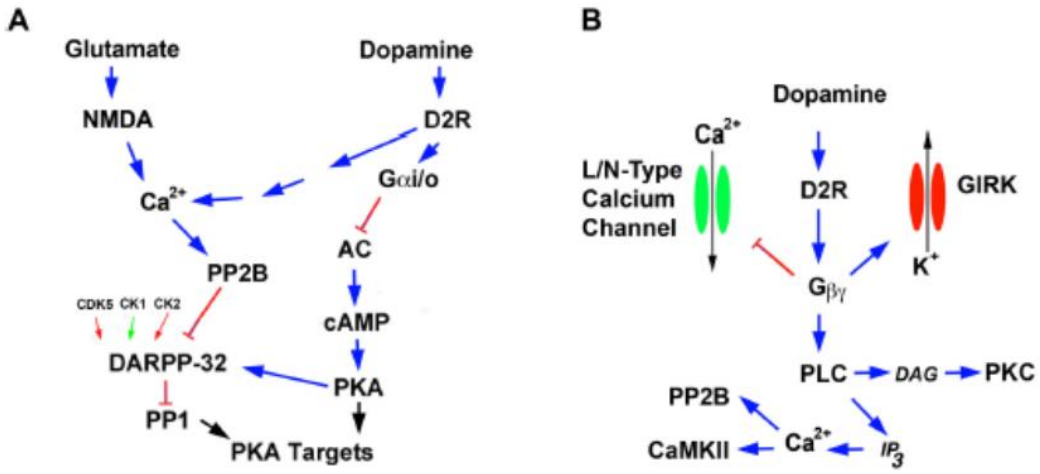

[Figure Intro 11: Signaling networks regulated by D2-class DA receptor.

***A**, regulation of Gαi/cAMP/PKA signaling by D2-class receptors.*

***B**, regulation of Gβγ signaling by D2-class receptors.*

The action of other neurotransmitters has been included to illustrate the role of many of these intermediates as signal integrators. Blue arrows indicate activation, red T-arrows indicate inhibition, and green arrows indicate the amplification of an already activated function. Black arrows indicate actions that can either be stimulatory or inhibitory on the function of specific substrates. ***From Beaulieu and Gainetdinov 2011]***

2.8 Signaling crosstalk between glutamate and DA

DA modifies the properties of various glutamate receptors. Dopamine bidirectionally modulates the function and membrane transport of NMDAR (Cepeda and Levine, 1998; Kotecha *et al.*, 2002; Lee *et al.*, 2002a; Tong and Gibb, 2008; Higley and Sabatini, 2010) and AMPAR (Roche *et al.*, 1996; Snyder *et al.*, 2000; Håkansson *et al.*, 2006; Santini *et al.*, 2007; Shepherd and Huganir, 2007; Alcacer *et al.*, 2012) with differential effects on the receptors, depending on their synaptic or non-synaptic distribution at the membrane, or on stimulation of D1 or D2 receptors—with various signaling pathways implicated.

DA-dependent modulation of glutamate evoked-response specific to the direct and indirect pathways has been further characterized in dSPNs and iSPNs using BAC transgenic mice (Cepeda *et al.*, 2008; André *et al.*, 2010). In particular, activation of D1R usually leads to potentiation of AMPA and NMDAR-dependent currents, while activation of D2R induces a decrease of NMDA and AMPAR-dependent responses (Cepeda *et al.*, 1993; Hernández-Echeagaray *et al.*, 2004; Skeberdis *et al.*, 2006; André *et al.*, 2010).

2.9.1 Actions of D2R on glutamate receptors

D2R stimulation diminishes presynaptic release of glutamate (Bamford *et al.*, 2004; André *et al.*, 2010), although it is not clear whether the D2R involved are located pre- or post-synaptically (Cepeda *et al.*, 1993; Hernández-Echeagaray *et al.*, 2004; Yin and Lovinger, 2006). D2R–triggered dephosphorylation of GluR1 subunits at Ser 845 should promote trafficking of AMPAR out of the synaptic membrane (Håkansson *et al.*, 2006). Recent work using glutamate uncaging on proximal dendritic spines and Ca^{2+} imaging failed to find any acute effect of D2R stimulation on AMPAR currents but has shown a decrease of NMDAR-induced responses (Higley and Sabatini, 2010). D2R signaling was found to decrease Ca^{2+} entry through NMDAR, keeping with the effect on voltage-dependent Ca^{2+} channels.

Direct interaction between D2R and NMDAR occurs at the postsynaptic density. DA stimulation enhances interactions of the third intracellular loop of D2R with the COOH terminal tail of GluN2B, reduces CaMKII and GluN2B association and the CaMKII-dependent phosphorylation of GluN2B at Ser 1303 and, as previously mentioned, inhibits NMDAR-mediated calcium currents (Liu *et al.*, 2006).

2.9.2 Actions of D1R on glutamate receptors

D1R signaling, in contrast to D2R signaling, has positive effects on AMPAR and NMDAR function and trafficking. D1R stimulation stabilizes AMPA currents (Cepeda *et al.*, 1993; Galarraga *et al.*, 1997; Yan *et al.*, 1999). This stabilization may be mediated by both PKA-catalyzed phosphorylation of the GluR1 subunit at Ser845 and DARPP-32 inhibition of PP1-catalyzed dephosphorylation of the residue (Yan *et al.*, 1999; Snyder *et al.*, 2000; Chao *et al.*, 2002). Activation of D1R also leads to a potentiation of NMDAR-dependent currents seemingly via DARPP-32 inhibition of PPA (Flores-Hernández *et al.*, 2002). DA action on specific NMDAR or AMPAR subunits could affect spine morphology and structural plasticity. Treatment with a D1R agonist leads to an increase in spine head width, further increased by a GluN2A antagonist co-administration and blocked by a GluN2B antagonist co-administration (Vastagh *et al.*, 2012). The same specific NMDAR subunits regulation of D1 evoked NMDA responses were described (Jocoy *et al.*, 2011).

There are multiple levels of interaction between D1R and NMDAR. First, trafficking and localization may be affected by direct protein-protein interaction between D1R and NMDAR (Dunah *et al.*, 2000; Lee *et al.*, 2002a; Scott *et al.*, 2006). Possible direct molecular interaction is suggested by the co-existence of D1R and NMDAR at synapses in SPNs (Hara and Pickel, 2005; Kruusmägi *et al.*, 2009;

Jocoy *et al.*, 2011; Vastagh *et al.*, 2012). Co-immunoprecipitation of D1R with GluN1/GluN2A subunits of the NMDAR also supports this idea. In addition, the fact that D1R interaction with GluN1 decreases when D1R is stimulated suggests a dynamic process (Lee *et al.*, 2002a). This interaction abolishes D1R internalization, a crucial adaptive response that normally occurs upon agonist stimulation (Fiorentini *et al.*, 2003). A competition between PSD-95 and NMDAR for interaction with the COOH terminal of D1R might modulate internalization by uncoupling D1R from NMDAR, thereby liberating the D1R and allowing for their internalization (Zhang *et al.*, 2009). Association of D1R with NMDAR also alters their trafficking along the surface of the plasma membrane. Works on hippocampal synapses suggest that D1R activation reduces D1R/GluN1 interaction at perisynaptic sites allowing fast lateral diffusion of NMDAR at the postsynaptic density, favoring LTP induction (Ladepeche *et al.*, 2013). Works on SPNs suggest that the direct interaction with NMDAR would "trap" the D1R to the synapse (Scott *et al.*, 2006).

D1R stimulation can also activate Src-family kinase (SFK), resulting in the tyrosine phosphorylation of NMDAR, mainly the GluN2B subunit (Tyr-1472 residue) and possibly GluN2A (Nakazawa *et al.*, 2001) . D1R stimulation activates Fyn in a G-protein dependent but cAMP-independent way (Dunah *et al.*, 2004; Pascoli *et al.*, 2011a), The tyrosine phosphorylation may increase NMDAR permeability, and particularly the NMDAR-mediated Ca^{2+} influx (Skeberdis *et al.*, 2006) (**Figure Intro 10**). The phosphatase STEP dephosphorylates GluN2B at Tyr-1472 (Won *et al.*, 2016). Interestingly, the activity of STEP is down-regulated by cAMP/PKA signaling as previously mentioned and D1R stimulation could promote tyrosine phosphorylation of NMDAR via this signaling pathway. The tyrosine kinase Fyn and protein phosphatase STEP appear to be important regulators of glutamate receptor surface expression (Braithwaite *et al.*, 2006; Salter *et al.*, 2009).

2.9 Adenosine receptors and adenosine signaling in SPNs

2.9.1 Adenosine receptors

Adenosine is a nucleoside distributed ubiquitously throughout the body as a metabolic intermediary. In the brain, adenosine does not act as a classical neurotransmitter, since it is not stored in vesicles, not released in response to action potential, and does not only act at synapses level to transfer information (Ribeiro *et al.*, 2002). Equilibrative nucleoside transporters, ENT1 and ENT2 allow adenosine to quickly cross the cell membrane bidirectionally (King *et al.*, 2006).

There are four subtypes of GPCRs, A1, $A2_A$, $A2_B$, and A3, each with specific adenosine affinity (Fredholm, 2010). The A2 receptor has two different subtypes categorized according to their high- ($A2_A$) or low- ($A2_B$) affinity for adenosine. A1 and $A2_A$ receptors have binding affinities for adenosine in the range of nanomolars, while its affinity for A2B and A3 receptors is in the range of micromolars. These latter receptors are only activated when high local concentrations of adenosine are present. Under physiological conditions, endogenous adenosine level is 20–250 nM in the brain (Ballarín *et al.*, 1991; Latini and Pedata, 2001; Pedata *et al.*, 2001), which is sufficient to activate receptors where they are very highly expressed-as for instance in the basal ganglia for A2AR on iSPN (Fredholm *et al.*, 2001; Fredholm, 2010). Under stress conditions, during ischemia for instance, this concentration can reach 30 µM at the receptor level allowing for all adenosine receptor subtypes to be activated (Pedata *et al.*, 2001).

The A1 and A3 receptors (A1R and A3R) are coupled to the Gαi family of G proteins and inhibit cAMP synthesis. A1R and A3R are both expressed in the brain, A3R at lower concentrations (Dixon *et al.*, 1996). A1R are expressed at lower levels in the striatum as compared to cortex (Mahan *et al.*, 1991),

mediating neuronal activity inhibition through inhibition of glutamate release at corticostriatal terminals in the striatum (Dunwiddie and Masino, 2001). A1R are also expressed on cholinergic interneurons.

$A2_AR$ are Gαs/olf coupled, stimulate AC, raise cAMP levels, activating the cAMP/PKA pathway via coupling to Gαolf (Kull *et al.*, 2000; Corvol *et al.*, 2001; Chen *et al.*, 2014) (**Figure Intro 10**). $A2_AR$ are homogeneously distributed throughout the lateral, medial, and ventromedial areas of the striatum (Rosin *et al.*, 2003). $A2_AR$ are highly concentrated post-synaptically, mainly at asymmetric excitatory striatal synapses, in dorsal and ventral striatum in D2R expressing SPNs, but not in D1R expressing SPNs, and at lower concentrations at presynaptic sites in corticostriatal terminals (Schiffmann *et al.*, 1991; Dixon *et al.*, 1996; Svenningsson *et al.*, 1997, 1998, 1999; Rebola *et al.*, 2005). $A2_ARs$ at presynaptic sites seem o be preferentially situated on corticostriatal terminals making contact with D1R expressing dSPNs (Quiroz *et al.*, 2009). They are colocalized with A1Rs, as well as in other heteromers with mGluR5 receptors, to regulate glutamate release at these glutamatergic striatal terminals (Rebola *et al.*, 2005; Rodrigues *et al.*, 2005; Ciruela *et al.*, 2006). $A2_ARs$ are also localized on glial cells in the caudate nucleus and putamen (Rosin *et al.*, 2003), in cholinergic interneurons (Preston *et al.*, 2000; Song *et al.*, 2000), and SPN axon collaterals (Hettinger *et al.*, 2001).

Blockade of adenosine receptors (in particular the $A2_ARs$) stimulates motor activity, while activation of the $A2_AR$ (and to a lesser extent the A1R) inhibits motor activity. The spontaneous locomotor activity of $A2_AR$ knockout ($A2_AR$-KO) mice is significantly reduced (Ledent *et al.*, 1997; Yang *et al.*, 2009; Taura *et al.*, 2018). The $A2_AR$ agonist CGS 21680 strongly reduces spontaneous locomotor activity in WT mice but had no significant effect on $A2_AR$-KO mice (Ledent *et al.*, 1997).

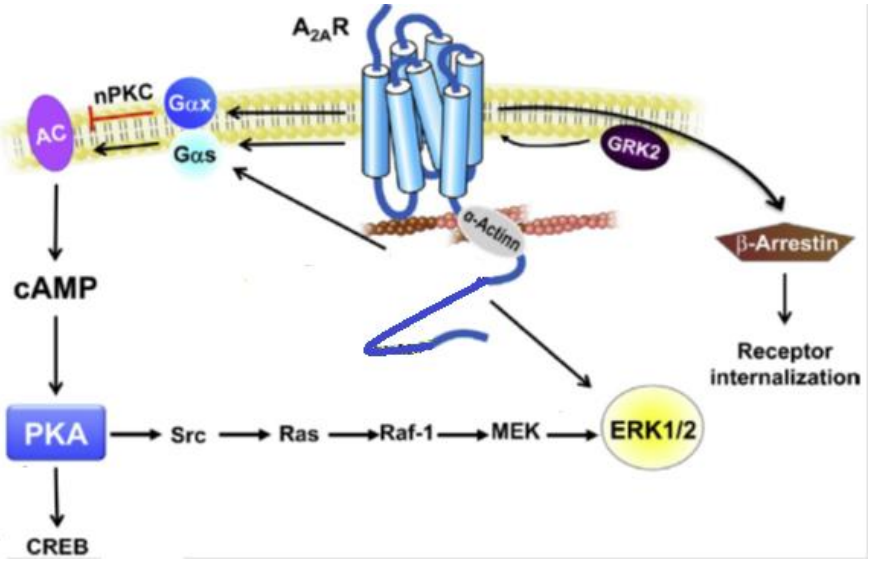

[Figure Intro 12. Major signaling pathway of $A2_A$ adenosine receptor ($A2_AR$), adapted from Chen et al 2014]

2.9.2 Adenosine receptors interaction with DA and glutamate neurotransmission in the striatum

The antagonistic interaction of combined adenosine and DA receptor stimulations appears different depending on the SPN type considered. While A1R and D1R communicate mainly in dSPNs, interaction between $A2_AR$ and D2R occurs in iSPNs. $A2_A$ and A1 antagonism is synergistic as A1R inhibition facilitates release of DA, while $A2_AR$ inhibition increases responses to DA postsynaptically. The A1R forms an oligomer with the D1R in basal ganglia (Fuxe *et al.*, 2007) regulated by agonist binding (Ginés *et al.*,

2000). Antagonists of A1Rs facilitate release of DA, and like A2AR antagonists, they increase DA-mediated responses (Ballarin *et al.*, 1995; Okada *et al.*, 1996).

The presence of $A2_AR$ in different receptor heteromers with neurotransmitters and neuromodulators receptors allows controlling other key glutamatergic synapses modulators like DA, glutamate and endocannabinoids (Fuxe *et al.*, 2003; Ferré *et al.*, 2011). The $A2_AR$ can form higher order oligomers with themselves (Vidi *et al.*, 2008) and have multiple binding partners including the A1R (Ciruela *et al.*, 2006; Navarro *et al.*, 2018a), the D2R (Hillion *et al.*, 2002), the D3R (Torvinen *et al.*, 2005), the mGluR5 (Díaz-Cabiale *et al.*, 2002; Kachroo *et al.*, 2005), and the cannabinoid CB1 receptor (Carriba *et al.*, 2007; Moreno *et al.*, 2018).

$A2_AR$ associate physically to form a functional complex with D2R (Fuxe *et al.*, 2005; Cabello *et al.*, 2009; Trifilieff *et al.*, 2011; Bonaventura *et al.*, 2015; Fernández-Dueñas *et al.*, 2015). Reciprocal antagonistic interactions occur within the $A2_AR$-D2R heteromer (Fuxe *et al.*, 2007). The stimulation or blockade of $A2_AR$ alters in opposite direction the binding affinity, decreasing or increasing it respectively, of D2R to its ligands; in particular to DA (Ferré *et al.*, 1999, 2016; Díaz-Cabiale *et al.*, 2001) and also to β-arrestin2, which disturbs D2R internalization (Torvinen *et al.*, 2004; Borroto-Escuela *et al.*, 2011). A reciprocal interaction was described, by which D2R agonists decrease the binding of $A2_AR$ ligands (Fernández-Dueñas *et al.*, 2013). In addition, a strong antagonistic interaction at the AC level has been described, which depends on the ability of D2R-mediated Gi activation to inhibit Golf activation elicited by $A2_AR$ activation (Ferré *et al.*, 2016). The recent hypothesis of the formation of $A2_AR$ -D2R heterotetrameric structures could explain the simultaneous existence of both types of receptor-receptor interactions: direct physical interaction in heteromer and counteraction by D2R Gi-coupled GPCR of AC activation mediated by $A2_AR$ Gs-coupled GPCR (Bonaventura *et al.*, 2015; Ferré *et al.*, 2016). A recent study has provided evidence for the existence of functional precoupled complexes of $A2_AR$ and D2R homodimers, their cognate Golf and Gi proteins and AC5, and demonstrated that this macromolecular complex provides the sufficient but necessary condition for the Golf–Gi interactions at the AC level (Navarro *et al.*, 2018b).

Besides adenosine A2AR and D2R, mGluR5 are also known to interact and colocalize in heteromeric receptor complexes postsynaptically in the iSPN (Conn *et al.*, 2005; Cabello *et al.*, 2009; Bogenpohl *et al.*, 2012). This provides a structural basis for the existence of multiple functional interactions of $A2_A$, D2, and mGlu5 receptors. $A2_A$ and mGlu5 receptor agonists lead to a synergistic decrease of DA receptors affinity and to a decrease of the motor behavior response to a D2 agonist (Ferré *et al.*, 1999; Popoli *et al.*, 2001). Activation of both receptors induces an increase of extracellular GABA levels in the ventral pallidum, indicating activation of iSPNs (Díaz-Cabiale *et al.*, 2002). The induction of c-fos expression is also increased in iSPNs when $A2_AR$ and mGlu5 receptors are coactivated (Ferré *et al.*, 2002; Nishi *et al.*, 2003) but maybe via a presynaptic activation of $A2_AR$ on glutamatergic terminals rather than a direct physical interaction (Shen *et al.*, 2013). Each mGluR5 and A2AR effect needs the coactivation of the other receptor by endogenous adenosine and glutamate respectively, to happen (Nishi *et al.*, 2003) and potentiate their effect (Domenici *et al.*, 2004). A molecular basis for this functional interaction via the phosphorylation of DARPP-32 has been suggested, and the mGluR5 effect seems to be ERK dependent (Nishi *et al.*, 2003; Shen *et al.*, 2013). When glutamatergic neurotransmission is active, it has also been suggested that a glutamatergic pathway via NMDAR

activation induces further adenosine release stimulating $A2_AR$ (Pedata *et al.*, 1991; Manzoni *et al.*, 1994; Nash and Brotchie, 2000).

Together these results point to a synergistic action of glutamate and adenosine signalings in iSPNs and reciprocal regulating interactions with D2R signaling. The respective roles of these mechanisms and those involving direct protein-protein interactions still need to be further investigated.

2.10 Calcium signaling

The regulation of Ca^{2+} signaling is crucial for cellular homeostasis and responses to extracellular stimuli. Ca^{2+} ions are the most common second messengers of eukaryotic cells. Ca^{2+} levels are finely tuned using a ubiquitous broad group of gene products: channels, pumps, transporters, and binding proteins (**Figure intro 13**).

Cell-to-cell signaling can be mediated through Ca^{2+}. Depolarization of the cell will activate voltage-gated Ca^{2+} channels (VGCC, CaV), Ca^{2+} rise being an intracellular signal mirroring neuronal electrical activity. Localized Ca^{2+} signals by VGCC control synaptic release by triggering vesicle fusion at active zones for neurotransmitter release (Sudhof, 2004; Schneggenburger and Neher, 2005). Ca^{2+} entry via neurotransmitter-gated Ca^{2+} permeant ion channels (such as NMDAR or GluA2-lacking AMPAR) lead to a local Ca^{2+} increase near the site of Ca^{2+} entry in the postsynaptic area, and can also initiate a cascade of events that can reach the nucleus and activate gene expression (Greer and Greenberg, 2008; Bading, 2013). An increase in cytosolic levels of Ca^{2+} activates kinases and phosphatases that affect the function and trafficking of various proteins, kinases, receptors and channels. Ca^{2+} entry can affect several Ca^{2+}-sensitive enzymes that convert changes in Ca^{2+} concentration ($[Ca^{2+}]$) into defined cell actions (Clapham, 2007; Giorgi *et al.*, 2018).

The Ca^{2+}-dependent signaling system is versatile and dynamic to ensure these vital roles. Since Ca^{2+} cannot be synthetized or destroyed, it requires a regulation of Ca^{2+} homeostasis.

2.10.1 Intracellular calcium homeostasis

The concentration of free Ca^{2+} in the cytosol ($[Ca^{2+}]c$) has to be maintained by cells to a 20,000-fold lower concentration between the intracellular (100 nM free) and extracellular (≈2mM) environments (Clapham, 2007). Indeed, minimal changes in $[Ca^{2+}]c$ are perceived as specific signals. Given the steep electrochemical gradient, increases in $[Ca^{2+}]c$ can be elicited by both Ca^{2+} entry from the extracellular space through plasma membrane channels and Ca^{2+} release from intracellular stores (Clapham, 2007; Giorgi *et al.*, 2018). The Ca^{2+} channels at the plasma membrane are of various types: VGCCs and nonvoltage-gated channels. VGCCs belong to the voltage-operated Ca^{2+} channel family and are activated by depolarizing membrane potentials, while nonvoltage-gated channels include ligand-gated channels such as NMDAR and GluA2-lacking AMPAR.

Storage in intracellular organelles: endoplasmic reticulum and mitochondria

This intracellular Ca^{2+} storage by the ER and Golgi apparatus have a critical role both in the maintenance of low $[Ca^{2+}]c$ in resting conditions and as a source of Ca^{2+} to be released by specific signals. Increased cytosolic Ca^{2+} levels can be further enhanced by Ca^{2+} release from intracellular stores mediated by the activation of IP3Rs on one hand, or CICR by ryanodine receptors (RyRs) on the other hand, and generate Ca^{2+} waves (Berridge, 1998). GPCR activation at the PM activates different isoforms of PLC that hydrolyze the PM lipid phosphatidylinositol-4,5-bisphosphate (PIP2) to generate (i) IP3, that will lead to the opening of IP3R, and (ii) DAG that will activate PKC.

Mitochondria can also accumulate high levels of Ca^{2+} that can be more than 20 times higher than those in the cytosol, leading to ATP production. This Ca^{2+} accumulation inside the matrix is achieved through the presence of juxtapositions with ER membranes (mitochondria-associated membranes, MAMs), an electrochemical gradient (≈-180 mV inside), and the mitochondrial calcium uniporter (MCU) complex (Marchi and Pinton, 2014).

Once the ER Ca^{2+} content is depleted, extracellular Ca^{2+} influxes through membrane channels restore the resting conditions of the ER [Ca^{2+}]. This mechanism is called store-operated Ca^{2+} entry (SOCE) (Stathopulos and Ikura, 2013). ATPase pumps such as Sarco/endoplasmic reticulum Ca^{2+}-ATPase (SERCA) pumps situated on the ER and the plasma membrane Ca^{2+}-ATPase (PMCA), as well as the NCX and NCKX exchangers, also pump out Ca^{2+} from the cytoplasm to re-establish basal Ca^{2+} levels (Clapham, 2007; Vandecaetsbeek *et al.*, 2011)(**Figure Intro 13**).

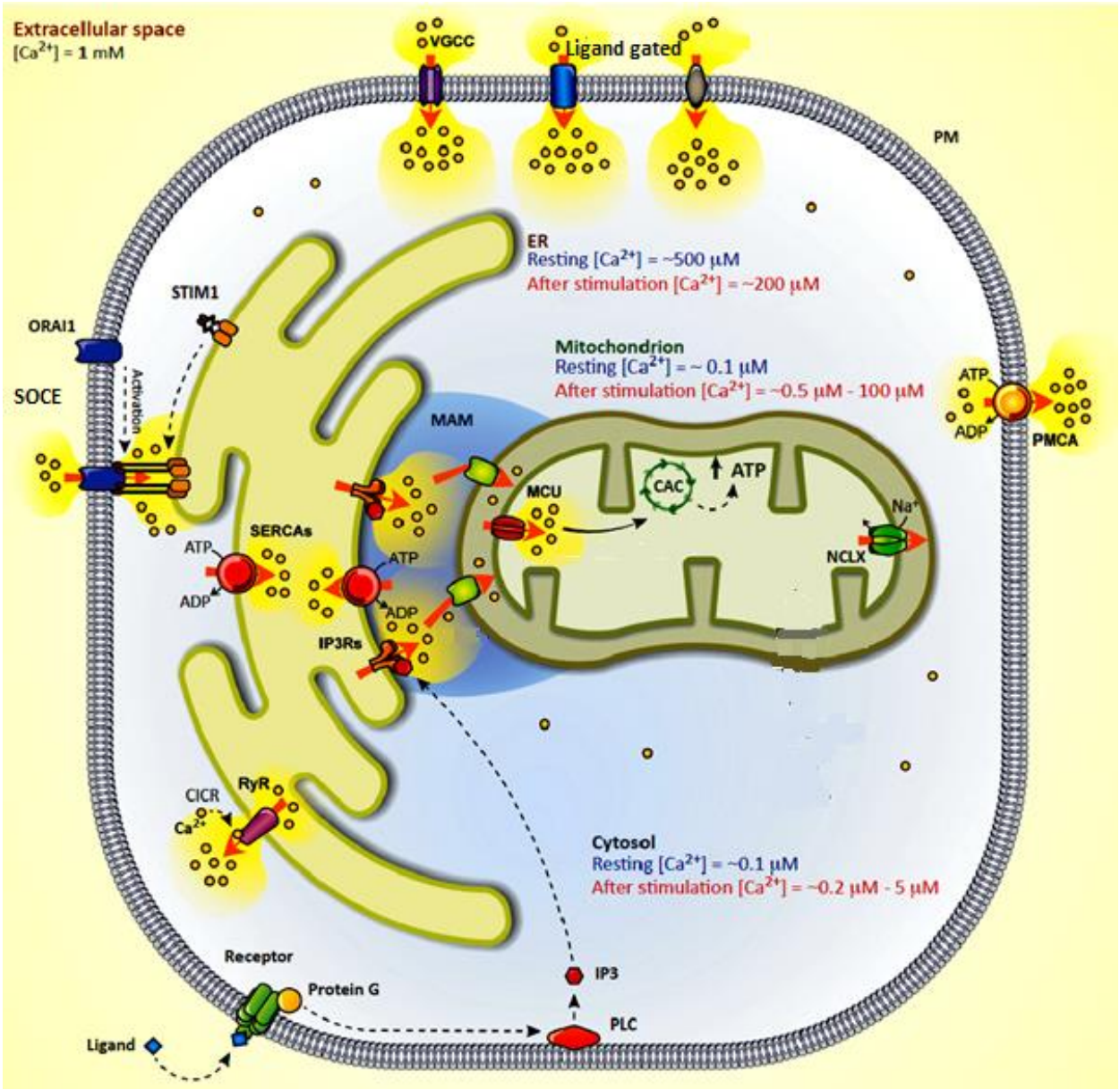

[Figure Intro 13: Intracellular Calcium (Ca^{2+}) homeostasis and signaling. Adapted from Giorgi et al 2018]

2.10.2 Regulation of intracellular Ca^{2+} in signal transduction

Ca^{2+} has a pivotal role as a second messenger of electrical signals in excitable cells (Santulli and Marks, 2015). In neural populations, the consequences of excessive Ca^{2+} signals vary according to their magnitude and duration and the type of neuron affected. Elevated Ca^{2+} is involved and required for striatal synaptic plasticity, sensitive to temporal and spatial patterns (Kim *et al.*, 2013). Synaptic transmission can result in elevated [Ca^{2+}]c levels via release from the ER or extracellular Ca^{2+} influx.

In the striatum, multiple levels of interactions with multiple neurotransmitters can trigger Ca^{2+} signaling. Indeed, direct entry of Ca^{2+} can occur through NMDAR or Ca^{2+}-permeable AMPAR or subsequent depolarization that triggers Ca^{2+}-entry through L-type VGCCs. Glutamate synaptic input on ionotropic receptors evoke EPSPs, that can generate an action potential if over threshold, that will backpropagate into the dendrites and cause the opening of VGCC through depolarization, and that will additionnaly increase NMDAR Ca^{2+} entry via relieving its Mg^{2+} block (Carter and Sabatini, 2004; Nevian and Sakmann, 2004; Bading, 2013; Plotkin *et al.*, 2013). A Ca^{2+} wave propagating through the sequential activation of IP3Rs along the dendrite can also be initiated through IP3 production from GPCR activation leading to mobilization of intracellular Ca^{2+} stores (Bading, 2013).

In SPNs, Ca^{2+} influx and propagation are tightly regulated. Back-propagating action potential, important for corticostriatal plasticity and adaptations to diseases such as PD, can evoke Ca^{2+} transients in the dendrites and spines, propagating more distally in D2-expressing iSPN than D1-expressing dSPN (Carter and Sabatini, 2004; Kerr and Plenz, 2004; Day *et al.*, 2008). More generally, increases in cytosolic Ca^{2+} arise from a number of sources including : (i) the above mentioned activations of PLC and PKC after GPCR activation, (ii) the direct entry via ionotropic glutamate receptors, (iii) but most of the Ca^{2+} influx comes from VGCCs, which open as the SPNs depolarize. The cooperative gating of clustered Ca^{2+} channels CaV1.3 (≈eight) could generate a more-persistent and greater Ca^{2+} influx (Moreno *et al.*, 2016).

Most isoforms of VGCCs are expressed in SPNs and are localized to distinct parts of the neuron. The Cav1 (L-type) and Cav3 (T-type) channels are less abundantly expressed than the Cav2 family of channels, including P/Q-, N-, and R-type channels, which have the highest level of expression (Hurley and Dexter, 2012). L-type (mostly Cav1.3), R-type, and T-type channels are mostly in SPN spines and shafts (Carter and Sabatini, 2004; Day *et al.*, 2006; Carter *et al.*, 2007). These channels are crucial for dendritic signal integration, generation of Ca^{2+} waves and corticostriatal plasticity in SPNs (Konradi *et al.*, 2003; Higley and Sabatini, 2008, 2010; Plotkin *et al.*, 2013; Warren EB, Sillivan SE, Konradi C, 2017).

2.10.3 Targets of intracellular Ca^{2+} in signal transduction and Ca^{2+} signaling in SPNs

Ca^{2+} entering through VGCCs or Ca^{2+}-permeable ionotropic NMDAR receptors activates second messengers including Ca^{2+}-calmodulin (CaM) (Faas *et al.*, 2011), Ca^{2+}/CaM-dependent protein kinases (CaMK) II and IV, phosphatases such as PP2B or calcineurin (Xia and Storm, 2005) and signaling proteins such as RasGRPs.

CaM, a 17 kDa protein, undergoes a conformational switch upon the binding of four Ca^{2+} ions. The quick buffering of Ca^{2+} by the soluble and cytosolic Ca^{2+} sensor Calmodulin (CaM) can prolonge its action through interaction with hundreds of target proteins, such as AC, CaMK II and the phosphatase Calcineurin (Clapham, 2007). CaM increases its Ca^{2+} affinity in the presence of target molecules (Swulius and Waxham, 2008). CaM thus captures transient Ca^{2+} signals and translates them into more prolonged signals. CaMKs are Ser/Thr kinases separated into two groups: multifunctional CaMKs [CaM kinase kinase (CaMKK), CaMKI, CaMKII, and CaMKIV], with multiple downstream targets, and substrate-specific CaMKs

(CaMKIII). At basal Ca^{2+} levels, CaMKs are inhibited by an autoinhibitory domain, which prevents substrate binding to the catalytic domain. Upon binding of Ca^{2+}-bound-CaM to CaMK, the autoinhibition of CaMK is relieved. CaMKs can be activated/phosphorylated by a CaMKK (Soderling, 1999). CaMKI is only expressed at low levels in the basal ganglia and does not seem to play a significant role in any specific signaling cascades. In contrast, CaMKII (predominantly the αCaMKII and βCaMKII isoforms) is expressed at very high levels in the striatum, ie in the SPNs, corticostriatal glutamatergic terminals, and dopaminergic terminals (Warren EB, Sillivan SE, Konradi C, 2017). CaMKII becomes hyperactive following striatal DA depletion, and its inhibition alleviates motor deficits in PD (Picconi *et al.*, 2004b; Brown *et al.*, 2005). Activation of CaMKs and particularly αCaMKII in SPNs can initiate multiple activations of various signaling cascades such as NMDAR-mediated LTP, SPN excitability and gene expression and phosphorylation of a number of activity-dependent transcription factors such as CREB for CaMKIV (Soderling, 1999; Picconi *et al.*, 2004b; Swulius and Waxham, 2008; Klug *et al.*, 2012; Wang *et al.*, 2017).

VGCCs are also one of many sites of interaction of cAMP and Ca^{2+} pathways (Konradi *et al.*, 2003): PKA phosphorylation slows VGCC inactivation, and PP2B-mediated dephosphorylation accelerates it (Budde et al., 2002; Evans et al., 2015). Dopamine also modulates VGCC conductances. In the striatum, D1R stimulation decreases N-, P/Q-type Ca^{2+} channel conductances via activation of PKA and DARPP-32 and increases L-type channel conductances (Surmeier et al 1995). D2R stimulation inhibits L-type Ca^{2+} channels (Hernandez-Lopez *et al.*, 2000).

Thus Ca^{2+} has a central role as a second messenger leading to multiple activations implicated in the transduction of multiple signaling cascades as mentioned above.

3- PD and striatal alterations in the absence of dopamine

3.1 Animal models of PD

The main feature of all forms of PD is the loss of dopaminergic neurons in the SNc. In most cases, this degeneration is associated with Lewy pathology consisting of Lewy bodies and Lewy neurites accumulating in the SNc neurons and neurons of other structures. Importantly, α-synuclein (α-syn) is the major component of the Lewy bodies. Its accumulation is considered a key player in PD pathogenesis. The progressive loss of the dopaminergic system in PD is not uniform, but rather follows a specific regional pattern that first involves the postcommisural sensorimotor putamen, followed by the caudate nucleus and more anterior associative regions of the putamen, while the limbic system-related ventral striatal regions are the least sensitive areas to DA denervation in PD (Damier *et al.*, 1999; Hornykiewicz, 2001; Dauer and Przedborski, 2003).

Animal models of PD provide valuable information at two levels: 1) to investigate the pathophysiogy of the disease and 2) to identify potential targets for disease intervention. But no existing animal model of PD recapitulates all the features of human pathology. The traditional models are based on the destruction of DA neurons by toxins, that is either the 6-hydroxydopamine (6-OHDA) in rats and mice, or 1-methyl-4-phenyl-1,2,3,6-tetrahydropyridine (MPTP) in non human primates (NHPs) and mice. These models induce selective and complete degeneration of SNc DA neurons but not the synucleopathy characteristic of the human disease. They have been proved useful in investigating the biological defects following the disappearance of the DA neurons, in developing symptomatic treatments for PD and in studying side effects associated with dopamine-replacement therapies such as LID (Cenci and Crossman, 2018). However, they are not as usefull to investigate disease-modifying drugs that can slow or halt degeneration process. The toxins act acutely and are rapidly killing DA neurons. They may not reflect those in PD characterized by synucleopathy and progressive loss in dopamine. More recent models have been developed to replicate the core, progressive, degenerative process driven by α-syn dysfunction. They consist of rodent transgenic lines that overexpress α-syn, viral vector-based overexpression of α-syn in rodents and NHP, and inoculation of various pathogenic α-syn protein aggregates. These various approaches lead to the development of synucleopathies with similarities to those seen in PD patients. They provide valuable reseach tools for discovery of drugs specifically targeting the neurodegenerative processes of PD.

Our research project focuses on the motor disorders in advanced PD and the side-effects of L-DOPA, which appear at even more advanced stages of the disease. These pathological processes result essentially from the loss of dopamine in the striatum. This is why I will focus the introduction on the present knowledge on the multiple levels of dysfunctions in striatal neurons caused by the disappearance of DA afferents. In addition during my work it was chosen to use the destruction of DA neurons by 6-OHDA as it represents a widely validated approach. It is widely validated to study the consequences of the loss of DA innervation in the striatum and to investigate the molecular mechanisms of therapeutic and harmful effects of L-DOPA treatment.

3.2 Striatal alterations in PD and dopamine deficiency

3.2.1 Alterations of basal ganglia loops

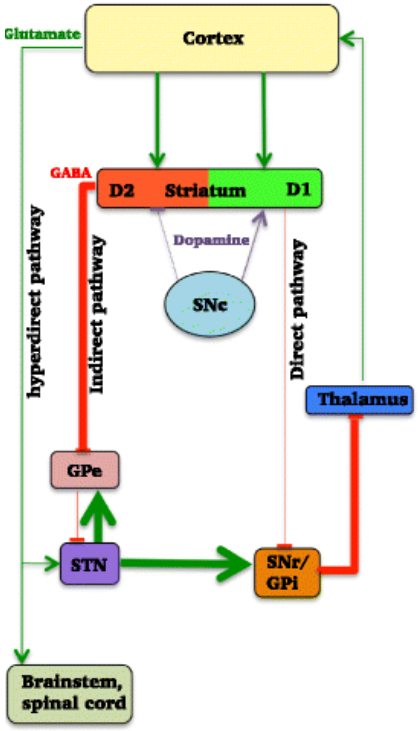

[Figure Intro 14. Model of alterations in the basal ganglia-thalamo-cortical motor circuit in the parkinsonian state.
*Degeneration of the SNc in early PD leads to decreased and increased activities in direct and indirect pathways, respectively (**from You, Mariani et al 2018**)]*

In PD, the loss of dopaminergic stimulation induces a dysfunction of the cortico-striato-thalamo-cortical loop, which is responsible for the motor symptoms with an overactive indirect pathway and an underactive direct pathway (Albin *et al.*, 1989; DeLong, 1990; Mallet *et al.*, 2006; Kravitz *et al.*, 2010) (**Figure Intro 14**). Because the indirect pathway normally inhibits unwanted movements, its overactivity may lead to the inhibition of wanted movements and previously learned motor routines. On the other hand, if direct pathway activity normally selects appropriate movements, its underactivity may additionally contribute to difficulties in initiating and performing movements in PD. Striatal DA depletion leads to enhanced iSPN output and decreased dSPN output, and a consequent decrease in activity in GPe and increase in GPi, as supported by results from studies in both animal models of PD (Filion and Tremblay, 1991; Mallet *et al.*, 2006) and in human PD patients (Obeso *et al.*, 2000). In line with this model, reducing activity in the indirect pathway by lesioning the STN alleviates the parkinsonian symptoms in MPTP-lesioned monkeys (Bergman *et al.*, 1990). Genetic deletions of specific subpopultations of either dSPN or iSPN also further support this model (Durieux *et al.*, 2009, 2012; Révy *et al.*, 2014). Optogenetic or chemogenetic stimulations of iSPNs elicit a parkinsonian state in mice (Kravitz *et al.*, 2010; Alcacer *et al.*, 2017). In addition, optogenetic or chemogenetic stimulations of dSPN rescue the parkinsonian deficits observed in mouse models of PD (Kravitz *et al.*, 2010; Alcacer *et al.*, 2017). The replacement of DA stimulation through exogenous L-DOPA restores the balance between direct and indirect pathways and the function of the basal ganglia system, improving motor symptoms. Taken together, this line of evidence establishes a critical role of bidirectional dysregulation of dSPNs and iSPNs in the motor defects of PD patients.

3.2.2 Alteration of SPN activity in human and non-human primates

The spontaneous activity of SPNs in normal animals is usually below 2 Hz and irregular with long periods of silence. Spiking with typical bursts is increased during movement execution. This activity pattern has been found consistently across intact rodents and NHPs (Crutcher and DeLong, 1984; Kimura *et al.*, 1992;

Wilson, 1993). DA depletion induces changes in SPN activity across species. Single cell recordings in the striatum of PD patients were performed during surgery for STN or GPi deep-brain stimulation (Singh *et al.*, 2016). SPNs of PD patients at rest were found spontaneously overactive, with a mean firing frequency of SPNs avering 30 Hz, much higher that other patient groups. In another study in advanced parkinsonian NHPs, the firing frequencies of SPNs in the baseline parkinsonian stage was averaging 28 ± 1.5 Hz in putamen and 23.5 ± 1 Hz in caudate (Liang *et al.*, 2008). The abnormally high activity of SPNs in PD patients at rest is also significantly patterned by brief spike bursts in a large proportion of units. In line with findings from imaging studies and magnetic stimulation in PD patients showing increased cortical activities, this hyperexcitability of SPNs has been hypothesized to be caused by a corticostriatal glutamatergic upregulation (Kojovic et al. 2015; Tang et al. 2010).

Following L-DOPA administration, in the transition to the ‘‘on’’ state (disappearance of parkinsonian symptoms), the firing rate of individual SPNs increases or decreases, with effects of approximately similar magnitudes (±13 to 15 Hz) (Liang *et al.*, 2008). Surprisingly, a higher proportion of SPNs (64%) increase their firing rates compared to the number of SPNs that respond with activity decrease (34%) which questions the mechanism underlying these responses, because not reflecting the approximate 50% repartition between D1-dSPN and D2-iSPN.

3.2.3 Alteration of SPN activity in rodents

In vivo studies have consistently shown that, on average, the discharge activity of unidentified SPNs is enhanced in 6-OHDA-lesioned rats (Schultz and Ungerstedt, 1978; Kish *et al.*, 1999; Chen *et al.*, 2001; Tseng *et al.*, 2001). Extracellular recordings in rats with unilateral 6-OHDA lesions show increased firing of SPNs averaging 5–12 Hz (Galarraga *et al.*, 1987; Tseng *et al.*, 2001; Kita and Kita, 2011). This could be attributed after DA depletion, as already suggested above in humans, to up-regulated corticostriatal glutamatergic inputs (Calabresi *et al.*, 1993; Tang *et al.*, 2001; Gubellini *et al.*, 2002; Picconi *et al.*, 2004a). Enhanced activity is characterized by recurrent bursting accompanied by numerous periods of spontaneous synchronization of striatal neuron activity, not seen in the controls (Raz *et al.*, 2000; Hammond *et al.*, 2007; Jáidar *et al.*, 2010; Zold *et al.*, 2012). Mallet et al (2006) observed that spontaneous activity of SPNs projecting to the SNr (dSPN) is decreased in DA-depleted striatum and that of SPNs without projection to SNr (presumably iSPN) is increased. In addition they showed that the absolute increase in the spontaneous activity of iSPNs greatly exceeded the decrease observed in dSPNs, providing an explanation to the general enhancement of firing rate observed in unidentified SPNs.

A decrease in the threshold current required to evoke responses to cortical stimulation has also been reported in SPNs after 6-OHDA lesion and shows an overall hyperexcitability of SPNs to cortical inputs (Nisenbaum and Berger, 1992; Florio *et al.*, 1993). Others have demonstrated that this increased responsiveness affects only iSPNs (Mallet *et al.*, 2006; Flores-Barrera *et al.*, 2010). They also described a pronounced decrease in the responsiveness of dSPN that was not seen in previous investigations, probably because DA depletion makes many of these dSPN completely silent. Conversely, dSPN responsiveness to cortical stimulation was found to be decreased by 10-fold. The one of iSPNs was reported to be increased and correlated with motor deficit in mice with extensive striatal DA depletion (Escande *et al.*, 2016). The responsiveness to thalamostriatal inputs was found affected similarly to the corticostriatal inputs in both types of SPN (Escande *et al.*, 2016). Hence, DA depletion inhibits the discharge activity of dSPNs and their responsiveness to cortical and thalamic inputs and enhances those

of iSPNs. Thus, these in vivo studies directly demonstrate the imbalance in dSPN and iSPN activities hypothesized by classical models of PD.

3.2.4 Alteration of SPN excitability

The long-term changes in firing rate and responses to excitatory inputs in the parkinsonian striatum could appear paradoxical given the homeostatic processes that should counterbalance these alterations. It is well established in numerous neuronal models that homeostatic plasticity processes keep average spike rate within a range, specific of a neuron. In neuronal networks, "the more things change, the more they stay the same" meaning those changes are necessary to stabilize neuronal and circuit activity (Turrigiano, 1999, 2012). Homeostatic plasticity with neuronal intrinsic and extrinsic changes should ameliorate the perturbations in SPN spiking that result from the loss of dopamine signaling.

Consistent with these principles, in iSPNs of DA-depleted striatum, hyperactivity maybe partially compensated by the loss of D2R signaling also leads to reduced intrinsic excitability over time. In parallel, loss of D1R signaling in DA-depleted dSPNs leads to compensatory elevation in intrinsic excitability (Fieblinger *et al.*, 2014a). But surprisingly the excitability of dendrites is unaffected in dSPNs while decreased in iSPNs. In addition, the strength of corticostriatal synapses is decreased in dSPN but increased in iSPN, in agreement with the results of in vivo recordings of SPN responses evoked by cortical stimulation. These results show that homeostatic plasticity could not completely compensate the deficits linked to the loss of DA inputs and the activity of both dSPN and iSPN remained disrupted despite these processes.

3.2.5 Morphological alterations of SPNs

- *Morphological alterations of dendritic trees*

Paper	Species	PD Model	Method to Distinguish SPNs	Visualization Technique	Spine Changes*
Suarez et al.	*Mouse*	6-OHDA Intrastriatal injection	dSPNs: BAC-*Drd1a*-tdTomato iSPNs: BAC-*Drd2*-eGFP	Lucifer Yellow-filling in fixed tissue Confocal microscopy	PD: ↓ Spine density in iSPNs and dSPNs LID: ↑ Spine density in iSPNs
Zhang et al.	*Rat*	6-OHDA MFB injection	SPNs not distinguished	Electron microscopy	PD: ↓ VGluT1-positive synapses LID: ↑ VGluT1-positive synapses
Zhang et al.	*Rat*	6-OHDA MFB injection	SPNs not distinguished	Golgi-Cox staining Brightfield microscopy	PD: ↓ Spine density LID: ↑ Spine density, ↑"mushroom" spines
Nishijima et al.	*Rat*	6-OHDA MFB injection	Retrograde labeling dSPNs: SNr-STR, iSPNs: GPe-STR	Lucifer Yellow-filling in fixed tissue Confocal microscopy	PD: ↓ Spine density in iSPNs LID: ↓ Spine density in dSPNs
Fieblinger et al.	*Mouse*	6-OHDA MFB injection	dSPNs: BAC-*Drd1a*-tdTomato BAC-*Drd1a*-eGFP iSPNs: BAC-*Drd2*-eGFP	Alexa dye-filling through patch pipette 2-Photon microscopy	PD: ↓ Spine density in iSPNs LID: ↑ Spine density in iSPNs, ↓ Spine density in dSPNs

*Downward arrows ↓, reduced compared to healthy control; upward arrows ↑, increased compared to PD (comparable to healthy control values).
6-OHDA, 6-hydroxydopamine; PD, Parkinson's disease; SPN, spiny projection neurons; dSPN, direct pathway spiny projection neurons; iSPN, indirect pathway spiny projection neurons; GPe, globus pallidus pars externa; LID, L-DOPA-induced dyskinesia; MFB, medial forebrain bundle; SNr, substantia nigra pars reticulata; STR, Striatum.

[Table 4: Spine changes in SPN in PD. From Fieblinger et al 2015]

Nigrostriatal degeneration in PD and subsequent loss of DA innervation induces complex morphological neuroadaptations in SPNs (Day *et al.*, 2006; Villalba and Smith, 2011). Striatal dendrites were reported to be affected in advanced PD, with dendritic atrophy and reduced overall dendritic length (McNeill *et al.*, 1988). These observations were largely confirmed later by other studies in PD patients (Stephens *et al.*, 2005; Zaja-Milatovic *et al.*, 2005). However, in these post-mortem studies, the causes of this atrophy of SPN dendrites in PD striatum could not be definitely established. Fieblinger et al (2014) showed in mice

that lesion of DA neurons was associated with a significant reduction in dendritic branching and total dendritic arbor length in both dSPNs and iSPNs. The reduction in dendritic length was 25% in dSPNs and 20% in iSPNs (Fieblinger *et al.*, 2014a). Remarkably, dendritic atrophy was not reversed by L-DOPA administration, which could explain why dendritic alterations were also detected in post-mortem studies in patients who were treated by L-DOPA for most part. The lack of reversion by L-DOPA suggests that dendritic atrophy is not caused by deficits in striatal DA release per se, but maybe from molecules co-released by DA terminals. Fieblinger et al suggest the brain-derived neurotrophic factor (BDNF) which is expressed in the DA neurons and known to promote dendritic growth in many types of neurons (Seroogy *et al.*, 1994; Baquet *et al.*, 2005).

- *Alterations of spine density*

A loss of spines has been reported several times in animal models and patients with PD (Stephens *et al.*, 2005; Zaja-Milatovic *et al.*, 2005; Villalba and Smith, 2011; Zhang *et al.*, 2013; Nishijima *et al.*, 2014; Suárez *et al.*, 2014)(**Figure Intro 15**; **Table 4**). The degree of striatal spine loss is closely correlated with the progressive striatal denervation pattern seen in PD, i.e. the most severely DA-depleted striatal regions in PD are more severely affected than the less DA-denervated regions (Zaja-Milatovic *et al.*, 2005; Suárez *et al.*, 2014). In the same way, an electrophysiological study of corticostriatal plasticity shows different results depending on the degree of DA depletion (Paillé *et al.*, 2010). Similar correlations have been also reported in NHPs (Villalba *et al.*, 2009; Villalba and Smith, 2011). As studies in PD patients, animal models of PD show a loss of spines across large populations of Golgi-impregnated striatal SPNs (Ingham *et al.*, 1989; Smith *et al.*, 2009; Villalba *et al.*, 2009; Zhang *et al.*, 2013). This general effect could mainly take place in iSPNs since it is well established that the iSPNs undergo spine loss following DA depletion (Day *et al.*, 2006; Smith *et al.*, 2009; Fieblinger *et al.*, 2014a; Nishijima *et al.*, 2014; Suárez *et al.*, 2014) suggesting a reduced synaptic convergence onto indirect pathway SPNs (Fieblinger *et al.*, 2014a)**.** At the same time, iSPNs exhibit increased firing rates (Mallet *et al.*, 2006), and increased excitability (Fino *et al.*, 2007) which suggests that this decrease in spine density may reflect a compensatory mechanism aimed at reducing overexcitation. DA is unlikely to be the only transmitter involved in this phenomenon. In vitro and in vivo data in rats, demonstrated that decortication prevents the loss of striatal spines induced by DA denervation, thereby suggesting that glutamate is another key determining factor of this pathology (Cheng *et al.*, 1997; McNeill *et al.*, 2003; Deutch *et al.*, 2007; Neely *et al.*, 2007; Garcia *et al.*, 2010). Elimination of spines in iSPNs is dependent on L-type Ca2+ channel (Cav1.3), suggesting that dysregulation of Ca^{+2} signaling could mediate this effect (Day *et al.*, 2006; Deutch *et al.*, 2007; Surmeier *et al.*, 2007).

The consequences of DA neuron loss on spine density on dSPN dendrites are more debated. One group (Suárez *et al.*, 2014) reported that dSPN dendrites lose spines after DA depletion whereas two other groups (Day *et al.*, 2006; Fieblinger *et al.*, 2014a; Nishijima *et al.*, 2014) observed no alteration in spine density following DA-denervationg lesion. Methodological approaches were not identical and this may explain this discrepancy (see (Fieblinger and Cenci, 2015)).

- *Alterations of spine morphology*

Morphological changes of asymmetric synapses consistent with increased synaptic activity in the DA-denervated striatum were reported in rodents, NHPs and humans (Ingham *et al.*, 1998; Meshul *et al.*, 1999; Meshul and Allen, 2000; Villalba *et al.*, 2009). It appears the remaining spines and their glutamatergic afferents from both corticostriatal and thalamostriatal inputs undergo an increase of the

size and length of the spine heads. This may support some of the electrophysiological data suggesting increased glutamatergic transmission at corticostriatal synapses in animal models of PD (Gubellini *et al.*, 2002; Calabresi *et al.*, 2007; Picconi *et al.*, 2012). However, these studies did not identify whether the SPNs belonged to the direct or indirect pathways. More recent studies indicated that the combination of spine loss and strengthening of remaining spines preferentially affected the iSPNs (Fieblinger *et al.*, 2014a). In contrast, the number of corticostriatal synapses onto dSPN dendrites appears unaffected by the DA lesion, but the strength of those synapses decreases on average. This study highlights the importance to further analyze the differential alterations of spine morphology specifically in dSPN and iSPN following the loss of dopaminergic neurons.

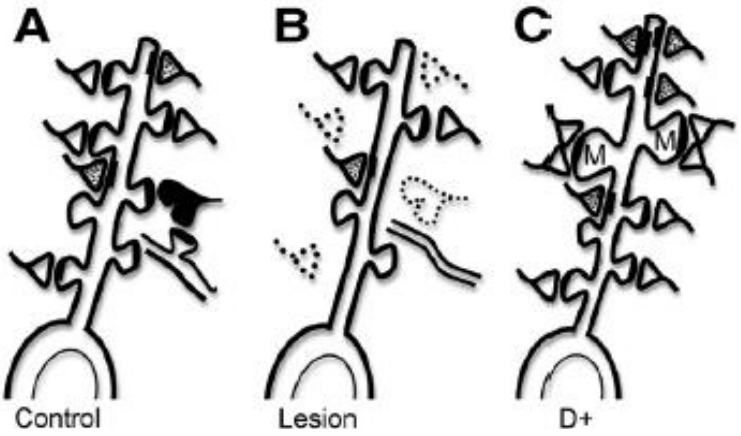

[Figure Intro 15 : Spine density in striatal SPNs**. After DA depletion (PD), the spine density in SPNs is decreased, more probably on iSPNs. Chronic L-DOPA treatment reverses the spine loss of PD selectively in D2-SPNs in mice showing dyskinesia with an aberrant increase in multisynaptic (mushroom) spines. **Adapted from Zhang et al 2013]

3.2.6 Alterations of synaptic plasticity

Regarding plasticity, a complete DA denervation abolishes both forms of corticostriatal plasticity (Calabresi *et al.*, 1992, 2007; Kreitzer and Malenka, 2007; Paillé *et al.*, 2010; Bagetta *et al.*, 2011). In fact, distinct degrees of DA denervation influence the two forms of plasticity: full DA denervation blocks the induction of both LTP and LTD, while partial DA depletion (≈75%) allows LTP induction but not its maintenance, leaving LTD induction and maintenance unaffected (Paillé *et al.*, 2010). In PD patients, LTP-like plasticity is deficient and restored by L-DOPA in non dyskinetic patients (Morgante *et al.*, 2006).

Other studies in genetically tagged SPN have explored the unbalance of striatal plasticity in the DA depleted situation. In D2-iSPNs, instead of LTD, LTP can be observed with a stimulus protocol that would normally induce LTD in intact striatum (Kreitzer and Malenka, 2007; Shen *et al.*, 2008). This shift from LTD to LTP may importantly contribute to the increased activity in the indirect pathway, ultimately resulting in excessive inhibition of movement. In contrast, it has been shown that direct pathway SPNs could exhibit LTD instead of LTP following DA-depletion (Shen *et al.*, 2008). Further studies are necessary to fully understand these complex synaptic changes.

3.2.7 Alterations of lateral inhibition between SPNs

Electrophysiological evidence indicates that SPNs receive collateral GABAergic inputs from other SPNs. Both dSPNs and iSPNs formed high-rate, one-way collateral connections with a homotypic preference (dSPN→dSPN or iSPN→iSPN) in the striatum. These collateral connections between SPNs were

dramatically downregulated in models of DA depletion mimicking PD (Taverna *et al.*, 2008). Although not found in all animal models of PD (Wei *et al.*, 2017). the attenuation of collateral inhibition among SPNs could have significant effects on striatal processing of excitatory input and diminished network control of synaptic plasticity. One of the main actions of collateral synapse is the regulation of backpropagating action potentials (bAPs) in SPNs (Plenz, 2003). The attenuation of shunting GABAergic synaptic activity could lead to enhanced bAP invasion of SPN dendritic trees and inappropriate alterations in the strength of glutamatergic synaptic connections. These alterations could be particularly important in iSPNs, whose excitability is elevated by DA depletion (Day *et al.*, 2006; Mallet *et al.*, 2006; Shen *et al.*, 2007). These adaptations of collateral synapses could be a major factor in the attenuation of differences between direct- and indirect pathway SPNs to repetitive cortical stimulation in PD models (Flores-Barrera *et al.*, 2010). Denervation changes the relation affecting the connections within a pathway and among the pathways, altering all the circuit dynamics (Carrillo-Reid *et al.*, 2008; Jáidar *et al.*, 2010).

3.3 Physiological and signaling alterations in SPNs in the absence of dopamine

3.3.1 Increase of D1R and D2R signaling in PD

In the DA-depleted striatum, direct pathway neurons display a supersensitive response to D1R stimulation by L-DOPA treatment or D1R agonists, which leads to abnormally high activations of cAMP/PKA pathway and ERK1/2/MAP kinase (Gerfen *et al.*, 2002; Pavón *et al.*, 2006; Santini *et al.*, 2007, 2009; Westin *et al.*, 2007; Darmopil *et al.*, 2009). These supersensitive responses lead to the induction of immediate early genes (IEGs), such as c-fos, FosB/ΔFosB or zif268 (Robertson *et al.*, 1990; Gerfen *et al.*, 1995; Steiner and Gerfen, 1996; Berke *et al.*, 1998; Cenci *et al.*, 1999; Bastide *et al.*, 2014; Heiman *et al.*, 2014a; Charbonnier-Beaupel *et al.*, 2015) via the activation of nuclear transcription factors, including Elk1 and CREB, the phosphorylation (and activation) of histone kinase proteins, such as MSK1 (Alcacer *et al.*, 2014), and the phosphorylation of histones such as histone H3 (Santini *et al.*, 2009).

This supersensitivity is not linked to an increase of D1R as their levels were found to be unchanged or lowered following DA denervation in animal models (Savasta *et al.*, 1988; Herve *et al.*, 1989; Missale *et al.*, 1989; Gerfen *et al.*, 1990; Hervé *et al.*, 1992; Pavón *et al.*, 2006; Hervé, 2011). Analysis in PD patients revealed no significant alteration in D1R expression in the striatal areas (Nikolaus *et al.*, 2009) but an increase in activation of AC by DA in the striatum (Pifl *et al.*, 1992; Tong *et al.*, 2004). Levels of Gαolf and Gγ7 were found to be increased in the brain of Parkinsonian patients and rodents after DA depletion (Hervé *et al.*, 1993; Marcotte *et al.*, 1994; Penit-Soria *et al.*, 1997; Corvol *et al.*, 2004; Alcacer *et al.*, 2012; Ruiz-DeDiego *et al.*, 2015; Morigaki *et al.*, 2017). However, this upregulation of the Gαolf protein levels is not associated with a parallel increase of the Gαolf mRNA expression. In line with a preponderant role of Gs/olf pathways, chemogenetic stimulation, with a DREADD approach, of dSPNs mimicks, while stimulation of iSPNs abolishes, the therapeutic action of L-DOPA in PD mice; with much stronger effects of DREADD Gs than Gq (Alcacer *et al.*, 2017). Accordingly, the homeostatic regulation of Gαolf protein levels is thought to occur through post-translational mechanisms in the striatum, where the altered expression of the Gαolf protein depends directly on its usage rate (Hervé, 2011). The persistent lack in the use of D1R and Gαolf could lower the Gαolf degradation rate and thereby could result in the accumulation of Gαolf protein in the DA-denervated striatum of PD models. In agreement with this hypothesis, works in D1R KO mice and A2AR KO mice showed a significant increase of the Gαolf protein levels without any changed expression of Gαolf mRNAs in the striatum of mutant mice

transcripts (Hervé *et al.*, 2001). The agonist-induced activation of D1R or $A2_AR$ might lead to the degradation of Gαolf proteins in striatal SPNs through a post-translational usage-dependent mechanism (Hervé *et al.*, 2001; Corvol *et al.*, 2004; Alcacer *et al.*, 2012; Ruiz-DeDiego *et al.*, 2015). These studies indicate that one of the main factors leading to sensitized AC responses to D1R stimulation is the increase of Golf levels in dSPNs. However, other mechanisms could also contribute to sensitized responses to D1R stimulation such as the lower internalization of D1R and increase in AC levels induced by DA depletion (Berthet *et al.*, 2009; Rangel-Barajas *et al.*, 2011). Following D1R activation, the cAMP/PKA/DARPP-32/PP1 pathway is necessary for the Ras/MEK/ERK pathway activation, probably in association with other signaling mechanisms, (Santini *et al.*, 2007, 2010; Lebel *et al.*, 2010; Alcacer *et al.*, 2012).

In patients with PD, the pattern of changes in D2R expression is extremely complex and is likely to depend on the stage of the disease, with a slight increase in D2R binding observed at the earlier stages and a decrease observed at the later stages (Beaulieu and Gainetdinov, 2011).

3.3.2 Alterations of cAMP and cGMP metabolism in PD

In patients and animal models of PD, impaired cyclic nucleotide levels have been reported (Volicer *et al.*, 1986; Sancesario *et al.*, 2004). In the denervated striatum, basal levels of cGMP were decreased and cAMP levels were increased (Sancesario *et al.*, 2004). The combine lacks of D1R-mediated stimulation and D2R-mediated inhibition on the cAMP production in the DA-depleted striatum could explain these findings. A down-regulation of the NO-cGMP pathway could also be involved regarding cGMP levels.

Levels of cAMP and cGMP also depend on PDEs that degrade them. In humans with PD, PDE mRNAs have been reported as decreased in the striatum, hypothalamus, thalamus and cortex for PDE4 (Niccolini *et al.*, 2017) and in the striatum and pallidum for PDE10 (Niccolini *et al.*, 2015; Heckman *et al.*, 2018). In PD patients taking DA replacement therapy, loss of striatal and pallidal PDE10 levels seems to be correlated with disease duration and severity, and its complications (Niccolini *et al.*, 2015). In the same way, in an animal model of PD, PDE10A transcripts were found to be reduced in striatal tissue after 6-OHDA lesion (Giorgi *et al.*, 2011). Further studies are necessary to determine how the down-regulation affects the specific dSPNs or iSPNs subpopulations. As presented above in the PDE subsection, in addition to the main Ca^{2+}-independent PDEs in the striatum PDE4 and PDE10A, Ca^{2+}–calmodulin-dependent PDE isoforms are also expressed, the most prevalent being PDE1B. An upregulation of PDE1B transcription was found in the striatum of 6-OHDA lesioned rats (Sancesario *et al.*, 2004). In line with this finding, some classic anti-parkinsonian drugs, such as deprenyl and amantadine inhibit PDE1A2 isoform and suggest a possible mechanism of their beneficial effects in PD (Heckman *et al.*, 2018).

Besides a potential symptomatic effect by further decreasing the degradation of cAMP, PDE inhibitors could also be tested as disease-modifying drugs since they seem to reduce neurotoxicity in experimental parkinsonism (Yamashita *et al.*, 1997; Yang *et al.*, 2008; Morales-Garcia *et al.*, 2011, 2015).

3.2.3 Alterations of glutamate transmission

Modifications of glutamate receptors were found following DA denervation in PD models.

Regarding NMDAR, the most proeminent changes observed in the DA-depleted striatum, are the changes in subunit composition of NMDAR at the glutamatergic synapse, in NMDAR subunit level at the cell surface and phosphorylation of specific subunits.

A reduction in the abundance of NR1 and NR2B proteins was found in the synaptic membrane

fractions, without significant alteration in the abundance of NR2A in both parkinsonian rodents and NHPs (Dunah *et al.*, 2000; Hallett *et al.*, 2005). Changes as increased GluN1 and GluN2B expression levels at the surface of striatal cells with a stable GluN2A surface expression were reported in 6-OHDA lesioned rats (Gan *et al.*, 2014). This leads to alterations of NMDAR subunit composition at the glutamate synapses in the DA-depleted striatum (Sgambato-Faure and Cenci, 2012; Mellone and Gardoni, 2013). Changes in synaptic NMDAR GluN2A/GluN2B subunit ratio in striatal SPNs correlate with the motor behavior abnormalities observed in a rat model of PD (Gardoni *et al.*, 2006; Mellone and Gardoni, 2013). More precisely, levels of GluN2B were specifically reduced in the absence of GluN2A alterations in synaptic fractions from fully-lesioned 6-OHDA rats (Picconi *et al.*, 2004b; Gardoni *et al.*, 2006; Paillé *et al.*, 2010). In addition, in the 6-OHDA model of PD, rats with a partial lesion of the nigrostriatal pathway (about 75%) showed a dramatic increase in the GluN2A immunostaining at the synapse without any modification of GluN2B (Paillé *et al.*, 2010). Overall these data indicate an increased GluN2A/GluN2B ratio at SPNs synapses at different stages of DA denervation in experimental rat models of PD. Dopamine denervation leads to modifications in the DA and Glutamate systems interactions among which interactions between receptors. Decrease in interactions between D1R and NMDAR were reported after DA-depletion and normalized by L-DOPA treatment only in non-dyskinteic animals (Fiorentini *et al.*, 2006). Stimulation of D1Rs also normalizes NMDAR subunit composition and improves motor behavior in a model of early PD (Paillé *et al.*, 2010). These findings underscore the importance of interactions between DA and Glutamate systems in regulating abnormal responses observed in PD.

Phosphorylations of NMDAR subunits also seem modified. The phosphorylation of GluN1 subunit at serine 890 and serine 896, but not at serine 897, was decreased in the membrane fraction (containing synaptic membranes) of lesioned striatum. In this fraction, the tyrosine phosphorylation of GluN2B but not GluN2A is decreased while globally the tyrosine phosphorylation of GluN2B is increased in crude homogenates of striatum (Menegoz *et al.*, 1995; Oh *et al.*, 1998). GluN2B total amount was unchanged. These data suggest changes in the subcellular localization of tyrosine-phosphorylated GluN2B. Interestingly, phosphorylation modulates the activity of NMDA receptors by modulating their electrophysiological properties as well as their localization at synapses (Chen and Roche, 2007).

In 6-OHDA-treated rats, mRNA levels of AMPAR subunits, GluA1 and GluA2, were found significantly higher in the DA-deafferented striatum (Tremblay *et al.*, 1995). But, such effects were not confirmed by another study which reported no significant changes in the dorsal striatum of 6-OHDA-lesioned rats (Kobylecki *et al.*, 2013). In MPTP-treated monkeys, GluA1 protein expression is markedly increased in caudate and putamen (Betarbet *et al.*, 2000). This effect is more pronounced in the striosomes, than in the matrix, suggesting that some discrepancies in literature could be related to the striatal regions evaluated. Further studies are needed to determine also if these changes occur in one or both types of SPNs.

3.2.4 Role of adenosine

In animal with 6-OHDA-lesions, persistent DA depletion per se has been shown to cause no apparent changes (Ballarin *et al.*, 1987; Herrera-Marschitz *et al.*, 1994; Nomoto *et al.*, 2000) or mild decrease (Pinna *et al.*, 2002) in the extracellular levels of adenosine in the lesioned striatum.

Roles of adenosine A1R in PD remain less investigated than those of adenosine $A2_AR$ which have been explored more extensively, in part due to the strategic selective localization of $A2_AR$ to the indirect output pathway from the striatum and their ability to control GABAergic, glutamatergic, and cholinergic

function. A recent positron emission tomography (PET) study with ^{11}C-MPDX found that A1R were not altered in early PD (Mishina *et al.*, 2017) and A1R antagonist have been reported not to improve motor symptoms in models of PD . Asymmetrical down-regulation of $A2_AR$s found in the putamen of early PD (Mishina *et al.*, 2011, 2017), which was normalized in advanced PD treated by L-DOPA (Martinez-Mir *et al.*, 1991), may likely be compensatory mechanisms in response to a decrease in DA and subsequent DA replacement therapy, because $A2_AR$ function is thought to be the opposite of D2R.

$A2_AR$ antagonists could reverse the altered motor function occurring in PD by various levels of action (Kase *et al.*, 2003; Mori and Shindou, 2003; Shindou *et al.*, 2003), among which important ones could be:

- First, antagonizing $A2_AR$ signaling could restore the brake on its excitatory modulation of iSPN pathway that was normally previously exerted by D2R signaling in the normal striatum without DA-denervation. Indeed, upregulated pallidal GABA levels and motor symptoms in the rat PD model were ameliorated by the $A2_AR$ antagonists (Koga *et al.*, 2000; Ochi *et al.*, 2000; Kelsey *et al.*, 2009).
- Second, disrupting $A2_AR$–D2R–mGluR5 hetero-oligomers activity could release D2R and increase its inhibitory signaling on iSPNs as suggested by results of combined modulations of $A2_AR$ and mGluR5 on D2R signaling (Coccurello *et al.*, 2004; Beggiato *et al.*, 2016).

The first-in-class adenosine $A2_AR$ antagonist istradefylline (KW-6002) was launched in Japan in 2013, as a result of preclinical and clinical studies (Hauser et al. 2008; LeWitt et al., 2008; Mizuno et al., 2010; Mizuno, Kondo, & the Japanese Istradefylline Study Group, 2013; Stacy et al., 2008). The effects observed in models of PD have been more or less the same for all selective $A2_AR$ antagonists studied (Morelli et al, 2009). In unilateral 6-OHDA-lesioned rats, the administration of $A2_AR$ antagonists alone might have some mild symptomatic action relevant to early PD but this is not observed with all $A2_AR$ antagonists tested (Rose et al 2007). When combined with L-DOPA or a DA agonist, adenosine $A2_AR$ antagonists potentiate their effect in PD patients and animal models of PD (Kase *et al.*, 2003; Pinna *et al.*, 2005; Rose *et al.*, 2007). Clinical studies showed also that $A2_AR$ antagonists significantely reduce the daily "off" time in patient treated with L-DOPA or other dopaminergic medications with no or "nontroublesome" increase of dyskinesia (Hauser *et al.*, 2008, 2011; LeWitt *et al.*, 2008; Mizuno *et al.*, 2013). These data suggest that $A2_AR$ antagonists could be used as adjunct therapy to L-DOPA in early PD patients where L-DOPA sparing strategies are most needed.

4- L-DOPA-induced dyskinesia

4.1 Clinical features

In spite of its spectacular improvement of the core motor symptoms, L-DOPA is far from an ideal drug, as it does not fulfil all the needs of patients. Particularly, the long-term outlook for PD patients is hampered by the occurrence of L-DOPA-induced motor complications, including motor fluctuations (ON-OFF problems) and dyskinesia (**Figure Intro 16**).

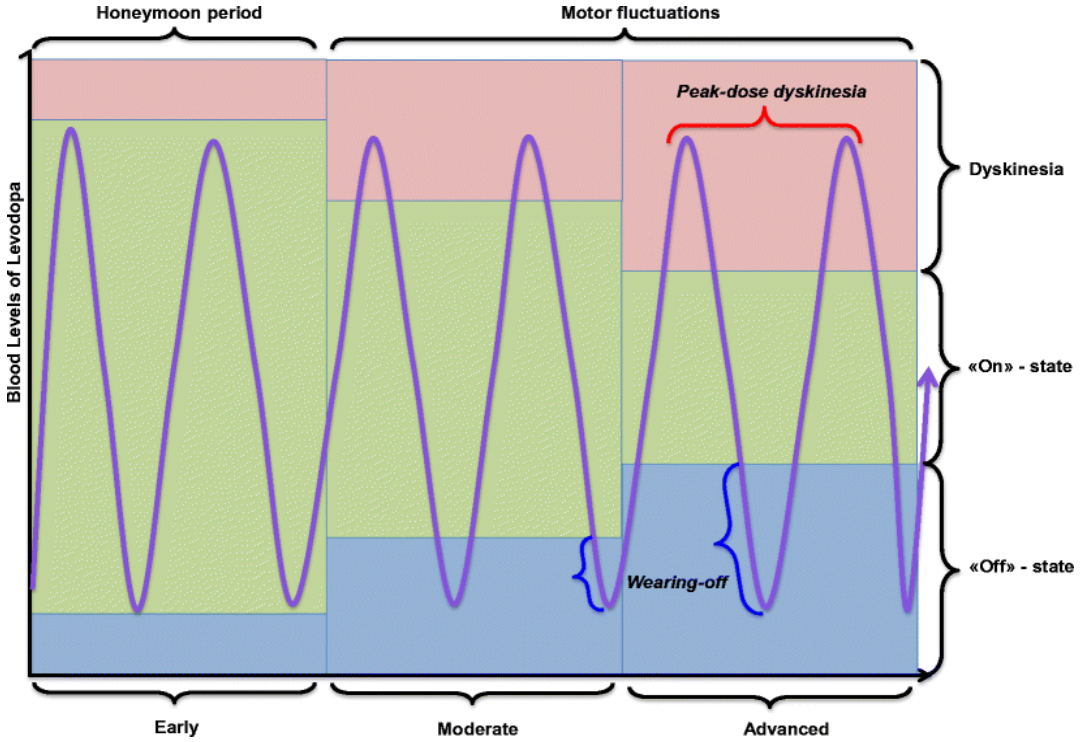

[Figure Intro 16: Motor complications in PD associated with levodopa. (from You, Mariani et al 2018) *During the honeymoon period, patients show no clinical motor fluctuations or LID when taking L-DOPA. As the neurodegenerations in PD progress, L-DOPA response fluctuations of the wearing-off and delayed-on types, as well as peak-dose and/or diphasic LID become more frequent narrowing the window of therapeutic efficiency of L-DOPA. This evolution could be also linked to fluctuations of L-DOPA blood levels due to disturbed intestinal absorption.**]***

Motor fluctuations are characterized by wearing-off, i.e., worsening or reappearance of motor symptoms before the next L-DOPA dose resulting in an 'off' state that improves when the next dose is taken ('on' state). Dyskinesias are abnormal movements of the limbs, trunk and face induced by the dose of L-DOPA. Dyskinesias are dystonic just after the administration and at the end of the dose (biphasic dyskinesia) and choreic at the peak of the dose. Motor fluctuations and dyskinesia affect virtually all patients but the delay in their occurrence is highly variable, affecting ~10% of patients per year. Dyskinesia has been reported to affect 30–50% of PD patients after 5 years and 70–90% after 10 years (Rascol *et al.*, 2000; Ahlskog and Muenter, 2001; Mazzella *et al.*, 2005). Beyond 10 years, more than 90% of PD patients have motor complications (Hely *et al.*, 1999; Mazzella *et al.*, 2005). PD patients not treated with dopaminergic drugs do not develop motor complications. On the other hand, long-term dopaminergic therapy in subjects without dopaminergic denervation does not induce motor complications.

Clinical risk factors of an early development of motor complications are a younger age at onset (Kostic *et al.*, 1991), longer disease duration and a more severe DA denervation (Lesser *et al.*, 1979; Schrag and Quinn, 2000; Fahn *et al.*, 2004; Schrag *et al.*, 2007). In addition, motor complications have been associated with higher dose and longer duration of L-DOPA treatment (Schrag and Quinn, 2000). Both the disease and dopaminergic therapy are thus required to develop motor complications but the question about the cause and the effect, hence the chicken and egg question, has led to decades of controversies and is still a matter of debate (Cenci, 2014). But in this case, it appears that the conjunction of two causes (lesion and L-DOPA) is required for the effect (dyskinesia).

LIDs involve a transient drug-induced excess of DA with predominance in the dorsal striatum in PD. They are associated with high L-DOPA levels in brain and plasma. L-DOPA has very low effect in the normal striatum but exerts a powerful effect in DA-denervated tissue. Neither gene changes nor LIDs are reported when L-DOPA or DA-agonist is given by continuous infusion. In contrast, repeated pulsatile administrations of L-DOPA lower dose threshold inducing LID and increase its severity (Morissette *et al.*, 1997; Lebel *et al.*, 2010). Hence pulsatile L-DOPA treatment is crucial in the genesis of LID in the supersensitive denervated striatum.

4.2 Model of basal ganglia circuit alterations in the dyskinetic state

In the dyskinetic state, L-DOPA pulsatile administration in the DA-denervated striatum with a predisposed supersensitive direct pathway in PD leads to (i) an overactivation of the direct pathway and (ii) and inhibition of the indirect pathway (Cenci, 2007; Cenci *et al.*, 2018) (**Figure Intro 17**). This imbalance of both pathways, in favor of hyperkinetic phenomenons, could be leading to LIDs.

Alterations in dSPNs could be critically involved in LID development since ablation of dSPNs impairs the arising of LID (Révy *et al.*, 2014). Moreover, a recent study, combining optogenetics and targeted recombination in active populations (TRAP) approaches, has shown that a distinct subset of dSPNs is causally involved in LID (Girasole *et al.*, 2018). However, chemogenetic stimulation of dSPN leads to the dyskinetic response to L-DOPA, only when it is associated with a D2R agonist administration, showing that both dSPN and iSPN are involved in severity of LID. Chemogenetic stimulation of iSPN was shown to reduce L-DOPA dyskinetic responses, demonstrating the modulatory role of iSPNs (Alcacer *et al.*, 2017).

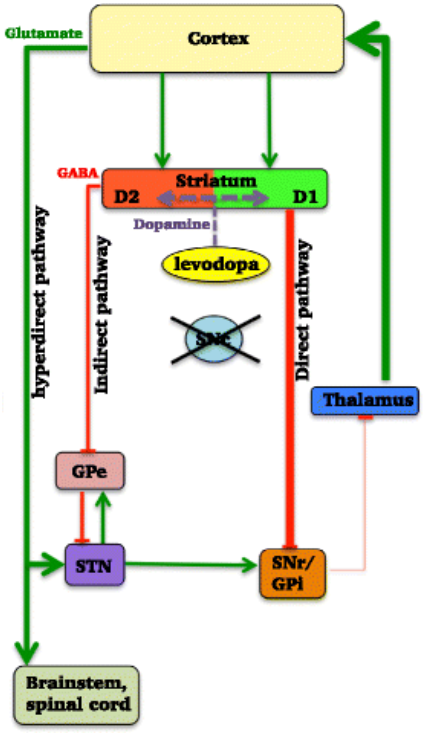

[Figure Intro 17. ***Model of the basal ganglia-thalamo-cortical motor circuit in the dyskinetic state.*** *In advanced PD with almost complete degeneration of nigrostriatal projections, L-DOPA substitutes for the lack of striatal DA. Hypersensitivity of D1R to DA produced from L-DOPA results in an increase in direct pathway activity* ***from You, Mariani et al*****]**

4.3 Postsynaptic and presynaptic mechanisms of LIDs

A large DA neuron lesion predisposes to LID via both presynaptic and postsynaptic mechanisms.

Following L-DOPA intake, perturbations in DA storage in the DA-denervated brain lead to transient large increases of DA extracellular levels (Abercrombie *et al.*, 1990; Meissner *et al.*, 2006; Lindgren *et al.*, 2010). Serotonin-associated mechanisms are also clearly crucial in LID, as they ensure DA synthesis from L-DOPA in the denervated brain and are at least partly responsible for the peaks of DA and LID (Carta *et al.*, 2007; Lindgren *et al.*, 2010).

Due to the degeneration of dopaminergic terminals and the dependence on intermittent dosing with exogenous levodopa, the pattern of normal tonic firing in nigrostriatal dopamine transmission changes to a phasic pattern. The surges of DA could transiently overactivate postsynaptic receptors with downstream changes in genes, proteins and neurotransmitter systems. At the postsynaptic level, the most widely documented consequence of DA denervation consists in a supersensitivity of DA receptor-dependent signaling and gene expression in striatal neurons (see below and review by (Jenner, 2008; Cenci and Konradi, 2010). In fact, basic research in animal models has shown that both presynaptic and postsynaptic factors contribute to the development of LID (Cenci and Lundblad, 2006).

4.4 Changes in structural and synaptic plasticity in LIDs

4.4.1 Morphological changes in LID

As discussed previously (see 3.2.5), an important remodeling of SPN morphology occurs in the DA-depleted striatum of PD patients and PD-model animals. One of the best-established changes concerns the loss of dendritic spines and glutamatergic synapses on iSPNs (Day *et al.*, 2006). After reintroduction of L-DOPA treatment, the initial post-lesion synaptic loss is followed by a restoration of corticostriatal synapses, associated with an increase of spine density on dendrites (Zhang *et al.*, 2013; Fieblinger *et al.*, 2014a; Nishijima *et al.*, 2014; Suárez *et al.*, 2014). Therefore, in LID state, there is a rewiring of corticostriatal, but likely not thalamostriatal, synaptic contacts onto iSPNs with an enlargement of striatal dendritic spines that receive cortical inputs (Zhang *et al.*, 2013; Nishijima *et al.*, 2014); **Figure Intro 15**). This restoration was partial in non dyskinetic rats, but increased to control levels in the iSPN of dyskinetic rats. However, synaptogenesis in dyskinetic rats involved the establishment of multiple inputs onto individual spines and the addition of inputs onto dendrites (**Figure Intro 15**). Therefore, it is possible that the reborned spines of iSPNs form abnormal synapses that contribute to dyskinesia. In contrast, L-DOPA treatment producing LID in 6-OHDA-lesioned mice was shown to decrease the dendritic density of spine in the dSPN (Fieblinger *et al.*, 2014a), this density being minimally affected by DA depletion alone. This loss in dyskinetic mice which is associated with reductions of number and strength of corticostriatal synapses could contribute also to dyskinesia development.

4.4.2 Changes of SPN activity associated with LID

In NHPs with LIDs, in vivo recordings show that the SPN firing response to DA that is observed after L-DOPA treatment at the onset of the ‘‘on’’ state is altered during the occurrence of dyskinesia (Beck *et al.*, 2018b). The frequency changes seen after L-DOPA administration are, at the time of dyskinesias, amplified in some neurons but decreased in others (Liang *et al.*, 2008). This pattern of response inversion is not found in under lower non dyskinesogenic doses of L-DOPA, thus, the inversion of DA responses seems specifically associated with LID (Liang *et al.*, 2008). Inversion of DA responses occurs in SPNs with

opposite responses to DA, and therefore, indicating that likely both pathways are involved in the mechanisms of dyskinesias (Beck *et al.*, 2018b).

4.4.2 Changes in synaptic plasticity associated with LID

Several forms of corticostriatal plasticity are modified in situation of LID. A large number of ex-vivo studies have shown altered plasticity (loss of LTP and LTD) at corticostriatal synapses as discussed in section 3.2.4 in PD models, but also including the complications induced by DA replacement treatment (Picconi *et al.*, 2003, 2008; Calabresi *et al.*, 2008; Fieblinger *et al.*, 2014a; Thiele *et al.*, 2014). LTP operates by positive feedback driving neuronal circuits toward maximal action potential firing, which can lead to synaptic saturation. Thus, the ability to "forget" or "ignore" irrelevant synaptic signals is critical to neurons to encode subsequent plastic changes. The main mechanism for synaptic forgetting is called "depotentiation". Synaptic depotentiation, results from the reversal of an established LTP by the application of low frequency stimulation (LFS) of corticostriatal fibers (O'Dell and Kandel, 1994). Interestingly, this ability to forget irrelevant synaptic signals is selectively lost only in dyskinetic animals chronically treated with L-DOPA, whereas non dyskinetic animals maintain the physiological reversal of synaptic strength after LFS (Picconi *et al.*, 2003). This lack of depotentiation might be due to abnormal RasGRF1-Ras- and DARPP-32-dependent ERK activation in dyskinetic animals which still needs further explorations (Picconi *et al.*, 2003; Cerovic *et al.*, 2015).

4.5 Molecular bases of LID

4.5.1 Role of D1R coupling to AC5 in LID

The hypersensitivity to DA of the denervated striatum is in part due to an increased coupling of D1R through increased levels of Gαolf (Corvol *et al.*, 2004). In addition, impaired D1R internalization and trafficking is also associated with LID (Guigoni *et al.*, 2007; Berthet *et al.*, 2009). Pharmacological or genetic inactivation of D1R reduces LID and decreases the associated molecular alterations (Westin *et al.*, 2007; Jenner, 2008; Darmopil *et al.*, 2009; Lebel *et al.*, 2010). A translational profiling study in the mouse has shown that LID is associated with multiple gene expression changes in dSPNs, whereas iSPNs show a more modest response (Heiman *et al.*, 2014a).

The DA-denervated striatum is associated with Gαolf and AC5 protein overexpression in striatal neurons, which correlate with dyskinesia severity in dyskinetic animals (Aubert *et al.*, 2005; Berthet *et al.*, 2009, p. 20; Rangel-Barajas *et al.*, 2011; Alcacer *et al.*, 2012). Both the G-protein-coupling efficiency and the trafficking of D1R tend to be normalized by chronic L-DOPA treatment, but only if the treatment does not induce LID (Aubert *et al.*, 2005; Fiorentini *et al.*, 2006; Berthet *et al.*, 2009). Several other studies found that the increased Gαolf levels in PD could be reduced by DA replacement with a daily exposure to L-DOPA in rodent models for PD with LID (Corvol *et al.*, 2004; Rangel-Barajas *et al.*, 2011; Ruiz-DeDiego *et al.*, 2015). More recently, in situ proximity ligation assay (PLA) disclosed cell-type specific changes in the Gαolf levels in close proximity to the D1R protein (D1R-Gαolf) or $A2_AR$ protein ($A2_AR$-Gαolf) in the DA-depleted striatum of mice with and without LID (Morigaki *et al.*, 2017). DA depletion caused a marked (≈90%) increase in the striatal levels of D1R-Gαolf, that is reduced by a daily administration of L-DOPA. However, there remained a significant (≈50%) increase in the striatal D1R-Gαolf in mice with LID when compared with normal controls. A daily treatment with L-DOPA, but not DA depletion per se, caused a significant (≈40%) decrease in the striatal A2AR-Gαolf in the DA-depleted striatum of mice with LID. Thus, in the DA-depleted striatum, DA replacement could blunt the increase of

Gαolf protein levels in dSPNs and reduce those in the iSPNs. The role of increase of Gαolf levels and cAMP signaling has been questioned by the lack of impairment of LID in mutant mice with reduced Gαolf expression (Alcacer *et al.*, 2012). However, in these experiments, both dSPNs and iSPNs are affected and it can not be ruled out that opposite effects in the two neuronal populations abraded the resultant effects.

4.5.2 Role of D1R-dependent ERK and PKA activations in LID

Following L-DOPA administration, D1R supersensitivity is mainly reflected by increased PKA-signaling pathways and aberrant overactivation of ERK signaling cascades. Regarding mechanisms mediating D1R supersensitivity, we mentioned previously the enhancement of D1R coupling and AC5. Other pathways can also be involved but out of the scope of the present PhD and will not be discussed in detail here.

In part as a consequence of increased D1R signaling, L-DOPA induces a strong phosphorylation of ERK that correlates with LID level (Santini *et al.*, 2007; Westin *et al.*, 2007). The ERK pathway appears to be important and causal for LID, as the occurrence of LIDs is prevented by genetic targeting of Ras/ERK signaling components or pharmacological blockade of ERK activation (Santini *et al.*, 2007; Lindgren *et al.*, 2009; Schuster *et al.*, 2009; Fasano *et al.*, 2010; Ding *et al.*, 2011; Cerovic *et al.*, 2015). Various observations suggest that different pathways may regulate D1R-dependent ERK activation in the intact versus the DA-denervated striatum (Valjent *et al.*, 2000; Gerfen *et al.*, 2002; Rylander *et al.*, 2009; Pascoli *et al.*, 2011a; Fieblinger *et al.*, 2014b). In heterozygous mice for Gαolf, L-DOPA-induced cAMP dependent signalling was attenuated while ERK activity and LIDs remained high, suggesting that the role of ERK is preponderant over that of canonical Gαolf-mediated signalling in inducing LIDs (Alcacer *et al.*, 2012). While acute L-DOPA treatment induces phospho-ERK in all DA-denervated animals, the response to chronic L-DOPA treatment differs significantly between dyskinetic and nondyskinetic animals. Rodents that develop dyskinesia respond to each dose of L-DOPA with a sustained phosphorylation of ERK, whereas nondyskinetic animals show a much-attenuated response (Pavón *et al.*, 2006; Santini *et al.*, 2007; Westin *et al.*, 2007). Hence, the core signaling abnormality in LID could consist of an inability to downregulate ERK activation upon repeated drug exposure. Direct coupling of D1R to ERK signalling is believed to play a crucial role in LID and a novel mechanism has been proposed in which the D1R-mediated ERK activation in the striatum is dependent on the formation of a signalling complex containing the protein tyrosine phosphatase Shp-2 that persists in dyskinetic animals (Fiorentini *et al.*, 2011, 2013).

PKA-mediated phosphorylation of several targets, such as DARPP-32 (Picconi *et al.*, 2003; Santini *et al.*, 2007) and GluA1 AMPAR subunit (Santini *et al.*, 2007; Alcacer *et al.*, 2012; Fieblinger *et al.*, 2014b) are increased and not normalized after chronic L-DOPA treatment (Tong *et al.*, 2004; Santini *et al.*, 2010). PKA activation is necessary to LID development (Lebel *et al.*, 2010). Hence, DARPP-32 phosphorylation is also increased and seems to be important for ERK activation and generation of LID, as they are both attenuated in DARPP-32 knockout mice (Santini *et al.*, 2007; Bateup *et al.*, 2010). Although, other authors have observed a persistent ERK phosphorylation in these mutant mice (Gerfen *et al.*, 2008). LID severity increases with DARPP-32 phosphorylation level (Picconi *et al.*, 2003; Santini *et al.*, 2007, 2010; Lebel *et al.*, 2010).

4.5.4 Role of gene transcription downstream ERK

Little is known about how the large striatal activation of ERK signaling produced by L-DOPA treatment leads to dyskinesia. Studies performed in animal models of LID have focused on nuclear signaling components downstream of ERK. Epigenetic mechanisms might contribute to the development of unwanted side effects in response to treatment with L-DOPA, as for instance, ERK phosphorylation is accompanied with strong phosphorylations of MSK1 and H3 in dSPN (Santini *et al.*, 2007, 2009; Alcacer *et al.*, 2014). Striatal histone modifications found in LID (Santini *et al.*, 2007; Nicholas *et al.*, 2008) are known to be involved in gene transcription. Changes in gene expression have been shown in both dSPNs and iSPN (Heiman *et al.*, 2014a), and some were confirmed in human postmortem studies such as for fosB/ΔfosB and pre-proenkephalin (Henry *et al.*, 2003; Lindgren *et al.*, 2011).

Some of these gene expression induced and implicated in LID were individually investigated. New strategies for pathway investigations and search for therapeutic targets using discovery-based approaches, such as DNA microarrays or proteomics methods, have also been used to investigate the molecular changes in animal models of LID. In a study by Konradi et al, the proeminent features of the mRNA expression changes associated to LID showed increased transcriptional activity in GABAergic neurons, structural and synaptic plasticity, altered calcium homeostasis and calcium-dependent signaling, and an imbalance between metabolic demands and capacity for energy production in the striatum (Konradi *et al.*, 2004). Several independent studies, revealed associations between LID and structural changes of neurons such as changes in gene expression involved in neurite outgrowth, synaptogenesis, and cell proliferation (El Atifi-Borel *et al.*, 2009; Lortet *et al.*, 2013; Fieblinger and Cenci, 2015). Further transcriptomics studies found several gene changes confirming ERK signaling and its targets as major markers of the response to LIDs, notably in D1R-SPNs (Heiman *et al.*, 2014a; Charbonnier-Beaupel *et al.*, 2015). Other changes like the upregulation of MAPK-signaling phosphatases suggested an attempt by these neurons to counteract the abnormally high activity of MAPK in LID. However, these homeostatic mechanisms fail to prevent several well-known genes induced by LID such as the jun and fos families (Heiman *et al.*, 2014a). Transcriptomics data from 6-OHDA-lesioned mice treated by L-DOPA identified the Nptx2 gene coding for Narp protein, whose L-DOPA-induced transcription is dependent on ERK activation and positively correlates with LID severity. Narp that binds to the extracellular surface of AMPAR at synapses and regulates their synaptic clustering, is causally linked to the development of LID, suggesting that changes in AMPAR activity are involved in the pathophysiology of LID (Charbonnier-Beaupel *et al.*, 2015).

4.5.4 Role of D2R signaling in LID

D2R involvement in LID has been less thoroughly investigated as it is not as clear and robust as for D1R involvement. The classic concept of imbalance in the activity of the two major striatal output pathways through over-activation by D1R and over-inhibition by D2R on the direct and indirect pathway, respectively, is in favor of further investigating D2R signaling implication. Pharmacological evidence shows that D2R agonists can induce LIDs (Jenner, 2008; Bastide *et al.*, 2015). As for D1R expression, D2R expression but also distribution do not seem to be affected by chronic L-DOPA treatment (Aubert *et al.*, 2005; Guigoni *et al.*, 2007). The role of the D2R is therefore often indirectly emphasized, through, for instance, the adenosine $A2_AR$ localized on iSPNs. An interaction between CaMKII and D2R, described in section 2.9.1, was shown to be enhanced in dyskinetic 6-OHDA-lesioned rats. Disruption of such interaction or inhibition of CaMKII reduces LID (Yang *et al.*, 2013; Zhang *et al.*, 2014). A more recent

study has investigated the two pathways contribution to different motor features using SPN type–specific chemogenetic stimulation in rodent models of PD and LID and has confirmed a role, not only of dSPNs, but also of iSPNs (Alcacer *et al.*, 2017).

4.6 Role of glutamate transmission in LID

4.6.1 Disruption of glutamate homeostasis in LID

Alternatives to current treatments that avoid LID may lie in nondopaminergic manipulations of basal ganglia, particularly the modulation of glutamate transmission (Verhagen Metman *et al.*, 1998a; Bibbiani *et al.*, 2005). More than 20 years ago, amantadine a glutamate NMDAR inhibitor has been shown to improve LID in animal models and PD patients and still has a preponderant place in the treatment of LID in 2018 (Verhagen Metman *et al.*, 1998b; Fox *et al.*, 2018).

Dysfunctions of glutamate transmission are implicated in PD, LID and other complications of L-DOPA therapy as indicated by molecular and corticostriatal synaptic plasticity modifications described in many previous studies (Sgambato-Faure and Cenci, 2012)(**Table 5 and see section 4.4.2**). Increased Glutamate recruits perisynaptic and extra-synaptic glutamate receptors whose activities are normally low under physiological conditions. Ionotropic receptor undergo changes in subcellular localization, subunit composition and phosphorylation (**Figure Intro 18**).

Indices of alteration	Species	LID
Extracellular glutamate	Rodent	Robelet et al. (2004), Dupre et al. (2011), Mela et al. (2011)
	NHP	ND
	Human	ND
Glutamate transporters	Rodent	Liévens et al. (2001) (GLT1); Robelet et al. (2004) (GLT1, VGLUT1,2), Konradi et al. (2004) (GLT1); Weiss et al. (2008) (VGLUT1,2,3)
	NHP	Rico et al. (2010) (VGLUT2)
	Human	ND
Glutamate receptors		
Expression or radioligand studies	Rodent	Oh et al. (1998) (NR2A/2B); Dunah et al. (2000) (NR1/2A/2B; GluR2/3); Konradi et al. (2004) (mGluR3,5, NR1); Gardoni et al. (2006) (NR2A/2B); Quintana et al. (2010) (NR2B)
	NHP	Hallett et al. (2005) (NR1/2A/2B); Hurley et al. (2005) (NR1/2B); Samadi et al. (2008) (mGluR5); Ouattara et al. (2010) (AMPA); Ouattara et al. (2011) (AMPA, mGluR5)
	Human	Calon et al. (2003) (NR1/2B, AMPA); Ahmed et al. (2011) (NMDA); Ouattara et al. (2011) (mGluR5)
Phosphorylation studies	Rodent	Oh et al. (1998) (NR1/2A/2B); Dunah et al. (2000) (NR1/2A/2B); Bibbiani et al. (2003) (GluR1); Gardoni et al. (2006) (NR2B); Santini et al. (2007) (GluR1); Quintana et al. (2010) (NR2B)
	NHP	Hallett et al. (2005) (NR1/2A/2B); Santini et al. (2010) (GluR1)
	Human	ND
Subcellular distribution studies	Rodent	Fiorentini et al. (2006) (D1/NR1/2B); Gardoni et al. (2006) (NR1/2A/2B); Gardoni et al. (2011) (NR2A/2B)
	NHP	Hallett et al. (2005) (GluR2/3; NR1/2A/2B); Silverdale et al. (2010) (GluR1,2/3)
	Human	ND

Abbreviations: ND; not determined; NHP; non-h

[Table 5: Altered glutamate transmission in LID. from Sgambato-Faure and Cenci 2012]

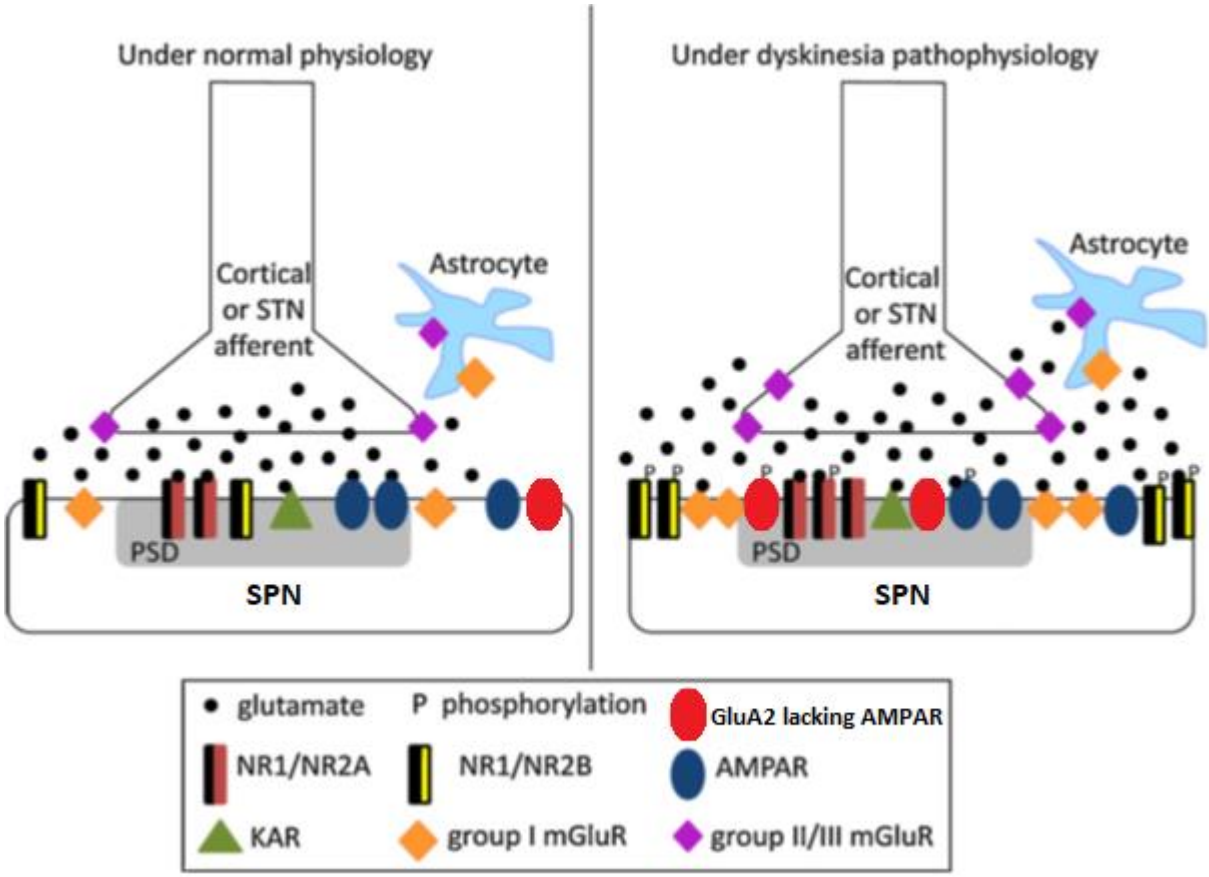

*[**Figure Intro 18: Some of the glutamatergic mechanisms involved in LID**.*
Drawings represent glutamatergic corticostriatal synapses with nearby astrocytes. Ionotropic glutamate receptors are mainly clustered in the post-synaptic density (PSD), whereas metabotropic receptors have a peri- or extra-synaptic localization. Under physiological conditions, glutamate stimulation remains largely confined to AMPA and NMDA receptors in the post-synaptic membrane. LID conditions result in changes in the subcellular localization, and phosphorylation state of ionotropic Glutamate receptors. Glutamate spillover from the synaptic cleft and/or glutamate release from astrocytes also cause a prominent activation of perisynaptic and extra-synaptic receptors. This effect concurs with. ***Adapted from Sgambato-Faure and Cenci 2012****]*

4.6.2 Role of AMPAR

Changes in phosphorylation levels of both AMPA and NMDA receptor subunits (Dunah *et al.*, 2004; Santini *et al.*, 2007; Fieblinger *et al.*, 2014b), subunit compositions (Hallett *et al.*, 2005; Gardoni *et al.*, 2006; Bagetta *et al.*, 2012) and subcellular localization (Silverdale *et al.*, 2010) have been reported in SPNs of dyskinetic animals.

Pharmacological blockade of AMPARs decreases LID and possibly enhances the antiparkinsonian effect of L-DOPA in animal models of LIDs (Konitsiotis *et al.*, 2000; Bibbiani *et al.*, 2005; Kobylecki *et al.*, 2010). More specifically, similar results were observed following administration of an antagonist of Ca^{2+}-permeable AMPAR IEM 1460 (Kobylecki *et al.*, 2010). Conversely, AMPAR agonists, alone or in combination with L-DOPA, triggered dyskinesias (Konitsiotis *et al.*, 2000). Specific radioligand binding to AMPARs was increased in the striatum of PD patients with LID and dyskinetic animals (Calon *et al.*, 2002, 2003; Ouattara *et al.*, 2010). These data suggest that an increased stimulation of AMPAR participates in

the pathophysiological adaptations of SPNs caused by DA depletion and chronic L-DOPA treatment and leading to LID.

The state of phosphorylation and intracellular trafficking of GluA1 seems to be altered in LID. As mentioned in section 4.5.2, In keeping with the increased phospho-DARPP-32 level, increased striatal phosphorylation by PKA of the Serine 845 of GluA1 is associated with LIDs. Phosphorylation of GluA1 on this residue promotes glutamate transmission by increasing open AMPA channel and surface expression (Banke *et al.*, 2000; Mangiavacchi and Wolf, 2004).

An altered trafficking of AMPAR in striatal neurons has been implicated in LID in a study performed in MPTP-lesioned monkeys (Silverdale *et al.*, 2010). Also an increased synaptic expression of AMPAR was suggested by the upregulation of Narp in LID (Charbonnier-Beaupel *et al.*, 2015). Chronically L-DOPA-treated dyskinetic monkeys showed a marked enrichment of the GluA2/3 subunit and trend for the GluA1 subunit enrichment, in a post-synaptic membrane fraction relative to a cytoplasmic vesicular fraction (Silverdale *et al.*, 2010). This GluA2 enrichement at post-synaptic membrane could be more specifically of the GluA2-flip splice variant as suggested by Kobylecki et al (2013). Increased expression of this specific splicing variant of the GluA2 subunit (GluA2-flip) may suggest slower desensitization and larger amplitudes of AMPA-mediated synaptic currents (Kobylecki *et al.*, 2013). The increased relative abundance of GluA2/3 in the post-synaptic membrane may render striatal neurons more sensitive to glutamate. In contrast with these results, an increased proportion of GluA2-lacking Ca^{2+}-permeable AMPARs at synaptic level were found in lesioned animals after either treatment by L-DOPA or high dose of the D2-agonist pramipexole (Bagetta *et al.*, 2012), which is in line with the results of Kobylecki et al (2010) mentioned above. This could be linked to abnormal NMDAR signaling as it is essential in GluA2 subunit internalization in physiological condition through the participation of the phosphorylation at the Tyr 876 residue of GluA2 by Src kinase (Hayashi and Huganir, 2004). Increased insertion of GluA2-lacking receptors could trigger "abnormal" cellular Ca^{2+} dynamics, related downstream pathways, and eventually pathological synaptic plasticity in a vicious cycle that would lead to the amplification of NMDAR dysfunction. Altogether, these data an important role for an altered AMPAR function in the striatal adaptations that are associated with LID, but it remains unknown as of to which SPN population(s) is (are) affected.

4.6.3 Role of NMDAR

As mentioned above, today, amantadine, a weak non-competitive NMDAR antagonist, represents the only clinically prescribed drug for the treatment of LID. Effects of amantadine have been taken as indications that NMDARs are involved in both parkinsonian motor symptoms and LID but one should keep in mind that amantadine can bind several other targets than the NMDAR and its effects are still modest.

Several studies performed in animal models of PD and LIDs have pointed at a possible important role of the NR2B subunit. Indeed high striatal levels of phosphorylation of the GluN2B subunit on the Tyr 1472 residue have been observed in several animal models of LID (Oh *et al.*, 1998; Dunah *et al.*, 2000; Hurley *et al.*, 2005; Quintana *et al.*, 2010). Increased GluN2B-containing NMDARs were reported in the putamen of dyskinetic PD patients and NPH (Calon *et al.*, 2002, 2003). However, GluN2B-selective antagonist' use in animal models of LID and motor fluctuations have produced variable results (Nash *et al.*, 2004; Nutt *et al.*, 2008; Rylander *et al.*, 2009). In the same way, in 6-OHDA lesioned mice, dyskinetic animals showed the same level of pGluN2B at Tyr-1472 residue as compared to controls (Mariani et al

unpublished personal data). In *knock in* Y1472F-GluN2B mice, where the residue 1472 is non phophorylable, increase of locomotor activity and ERK hyperphosphorylation induced by cocaine injection was not changed compared to wild-type controls (Mariani et al unpublished personal data). These data suggest that phosphorylation of the Tyr-1472 in GluN2B is not specifically responsible of ERK phosphorylation and LIDs generation and that other NMDAR changes are involved.

Altered trafficking of NMDA subunits between synaptic and extra-synaptic membranes also seems to play an important role (Gardoni *et al.*, 2006, 2012; Ahmed *et al.*, 2011). Studies in 6-OHDA-lesioned rats showed an association between LID and a reduction in the synaptic localization of NR2B (Fiorentini *et al.*, 2006; Gardoni *et al.*, 2006), with an increase in the GluN2A/GluN2B ratio in the striatal post-synaptic membrane (Hallett *et al.*, 2005; Fiorentini *et al.*, 2006; Gardoni *et al.*, 2006, 2011; Bagetta *et al.*, 2012). In organotypic cultures of SPNs, D1R activation facilitates the insertion of GluN2B-containing NMDAR in the postsynaptic membrane and vice versa which are tyrosine phosphorylation-dependent (Hallett *et al.*, 2006). Altered trafficking mechanisms may also affect NR1. Indeed, an association between dyskinesia and a loss of synaptic D1R/GluN1-GluN2B-containing receptor complexes was evidenced using striatal tissue from 6-OHDA-lesioned rats chronically treated with L-DOPA (Fiorentini *et al.*, 2006). Thus, the super-sensitization of the D1R could at leat partly lead to the abnormal trafficking of glutamate receptors observed in LIDs.

4.6.4 Role of mGluR5:

mGluR reprensent attractive pharmacological targets for the treatment of PD and LID due to their ability to modulate the actions of both glutamate and DA without blocking fast excitatory neurotransmission (Gasparini *et al.*, 2013; Sebastianutto and Cenci, 2018).

Multiple preclinical and clinical studies have pointed group I mGluR antagonism as promising to improve motor function and reduce LID and in particular by pharmacological blockade of mGluR5 receptors (Reviewed in (Rascol *et al.*, 2014; Litim *et al.*, 2017; Sebastianutto and Cenci, 2018). These studies were supported by previous findings of upregulation of mGluR5 in LID. Increased striatal expression of mGluR5 has been found in relation to L-DOPA treatment and LID (Samadi *et al.*, 2008; Ouattara *et al.*, 2010; Jourdain *et al.*, 2015). In addition to reducing LID, selective mGluR5 antagonism can attenuate molecular changes associated with LID, such as the hyperactivation of ERK and other markers related to either D1R or D2R signaling (Levandis *et al.*, 2008; Rylander *et al.*, 2009; Morin *et al.*, 2014). In animals with 6-OHDA lesions, the D1R-mediated induction of ERK in striatal neurons seems dependent on the activity of mGluR5, but independent of NMDAR (Rylander *et al.*, 2009; Fieblinger *et al.*, 2014b). Togother these data support a strong involvement of mGluR5 in the regulation and crosstalks between DA and Glutamate systems leading to LIDs.

4.7 Role of PDEs

The pharmacological manipulation of PDE signaling pathways is complex and its relationship with LIDs is not completely understood. Systemic or intra-striatal injections of inhibitors of PDEs 5, 6 and 9 improve LID (Giorgi *et al.*, 2008; Picconi *et al.*, 2011). Interestingly, inhibition of these PDE in the striatum can rescue the LTD at corticostriatal synapses that was lost in LID (Picconi et al 2011).

Knowing that LIDs are characterized by over-inhibition of D2R-dependent cAMP pathway, PDE10A inhibitors biased towards iSPN could promote antidyskinetic effects by increasing intracellular cAMP levels and restoring LTP in striatopallidal MSNs, releasing this pathway from over-inhibition during

LID. A selective PDE10A inhibitor has been recently shown to reduce LID in MPTP-macaques without affecting the therapeutic antiparkinsonian action of L-DOPA and with a larger anti-LID effect than amantadine (Beck *et al.*, 2018a). In addition, the inhibition of PDE10A by another inhibitor, TP-10, dose-dependently reduced LID in 6-OHDA-lesioned rats (Padovan-Neto and West, 2017). However, another study using papaverine that inhibits efficiently PDE10A, among other PDE inhibitors, did not confirm the amelioration of LID in the 6-OHDA model (Sancesario *et al.*, 2014). Even though a loss of PDE10A is observed in PD (see 3.3.2), there does not seem to be a difference of expression between dyskinetic and non dyskinetic animals (Sancesario *et al.*, 2014). It is not clear if this effect is part of the underlying pathology causative for the symptoms or if it is an adaptive change due to reduced cyclic nucleotide levels that would attenuate the symptoms. Further studies are needed to evaluate a potential beneficial effect of PDE10A or other PDEs inhibition in LID.

4.8 Role of adenosine in LIDs

The role of the $A2_AR$ in LID has been extensively examined. PET imaging studies generally suggested that dyskinesia might involve adenosine $A2_AR$. Studies in patients with PD demonstrated that the putaminal density of adenosine $A2_AR$ was increased in patients with dyskinesia (Calon *et al.*, 2004; Mishina *et al.*, 2011; Ramlackhansingh *et al.*, 2011) and that there was no significant difference between *de novo* PD patients and normal controls (Mishina *et al.*, 2011). Similar effects were observed in dyskinetic animals from NPH and rodent models of PD (Morelli *et al.*, 1994; Pinna *et al.*, 2002; Tomiyama *et al.*, 2004; Morissette *et al.*, 2006; Zhou *et al.*, 2017).

The $A2_AR$ seems to play a crucial and functional role in the modulation of motor behavior and its inhibition can also reduce LID (Fredduzzi *et al.*, 2002; Chen *et al.*, 2003; Xiao *et al.*, 2006, 2011). Indeed, blockade of $A2_AR$ attenuates LID and the morphological alterations of corticostriatal synapses induced by L-DOPA (Huang *et al.*, 2011). Several behavioral studies in animal models and in PD patients have showed the beneficial effects of $A2_AR$ antagonism in treating or delaying LID (Fredduzzi *et al.*, 2002; Bara-Jimenez *et al.*, 2003; Bibbiani *et al.*, 2003; Chase *et al.*, 2003; Uchida *et al.*, 2015)(non exclusive list). This would suggest that adenosine $A2_AR$ antagonists may have a role in the early treatment of PD not only for symptomatic improvement but also for dyskinesia prevention. Monotherapy of istradefylline, in drug-naïve PD patients improves parkinsonian symptoms without provoking LID (Fernandez *et al.*, 2010). In PD patients, a meta-analysis comparing istradefylline 40 mg with placebo concluded to a significant reduction in dyskinesia (Zhu *et al.*, 2014). But there was no difference in case of 20 mg istradeffyline. Preclinical and many clinical studies of istradefylline also suggest that $A2_AR$ antagonists may not improve dyskinesia when coadministered with L-DOPA (Hauser *et al.*, 2008, 2011; LeWitt *et al.*, 2008; Mizuno *et al.*, 2013) (non exclusive list). Thus, despite the numerous preclinical and clinical studies performed, it is still difficult to conclude regarding the beneficial effect of A2AR antagonism in LID. Discrepancies may be due to the protocols used such as the dosage of the drugs.

$A2_AR$ and mGluR5 were also shown to interact in iSPNs and to reduce the affinity of D2R in the striatum (Ferré *et al.*, 1999, 2002). Studies suggest that the striatal $A2_AR$–D2R–mGluR5 multimeric receptor complexes are involved in the striatal plasticity and could be relevant for the management of PD and LID (Ferré *et al.*, 2002; Fuxe *et al.*, 2003; Morelli *et al.*, 2007).

5- Introduction to biosensor live imaging

The recent development of Föster resonance energy transfert (FRET)-based biosensors and genetically encoded Ca^{2+} indicators (GECIs) coupled to two-photon imaging, has allowed for a novel approach of signaling pathway activity monitoring, providing data with a temporal resolution of less than a second to hours in living neurons at the cellular and even subcellular level, opening a new avenue to understanding the integration processes in space and time.

Ca^{2+} dynamics and kinases activity, like many other cellular signals, take place in the complex multidimensional space of the living cell. The temporal dimension is obviously a critical one, as the signal rises following a stimulus and then declines over time as the stimulus is removed and/or feedback mechanisms cause the signal to revert towards baseline. The spatial dimension also plays a role since the concentration of signaling molecules decreases with distance. Protein-protein interactions maintain all partners of the signaling cascade in close proximity in so-called signaling microdomains. In addition to these factors, the geometry of the cell can affect signal integration, with a high surface to volume ratio favoring the accumulation of substrates and the activation of kinase in thin dendrites versus the cell body (Neves *et al.*, 2008; Li *et al.*, 2015). Therefore, since temporal and spatial measurements are of critical importance to the understanding of intracellular signaling, direct imaging of Ca^{2+} dynamics and cAMP/PKA and ERK signaling cascades is a highly desirable approach.

To visualize and quantify intracellular events with a good spatial and temporal resolution, various methods based on fluorescence have been developed. Historically, the first fluorescence-based techniques, such as immunohistochemistry (IHC), have allowed visualizing and locating specific cellular components in fixed tissues and cells. But using phosphoproteins specific antibodies can only give an image of the enzymatic activity at specific time points. Experiments performed at various time points were used to improve temporal characteristics but even with this approach, temporal resolution remains low and the temporal information comes from different samples. This is why dynamic imaging was developed, following the time course of a biological signal thanks to fluorescence variations (Moore *et al.*, 1990; Roe *et al.*, 1990; Zhang *et al.*, 2002; Miyawaki, 2003b; Yasuda, 2006).

Fluorescent biosensors are a class of artificial proteins made of one or more fluorescent proteins and a sensitive domain to a specific biological signal of interest. This biological signal will induce a change in the optical properties of the proteins, which will be detected by optical imaging. The genetically encoded biosensors are exclusively made of amino-acids that will allow them to be expressed in most of the cell types. Their non invasive introduction in the cells has the great advantage of keeping the cell membrane intact. Adding target domains or point mutations allows optimizing the properties of the sensors and targeting them to specific cell subtypes or cell compartments.

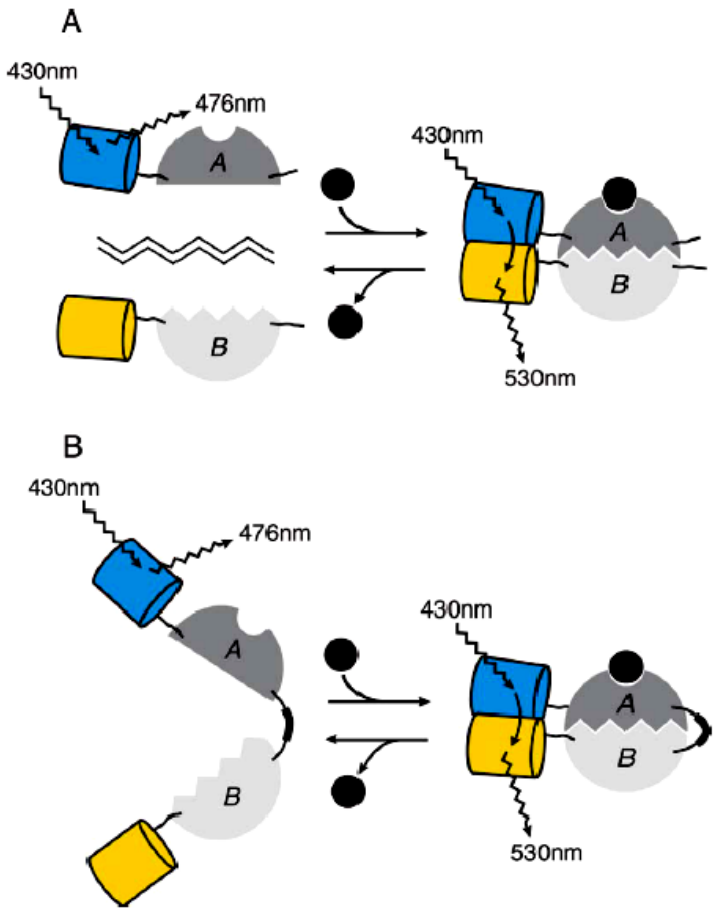

*[**Figure Intro 19. Basic Designs of Fluorescent Indicators Employing GFP-Based FRET***
***A.** The basic principle of bimolecular fluorescent indicators. CFP and YFP are fused to domains A and B, respectively, which interact with one another depending upon the ligand binding or modification of domain A. There are many variations in the design; CFP and YFP can be swapped, or signal-dependent dissociation of two domains can be used. Incoming and outgoing saw-toothed arrows indicate excitation and emission at the stated wavelengths.*
***B.** The basic design of unimolecular fluorescent indicators. **from (Miyawaki, 2003a)**]*

5.1 FRET principles

FRET relies on fluorescence resonance energy transfer described by Förster in 1948. The energy is transfered without any light emission from an excited fluorophore (donor) to a non excited fluorophore (acceptor). The acceptor is then excited and relaxation occurs emitting a photon at its own longer wave length (**Figure Intro 19**). This transfer of energy will result in a reduced fluorescence of the donor and an increased fluorescence of the acceptor. Various parameters are important for the energy transfer to happen. The emission spectrum of the donor must overlap the absorption spectrum of the acceptor. The efficiency of FRET strongly depends on the orientation and the distance between the donor and the acceptor, typically between 10 and 100 A° (Forster and Haas, 1993; Bastiaens and Pepperkok, 2000; Wouters and Bastiaens, 2001; Jares-Erijman and Jovin, 2003; Nagai *et al.*, 2004), making this phenomenon a useful tool for monitoring interactions between proteins that are fused to fluorophores (Miyawaki, 2003a; Umezawa, 2005).

Because FRET increases acceptor fluorescence and decreases donor fluorescence, the ratio between the fluorescence intensities in the donor and acceptor emission wavelengths is often used to measure FRET (Wallrabe and Periasamy, 2005). Ratiometric quantification of these sensors, composed of two fluorophores is another advantage. Indeed, in sensors with only one fluorophore, such as chemical Ca^{2+} sensors like fluo-3, changes in fluorescence are measured at a unique wave length. But these changes can be due to multiples artifacts: technical (excitation light intensity fluctuations, focal point drifting), linked to the cell (cell volume variations hence concentration of the indicator) or biosensor (quenching, photobleaching). Hence, if the measurement is done on two wave length, as for FRET biosensors, the confounding factor similarly modifies the fluorescence for both fluorophores which allows correcting these artifacts. Other concerns have to be addressed such as specificity of the signal or lack of cell physiology disturbances by the probe (buffering effect for instance).

A major breakthrough in this field resulted from the creation of FRET-based genetically encoded optical sensors, the first sensors being designed to report Ca^{2+} (Miyawaki *et al.*, 1997; Romoser *et al.*, 1997), eventually leading to sensors for various other biological signals. Since the first FRET-based Ca^{2+} sensors were developed (Miyawaki *et al.*, 1997), a number of genetically encoded FRET sensors of signaling have been created (most of them use FRET between eCFP and eYFP). For example, a class of kinase activity reporters has been produced, which consist of four linked components: a donor, a specific kinase target polypeptide, a phosphoamino-acid binding domain, and an acceptor (Ni *et al.*, 2006). Phosphorylation of the kinase target polypeptide causes binding between the kinase target polypeptide and the phosphoamino-acid-binding domain, thereby altering the FRET efficiency between the donor and the acceptor. Another class of kinase activity reporter uses fluorescent proteins tagged to both ends of the kinase to measure the conformational change of the kinase that occurs when the protein is activated (Takao *et al.*, 2005; Ni *et al.*, 2006). Most of these sensors are optimized for ratiometric imaging. Because FRET efficiency is sensitive to the distance and the angle between the two fluorophores, it depends on the length and the rigidity of the linkers connecting fluorophores and target proteins as well as the location of the fluorophore within the target protein (Miyawaki, 2003a). These parameters have to be optimized empirically (Miyawaki, 2003a). The optimum FRET efficiency is 100% for ratiometric imaging (Yasuda, 2006). Some limitations of biosensor imaging include sensitivity to photobleaching, pH and temperature, and it is therefore desirable to use the brightest as well as the most stable fluorophores in biosensor constructs.

5.2 An historical perspective on fluorescent probes

Aequorine, a bioluminescent protein discovered in the jellyfish Aequorea Victoria, was extracted and purified in 1962 (Shimomura *et al.*, 1962) and allowed reporting the first Ca^{2+} signals on muscular fibers (Ridgway and Ashley, 1967). While chemical Ca^{2+} sensors were developed giving a better temporal resolution and stronger signal intensity than Aequorine, leading to multiples breakthrough in the knowledge of intracellular Ca^{2+} dynamics. These chemical sensors only allowed for ion monitoring but not complex signal pathways. R. Tsien's team created a sensor for cAMP based on monitoring the dissociation of subunits of a recombinant PKA (Adams *et al.*, 1991). This biosensor called FlCRhR was used in invertebrate neurons (Bacskai *et al.*, 1993; Hempel *et al.*, 1996) and embryonic spinal neurons (Gorbunova and Spitzer, 2002). However, this first biochemical sensor remained impractical to use in vertebrate mature neurons because the recombinant and labeled holoenzyme had to be injected into

living cell, which proved to be a difficult task because needing a mechanical introduction in the cell through a microinjection or a patch pipet (Goaillard *et al.*, 2001; Vincent and Brusciano, 2001). This led to the wide use of fluorescent molecules, extracted from the jellyfish, easily introduced in the cells through a transgene (Ormö *et al.*, 1996; Shimomura, 2009). A short time after the publication of the sequence of the green fluorescent protein (GFP)(Prasher *et al.*, 1992), GFP mutants were created (Tsien, 1998). These mutations of GFPs generated had diverse overlapping excitation and emission spectra, and allowed to combine two different fluorophores hence suitable for FRET imaging. The eCFP–eYFP pair is the most popular for ratiometric imaging. After 1997 first GECIs, multiples kinases activity reporters were then created using the same structure, such as AKAR, CKAR and EKAR (Miyawaki, 2003a; Harvey *et al.*, 2008) and reporters protein tyrosine kinase activities such as Src, Abl and EGFR (Ting *et al.*, 2001). During the last two decades, a wide range of biosensors have been developed for monitoring various activities ranging from neurotransmitters such as glutamate (Dulla *et al.*, 2008; Marvin *et al.*, 2013), small molecules like "perceval" measuring the ratio of ATP/ADP (Berg *et al.*, 2009), for IP3 biosensors (Tanimura *et al.*, 2004) or second messengers sur as cAMP or cGMP (Honda *et al.*, 2001; Nikolaev *et al.*, 2004).

5.3 cAMP sensors

5.3.1 Probes based on PKA or Epac linking domain to cAMP

The first genetically encoded indicator for cAMP used the same design as FlCRhR, first replacing the chemical fluorophores fluorescein and rhodamine with the GFP and BFP fluorophores, and later on with blue CFP and yellow YFP variants of GFP (Zaccolo *et al.*, 2000; Lissandron *et al.*, 2005). This sensor reports the dissociation of the regulatory (CFP donor) and catalytic (YFP acceptor) subunits of PKA by a decrease in FRET between these fluorophores. This type of sensor needs equal expression of both subunits to form the holoenzyme in the transfected cell and excess of either subunit can complicate signal analysis. Moreover, this sensor still has a kinase activity and its expression in neurons will likely interfere with the cAMP/PKA signaling cascade. This probe derived from PKA has a poor temporal resolution (Dunn *et al.*, 2006) and activation speed reflects more the activation of PKA than cAMP concentration variations that are much faster. Improving this issue, genetically encoded single chain FRET biosensors devoid of catalytic activity were developed using the cAMP-binding domain B of RIIβ subunit of PKA as cAMP sensing domain (PKA-camps sensor) (Nikolaev *et al.*, 2004).

In parallel, other sensors were developed using either the whole Epac protein or truncated forms reducing its cAMP-binding or membrane binding domain (DiPilato *et al.*, 2004; Nikolaev *et al.*, 2004; Ponsioen *et al.*, 2004) and exhibit significantly faster kinetics than the sensor based on PKA holoenzyme. While most biosensors use the traditional CFP/YFP pair of fluorophores, or their close derivatives, it may be needed to perform recordings at other wavelength and various versions of Epac-based sensors have been created with GFP donor and various yellow and red acceptors (van der Krogt *et al.*, 2008; Hong *et al.*, 2011).

5.3.2 Probes reporting the equilibrium between PKA and phosphatase activities

One step downstream, the effects of cAMP on PKA activity can be investigated using the A-kinase activity reporter (AKAR). This is a family of FRET biosensors composed of CFP as FRET donor, a phosphor-amino-acid binding domain, a PKA-specific substrate, and YFP as FRET acceptor: when this protein is phosphorylated by PKA, the phosphoamino acid binding domain binds onto the phosphorylated PKA

substrate, driving a conformational change, which increases FRET between CFP and YFP. The initial proof of concept of AKAR1 consisted of fusions of eCFP and eYFP, a phosphoamino acid binding domain (14-3-3tau binding to phosphor-Ser/Thr), and a consensus substrate for PKA which is a sequence LRRASLP with a Serine targeted by PKA (Zhang *et al.*, 2001). It lacked reversibility maybe because of an excessive affinity of the 14-3-3r domain for the phosphotréonine of the substrate domain preventing its dephophorylation by phosphatases. Later were developed AKAR2 (Zhang *et al.*, 2005; Dunn *et al.*, 2006) a well-usable reporter where the 14-3-3r was replaced by a FHA1 domain with less affinity for the substrate and the consensus substrate for PKA was changed to LRRATLVD to match FHA1. The reversibility was improved in AKAR2.2 thanks to the use of a GFP variant (mutation A206K) preventing their dimerization (Zacharias *et al.*, 2002; Dunn *et al.*, 2006).

AKAR2 were rapidly superseded by AKAR3, where the acceptor was changed for a circularly permuted citrine cpVenus, a variant of eYFP less sensitive to pH and photobleaching and with greater signal amplitude (Allen and Zhang, 2006)(**Figure Intro. 20**). This probe was used in the present PhD study. Changing the CFP donor for the brighter Cerulean led to AKAR4 (Depry *et al.*, 2011) while Aquamarine led to AqAKARCit with improved photostability (Erard *et al.*, 2013). The insertion of a flexible EV linker has been proven to improve performances of AKAR3EV as compared to AKAR3 and AKAR4 (Komatsu *et al.*, 2011). Although commonly named “PKA sensors,” one must keep in mind that the phosphorylation level of the biosensor results from the equilibrium between PKA-dependent phosphorylation and dephosphorylation performed by phosphatases, and is therefore a reporter of the phosphorylation level of a PKA substrate. Hence an increase in the AKAR signal can result from the activation of PKA or the inhibition of phosphatases during the tonic activity of PKA. For instance, in the cortex, inhibition of PP2A and PP2B prevented AKAR2 dephosphorylation (Gervasi *et al.*, 2007).

Targeting AKAR to specific cellular compartments has been achieved through the fusion of a nuclear localization sequence to AKAR2.2 (Zhang *et al.*, 2005; Allen and Zhang, 2006) or AKAR3 (Allen and Zhang, 2006). In brain slices, the kinetics of PKA activation in neuron nucleus has been shown to be much slower than in the cytosol (Gervasi *et al.*, 2007).

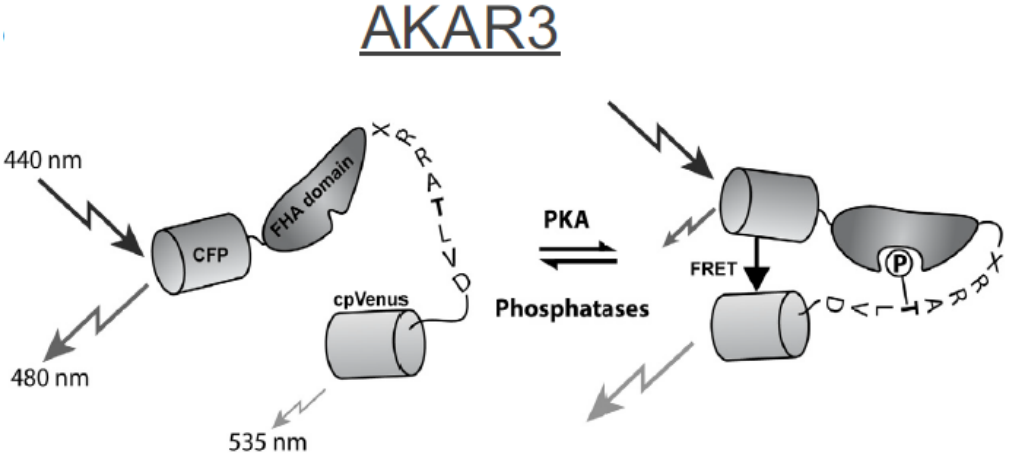

***[Figure Intro 20. The PKA FRET biosensor AKAR3. From** (Castro et al., 2016)]*

5.4 ERK sensors

After the development of Tyrosine kinase FRET biosensors (Ting *et al.*, 2001; Sato *et al.*, 2002) and following AKAR probes development (Ni *et al.*, 2006), a ERK activity reporter EKAR has been developed (Harvey *et al.*, 2008) and its second generation EKAR2G (Blum *et al.*, 2017).

EKAR is composed of a fluorescent protein-based FRET pair (mCerulean-mVenus or mRFP1-EGFP), a substrate phosphorylation peptide containing mitogen-activated protein kinase (MAPK) target sequence (PDVPRTPVGK) and docking site (FQFP), and the proline-directed WW phospho-binding domain (Harvey *et al.*, 2008). It has been demonstrated that the insertion of a flexible EV linker (116–244 amino acids) (Komatsu *et al.*, 2011) between WW domain and substrate phosphorylation peptide improves the sensitivity of EKAR when the Ypet-ECFP pair is used (EKAREV) (Komatsu *et al.*, 2011) (**Figure Intro. 21**). The EKAR-EV probe was used in the present PhD study.

As for AKAR, sensors of ERK activity specifically in the nucleus (EKARnuc) and the cytosol (EKAREV-cyto) have been more recently used (Zhai *et al.*, 2013; Tang and Yasuda, 2017). For instance, Zhai et al showed that the induction of LTP or Ca^{2+} entry via glutamate uncaging in only a few dendritic spines was sufficient to activate ERK in the nucleus and regulate downstream transcription factors. Signaling from individual spines was integrated over a wide range of time (>30 min) and space (>80 µm). Spatially dispersed inputs over multiple branches activated nuclear ERK much more efficiently than clustered inputs over one branch (Zhai *et al.*, 2013).

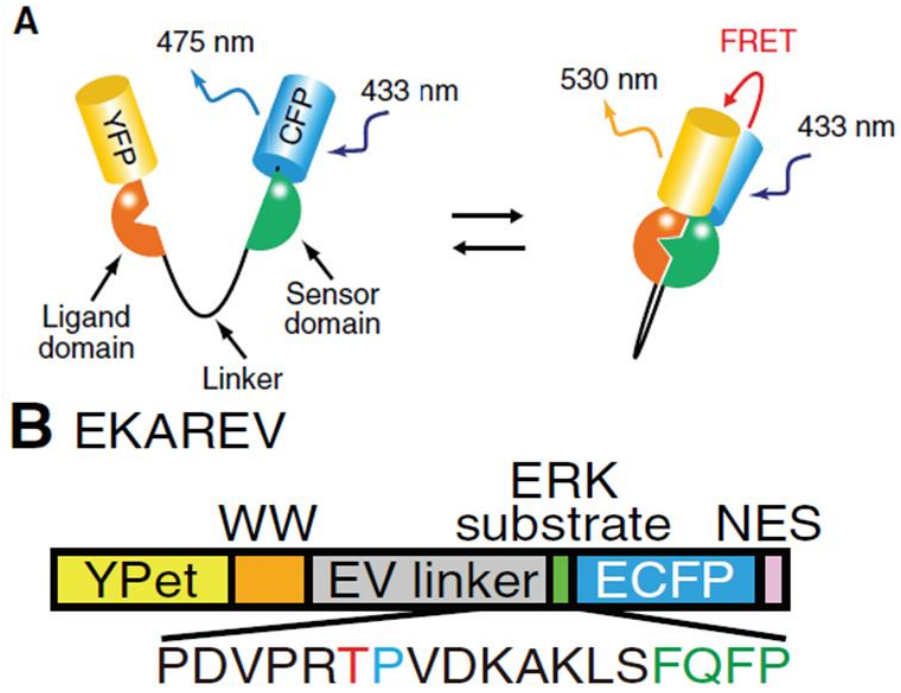

[Figure Intro 21. The ERK FRET biosensor EKAR-EV.

(A) Mode of action of the intramolecular FRET biosensor. (B) Structure of the EKAR-EV intramolecular FRET biosensor based on the Eevee backbone. In the substrate peptide sequence, red letters indicate the phosphorylation site. Blue letters indicate amino-acid substitutions to increase the affinity to either the WW domain. Green letters indicate the docking site of the kinase. ***Adapted from Komatsu et al. 2011****]*

5.5 Genetically encoded Ca^{2+} indicators (GECIs)

To assess Ca^{2+} dynamics, Ca^{2+} fluorescent indicators represent the most-feasible means of visualizing Ca^{2+} dynamics (Bootman *et al.*, 2013). These indicators permit the measurement of Ca^{2+} changes in subcellular to multicellular environments, as well as at high speed or as time-lapse images. Several methodological improvements, such as the development of two-photon and super-resolution microscopy have allowed refining the visualization of Ca^{2+} dynamics.

The first ratiometric quantifications were applied on the biochemical Ca^{2+} indicator fura-2 (Grynkiewicz *et al.*, 1985). The first GECIs were built on a Ca^{2+} sensitive domain surrounded by two fluorophores (Miyawaki *et al.*, 1997; Romoser *et al.*, 1997).

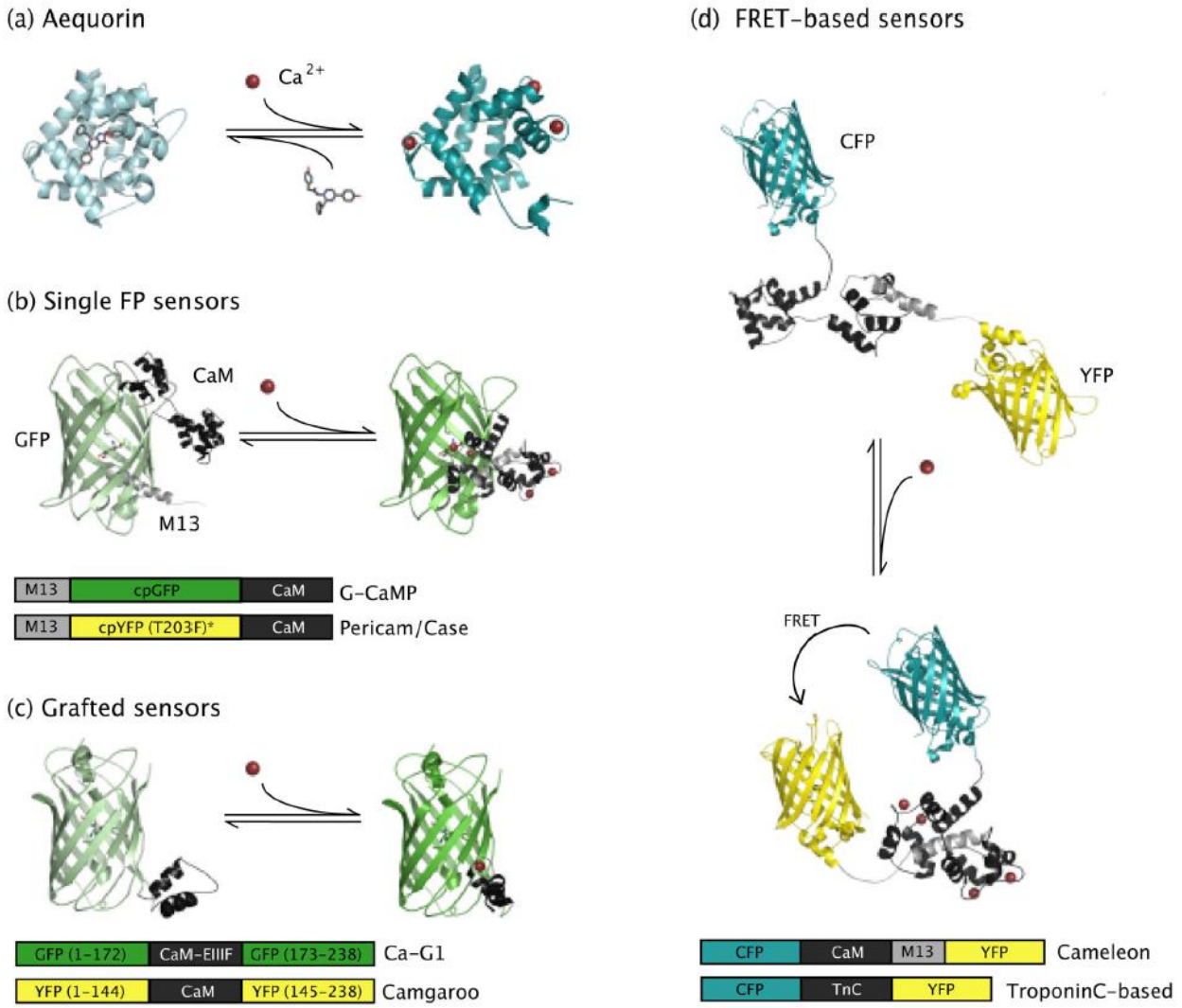

***[Figure Intro 22. Models of the classes of GECIs**. (a) The aequorin photoprotein is shown in complex with coelenterazine. Upon binding of Ca^{2+}, the aequorin undergoes a conformational change, releasing coelenteramide and emitting blue light. (b) Single FP sensors employing the Ca^{2+}- responsive element CaM and a CaM binding peptide attached to a circularly permutated FP. On binding Ca^{2+}, CaM executes a conformational change, interacting with the peptide and altering the protonation state of the chromophore, thus changing the fluorescence intensity of the protein. Note the Case sensors are built from a cpYFP with a T203F and a few other mutations. (c) Grafted sensors utilizing EF hands or portions of CaM inserted into a fluorescent protein. Binding of Ca^{2+} causes a*

change in protein conformation and a shift in the protonation state of the chromophore. (d) FRET-based sensors having a Ca^{2+} binding domain located between two flurophorescent proteins. As Ca^{2+} binds, the Ca^{2+} binding domain undergoes a conformational change, interacting with its binding peptide. This brings the two FPs closer together, increasing the efficiency of FRET. Below each model are maps for the various available families of GECIs. ***From (McCombs and Palmer, 2008)]***

Since the first demonstration of FRET–based prototypical sensors such as the Cameleons (Miyawaki *et al.*, 1997, 1999)(**Figure Intro 22**) and the first single fluorophore Ca^{2+} sensors (Baird *et al.*, 1999), these two major classes have evolved. High performance variants were developed. Signal strength was optimized in iterative steps of improvements and validation. Among FRET based sensors Cameleons, which exploit the interaction of Calmodulin with the binding peptide M13 as a Ca^{2+} sensing mechanism, saw several rounds of improvements of their signals strength allowing analysis of spontaneous Ca^{2+} activity in neuronal networks of up to 100,000 neurons (Nagai *et al.*, 2004; Horikawa *et al.*, 2010). Troponin C has been used as a more biocompatible alternative to Calmodulin in FRET sensors (Heim and Griesbeck, 2004). These sensors also underwent several rounds of engineering (Mank et al 2006, 2008). Among single fluorophore sensors, GCaMP type sensors (Nakai *et al.*, 2001) became the most popular class. Finally, large scale mutagenesis and screening approaches have resulted in GECIs that match or even exceed the in vivo sensitivity of the synthetic Ca^{2+} dye OGB-1, often referred to as a standard against which response properties of new GECIs were compared to (Chen *et al.*, 2013; Thestrup *et al.*, 2014).

The most optimized GECIs are single-wavelength green indicators based on the original GCaMP sensor (Nakai *et al.*, 2001). GCaMP and its progeny consist of circularly permuted GFP (cpGFP) (Baird *et al.*, 1999) the Ca^{2+}-binding protein calmodulin (CaM) and the CaM-interacting M13 peptide (Crivici and Ikura, 1995)(**Figure Intro 23**). The CaM–M13 complex is in proximity to the chromophore inside the cpGFP β-barrel (Akerboom *et al.*, 2009). Ca^{2+}-dependent conformational changes in CaM–M13 cause increased brightness with Ca^{2+} binding. Improvements have been facilitated both by crystal structure determination in the Ca^{2+}-free and Ca^{2+}-bound states (Wang *et al.*, 2008; Akerboom *et al.*, 2009), and high-throughput screening in bacterial colonies (Ibraheem *et al.*, 2011; Zhao *et al.*, 2011; Akerboom *et al.*, 2012) and lysates (Tian *et al.*, 2009). Variants with everincreasing sensitivity to neuronal activity were generated (Ohkura *et al.*, 2005, 2012; Tallini *et al.*, 2006; Tian *et al.*, 2009; Muto *et al.*, 2011), as were blue and red emitting color variants (Zhao *et al.*, 2011; Ohkura *et al.*, 2012; Akerboom *et al.*, 2013; Wu *et al.*, 2014). Sufficient structure/function relationships are known for GCaMP (Wang *et al.*, 2008; Akerboom *et al.*, 2009) and its constituent molecules, CaM (Chou *et al.*, 2001; Faas *et al.*, 2011; Stigler and Rief, 2012) and GFP (Ormö *et al.*, 1996; Tsien, 1998), to allow specific, semirational manipulation of critical sensor parameters including: Ca^{2+} affinity, on-and off-kinetics, protein stability, expression/degradation profiles, and baseline and activated fluorescence levels and sensor colors (Akerboom *et al.*, 2009, 2013; Tian *et al.*, 2009)(Akerboom et al 2009,2012b, 2013; Tian et al. 2009).

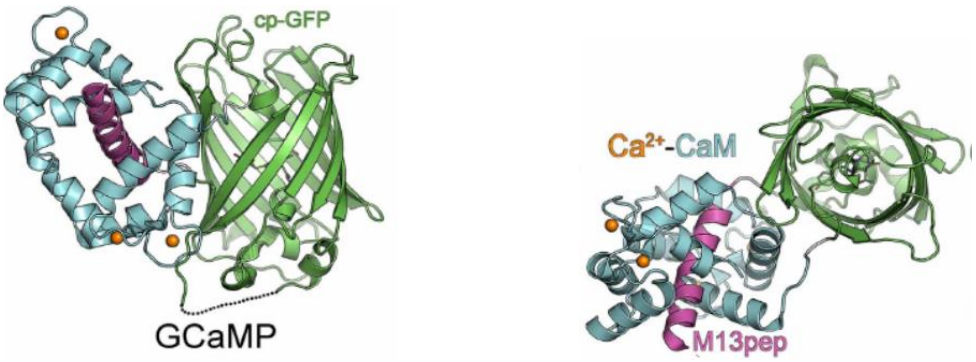

[Figure Intro 23. Crystal structure of Ca^{2+}-bound GCaMP in two orthogonal views.
Label indicates the coloring of the domains of GCaMP with cpGFP domain colored in green, M13 peptide in purple, CA $^{2+}$ in yellow and CaM in light blue. ***adapted from (Akerboom et al., 2013)]***

Among these variants, GCaMP6 variants with different characteristics **(Figure Intro 24)** were developed (GCaMP6s, 6m, 6f; for slow, medium and fast kinetics, respectively) and have been used to monitor even single action potentials (Chen *et al.*, 2013). These sensors vary in kinetics, with the more sensitive sensors having slower kinetics. Compared to GCaMP5G, the GCaMP6 sensors have similar baseline brightness and a 1.1- to 1.6-fold increase in dynamic range (ΔF/F0 at 160 action potentials). For small numbers of action potentials the most sensitive sensor, GCaMP6s, produced sevenfold larger signals (>10-fold larger than GCaMP3). GCaMP6 indicators were more sensitive and/or faster than other GCaMP variants. Compared to GCaMP5G, GCaMP6s exhibited threefold higher apparent affinity for Ca^{2+} and 1.3-fold higher saturated fluorescence, with similar baseline fluorescence. Ca^{2+} saturated GCaMP6s is 27% brighter than enhanced GFP (EGFP), its parent fluorescent protein. The fastest sensor, GCaMP6f, had two-fold faster rise time and 1.7-fold faster decay time than GCaMP5G (**Figure Intro 24**). GCaMP6f is the fastest GECIs for cytoplasmic free Ca^{2+} in neurons, with sensitivity comparable to OGB1-AM the commonly used synthetic Ca^{2+} indicators (Chen *et al.*, 2013). The most sensitive sensor, GCaMP6s, was used in in the present PhD study.

Further improvements of GECIs are proposed regularly based on specific objectives, among which the possibility of monitoring the activity of large population of neurons *in vivo* (Chisholm *et al.*, 2018) also via development of genetic reporter mouse models (Zariwala *et al.*, 2012), tracking the same neurons across multiple days in Ca^{2+} imaging (Sheintuch *et al.*, 2017), development of a photoconverible fluorescent protein, CaMPARI and CaMPARI2, that can detect the coincidence of light and Ca^{2+} to mark neurons that are active during experimenter-defined periods (Fosque *et al.*, 2015; Moeyaert *et al.*, 2018). One drawback of green fluorescent GECIs, such as the widely used GCaMP6 variant, is that the blue wavelengths of light used to excite the GECI also activate optogenetic actuators such as channelrhodopsins, so other improvements has been proposed recently such as the development of a bioluminescent GECI, designated LUCI-GECO1, based on efficient bioluminescent resonance energy transfer (BRET) between the NanoLuc luciferase and a topological variant of GCaMP6s (Qian *et al.*, 2018).

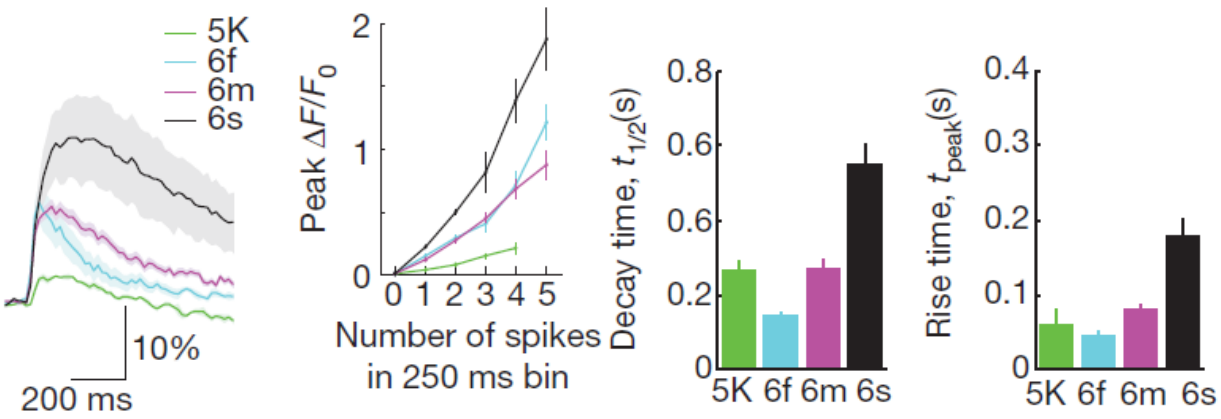

*[**Figure Intro 24. Comparisons of GCaMP6 indicators.***

Left panel: Median fluorescence change in response to one action potential for different Ca^{2+} indicators. *Shading corresponds to s.e.m., n=9 (GCaMP5K, data from Akerboom et al 2012), 11 (GCaMP6f), 10 (GCaMP6m), 9 (GCaMP6s) cells. GCaMP5K and GCaMP5G have similar properties (Akerboom et al 2012).*

Right panel: Peak fluorescence change as a function of number of action potentials in a 250ms bin *(5K: n=161, 65, 22, 4 events for 1, 2, 3, 4 action potentials; 6f: n=366, 120, 50, 15, 7 events for 1, 2, 3, 4, 5 action potentials; 6m: n=354, 105, 31, 11, 7 events for 1, 2, 3, 4, 5 action potential; 6s: n=250, 60, 20, 5, 4 events for 1, 2, 3, 4, 5 action potentials). Error bars correspond to s.e.m.*

Comparison of GCaMP indicators: *Half decay time. Rise time to peak. Error bars correspond to s.e.m.*

***Adapted from Chen et al 2013**]*

Results

Results

1- Cell-specific up-regulation of signaling pathways in the dopamine-depleted striatum

Main results of the article

1- After setting up the experimental model of biosensor imaging in corticostriatal slices of adult parkinsonian mice, we show two-photon imaging with various biosensors allows monitoring the signaling pathway dynamics in specific populations of SPN in adult mice and in a mouse model of PD.
In particular, we show that EKAR-EV biosensor can be used to follow ERK activation in neuronal culture, and in young and adult corticostriatal slices.
We also show that PKA dynamics can be monitored in adult brain slices with AKAR3.

2- First, we confirm the upregulation of ERK signaling pathway in response to D1R agonist after dopamine depletion by 6-OHDA. We also reveal that the combined pharmacological stimulation of dopamine and glutamate receptors does not produce a synergic activation of ERK in SPN but induce an increase in the percentage of responsive SPNs.

3- Second, we study PKA dynamics after dopamine depletion.
- we confirm that PKA response is specifically amplified in D1R-responsive SPN after 6OHDA lesion.
Using heterozygous Gαolf knock-out adult mice, we show that in controls, the activation of AC by D1R or A2AR is severely impaired when Gαolf protein is reduced by 50%, leading to a decreased PKA activation in both D1R- and A2AR-responsive SPN. AC activation is restored to normal levels only in D1R-responsive SPN of 6OHDA lesioned animals.
Our results are compatible with an increase in $G\alpha_{olf}$ leading to an increase of PKA activation in dSPNs after dopamine depletion.

- we explore the contribution of PDEs to the upregulated PKA activity after DA-depletion.
By applying a broad-spectrum PDE inhibitor, IBMX, we show that cAMP is tonically produced in adult striatal slices and PDE contributes significantly to its degradation.
We show that after DA depletion, there is a loss of regulation of PKA activity by PDEs only in the D1R-responsive cells.

4- Third, we study Ca^{2+} dynamics in distinct SPN subtypes after DA-depletion
- we show spontaneous Ca^{2+} activity is increased, in particular in dSPN.
- then, we show there is a specific upregulation of AMPA-induced intracellular Ca^{2+} dynamics in iSPN.

Altogether our data show cell-specific up-regulation of various signaling pathways after DA-depletion.

- Spontaneous Ca^{2+} transients in SPN are increased.
- ERK activation by dopamine and glutamate is increased.
- D1R- $G\alpha_{olf}$-PKA pathway is upregulated in dSPNs
- Intracellular Ca^{2+} transients in response to AMPAR stimulation are increased specifically in iSPN

Article

Cell-specific up-regulation of signaling pathways in striatal neurons following dopamine depletion

Louise-Laure MARIANI[1,2,3], Sophie LONGUEVILLE[1,2,3], Jean-Antoine GIRAULT[1,2,3], Denis HERVÉ[1,2,3], Nicolas GERVASI[1,2,3]

Affiliations

1- Inserm UMR-S 839, Paris, France
2- Sorbonne Université, Science and Engineering Faculty, Paris, France
3- Institut du Fer a Moulin, Paris, France

Abstract (<150 words)

Parkinson's disease (PD) results in the disappearance of dopamine (DA) from the dorsal striatum. L-DOPA replacement therapy long-term complications, including dyskinesia, may derive from altered striatal plasticity. To identify signaling dysregulations in striatal projection neurons (SPN) in the absence of dopamine we used 6-OHDA lesion in adult mice combined with virally-transduced biosensors to monitor signaling pathways by two-photon imaging of corticostriatal slices. DA lesion increased ERK and PKA activation in response to D1 receptors (D1R) stimulation. Augmented activation of PKA could be accounted for by an increase in Gαolf amplified by deficient phosphodiesterase activity in D1R-expressing neurons. Monitoring Ca^{2+} signals showed an increased spontaneous activity of D1R-expressing neurons in lesioned mice and an unexpected hypersensitivity of indirect pathway SPNs to stimulation of AMPA glutamate receptors. Our work reveals distinct cell type-specific signaling alterations in the two populations of SPNs and suggests possible mechanisms for these alterations.

Introduction

The striatum is the input structure of the basal ganglia circuits that play a major role in motor control, including the accurate selection of habitual or goal-directed motor actions (Redgrave *et al.*, 2010). The functions of the striatum are based on the balance of two distinct systems of GABAergic striatal projection neurons (SPNs). The direct pathway SPNs (dSPNs), directly project to the basal ganglia output structures (substantia nigra pars reticulata and globus pallidus pars interna) and promote one action, while the indirect pathway SPNs (iSPNs), projects to the same output structures via relays in the globus pallidus pars externa and subthalamic nucleus, and suppress other actions (Albin *et al.*, 1989; DeLong, 1990; Gerfen and Surmeier, 2011b). Dopamine (DA) release by afferent neurons from the substantia nigra pars compacta oppositely modulates dSPNs and iSPNs activities because of their preferential expression of DA D1 (D1R) and D2 (D2R) receptors, respectively (Gerfen *et al.*, 1990; Le Moine and Bloch, 1995). SPN activity is driven by abundant glutamate afferents from the entire cerebral cortex and some thalamic nuclei. Shaping SPN activity is thus dependent on specific regulations by DA on the glutamate synapses and their plasticity.

In Parkinson's disease (PD), DA afferents to the striatum are progressively damaged. This loss plays a major role in the motor and possibly non-motor symptoms of the disease. Especially, bradykinesia, akinesia and rigidity, that characterize PD, are attributed to the loss of dSPN activation and iSPN inhibition exerted in normal conditions by D1R and D2R, respectively (Albin *et al.*, 1989; Alexander and Crutcher, 1990; Mallet *et al.*, 2006; Kravitz *et al.*, 2010; Alcacer *et al.*, 2017). L-DOPA is particularly effective to restore dopaminergic tone in the PD striatum and reduce motor symptoms in early stages of the disease. However, as the disease progresses and more dopaminergic neurons degenerate, the L-DOPA dose needed to reduce the symptoms must be increased. In addition, uncontrolled fluctuations in therapeutic effects are observed and abnormal movements called dyskinesia emerge, leading to increasingly severe disabilities for patients. These phenomena are still poorly understood, but have been attributed to lasting alterations of SPNs caused by the loss of DA input that would lead to inappropriate responses to L-DOPA (Cenci and Konradi, 2010). They are thought to result from alterations of signaling pathways that differentially affect dSPNs and iSPNs. cAMP-, Ca^{2+}-, and extracellular signal-

regulated kinase (ERK)-dependent signaling pathways are markedly altered in SPNs of DA-depleted striatum, and these changes may lead to disruption of SPN responses in advanced PD stages, ultimately resulting in L-DOPA-induced complications including L-DOPA induced dyskinesia (LID) (Sgambato-Faure and Cenci, 2012; Fieblinger *et al.*, 2014a). Following lesion of DA neurons, L-DOPA induces a very strong activation of ERK that is not observed in the DA-intact striatum (Gerfen *et al.*, 2002; Pavón *et al.*, 2006; Santini *et al.*, 2007; Westin *et al.*, 2007). This activation of ERK is under the control of DA D1R and occurs selectively in dSPNs (Gerfen *et al.*, 2002; Santini *et al.*, 2007). Stimulation of cortico-striatal afferents can also activate ERK in the striatum (Sgambato *et al.*, 1998), mostly in iSPNs (Gerfen *et al.*, 2002). Importantly, pharmacological and genetic evidences showed that ERK inhibition prevents LID development and may even reverse already established LID (Santini *et al.*, 2007; Fasano *et al.*, 2010). In addition, the cAMP-dependent pathway is strongly activated in response to D1R stimulation in the DA-depleted striatum (Santini *et al.*, 2007; Bateup *et al.*, 2010). The levels of D1R being unchanged or even decreased (Marshall *et al.*, 1989; Gerfen *et al.*, 1990), the cAMP-dependent pathway hyperactivity after DA denervation is caused by increased downstream signal transduction, in particular the upregulation of Gαolf (Hervé *et al.*, 1993; Corvol *et al.*, 2004; Morigaki *et al.*, 2017), the G protein subunit which couples D1R to adenylyl cyclase in the striatum (Zhuang *et al.*, 2000; Corvol *et al.*, 2001). If the cAMP pathway is required in the striatal neurons for LID development (Lebel *et al.*, 2010; Park *et al.*, 2014), it seems however that its increase is not the primary cause of LID (Alcacer *et al.*, 2012). Alterations of NMDA and AMPA receptors, including their subunit composition, synaptic trafficking and phosphorylation, and the clustering protein Narp (Oh *et al.*, 1998; Dunah *et al.*, 2000; Fiorentini *et al.*, 2006; Gardoni *et al.*, 2006; Sgambato-Faure and Cenci, 2012; Charbonnier-Beaupel *et al.*, 2015) could sensitize SPNs to cortical glutamatergic input and thereby modify motor function. However the dynamics and cell type specificity of signaling alterations in SPNs resulting from the chronic absence of DA are still poorly characterized, hampering our understanding of pathophysiological consequences.

Here, to address this issue and identify the complex alterations of ERK, cAMP and Ca^{2+}-dependent pathways in dSPNs and iSPNs following total loss of DA input, we used protein sensors for two-photon imaging of identified living neurons in mouse striatal slices. We

monitored the activity of SPN populations with the Ca^{2+} indicator GCaMP6S (Chen *et al.*, 2013) and we examined protein kinase A (PKA) and ERK activity with Förster resonance energy transfer (FRET)-based biosensors, AKAR3 and EKAR-EV respectively (Allen and Zhang, 2006; Komatsu *et al.*, 2011; Castro *et al.*, 2013). Striatal DA terminals were lesioned by local microinjection of 6-hydroxydopamine (6-OHDA). The responses in intact and DA-depleted striatum were compared following applications of D1R agonist and/or AMPA for mimicking inputs from dopaminergic and corticostriatal afferents. We found that the cAMP and ERK-dependent pathways were upregulated in response to D1R stimulation in the dSPNs without any clear upregulation of Ca^{2+} signaling in response to AMPA. In contrast, the excitability of iSPN to AMPA stimulation was highly increased by the loss of DA input, while the cAMP and ERK-dependent pathways were not significantly affected. Hence our results indicate that dopamine and glutamate-induced responses are independently disrupted in the dSPN and iSPN. They also suggest that complications in the PD treatments at late stages are linked to the inability to appropriately regularize both dopamine and glutamate responses in dSPN and iSPN.

Results

Imaging ERK activity dynamics in striatal neurons

In order to monitor ERK activity in striatal neurons we used three FRET-based optical biosensors that allows quantitative real-time analysis of ERK activity dynamics with single cell resolution in tissue, $EKAR_{cyto}$, EKAR2G1 and EKAR-EV (Harvey *et al.*, 2008; Komatsu *et al.*, 2011; Fritz *et al.*, 2013). $EKAR_{cyto}$ is comprised of a fluorescent protein-based FRET pair (mCerulean-mVenus), a substrate phosphorylation peptide containing ERK target sequence (PDVPRTPVGK) and docking site (FQFP), and the proline-directed WW phospho-binding domain (Harvey *et al.*, 2008). EKAR2G1 uses the backbone of $EKAR_{cyto}$ with a substitution of mCerulean at the N terminus and mVenus at the C terminus by variants of mTFP1 (mTFP1/cp227) and Venus (Venus/cp173), respectively (Fritz *et al.*, 2013). EKAR-EV is optimized with fluorescent protein variant pair (Ypet/ECFP) and a long, flexible linker between WW domain and substrate phosphorylation peptide of $EKAR_{cyto}$ that markedly increased the gain of FRET signals (Komatsu *et al.*, 2011).

To test the sensitivity of these EKAR variants, we stimulated striatal neurons in culture (DIV 7) expressing these biosensors (transfection with lipofectamine) with brain-derived neurotrophic factor (BDNF) (10 ng/mL) for 5 min, which activates ERK signaling through BDNF receptors (**Fig. 1A**). EKAR-EV exhibited a larger BDNF-induced YFP/CFP emission ratio (FRET ratio) than $EKAR_{cyto}$ and EKAR2G1 (**Fig. 1A**, **middle panel**). To quantify FRET responses, we normalized the FRET ratio increases by their corresponding FRET ratio baselines [i.e., $\Delta R/R0$, as in previous studies (Gervasi *et al.*, 2007, 2010)]. EKAR-EV showed a higher FRET increase (12.5 ± 1.6%, mean ± S.E.M) compared to $EKAR_{cyto}$ (6.6 ± 0.9%) and EKAR2G1 (2.9 ± 0.3%) (**Fig. 1A**, **right panel**). Based on these results, we chose EKAR-EV to monitor ERK activity dynamics in striatal brain slices.

We started to monitor changes in ERK activity in real time by ratiometric two-photon microscopy using Sindbis viral vectors encoding EKAR-EV in striatal slice preparations from immature mice (P8-P12). Sindbis viruses were already successfully used to infect biosensors to monitor other signaling pathways in young brain slices (Gervasi *et al.*, 2007; Hepp *et al.*, 2007; Castro *et al.*, 2013; Tricoire and Lambolez, 2014; Luczak *et al.*, 2017). We first verified that EKAR-EV was able to report ERK activation in striatal neurons after a global depolarization. KCl (25 mM) application for 1 min produced a large increase in the FRET ratio in about 90% of the EKAR-EV-expressing neurons, which decreased after KCl washout (**Fig. 1B**). Application of AMPA (5 μM) for 30 s yielded a large, but less pronounced, increase in the FRET emission ratio. On average, AMPA increased the emission ratio to 4.7 ± 0.5% and KCl to 7.8 ± 0.6% (mean ± S.E.M., Student's t test, $p<0.05$).

To study ERK activity dynamics in 6-OHDA-lesioned mice, we had to perform ERK imaging in mature striatal network (over 8-week-old). Since Sindbis virus does not allow effective neuronal infection in adult striatal slices, we produced a recombinant adeno-associated virus (AAV, serotype 2/1) encoding EKAR-EV. The biosensor was expressed in the mouse striatum via AAV injection and was subsequently imaged in acute brain slices (2–4 weeks post injection, **Fig. 1C**). D1 agonist (SKF81297 10 μM) application for 30 s rapidly increased FRET emission ratio in the soma indicating an increase in ERK activity (**Fig. 1D**). Subsequent addition of KCl (25 mM) further increased FRET emission ratio (1.2 ± 0.2% for SKF81297 versus 3.4 ± 0.25% for KCl, **Fig.**

1E). The response to KCl application was used as a positive control for cell health and responsiveness in all experiments. The SKF81297- and KCl-induced increases in FRET emission ratio were dependent on the activity of MEK1/2, the kinases activating ERK, since all the responses were abolished in the presence of U0126 (5 μM), a selective inhibitor of MEK1/2 (**Fig. 1C-E**). We noticed that each local application, whatever the drug applied, was followed by a transient decrease in the FRET emission ratio. This decrease also occurred after local application of ACSF even if ACSF did not produce any increase in the FRET emission ratio (0.15 ± 0.09%). In addition, similar decreases were also recorded in the presence of U0126 for all the stimulations (**Fig. 1E**) and did not seem to result from changes in MEK1/2, suggesting they were artefactual but were short and did not preclude measurement of ERK activity. In summary, we showed that EKAR-EV biosensor was appropriate to monitor ERK activity in neurons in culture as well as in young and adult striatal slices.

ERK responses are increased after dopamine depletion induced by 6-OHDA lesion

Modifications of ERK responses to L-DOPA or DA agonists have been reported after lesion of the DA neurons in experiments using immunoblotting or immunofluorescence (Gerfen *et al.*, 2002; Santini *et al.*, 2007; Alcacer *et al.*, 2014). To analyze these changes, we investigated dynamics of ERK activity using EKAR-EV in dorsal striatum neurons of 6-OHDA-lesioned mice. We co-injected 6-OHDA and AAV expressing EKAR-EV biosensor into the dorsal striatum of 4-6-week-old mice that were allowed to recover for 4 weeks before acute brain slicing and two-photon imaging (**Fig. 2A**). Striatal depletion of DA terminals following 6-OHDA microinjection was checked by immunoblotting or immunofluorescence (**Fig. 2A**). As compared to controls, tyrosine hydroxylase (TH) immunoreactivity was dramatically decreased after 6-OHDA lesion, only on the side injected as indicated by immunoblotting and immunofluorescence (**Fig. 2A**). 6-OHDA microinjection and DA depletion did not alter the expression of the biosensor (**Fig. 2A**).

ERK signaling pathway has been reported to be activated by combination of DA and glutamate stimulations in the striatal neurons in the context of drug addiction (see (Girault *et al.*, 2007) for a review). Since the activation of ERK is particularly intense after the first L-DOPA

treatment in the DA-denervated striatum (Santini *et al.*, 2007), we compared ERK activity dynamics after DA and glutamate stimulation for 30 s in control and 6-OHDA-lesioned striata. In 6-OHDA lesioned slices, the amplitude of FRET emission ratio in striatal neurons was significantly increased as compared to non-lesioned control animals, after D1R stimulation by SKF81297 (mean ± SEM: non-lesioned, 0.9 ± 0.2%, lesioned, 2.1 ± 0.2%, **Fig. 2B**). AMPA application produced a statistically non-significant increase of FRET emission ratio in the 6-OHDA-lesioned striata as compared to the non-lesioned striata (**Fig. 2B**). The co-application of AMPA and SKF 81297 increased the FRET emission ratio in 6-OHDA-lesioned striata (non-lesioned, 0.95 ± 0.13%, lesioned, 1.7 ± 0.19%, **Fig. 2B**). However, this increase was not different from the response to SKF81297 alone. In contrast, the 6-OHDA lesion did not modify the FRET emission ratio response of striatal neurons to ACSF or KCl (**Fig. 2C**). We also compared the percentage of responsive neurons in the various conditions. In 6-OHDA-lesioned slices, the percentage of neurons showing ERK activation was significantly increased as compared to non-lesioned controls, only after AMPA and SKF81297 co-application (non-lesioned, 43 ± 3%, lesioned, 67 ± 4%, *p<0.05 **Fig. 2D**), although a non-significant increase in the lesioned striata was also observed after AMPA application alone (non-lesioned, 22 ± 6%, lesioned, 37 ± 4% for 6-0HDA, **Fig. 2D**). The proportion of responsive cells after SKF81297, ACSF alone or KCl application was not changed by the lesion (**Fig. 2D-E**).

These results confirmed the upregulation of ERK signaling pathway in response to D1R agonist after DA depletion by 6-OHDA. Although the combined D1 and AMPA receptors pharmacological stimulation did not increase the average ERK response amplitude as compared to D1R alone, it increased the percentage of responsive neurons. To address the possible mechanisms of these effects of the DA lesion on ERK, we further investigated, the dynamic changes in the signaling pathways leading to ERK activation in SPN, including the cAMP/PKA pathway and Ca^{2+} regulation.

PKA responses to D1R stimulation are increased in dSPN after 6-OHDA lesions in adult mice

Since increase in PKA signaling could explain the enhancement of ERK responsiveness to D1R agonist, we investigated PKA responses in control and 6-OHDA-lesioned animals. We injected an AAV vector encoding AKAR3, a sensor for PKA activity (Allen and Zhang, 2006), into the striatum of adult mice. We used corticostriatal slices 3-4 weeks later for real-time imaging of PKA activation as the FRET emission ratio in living striatal neurons with two-photon microscopy (**Fig. 3A and B**). Since previous studies from other laboratories used very young animals, we first validated our approach in adult mice (8-10 weeks old). As in previous studies, we stimulated the slices with D1R and $A2_AR$ agonists to differentiate putative dSPNs and iSPNs, expected to respond to D1R and $A2_AR$ agonists, respectively (Castro *et al.*, 2013; Polito *et al.*, 2015; Yapo *et al.*, 2017). In the dorsal striatum, application of SKF81297 for 1 min yielded an increase in the FRET emission ratio to 6.1 ± 0.3% (**Fig. 3C**) in about half of the neurons present in the field of view (46 ± 4%), revealing the D1R-expressing neurons. After 10 min of SKF81297 washout, application of the $A2_AR$ agonist CGS21680 for 1 min increased FRET emission ratio to 5.9 ± 0.2% in the other half of the neurons present in the field of view (40 ± 3%) (**Fig. 3D**), revealing the $A2_AR$-expressing SPN. This was consistent with previous studies showing that D1R and $A2_AR$ are segregated in the two major subsets of SPNs corresponding to the direct and indirect pathways, respectively (Bateup *et al.*, 2008; Bertran-Gonzalez *et al.*, 2008). These results were also in agreement with FRET biosensor studies performed in striatal slices from immature mice (Polito *et al.*, 2015; Yapo *et al.*, 2017). We randomly alternated the order of SKF81297 and CGS21680 application with no effect on either the amplitude of FRET emission ratio or the proportion of responsive SPNs. In all the experiments, a subsequent application of forskolin (FSK, 10 μM) that directly activates adenylyl cyclase (AC) produced a maximal increase of FRET emission ratio to 11.7± 0.3% in both D1R- and $A2_AR$-expressing SPNs, indicating the cell health and the correct AKAR3 responsiveness to AC activation in all experiments (**Fig. 3A-D**). We also measured the rise time of AKAR3 responses that was shorter for FSK than for SKF81297 and slower for CGS21680 (**Fig. 3A-C**).

Since these experiments showed that our experimental approach reliably allowed studying PKA responses in adult striatal slices, we then compared PKA activation in control and 6-OHDA-lesioned striata. We co-injected 6-OHDA with an AAV expressing AKAR3 in the dorsal striatum of 4-6-week-old mice. In 6-OHDA-lesioned striata, the increase in FRET emission ratio after application of SKF81927 was significantly larger than in non-lesioned striata (non-lesioned, 4.4 ± 0.3 %, lesioned, 7.7 ± 0.3%, **Fig. 3F**). In contrast, no significant change was detected after application of CGS21680 (non-lesioned, 4.7 ± 0.2%, lesioned, 4.9 ± 0.3%) nor after application of FSK (non-lesioned, 11 ± 0.5%, lesioned, 10.6 ± 0.4%, **Fig. 3F**). There was no significant change in the percentage of cells responsive to the D1R agonist after 6-OHDA lesion (non-lesioned, 44 ± 5%, lesioned, 50± 5%, **Fig. 3G**). The lesion did not alter either the percentage of cells responsive to the $A2_AR$ agonist (non-lesioned, 52 ± 4%, lesioned, 54 ± 5%) or FSK (non-lesioned 94 ± 3%, lesioned, 98 ± 2%, **Fig. 3G**). Together, these results show that PKA responses are specifically amplified in D1R-expressing SPNs after DA depletion by 6-OHDA lesion, without change in the number of responsive cells.

In *Gnal*$^{+/-}$ mice PKA activation is decreased but the specific upregulation in response to a D1R agonist after 6-OHDA lesions is conserved

In the dorsal striatum, D1R activates AC through its coupling to $G\alpha_{olf}$ (Hervé *et al.*, 1993; Corvol *et al.*, 2001). We previously observed increased $G\alpha_{olf}$ protein levels in the dorsal striatum of 6-OHDA-lesioned rodents (Hervé *et al.*, 1993; Alcacer *et al.*, 2012) and in the putamen of PD patients (Corvol *et al.*, 2004). So we used $G\alpha_{olf}$ gene mutant mice to investigate the mechanism of increased PKA activity after 6-OHDA lesion. Homozygous $G\alpha_{olf}$ gene knock-out mice (*Gnal*$^{-/-}$) have a severe phenotype combining olfactory and striatal deficits (Belluscio *et al.*, 1998; Zhuang *et al.*, 2000; Corvol *et al.*, 2001). These mice usually die in the early postnatal period and could not be used in our study. In contrast, *Gnal*$^{+/-}$ mice, which develop and breed normally, provide a very interesting model because they display a decrease of about 50% in $G\alpha_{olf}$ protein levels (Corvol *et al.*, 2007; Alcacer *et al.*, 2012).

We performed co-injections of saline or 6-OHDA with AAV expressing AKAR3 into the striatum of 4-6 week-old *Gnal*$^{+/-}$ and *Gnal*$^{+/+}$ littermates. When DA innervation was intact, we

recorded in the *Gnal*$^{+/-}$ mice a significant decrease in the FRET emission ratio in response to CGS21680 (*Gnal*$^{+/+}$, 5.2 ± 0.2%, *Gnal*$^{+/-}$, 3.6 ± 0.2%, **Fig. 4A**) and SKF81297 application (*Gnal*$^{+/+}$, 5.8 ± 0.2%, *Gnal*$^{+/-}$, 3.6 ± 0.3%, **Fig. 4B**). No change was detected after application of FSK (*Gnal*$^{+/+}$, 11.4 ± 0.3%, *Gnal*$^{+/-}$, 11.5 ± 0.2%) meaning that AC was not changed and could still be directly activated by FSK in the *Gnal*$^{+/-}$ mice (**Fig. 4C**). These results were consistent with previous measurements of AC activity in striatal membranes and the conclusion that Gαolf levels are limiting for the activation of AC in response to either D1R or $A2_AR$ stimulation (Hervé *et al.*, 1993; Corvol *et al.*, 2001, 2007). No significant change was observed in the percentage of responsive cells in *Gnal*$^{+/-}$ mice after CGS21680 (*Gnal*$^{+/+}$, 36 ± 3%, *Gnal*$^{+/-}$, 39 ± 2%), SKF81297 (*Gnal*$^{+/+}$, 50 ± 3%, *Gnal*$^{+/-}$, 48 ± 2%), or FSK (*Gnal*$^{+/+}$, 91 ± 1%, *Gnal*$^{+/-}$, 92 ± 2%). These results showed that the activation of AC by D1R or $A2_AR$ is markedly impaired when $G\alpha_{olf}$ protein is reduced leading to a decreased PKA activation in both D1R- and $A2_AR$-expressing SPNs. Our results are in contrast to a previous study in young mice (P8-12) that did not show any change in PKA dynamics in *Gnal*$^{+/-}$ mice (Castro *et al.*, 2013). This is likely due to the fact that the Gαs/Gαolf switch has not yet fully taken place at P8-12 (Iwamoto *et al.*, 2004) and that AC responses to D1R or $A2_AR$ agonists are less dependent on $G\alpha_{olf}$ levels.

After 6-OHDA-lesion in *Gnal*$^{+/-}$ mice no modification of the FRET emission ratio was observed when CGS21680 was applied when compared to non-lesioned *Gnal*$^{+/-}$ mice (non-lesioned, 3.7 ± 0.2%, lesioned, 3.6 ± 0.3%, **Fig. 4A**). In contrast, SKF81297 increased the FRET emission ratio to a higher level in 6-OHDA-lesioned *Gnal*$^{+/-}$ mice than in non-lesioned mutant mice (non-lesioned, 3.6 ± 0.2%, lesioned, 6.1 ± 0.5%, **Fig. 4B**). However this increase in FRET response did not reach the level attained in 6-OHDA-lesioned striata from wild type mice (7.8 ± 0.3% in 6-OHDA-lesioned wild type striata, indicated by a green dashed line in **Fig. 4B**). No significant change was observed in the FRET emission ratio after FSK application (**Fig. 4C**). In addition, the percentage of responsive cells was unaffected by the lesion in *Gnal*$^{+/-}$ mice after CGS21680 (non-lesioned, 39 ± 2%, lesioned, 42 ± 2%), SKF81297 (non-lesioned, 48 ± 2%, lesioned, 45 ± 2%), or FSK (non-lesioned, 92 ± 1%, lesioned, 89 ± 2%).

These results suggest that in 6-OHDA-lesioned animals, increased PKA activity after D1R stimulation in D1R-expressing SPNs is compatible with an increase in $G\alpha_{olf}$ levels. This increase is cell type-specific because no modification was observed in $A2_AR$-expressing SPNs.

Cell type-specific down-regulation of PDE activity in D1R-agonist responsive SPNs after 6-OHDA lesions

PDEs are important negative regulators of PKA activity. Regulation in the expression of PDE have been reported after 6-OHDA lesion with a down regulation of PDE4 and PDE10 in PD patients and animal models of PD (Niccolini *et al.*, 2015, 2017; Heckman *et al.*, 2018). Hence, we tested if PDE activity could be implicated in the cell type-specific upregulation of PKA activity observed after DA depletion. We examined the effects of application of a broad-spectrum PDE inhibitor, 3-isobutyl-1-methylxanthine (IBMX). We first observed that, as expected, the amplitude of AKAR3 activation was increased by IBMX in SPNs of adult non-lesioned mice in a dose dependent-manner (**Fig. 4D**). These results were similar to those previously reported in immature mice (Castro et al., 2010; Polito et al., 2015). They showed that in our conditions, cAMP was tonically produced in striatal slices and that PDEs constantly degraded it.

We then investigated PKA responses in adult striatal slices in the presence of a low concentration of IBMX (30 μM for 10 min) which had no or small effects on basal FRET emission ratio. At this concentration, IBMX enhanced the PKA responses to CGS 21680 (no IBMX, 5.4 ± 0.3%, IBMX 9.3 ± 0.5%, **Fig. 4E**), SKF81297 (no IBMX, 5.0 ± 0.3%, IBMX 9.0 ± 0.3%, **Fig. 4F**) and FSK (**Fig. 4G,H**). This confirmed that PDE activity exerted an important negative tuning of PKA responses in adult SPNs. In 6-OHDA-lesioned animals, although IBMX (30 μM) increased the amplitude of FRET emission ratio in response to CGS21680 (no IBMX, 3.4 ± 0.3%, IBMX, 8.1 ± 0.3%, **Fig. 4E**), it did not further increase the response to SKF81297 (no IBMX, 7.5 ± 0.3%, IBMX 8.2 ± 0.5%, **Fig. 4F**). Pretreatment with IBMX did not alter the proportion of responsive cells to D1R agonist in the 6-OHDA-lesioned striata as compared to non-lesioned ones (non-lesioned, no IBMX, 39 ± 7%, IBMX, 53 ± 4%, lesioned, no IBMX, 48 ± 6%, IBMX, 54 ± 5%) or $A2_AR$ agonist-responsive SPNs (non-lesioned, no IBMX, 44 ± 7%, IBMX, lesioned, no IBMX, 49 ± 3%, IBMX, 48 ± 4%). Our data show a loss of regulation of PKA activity by PDE in D1R agonist-responsive SPNs

after 6-OHDA lesion but not in $A2_AR$-responsive SPN. To test whether this loss of regulation by PDEs only impacts the D1R pathway or is more generalized, we analyzed FSK-induced PKA activity in both types of SPNs. Pretreatment with IBMX, increased the responses to FSK in the $A2_AR$-responsive SPNs of non-lesioned (no IBMX, 8.9 ± 0.4%, IBMX, 12.3 ± 0.7%) and 6-OHDA lesioned slices (no IBMX, 8.2 ± 0.3%, IBMX, 13.6 ± 0.5%, **Fig. 4G**). In contrast, the pretreatment with IBMX only increased the responses to FSK in the D1R-expressing SPNs of non-lesioned slices (no IBMX, 9.6 ± 0.5%, IBMX, 11.3 ± 0.4%, **Fig. 4H**). This effect was not observed in the 6-OHDA-lesioned slices where the FSK effect was already increased before IBMX application (no IBMX, 11.3 ± 0.4%, IBMX, 10.5 ± 0.5%, **Fig. 4H**). We also noticed that in the absence of IBMX, the FRET emission ratio after FSK was increased in the D1R-expressing SPNs of 6-OHDA-lesioned mice as compared to those of non-lesioned mice (**Fig. 4H**). Taken together these results suggested that PDE activity is down-regulated specifically in D1R-agonist-responding SPNs after DA depletion and this down-regulation is associated with an increase in PKA activity in response to D1R or AC stimulation.

Spontaneous Ca^{2+} transient activity is increased in 6-OHDA-lesioned D1R-expressing striatal neurons

Intracellular Ca^{2+} increase has been implicated in ERK activation in many models including *C. elegans* (Tomida *et al.*, 2012), CA1 pyramidal neurons in rodents (Zhai *et al.*, 2013), and SPNs in DA-depletion models (Fieblinger *et al.*, 2014b). Hence, we investigated intracellular free Ca^{2+} in the striatal neurons of non-lesioned and 6-OHDA-lesioned mice. We co-microinjected 6-OHDA and an AAV expressing GCaMP6S (Chen *et al.*, 2013) in the dorsal striatum and 3-4 weeks later, acute striatal slices were imaged under a multiphoton microscope. In our experimental conditions, some SPNs were spontaneously active and showed transient increases in intracellular Ca^{2+} detected by the normalized fluorescence ratio ($\Delta F/F0$). We therefore used the baseline period of our recordings to sort the striatal neurons into two categories as described in the Methods section: spontaneously active and silent striatal neurons (**Fig. 5A**). The number of spontaneously active SPNs was higher in 6-OHDA-lesioned than non-lesioned striata (non-lesioned, 13.1%, n= 274/2085, lesioned, 18.2%, n= 319/1748, **Fig. 5B**). To determine whether

this higher spontaneous activity affected dSPNs and/or iSPNs, we microinjected an AAV Cre-dependently expressing GCaMP6S (AAV-flex-GCaMP6s), into the striatum of *Drd1*::Cre (D1Cre) and *Adora2$_A$::*Cre (A2$_A$Cre) mice. In the 6-OHDA-lesioned *D1*Cre mice, dSPNs were spontaneously more active than in the non-lesioned animals (non-lesioned, 11.3%, n= 58/512, lesioned, 19.7%, n= 179/910, **Fig. 5B**). In the *A2$_A$*Cre mice, no significant difference was observed between lesioned and non-lesioned striata (non-lesioned 15.4%, n= 80/518, lesioned, 18.2%, n= 69/379, **Fig. 5B**). These results suggested that a higher proportion of dSPNs had spontaneous Ca^{2+} activity in DA-depleted striatum.

Specific upregulation of AMPA-induced intracellular Ca^{2+} dynamics in A2$_A$R-expressing striatal neurons after 6-OHDA lesion

As mentioned above, co-application of AMPA and SKF81297 activated ERK in a larger number (>50%) of neurons in the 6-OHDA-lesioned striatum than in the intact striatum (**Fig. 2B**). These effects could be indicative of alterations of Ca^{2+} responses to AMPAR stimulation in the DA-depleted striatum. To address this question, we monitored intracellular Ca^{2+} dynamics following a 30 s AMPA application in SPNs of 6-OHDA-lesioned and control mice. Our analysis was focused on the silent striatal neurons because the drug-induced Ca^{2+} responses were difficult to evaluate in spontaneously active neurons. In the non-lesioned animals, AMPA-induced Ca^{2+} responses, evaluated by the normalized fluorescence ratio, were very variable from one neuron to another, but the average response was small (**Fig. 6A**). In contrast, in the 6-OHDA-lesioned animals, we observed a prolonged increase of the fluorescence ratio in response to AMPA application, showing an increase of Ca^{2+} responses (area under the curve [AUC]: non-lesioned 1.966 $\pm$ 0.264 s.%.10^3, lesioned, 1.2552 $\pm$ 0.609 s.%.10^3, **Fig. 6A right lower panel**). We also found a significant increase in the percentage of responsive cells (non-lesioned 44.2%, n=206/466, lesioned, and 61.2%, n= 120/196, **Fig. 6A right upper panel**). When KCl (25 mM, 30 s) was applied at the end of all experiments, it produced a general and transient activation of all neurons expressing GCaMP6s in the slices (**Fig. 6A-C**). This stimulation allowed us to test the viability of striatal neurons in the brain slices and also to determine the number of cells present and thus the percentage of cells responding to the application of AMPA.

We then determined in which SPN subpopulation(s) the increase in AMPA-induced Ca^{2+} transients occurred in the DA-depleted striatum by microinjecting AAV-flex-GCaMP6s into the striatum of D1Cre mice. In these mice the lesion did not modify the AMPA-induced increase in normalized fluorescence ratio (AUC: non-lesioned, 0.5055 ± 0.0928 s.%.10^4, lesioned, 0.3503 ± 0.0521 s.%.10^4, **Fig. 6B right lower panel**). In addition, no change was detected in the percentage of responsive cells (non-lesioned, 23.8%, n=62/261, lesioned, 25.6%, n= 103/403, **Fig. 6B right upper panel**).

We then microinjected AAV-flex-GCaMP6s into the striatum of $A2_ACre$ mice to selectively study the iSPNs. In these mice, AMPA dramatically increased the normalized fluorescence ratio in 6-OHDA- lesioned compared to non-lesioned mice (AUC: non-lesioned, 0.7619 ± 0.1102 s.%.10^4, lesioned, 0.18379 ± 0.33013 s.%.10^4, **Fig. 6C right lower panel**). In addition, the percentage of AMPA-responsive iSPNs was strongly enhanced (non-lesioned, 57.8%, n=52/90, lesioned, and 83.9%, n= 47/56, **Fig. 6C right upper panel**). These results indicated a high iSPN-specific increase of intracellular Ca^{2+} transients after 6-OHDA lesion.

In conclusion this series of experiments shows that 6-OHDA lesion increases the amplitude of AMPA-induced Ca^{2+} responses and number of responsive cells, and that this effect is selectively taking place in $A2_AR$-expressing cells, presumably iSPNs.

Discussion

Our work, using for the first time 2-photon biosensor imaging in the DA-depleted striatum of adult mice confirms and extends previous observations on signaling dysregulations in the absence of DA. Our results show that DA lesion increases ERK and PKA activation in response to D1 receptors stimulation. Augmented activation of PKA could be accounted for by an increase in Gαolf amplified by deficient phosphodiesterase activity in D1R-expressing neurons. Monitoring Ca^{2+} signals showed an increased spontaneous activity of D1 neurons in lesioned mice and an unexpected hypersensitivity of indirect pathway SPNs to stimulation of AMPA glutamate receptors. Our work reveals distinct cell type-specific signaling alterations in the two populations of SPNs and suggests possible mechanisms for these alterations.

ERK phosphorylation is upregulated after 6-OHDA lesion

In keeping with the literature, we confirmed that ERK activity is upregulated after 6-OHDA lesion, in particular after D1R stimulation as previously shown by several groups (Gerfen *et al.*, 2002; Pavón *et al.*, 2006; Santini *et al.*, 2007, 2009; Westin *et al.*, 2007; Nicholas *et al.*, 2008; Darmopil *et al.*, 2009; Alcacer *et al.*, 2014). The increased amplitude of ERK activity that we found is consistent with a supersensitive D1R pathway. The number of responsive cells to the D1 agonist was not significantly increased and, in our very sensitive experimental conditions, it corresponded to 40% of KCl-responsive cells in non-lesioned and 44% in lesioned animals. Indeed, this is probably close to the maximum of potentially responsive neurons since D1-dSPNs correspond to about 50% of SPNs in the dorsal striatum (Bertran-Gonzalez *et al.*, 2010). Our data indicate that, in the DA-depleted striatum, the increase in ERK responses to D1R stimulation is attributable to greater activation in the vast majority of SPNs, but not to the emergence of a new cell population in which ERK responses to D1R stimulation is exacerbated. A low ERK activation is achieved in the majority of dSPNs in normal conditions and this activation appeared to be highly increased in most dSPNs in the 6-OHDA-lesioned striatum.

We also showed that pharmacological glutamate receptor stimulation, mimicking cortico/thalamo-striatal glutamatergic inputs, can activate ERK in SPNs. Indeed, previous works have shown that corticostriatal stimulation alone, in non-lesioned and lesioned animals, can induce ERK activation in SPNs (Sgambato *et al.*, 1998; Gerfen *et al.*, 2002; Quiroz *et al.*, 2009). We chose to use AMPA since ERK activation does not seem to be NMDAR-dependent after 6-OHDA lesion (Gerfen *et al.*, 2002; Rylander *et al.*, 2009), as opposed to findings in models of drug of abuse (Valjent *et al.*, 2000; Pascoli *et al.*, 2011a). AMPAR-mediated activation of ERK has also been previously reported in SPNs (Perkinton *et al.*, 1999; Mao *et al.*, 2004). Moreover administration of an AMPA agonist has the ability to induce LIDs, whereas blockade of AMPAR reduces LIDs (Konitsiotis *et al.*, 2000; Bibbiani *et al.*, 2005; Kobylecki *et al.*, 2010).

Interestingly, in our study, after glutamate AMPAR stimulation (alone or with a D1R agonist) a trend to an increase in the number of cells showing ERK activation was observed, reaching up to 67% of all SPNs when AMPA was co-administered with a D1R agonist. These results suggest that glutamate-induced ERK activation could be happening in another subtype of

SPN, such as iSPNs. This is in line with previous findings by Gerfen et al. (2002) who found that after DA-depletion, corticostriatal stimulation alone or with co-administration of a D1R agonist could elicit ERK activation in iSPN, identified by histochemical localization of enkephalin mRNA (Gerfen *et al.*, 2002). Corticostriatal involvement in the activation of ERK preferentially in iSPN has also been reported (Ferguson and Robinson, 2004) maybe through adenosine release since it is prevented by $A2_AR$ blockade (Quiroz *et al.*, 2006). Westin et al. (2007) also showed ERK upregulation after DA-depletion could be elicited in iSPN in dyskinetic animals, identified with enkephalin markers (Westin *et al.*, 2007). Interestingly, Santini et al (2009) showed that L-DOPA-induced ERK activation in animals with LIDs was D1R-dependent and occurred only in dSPN, using *Drd1*-GFP and *Drd2*-GFP mice (Santini *et al.*, 2009). These findings suggest that, after DA-depletion, ERK activation induced by AMPAR and D1R stimulation arises in different SPN types , a process that may be similar to that proposed for ERK activation induced by drugs of abuse based on the coincident synergy of glutamate and DA inputs in dSPN (Girault *et al.*, 2007; Pascoli *et al.*, 2011a), except that in the case of corticostriatal or AMPAR stimulation in the DA-depleted striatum, DA may be replaced by endogenous adenosine.

Another interesting point is the kinetics of ERK activation following pharmacological stimulation (see Figure 1). Our approach allowed seeing ERK activation occurring within individual cells seconds after the pharmacological stimulation of different receptors, and reaching a plateau after approximately 6 to 10 minutes and did not return to baseline during our experiments. No specific differences in the kinetics of ERK activation were seen between the non-lesioned and lesioned animals (data not shown). These findings are quite in agreement with previous works using less sensitive approaches, with fixed tissue at specific time points, where maximal ERK signal was found at 10 to 20 min; and then slowly declined from 30 to 45 min and returned to basal levels at 60 min in the intact striatum and at least 120 min in the lesioned striatum (Sgambato *et al.*, 1998; Vanhoutte *et al.*, 1999; Gerfen *et al.*, 2002; Pavón *et al.*, 2006; Westin *et al.*, 2007).

D1R-Gαolf-PKA pathway is upregulated in dSPNs after 6-OHDA lesion

We further investigated the dynamical changes in the upstream signaling pathways leading to ERK activation. We found that, as expected, PKA response was specifically amplified in SPN

responsive to D1R agonist after DA depletion. Since no modification of PKA signaling was observed after $A2_AR$ stimulation, these results suggest the upregulation of PKA signaling occurs in dSPN after DA-depletion and D1R supersensitivity is related to an upregulation of the PKA pathway. This is in agreement with previous studies in which an acute administration of L-DOPA increased the phosphorylation of the PKA targets, DARPP-32 at Thr34 and GluA1 at Ser845 (Santini *et al.*, 2007). This pathway seems to be implicated, at least in part, in ERK upregulation and LIDs intensity. Indeed, PKA signaling appears to be necessary for the intensity of LIDs. Pharmacological intrastriatal inhibition of PKA partially reduces LIDs (Lebel *et al.*, 2010). LIDs and ERK phosphorylation were partially decreased in DARPP-32-KO mice (Santini *et al.*, 2007) and a robust decrease in LIDs was observed in 6-OHDA-lesioned mice with a targeted invalidation of DARPP-32 in dSPNs (Bateup *et al.*, 2010). In keeping with this view, in homozygous Golf-/- mice ERK activation was blocked following treatment by a drug of abuse (Corvol *et al.*, 2007), but ERK upregulation and LIDs were not decreased in heterozygous Golf+/- 6-OHDA lesioned mice (Alcacer *et al.*, 2012). This suggests that PKA is necessary for ERK activation but that its upregulation is not the major mechanism of ERK pathway upregulation.

We further investigated the mechanisms underlying this upregulation of PKA signaling specifically observed in dSPN of DA-depleted mice. The supersensitivity of D1R-PKA pathway is not linked to an increase of D1R as their levels were found to be unchanged or lowered following DA denervation in animal models (Savasta *et al.*, 1988; Herve *et al.*, 1989; Missale *et al.*, 1989; Gerfen *et al.*, 1990; Hervé *et al.*, 1992; Pavón *et al.*, 2006; Hervé, 2011). Analysis in PD patients revealed no significant alteration in D1R expression in the striatum (Nikolaus *et al.*, 2009) but an increase in activation of AC by DA in the striatum (Pifl *et al.*, 1992; Tong *et al.*, 2004). In contrast, we observed increased Gαolf levels after lesion of DA neurons in rats and mice as well as in PD patients. Levels of Gαolf were increased in PD patients and rodents after DA depletion (Hervé *et al.*, 1993; Marcotte *et al.*, 1994; Penit-Soria *et al.*, 1997; Corvol *et al.*, 2004; Alcacer *et al.*, 2012; Ruiz-DeDiego *et al.*, 2015; Morigaki *et al.*, 2017). Therefore, we took advantage of heterozygous *Gnal*+/- mice, which develop and breed normally, and provide a very interesting model because they display a decrease of ≈50% in Gαolf protein levels (Alcacer *et al.*, 2012). We found that DA-depletion in *Gnal*+/- mice reversed the decreased PKA activity

specifically in dSPN. Our results suggest that an increase in Gαolf protein levels after DA-depletion contributes to increased PKA activity.

In line with a preponderant role of Gαolf-dependent pathways, chemogenetic stimulation of dSPNs mimicked, while stimulation of iSPNs abolished, the therapeutic action of L-DOPA in PD mice; with much stronger effects of DREADD activating Gs-type protein than Gq-type (Alcacer *et al.*, 2017). The homeostatic regulation of Gαolf levels is thought to occur through post-translational mechanisms in the striatum, where the altered expression of the Gαolf protein depends directly on its usage rate (Hervé, 2011). The agonist-induced activation of D1R or $A2_AR$ might lead to the degradation of Gαolf protein in striatal SPNs through this usage-dependent mechanism (Hervé *et al.*, 2001; Corvol *et al.*, 2004; Alcacer *et al.*, 2012; Ruiz-DeDiego *et al.*, 2015). In PD, because of DA-depletion, decreased usage of Gαolf could lead to its accumulation. In support of this hypothesis, in D1R KO and $A2_AR$ KO mice a significant increase of Gαolf protein levels was observed without any change in its mRNAs (Hervé *et al.*, 2001). These studies and our results indicate that one of the main factors leading to sensitized D1R-AC-PKA responses to D1R stimulation is the increase of Gαolf levels in dSPNs.

We investigated another key component of PKA regulation, PDEs. Our results suggest that PDE activity was down-regulated specifically in dSPN after DA depletion. Down-regulation in the expression of PDE in the striatum has been reported after DA-depletion in animal models and PD patients (Giorgi *et al.*, 2011; Niccolini *et al.*, 2015, 2017; Heckman *et al.*, 2018). This down-regulation is, consistent with the absence of efficacy of IBMX when co-applied with D1R agonist or FSK in the DA-depleted striatum that can be interpreted as an “occlusion” effect. We suggest that the decrease of PDE associated with an increase in cAMP production is likely to account for the enhanced PKA activity in response to DA or to direct AC stimulation in DA-depleted dSPNs. Preferential activity of specific PDEs remaining active in specific SPN subpopulations, such as PDE10 in iSPN (Nishi *et al.*, 2008), could also participate in this imbalance. Further investigations about which specific PDE subtype(s) could be down-regulated are needed.

Upregulation of Ca^{2+} signaling after glutamate receptors stimulations in SPNs in the DA-depleted striatum

Intracellular Ca^{2+} dynamics have been implicated in ERK activation in many models including C. elegans (Tomida *et al.*, 2012), CA1 pyramidal neurons (Zhai *et al.*, 2013) and DA-depleted SPNs in rodents (Fieblinger *et al.*, 2014b). Since we found that stimulation of AMPA activated ERK in SPNs after 6-OHDA-induced lesion, we investigated if Ca^{2+} dynamics were modified in SPNs. We observed an increase in intracellular Ca^{2+} in the DA-depleted striatum after AMPAR stimulation, indicating an increased SPN reactivity to corticostriatal activity. Ca^{2+} imaging was previously shown to reflect SPNs firing after electrical or glutamatergic stimulation in corticostriatal slices (Carrillo-Reid *et al.*, 2008). Decrease in the threshold current required to evoke responses to cortical stimulation has been reported in SPNs after 6-OHDA-induced lesion and interpreted as an overall hyperexcitability of SPNs to cortical inputs (Nisenbaum and Berger, 1992; Florio *et al.*, 1993). This excitability seems to be decreased by AMPAR antagonists as they reduced 50% of SPN activity in MPTP-lesioned monkeys (Singh *et al.*, 2018). Others have demonstrated that this increased responsiveness only affects iSPNs (Mallet *et al.*, 2006; Flores-Barrera *et al.*, 2010). Conversely, dSPN responsiveness to cortical stimulation was found to be decreased by 10-fold, whereas iSPNs responsiveness was increased and correlated with motor deficit in mice with extensive striatal DA depletion (Escande *et al.*, 2016). Increased AMPAR signaling could be due to increased synaptic expression and altered trafficking of AMPAR (Mangiavacchi and Wolf, 2004; Silverdale *et al.*, 2010). An increased synaptic expression of AMPAR in LID was also suggested by the upregulation of Narp, a secreted protein that clusters AMPAR (Charbonnier-Beaupel *et al.*, 2015). Chronically L-DOPA-treated dyskinetic monkeys showed a marked enrichment of the GluA2/3 subunit (and a trend for the GluA1), in a post-synaptic membrane fraction relative to a cytoplasmic vesicular fraction (Silverdale *et al.*, 2010). This GluA2 enrichment at post-synaptic membranes could more specifically affect the GluA2-flip splice variant as suggested by Kobylecki et al. (2013). Increased expression of this specific splice variant of the GluA2 subunit may suggest slower desensitization and larger amplitude of AMPA-mediated synaptic currents (Kobylecki *et al.*, 2013). A possible mechanism for increased AMPAR signaling is through its phosphorylation by PKA, since serine phosphorylation of GluA1 enhances

channel opening and conductance (Banke *et al.*, 2000; Mangiavacchi and Wolf, 2004). This is however unlikely to explain our observations in iSPNs since cAMP pathway hypersensitivity preferentially happens in D1R-expressing dSPNs after D1R stimulation.

AMPAR-mediated activation of ERK has been previously reported in SPNs through a Ca^{2+}-dependent pathway, possibly via a direct entry through Ca^{2+}-permeable AMPAR (Perkinton *et al.*, 1999; Mao *et al.*, 2004). A functional population of GluA2-lacking Ca^{2+}-permeable receptors in SPNs has been demonstrated (Carter and Sabatini, 2004). Interestingly, in PD, an increased proportion of GluA2-lacking Ca^{2+}-permeable AMPARs at synaptic level was found in lesioned animals after either treatment by L-DOPA or high dose of the D2-agonist pramipexole (Bagetta *et al.*, 2012). These results are in line with those of Kobylecki et al. reporting that administration of an antagonist of Ca^{2+}-permeable AMPAR, IEM 1460, reduced LIDs (Kobylecki *et al.*, 2010). Increased insertion of GluA2-lacking receptors could trigger "abnormal" cellular Ca^{2+} dynamics, increase in related downstream pathways, and eventually pathological synaptic plasticity. Interestingly, dSPNs express higher levels of GluA2 protein than iSPNs (Deng *et al.*, 2007). Hence, the increase in GluA2-lacking AMPAR could preferentially occur in iSPNs and be more visible in this subtype of neurons.

Differences in D1R-PKA signaling in SPNs of young and adult mice

In our hands, PKA activity was reduced in both types of SPNs of non-lesioned adult heterozygous *Gnal*$^{+/-}$ animals. This was expected since these animals show a decrease of ≈50% in Gαolf protein levels leading to decreased cAMP production and decreased activation of PKA targets in both types of SPNs (Corvol *et al.*, 2001; Alcacer *et al.*, 2012). In contrast, a previous study assessing PKA activity using the AKAR3 biosensor in the striatum failed to find any difference between PKA activity in SPNs of *Gnal*$^{+/-}$ mice and their *Gnal*$^{+/+}$ littermates (Castro *et al.*, 2013). This apparent discrepancy is certainly due to differences in the age of the animals used. Indeed, Castro et al (2013) monitored PKA activity in striatal slices from young P8-P12 mice. cAMP is tonically produced in striatal slices and PDEs contribute significantly to its degradation. Castro et al also found a basal PDE activity regulating PKA (Castro *et al.*, 2010; Polito *et al.*, 2015). But the PDE activity in adults could be stronger than in young mice. Indeed, we found that IBMX could further increase the response to FSK in SPNs of adult mice. Castro et al found cAMP production

in response to FSK was only increased by IBMX application in the cortex but not in the striatum of young mice (Castro *et al.*, 2013). This would mean that PDEs in the striatum of young mice are not sufficient to counteract the cAMP production elicited by forskolin.

Another point is the changes of expression of other actors of PKA signaling over development. Indeed, changes in expression of G-protein and AC occur during the postnatal to adult period (Iwamoto *et al.*, 2004). For instance, AC5, an AC inhibited by Ca^{2+}, predominates in the P56 adult brain and AC1, an AC stimulated by Ca^{2+}, has an expression restricted to scattered subset of cells in adults, whereas it is widely distributed in P7 young mice (Visel *et al.*, 2006). AC5 provides around 80% of basal AC activity in the adult striatum (Lee *et al.*, 2002b; Iwamoto *et al.*, 2003). This underlines the importance of working with adult animals when studying adult disorders, to avoid the different changes in signalling pathways occurring during development.

Increased spontaneous intracellular Ca^{2+} transients in SPNs in the DA-depleted striatum

During our Ca^{2+} dynamics experiments we observed that some SPNs are spontaneously active and show transient increases in intracellular Ca^{2+} before any drug application. The same kind of spontaneous activity has been reported by others during Ca^{2+} imaging of SPNs in corticostriatal slices (Jáidar *et al.*, 2010; Carrillo-Reid *et al.*, 2011). We found that these spontaneous intracellular Ca^{2+} transients were increased in the DA-depleted striatum, similarly to previous findings by others (Jáidar *et al.*, 2010). This could be reflecting that, SPNs are more excitable after DA-depletion (Fino *et al.*, 2007). Our preliminary analysis shows that these increased spontaneous Ca^{2+} transients seem to affect more dSPN than iSPN after DA-depletion. Assuming that they reflect an increased intrinsic excitability of SPNs, our results would be compatible with previous electrophysiological results in specific subpopulations of SPN showing that dSPN intrinsic excitability was elevated in a PD model without neuronal scaling of the strength of corticostriatal synapses (Fieblinger *et al.*, 2014a).

Interestingly, Jaidar et al. and Carillo-Reid et al. found that DA deprivation enhances cell assemblies activation, showing activation of a specific network of neurons, engaging into a dominant network state (Carrillo-Reid *et al.*, 2008; Jáidar *et al.*, 2010). This effect could be related to reduced mutual inhibition between SPNs because DA depletion is known to greatly decrease the local axon collaterals of SPNs (Tecuapetla *et al.*, 2005; Taverna *et al.*, 2008).

However the concept of network activation in the striatum, mostly comprised of inhibitory neurons remains to be clarified. Increased spontaneous Ca^{2+} transients could reflect corticostriatal hyperactivity as inhibition of NMDAR or AMPAR reduced the number of active cells and synchrony. However, some neurons remained active even in the presence of both glutamatergic antagonists (Jáidar *et al.*, 2010). This could reflect an increased intrinsic excitability or reactivity to other neurotransmitter modulations in those neurons.

The modulation of these putative striatal networks by DA has been explored and it was reported that activation of either D1R or D2R increased the correlated activity and synchrony of microcircuits in the DA-intact striatum (Carrillo-Reid *et al.*, 2011). After the application of a DA D1R agonist, the non-lesioned striatal network remained hyperactive. Peaks of synchronous activity continued to appear (Jáidar *et al.*, 2010), whereas L-DOPA significantly reduced the enhanced pathological activity of the DA-depleted circuit (Plata *et al.*, 2013). The mechanisms underlying these observations need to be further explored.

In conclusion, our work using 2-photon biosensor imaging in the DA-depleted striatum of adult mice confirms and extends previous observations on signaling dysregulations in the absence of DA. It reveals distinct cell type-specific alterations of cAMP, Ca^{2+} and ERK responses in the two populations of SPNs and suggests possible mechanisms for these alterations. We propose that the existence of altered signaling, with a predominant increase in pathways that normally lead to synaptic plasticity, contributes to the occurrence of later complications of L-DOPA treatment.

Methods

Animals

C57BL/6JRj mice (Janvier Labs; Le Genest Saint Isle, France) were used premature (between 8 and 12 days postnatal) or in adulthood (between 6 and 8 weeks postnatal). Gnal+/- mice ($Gnal^{tm1Rax}$, (Belluscio *et al.*, 1998)) were mated with C57BL/6J mice (Charles River Lab France; L'Arbresle, France) to produce male and female Gnal+/- and Gnal+/+ littermates. Adult D1-Cre [Tg(Drd1a-cre)EY262Gsat, (Gong *et al.*, 2007)] and A2A-Cre [Tg(Adora2a-cre)2MDkde, (Durieux

et al., 2009)] mice in which the Cre recombinase is targeted to neuronal subtypes expressing D1 and $A2_A$ receptor, respectively, were backcrossed for at least 10 generations on a C57Bl/6J background. We also used Drd1-KO mice (D1R-/-, Drd1tm1Jcd, (Drago *et al.*, 1994)) that were kept in a hybrid 129Sv-C57BL6/J background. The mice were genotyped by PCR analysis of genomic DNA using standard PCR protocols. The mice were kept in groups (maximum five per cage) on a 12 h light/dark cycle at a constant temperature of 22°C with access to food and water *ad libitum*. All experiments were in accordance with the guidelines of the French Agriculture and Forestry Ministry for handling animals (decree 87-848). The laboratory animal facility was approved to carry out animal experiments by the Sous-Direction de la Protection Sanitaire et de l'Environnement de la Préfecture de Police (arrêté préfectoral DTPP 2018-20, D 75-05-22). The experimental protocols were approved by the Charles Darwin ethic committee and the Ministère de l'Education Nationale, de l'Enseignement Supérieur et de la Recherche (02635.02 agreement).

6-OHDA lesions, AAV injections and postoperative care

Mice were anesthetized with a mixture of ketamine and xylazine (80 and 10 mg/kg, respectively, 10 ml/kg ip) (Centravet) and mounted in a digitalized stereotactic frame (Stoelting Europe) equipped with a mouse adaptor. 6-OHDA-HCl (6.0 mg/ml; Sigma-Aldrich) was dissolved in a solution containing 0.2 g/L ascorbic acid in saline. AAV virus was diluted (1/5) in the 6-OHDA solution. Mice received a unilateral injection (1.25 µL) of a mix of 6-OHDA and AAV vector into the right striatum at the following coordinates according to a mouse brain atlas (Paxinos and Franklin; 2001): anteroposterior (AP), +0.3 mm from bregma; lateral (L), +2.3 mm; dorsoventral (DV), -3.4 mm. Sham mice were injected with vehicle only (ascorbic acid in saline) in which the AAV virus (5X) was diluted. Before and after surgery, the mice received a subcutaneous injection of a non-steroidal anti-inflammatory drug (flunixin meglumine, 4 mg/kg; Sigma-Aldrich) and were placed on a warm plate (34°C) during about ≈10 h after surgery to avoid hypothermia. Mice were allowed to recover for 3 weeks before sacrifice and brain slicing. Lesions were assessed at the end of experiments by determining the striatal levels of tyrosine hydroxylase (TH) using immunoblotting (see below). DA depletion was analyzed by TH immunofluorescence in a few animals as previously described (Alcacer *et al.*, 2012). Only animals with a TH level

reduction by >80% in the lesioned striatal area compared with the control side were included in the analyses (corresponding to more than 85% of surviving lesioned mice).

Biosensors and viral vectors

The GECI GCaMP6s (Chen *et al.*, 2013), the FRET-based A-kinase activity reporter AKAR3 (Allen and Zhang, 2006) and ERK activity reporter EKAR-EV (Komatsu *et al.*, 2011) were used in the present study.

pAAV.Syn.GCaMP6s.WPRE.SV40 and pAAV.Syn.Flex.GCaMP6s.WPRE.SV40 were a gift from The Genetically Encoded Neuronal Indicator and Effector Project (GENIE) & Douglas Kim (Addgene viral prep # 100843-AAV9 (100µL at titer ≥1.10^{13}vg/mL) and Addgene viral prep # 100845-AAV1 (100µL at titer ≥1.10^{13}vg/mL), respectively).

pAAV.hSyn.AKAR3.WPRE was a gift from Ted Abel's team (UPenn).

For EKAR-EV biosensor, pAAV.hSyn.EKAREV.WPRE was prepared from plasmids provided by GenScript HK (USA) and the AAV was prepared by Ted Abel's team (UPenn) The Sindbis viruses encoding EKARcyto, EKAR2G1 and EKAR-EV were prepared as previously described for Sindbis viruses preparations (Gervasi *et al.*, 2007).

Preparation of brain slices and primary striatal cultures

The animals were anesthetized with a mixture of ketamine and xylazine (80 and 10 mg/kg, respectively, 10 ml/kg ip), following the guidelines of our institution. Then ice-cold "cutting" choline-artificial cerebrospinal fluid (choline-ACSF) solution, containing 110 mM Choline Cl, 0.5 mM $CaCl_2$, 7 mM $MgCl_2$, 1.25 mM NaH_2PO_4, 25 mM $NaHCO_3$, 2.5 mM KCl, 11.6 mM ascorbic acid, 3.1 mM sodium pyruvate and 25 mM glucose, saturated with 5% CO_2 and 95% O_2, was perfused by intracardiac injection. Brains were quickly isolated and placed in ice-cold "cutting" choline-ACSF solution. Sections (250 µm) were made using a vibrating microtome (Thermo Scientific) in a parahorizontal plane as described previously (Kawaguchi et al., 1989; Kita, 1996; Wickens et al. 1998; Fino et al 2005, Smeal et al 2007). After cutting, brain slices were transferred 15 min to recovery in "recording" standard ACSF solution at 35°C, containing 125 mM NaCl, 0.5 to 1 mM $CaCl_2$, 1 mM $MgCl_2$, 1.25 mM NaH_2PO_4, 26 mM $NaHCO_3$, 2.5 mM KCl and

25 mM glucose, saturated with 5% CO_2 and 95% O_2. Brain slices were then kept in a custom-made interface chamber on an optic paper lying on a non-woven compress net that were placed at the interface between the ACSF solution bubbled with 95% O_2/5% CO_2 and incubated for 1 h at room temperature in 95% O_2/5% CO_2 for recovery of the pH and metabolic equilibrium.
Primary striatal cultures were prepared as previously described (Li et al 2015).

Two-photon slice imaging and drugs

On the microscope stage, a nylon/platinum harp stabilized the brain slice while suspended on a nylon mesh to facilitate continuous perfusion over the whole slice at 3 mL/min with ‘‘standard” ACSF at 32°C. Two-photon imaging was performed using an upright Leica TCS MP5 microscope with resonant scanning (8 kHz), a Leica 25X/0.95 HCX IRAPO immersion objective and a tunable Ti:sapphire laser (Coherent Chameleon Vision II) with dispersion correction set to 860 nm for CFP excitation and 920 or 940nm for GFP excitation. The emission path consisted of an initial 700 nm low-pass filter to remove excess excitation light (E700 SP, Chroma Technologies), 506 nm dichroic mirror for orthogonal separation of emitted signal, 479/40 CFP emission filter, 542/50 YFP emission filter (FF506-Di01-25 x 36; FF01-479/40; FF01-542/50; Brightline Filters; Semrock) for AKAR3 and EKAR-EV imaging, and a GFP emission filter for GcAMP6s experiments, and a two-channel Leica HyD detector for simultaneous acquisition. Due to the high quantum efficiency and low dark noise of the HyD photodetectors, detector gain was typically set at 10–20% with laser power at 1–5%. For AKAR3 and EKAR-EV image acquisition, Z-stack images (16-bit; 512 x 512) were typically acquired every 15 s. The z-step size was 1–2 µm and total stack size was typically 40–60 sections depending on the slice (≈ 40–120 µm). For GCaMP6s imaging, z-stack images (12-bits, 512x512) were typically acquired every 1s. The z-step size was 5 µm and total stack size was typically 3 to 5 sections depending on the slice (≈ 10 to 20µm).
Drug solutions were freshly diluted from concentrated stocks in standard ACSF saturated with 95% O_2/5% CO_2 and continuously bubbled during perfusion. (RS)-AMPA hydrobromide (0.5 µM; Tocris), SKF81297 hydrobromide (10 µM, Tocris) and CGS21680 hydrochloride (10 µM, Biotechne) were freshly prepared in ultrapure Milli-Q water. Forskolin (10 mM; Sigma), UO126

(5 µM, Tocris), and IBMX (10-300 mM; 3,7-Dihy dro-1-methyl-3-(2-methylpropyl)-1H-purine-2,6-dione; Tocris) were prepared in 100% DMSO.

Drug application

The imaging chamber on the microscope was continuously perfused with the recording ACSF solution saturated with 95% O2/ 5% CO2 at a rate of 3 ml/min. For bath application, smoothly switching between different reservoirs allowed for changing the bathing solution to a solution containing drugs, without mechanically disturbing the preparation. For more precise application of the drug, the pipette is linked to a Valvebank®4 circuitry (AutoMate Scientific, Inc.) designed for solution-switching use with valve opened at the desired time of compound application with 10 ms accuracy. The pipette holder is mounted onto a micromanipulator, like the ones used for patch-clamp experiment. The pipette is filled with ACSF (Control) or the drug of interest at its final concentration and positioned with the micromanipulator system in close proximity to the slice.

Immunoblotting

At the end of the imaging experiment, striata from both sides were separately dissected from each 250 µm-thick brain slice and were immediately frozen at -80°C. Striata were sonicated in 10 g/L SDS, and placed at 100°C for 5 min. Aliquots (5 µl) of the homogenate were used for protein determination using a bicinchoninic acid assay kit (Pierce Europe). Equal amounts of total protein (20 µg) were separated by SDS-PAGE on 4–15% precast gels (Bio-Rad) and transferred electrophoretically to nitrocellulose membranes (GE Healthcare). The membranes were then incubated in chicken anti-TH (polyclonal, AVES, dilution 1:1000), rabbit anti-GFP (polyclonal, Invitrogen, A-6455) and mouse anti-actin (monoclonal, Sigma-Aldrich, dilution 1:5000) antibodies. Secondary antibodies (1:5000) were IRDye 800CW-conjugated anti-chicken IgG; IRDye 800 CW-conjugated anti-mouse IgG, IRDye 700 CW-conjugated anti-mouse IgG and IRDye 700 CW-conjugated anti-rabbit IgG (Rockland Immunochemical). Bound antibodies were visualized using an Odyssey infrared fluorescence detection system (LI-COR), followed by

quantification by Odyssey version 1.2 software. Fluorescence intensity values were normalized to actin values for variations in loading and transfer.

Image analysis and post-acquisition processing

Images were processed in ImageJ and Icy softwares by using maximum z projections (ICY-A9L7V2) followed by translation and rotation corrections to compensate x/y movements to correct for temporal drift (ICY-E4L7S9). Regions of interest (ROIs), corresponding to neuronal cell bodies, were selected if they could only be measured for the whole experimental time course for AKAR3 and EKAR-EV experiments. For GCaMP6s experiments, ROI were selected if they appeared during the time course of the experiment or after KCl application, as basal GCaMP6s fluorescence are usually low and only increase when a response is observed. ROIs were placed around the periphery of the neuron soma. After ROI placement, raw CFP and YFP or GFP intensity measurements for the entire time course were imported into Microsoft Excel (ICY-Y5X4A1). A fluorescence ratio was calculated for each time point in each ROI series and was normalized to the average baseline ratio for each respective ROI (average of 20 to 30 frames, i.e. 20-30 s for GCaMP6s and 5-7.5 min for AKAR3 and EKAR-EV, during the period before first stimulus) as ΔR [YFP/CFP]/R0 for AKAR3 or EKAR-EV experiments and ΔF/F0 for GCaMP6s experiments. For each ROI, peak amplitudes were determined by finding the maximum point during the stimulus interval (e.g. treatment), and taking the average of 5 to 7 points on either side of the max (average of 10 to 15 points total). For each ROI, the rise time was determined by measuring the maximum slope over 4–5 points of the rising phase. If amplitude of the fluorescent signal (ΔF/F0) increased over > 3 standard deviation (SD) (i) during baseline recording, the cell was considered as “spontaneously active” or (ii) after pharmacological stimulation, the cell was considered as “responsive to treatment”.

Statistical methods

Statistical analysis was performed in Matlab and GraphPad Prism. Categorical variables are expressed as the ratio of the number of responsive cells to a stimulus over the total number of cells assessed and as percentages [n/N (%)]; and continuous variables as mean ± SEM. Quantitative variables were compared using a one-way analysis of variance (ANOVA) followed

by Holm-Sidak's multiple comparison test in case of Gaussian distribution, or Kruskall-Wallis test followed by Dunn's multiple comparison test in case of non-Gaussian distribution, when there were three or more groups. Two-tailed, unpaired Student t-test in case of Gaussian distribution, or Mann-Whitney test in case of non-Gaussian distribution, was used to compare quantitative variables when two groups were compared. Categorical variables were compared using the chi-square test or with Fisher exact test when numbers were too small.

References

Albin RL, Young AB, Penney JB. The functional anatomy of basal ganglia disorders. Trends Neurosci. 1989; 12: 366–375.

Alcacer C, Andreoli L, Sebastianutto I, Jakobsson J, Fieblinger T, Cenci MA. Chemogenetic stimulation of striatal projection neurons modulates responses to Parkinson's disease therapy. J. Clin. Invest. 2017; 127: 720–734.

Alcacer C, Charbonnier-Beaupel F, Corvol J-C, Girault J-A, Hervé D. Mitogen- and stress-activated protein kinase 1 is required for specific signaling responses in dopamine-denervated mouse striatum, but is not necessary for L-DOPA-induced dyskinesia. Neurosci. Lett. 2014; 583: 76–80.

Alcacer C, Santini E, Valjent E, Gaven F, Girault J-A, Hervé D. Gα(olf) mutation allows parsing the role of cAMP-dependent and extracellular signal-regulated kinase-dependent signaling in L-3,4-dihydroxyphenylalanine-induced dyskinesia. J. Neurosci. Off. J. Soc. Neurosci. 2012; 32: 5900–5910.

Alexander GE, Crutcher MD. Functional architecture of basal ganglia circuits: neural substrates of parallel processing. Trends Neurosci. 1990; 13: 266–271.

Allen MD, Zhang J. Subcellular dynamics of protein kinase A activity visualized by FRET-based reporters. Biochem. Biophys. Res. Commun. 2006; 348: 716–721.

Bagetta V, Sgobio C, Pendolino V, Del Papa G, Tozzi A, Ghiglieri V, et al. Rebalance of striatal NMDA/AMPA receptor ratio underlies the reduced emergence of dyskinesia during D2-like dopamine agonist treatment in experimental Parkinson's disease. J. Neurosci. Off. J. Soc. Neurosci. 2012; 32: 17921–17931.

Banke TG, Bowie D, Lee H, Huganir RL, Schousboe A, Traynelis SF. Control of GluR1 AMPA receptor function by cAMP-dependent protein kinase. J. Neurosci. Off. J. Soc. Neurosci. 2000; 20: 89–102.

Bateup HS, Santini E, Shen W, Birnbaum S, Valjent E, Surmeier DJ, et al. Distinct subclasses of medium spiny neurons differentially regulate striatal motor behaviors. Proc. Natl. Acad. Sci. U. S. A. 2010; 107: 14845–14850.

Bateup HS, Svenningsson P, Kuroiwa M, Gong S, Nishi A, Heintz N, et al. Cell type-specific regulation of DARPP-32 phosphorylation by psychostimulant and antipsychotic drugs. Nat. Neurosci. 2008; 11: 932–939.

Belluscio L, Gold GH, Nemes A, Axel R. Mice deficient in G(olf) are anosmic. Neuron 1998; 20: 69–81.

Bertran-Gonzalez J, Bosch C, Maroteaux M, Matamales M, Hervé D, Valjent E, et al. Opposing patterns of signaling activation in dopamine D1 and D2 receptor-expressing striatal neurons in response to cocaine and haloperidol. J. Neurosci. Off. J. Soc. Neurosci. 2008; 28: 5671–5685.

Bertran-Gonzalez J, Hervé D, Girault J-A, Valjent E. What is the Degree of Segregation between Striatonigral and Striatopallidal Projections? Front. Neuroanat. 2010; 4

Bibbiani F, Oh JD, Kielaite A, Collins MA, Smith C, Chase TN. Combined blockade of AMPA and NMDA glutamate receptors reduces levodopa-induced motor complications in animal models of PD. Exp. Neurol. 2005; 196: 422–429.

Carrillo-Reid L, Hernández-López S, Tapia D, Galarraga E, Bargas J. Dopaminergic modulation of the striatal microcircuit: receptor-specific configuration of cell assemblies. J. Neurosci. Off. J. Soc. Neurosci. 2011; 31: 14972–14983.

Carrillo-Reid L, Tecuapetla F, Tapia D, Hernández-Cruz A, Galarraga E, Drucker-Colin R, et al. Encoding network states by striatal cell assemblies. J. Neurophysiol. 2008; 99: 1435–1450.

Carter AG, Sabatini BL. State-dependent calcium signaling in dendritic spines of striatal medium spiny neurons. Neuron 2004; 44: 483–493.

Castro LRV, Brito M, Guiot E, Polito M, Korn CW, Hervé D, et al. Striatal neurones have a specific ability to respond to phasic dopamine release. J. Physiol. 2013; 591: 3197–3214.

Castro LRV, Gervasi N, Guiot E, Cavellini L, Nikolaev VO, Paupardin-Tritsch D, et al. Type 4 phosphodiesterase plays different integrating roles in different cellular domains in pyramidal cortical neurons. J. Neurosci. Off. J. Soc. Neurosci. 2010; 30: 6143–6151.

Cenci MA, Konradi C. Maladaptive striatal plasticity in L-DOPA-induced dyskinesia. Prog. Brain Res. 2010; 183: 209–233.

Charbonnier-Beaupel F, Malerbi M, Alcacer C, Tahiri K, Carpentier W, Wang C, et al. Gene expression analyses identify Narp contribution in the development of L-DOPA-induced dyskinesia. J. Neurosci. Off. J. Soc. Neurosci. 2015; 35: 96–111.

Chen T-W, Wardill TJ, Sun Y, Pulver SR, Renninger SL, Baohan A, et al. Ultrasensitive fluorescent proteins for imaging neuronal activity. Nature 2013; 499: 295–300.

Corvol J-C, Muriel M-P, Valjent E, Féger J, Hanoun N, Girault J-A, et al. Persistent increase in olfactory type G-protein alpha subunit levels may underlie D1 receptor functional hypersensitivity in Parkinson disease. J. Neurosci. Off. J. Soc. Neurosci. 2004; 24: 7007–7014.

Corvol JC, Studler JM, Schonn JS, Girault JA, Hervé D. Galpha(olf) is necessary for coupling D1 and A2a receptors to adenylyl cyclase in the striatum. J. Neurochem. 2001; 76: 1585–1588.

Corvol J-C, Valjent E, Pascoli V, Robin A, Stipanovich A, Luedtke RR, et al. Quantitative changes in Galphaolf protein levels, but not D1 receptor, alter specifically acute responses to psychostimulants. Neuropsychopharmacol. Off. Publ. Am. Coll. Neuropsychopharmacol. 2007; 32: 1109–1121.

Darmopil S, Martín AB, De Diego IR, Ares S, Moratalla R. Genetic inactivation of dopamine D1 but not D2 receptors inhibits L-DOPA-induced dyskinesia and histone activation. Biol. Psychiatry 2009; 66: 603–613.

DeLong MR. Primate models of movement disorders of basal ganglia origin. Trends Neurosci. 1990; 13: 281–285.

Deng YP, Xie JP, Wang HB, Lei WL, Chen Q, Reiner A. Differential localization of the GluR1 and GluR2 subunits of the AMPA-type glutamate receptor among striatal neuron types in rats. J. Chem. Neuroanat. 2007; 33: 167–192.

Drago J, Gerfen CR, Lachowicz JE, Steiner H, Hollon TR, Love PE, et al. Altered striatal function in a mutant mouse lacking D1A dopamine receptors. Proc. Natl. Acad. Sci. U. S. A. 1994; 91: 12564–12568.

Dunah AW, Wang Y, Yasuda RP, Kameyama K, Huganir RL, Wolfe BB, et al. Alterations in subunit expression, composition, and phosphorylation of striatal N-methyl-D-aspartate glutamate receptors in a rat 6-hydroxydopamine model of Parkinson's disease. Mol. Pharmacol. 2000; 57: 342–352.

Durieux PF, Bearzatto B, Guiducci S, Buch T, Waisman A, Zoli M, et al. D2R striatopallidal neurons inhibit both locomotor and drug reward processes. Nat. Neurosci. 2009; 12: 393–395.

Escande MV, Taravini IRE, Zold CL, Belforte JE, Murer MG. Loss of Homeostasis in the Direct Pathway in a Mouse Model of Asymptomatic Parkinson's Disease. J. Neurosci. Off. J. Soc. Neurosci. 2016; 36: 5686–5698.

Fasano S, Bezard E, D'Antoni A, Francardo V, Indrigo M, Qin L, et al. Inhibition of Ras-guanine nucleotide-releasing factor 1 (Ras-GRF1) signaling in the striatum reverts motor symptoms associated with L-dopa-induced dyskinesia. Proc. Natl. Acad. Sci. U. S. A. 2010; 107: 21824–21829.

Ferguson SM, Robinson TE. Amphetamine-evoked gene expression in striatopallidal neurons: regulation by corticostriatal afferents and the ERK/MAPK signaling cascade. J. Neurochem. 2004; 91: 337–348.

Fieblinger T, Graves SM, Sebel LE, Alcacer C, Plotkin JL, Gertler TS, et al. Cell type-specific plasticity of striatal projection neurons in parkinsonism and L-DOPA-induced dyskinesia. Nat. Commun. 2014a; 5: 5316.

Fieblinger T, Sebastianutto I, Alcacer C, Bimpisidis Z, Maslava N, Sandberg S, et al. Mechanisms of dopamine D1 receptor-mediated ERK1/2 activation in the parkinsonian striatum and their modulation by metabotropic glutamate receptor type 5. J. Neurosci. Off. J. Soc. Neurosci. 2014b; 34: 4728–4740.

Fino E, Glowinski J, Venance L. Effects of acute dopamine depletion on the electrophysiological properties of striatal neurons. Neurosci. Res. 2007; 58: 305–316.

Fiorentini C, Rizzetti MC, Busi C, Bontempi S, Collo G, Spano P, et al. Loss of synaptic D1 dopamine/N-methyl-D-aspartate glutamate receptor complexes in L-DOPA-induced dyskinesia in the rat. Mol. Pharmacol. 2006; 69: 805–812.

Flores-Barrera E, Vizcarra-Chacón BJ, Tapia D, Bargas J, Galarraga E. Different corticostriatal integration in spiny projection neurons from direct and indirect pathways. Front. Syst. Neurosci. 2010; 4: 15.

Florio T, Di Loreto S, Cerrito F, Scarnati E. Influence of prelimbic and sensorimotor cortices on striatal neurons in the rat: electrophysiological evidence for converging inputs and the effects of 6-OHDA-induced degeneration of the substantia nigra. Brain Res. 1993; 619: 180–188.

Fritz RD, Letzelter M, Reimann A, Martin K, Fusco L, Ritsma L, et al. A versatile toolkit to produce sensitive FRET biosensors to visualize signaling in time and space. Sci. Signal. 2013; 6: rs12.

Gardoni F, Picconi B, Ghiglieri V, Polli F, Bagetta V, Bernardi G, et al. A critical interaction between NR2B and MAGUK in L-DOPA induced dyskinesia. J. Neurosci. Off. J. Soc. Neurosci. 2006; 26: 2914–2922.

Gerfen CR, Engber TM, Mahan LC, Susel Z, Chase TN, Monsma FJ, et al. D1 and D2 dopamine receptor-regulated gene expression of striatonigral and striatopallidal neurons. Science 1990; 250: 1429–1432.

Gerfen CR, Miyachi S, Paletzki R, Brown P. D1 dopamine receptor supersensitivity in the dopamine-depleted striatum results from a switch in the regulation of ERK1/2/MAP kinase. J. Neurosci. Off. J. Soc. Neurosci. 2002; 22: 5042–5054.

Gerfen CR, Surmeier DJ. Modulation of striatal projection systems by dopamine. Annu. Rev. Neurosci. 2011; 34: 441–466.

Gervasi N, Hepp R, Tricoire L, Zhang J, Lambolez B, Paupardin-Tritsch D, et al. Dynamics of protein kinase A signaling at the membrane, in the cytosol, and in the nucleus of neurons in mouse brain slices. J. Neurosci. Off. J. Soc. Neurosci. 2007; 27: 2744–2750.

Gervasi N, Tchénio P, Preat T. PKA dynamics in a Drosophila learning center: coincidence detection by rutabaga adenylyl cyclase and spatial regulation by dunce phosphodiesterase. Neuron 2010; 65: 516–529.

Giorgi M, Melchiorri G, Nuccetelli V, D'Angelo V, Martorana A, Sorge R, et al. PDE10A and PDE10A-dependent cAMP catabolism are dysregulated oppositely in striatum and nucleus accumbens after lesion of midbrain dopamine neurons in rat: a key step in parkinsonism physiopathology. Neurobiol. Dis. 2011; 43: 293–303.

Girault J-A, Valjent E, Caboche J, Hervé D. ERK2: a logical AND gate critical for drug-induced plasticity? Curr. Opin. Pharmacol. 2007; 7: 77–85.

Gong S, Doughty M, Harbaugh CR, Cummins A, Hatten ME, Heintz N, et al. Targeting Cre recombinase to specific neuron populations with bacterial artificial chromosome constructs. J. Neurosci. Off. J. Soc. Neurosci. 2007; 27: 9817–9823.

Harvey CD, Ehrhardt AG, Cellurale C, Zhong H, Yasuda R, Davis RJ, et al. A genetically encoded fluorescent sensor of ERK activity. Proc. Natl. Acad. Sci. U. S. A. 2008; 105: 19264–19269.

Heckman PRA, Blokland A, Bollen EPP, Prickaerts J. Phosphodiesterase inhibition and modulation of corticostriatal and hippocampal circuits: Clinical overview and translational considerations. Neurosci. Biobehav. Rev. 2018; 87: 233–254.

Hepp R, Tricoire L, Hu E, Gervasi N, Paupardin-Tritsch D, Lambolez B, et al. Phosphodiesterase type 2 and the homeostasis of cyclic GMP in living thalamic neurons. J. Neurochem. 2007; 102: 1875–1886.

Hervé D. Identification of a specific assembly of the g protein golf as a critical and regulated module of dopamine and adenosine-activated cAMP pathways in the striatum. Front. Neuroanat. 2011; 5: 48.

Hervé D, Le Moine C, Corvol JC, Belluscio L, Ledent C, Fienberg AA, et al. Galpha(olf) levels are regulated by receptor usage and control dopamine and adenosine action in the striatum. J. Neurosci. Off. J. Soc. Neurosci. 2001; 21: 4390–4399.

Hervé D, Lévi-Strauss M, Marey-Semper I, Verney C, Tassin JP, Glowinski J, et al. G(olf) and Gs in rat basal ganglia: possible involvement of G(olf) in the coupling of dopamine D1 receptor with adenylyl cyclase. J. Neurosci. Off. J. Soc. Neurosci. 1993; 13: 2237–2248.

Hervé D, Trovero F, Blanc G, Glowinski J, Tassin JP. Autoradiographic identification of D1 dopamine receptors labelled with [3H]dopamine: distribution, regulation and relationship to coupling. Neuroscience 1992; 46: 687–700.

Herve D, Trovero F, Blanc G, Thierry AM, Glowinski J, Tassin JP. Nondopaminergic prefrontocortical efferent fibers modulate D1 receptor denervation supersensitivity in specific regions of the rat striatum. J. Neurosci. Off. J. Soc. Neurosci. 1989; 9: 3699–3708.

Iwamoto T, Iwatsubo K, Okumura S, Hashimoto Y, Tsunematsu T, Toya Y, et al. Disruption of type 5 adenylyl cyclase negates the developmental increase in Galphaolf expression in the striatum. FEBS Lett. 2004; 564: 153–156.

Iwamoto T, Okumura S, Iwatsubo K, Kawabe J-I, Ohtsu K, Sakai I, et al. Motor dysfunction in type 5 adenylyl cyclase-null mice. J. Biol. Chem. 2003; 278: 16936–16940.

Jáidar O, Carrillo-Reid L, Hernández A, Drucker-Colín R, Bargas J, Hernández-Cruz A. Dynamics of the Parkinsonian striatal microcircuit: entrainment into a dominant network state. J. Neurosci. Off. J. Soc. Neurosci. 2010; 30: 11326–11336.

Kobylecki C, Cenci MA, Crossman AR, Ravenscroft P. Calcium-permeable AMPA receptors are involved in the induction and expression of l-DOPA-induced dyskinesia in Parkinson's disease. J. Neurochem. 2010; 114: 499–511.

Kobylecki C, Crossman AR, Ravenscroft P. Alternative splicing of AMPA receptor subunits in the 6-OHDA-lesioned rat model of Parkinson's disease and L-DOPA-induced dyskinesia. Exp. Neurol. 2013; 247: 476–484.

Komatsu N, Aoki K, Yamada M, Yukinaga H, Fujita Y, Kamioka Y, et al. Development of an optimized backbone of FRET biosensors for kinases and GTPases. Mol. Biol. Cell 2011; 22: 4647–4656.

Konitsiotis S, Blanchet PJ, Verhagen L, Lamers E, Chase TN. AMPA receptor blockade improves levodopa-induced dyskinesia in MPTP monkeys. Neurology 2000; 54: 1589–1595.

Kravitz AV, Freeze BS, Parker PRL, Kay K, Thwin MT, Deisseroth K, et al. Regulation of parkinsonian motor behaviours by optogenetic control of basal ganglia circuitry. Nature 2010; 466: 622–626.

Lebel M, Chagniel L, Bureau G, Cyr M. Striatal inhibition of PKA prevents levodopa-induced behavioural and molecular changes in the hemiparkinsonian rat. Neurobiol. Dis. 2010; 38: 59–67.

Lee K-W, Hong J-H, Choi IY, Che Y, Lee J-K, Yang S-D, et al. Impaired D2 dopamine receptor function in mice lacking type 5 adenylyl cyclase. J. Neurosci. Off. J. Soc. Neurosci. 2002; 22: 7931–7940.

Le Moine C, Bloch B. D1 and D2 dopamine receptor gene expression in the rat striatum: sensitive cRNA probes demonstrate prominent segregation of D1 and D2 mRNAs in distinct neuronal populations of the dorsal and ventral striatum. J. Comp. Neurol. 1995; 355: 418–426.

Luczak V, Blackwell KT, Abel T, Girault J-A, Gervasi N. Dendritic diameter influences the rate and magnitude of hippocampal cAMP and PKA transients during β-adrenergic receptor activation. Neurobiol. Learn. Mem. 2017; 138: 10–20.

Mallet N, Ballion B, Le Moine C, Gonon F. Cortical inputs and GABA interneurons imbalance projection neurons in the striatum of parkinsonian rats. J. Neurosci. Off. J. Soc. Neurosci. 2006; 26: 3875–3884.

Mangiavacchi S, Wolf ME. D1 dopamine receptor stimulation increases the rate of AMPA receptor insertion onto the surface of cultured nucleus accumbens neurons through a pathway dependent on protein kinase A. J. Neurochem. 2004; 88: 1261–1271.

Mao L, Tang Q, Samdani S, Liu Z, Wang JQ. Regulation of MAPK/ERK phosphorylation via ionotropic glutamate receptors in cultured rat striatal neurons. Eur. J. Neurosci. 2004; 19: 1207–1216.

Marcotte ER, Sullivan RM, Mishra RK. Striatal G-proteins: effects of unilateral 6-hydroxydopamine lesions. Neurosci. Lett. 1994; 169: 195–198.

Marshall JF, Navarrete R, Joyce JN. Decreased striatal D1 binding density following mesotelencephalic 6-hydroxydopamine injections: an autoradiographic analysis. Brain Res. 1989; 493: 247–257.

Missale C, Nisoli E, Liberini P, Rizzonelli P, Memo M, Buonamici M, et al. Repeated reserpine administration up-regulates the transduction mechanisms of D1 receptors without changing the density of [3H]SCH 23390 binding. Brain Res. 1989; 483: 117–122.

Morigaki R, Okita S, Goto S. Dopamine-Induced Changes in Gαolf Protein Levels in Striatonigral and Striatopallidal Medium Spiny Neurons Underlie the Genesis of l-DOPA-Induced Dyskinesia in Parkinsonian Mice. Front. Cell. Neurosci. 2017; 11: 26.

Niccolini F, Foltynie T, Reis Marques T, Muhlert N, Tziortzi AC, Searle GE, et al. Loss of phosphodiesterase 10A expression is associated with progression and severity in Parkinson's disease. Brain J. Neurol. 2015; 138: 3003–3015.

Niccolini F, Wilson H, Pagano G, Coello C, Mehta MA, Searle GE, et al. Loss of phosphodiesterase 4 in Parkinson disease: Relevance to cognitive deficits. Neurology 2017; 89: 586–593.

Nicholas AP, Lubin FD, Hallett PJ, Vattem P, Ravenscroft P, Bezard E, et al. Striatal histone modifications in models of levodopa-induced dyskinesia. J. Neurochem. 2008; 106: 486–494.

Nikolaus S, Antke C, Müller H-W. In vivo imaging of synaptic function in the central nervous system: I. Movement disorders and dementia. Behav. Brain Res. 2009; 204: 1–31.

Nisenbaum ES, Berger TW. Functionally distinct subpopulations of striatal neurons are differentially regulated by GABAergic and dopaminergic inputs--I. In vivo analysis. Neuroscience 1992; 48: 561–578.

Nishi A, Kuroiwa M, Miller DB, O'Callaghan JP, Bateup HS, Shuto T, et al. Distinct roles of PDE4 and PDE10A in the regulation of cAMP/PKA signaling in the striatum. J. Neurosci. Off. J. Soc. Neurosci. 2008; 28: 10460–10471.

Oh JD, Russell DS, Vaughan CL, Chase TN, Russell D. Enhanced tyrosine phosphorylation of striatal NMDA receptor subunits: effect of dopaminergic denervation and L-DOPA administration. Brain Res. 1998; 813: 150–159.

Park H-Y, Kang Y-M, Kang Y, Park T-S, Ryu Y-K, Hwang J-H, et al. Inhibition of adenylyl cyclase type 5 prevents L-DOPA-induced dyskinesia in an animal model of Parkinson's disease. J. Neurosci. Off. J. Soc. Neurosci. 2014; 34: 11744–11753.

Pascoli V, Besnard A, Hervé D, Pagès C, Heck N, Girault J-A, et al. Cyclic adenosine monophosphate-independent tyrosine phosphorylation of NR2B mediates cocaine-induced extracellular signal-regulated kinase activation. Biol. Psychiatry 2011; 69: 218–227.

Pavón N, Martín AB, Mendialdua A, Moratalla R. ERK phosphorylation and FosB expression are associated with L-DOPA-induced dyskinesia in hemiparkinsonian mice. Biol. Psychiatry 2006; 59: 64–74.

Penit-Soria J, Durand C, Besson MJ, Herve D. Levels of stimulatory G protein are increased in the rat striatum after neonatal lesion of dopamine neurons. Neuroreport 1997; 8: 829–833.

Perkinton MS, Sihra TS, Williams RJ. Ca(2+)-permeable AMPA receptors induce phosphorylation of cAMP response element-binding protein through a phosphatidylinositol 3-kinase-dependent stimulation of the mitogen-activated protein kinase signaling cascade in neurons. J. Neurosci. Off. J. Soc. Neurosci. 1999; 19: 5861–5874.

Pifl C, Nanoff C, Schingnitz G, Schütz W, Hornykiewicz O. Sensitization of dopamine-stimulated adenylyl cyclase in the striatum of 1-methyl-4-phenyl-1,2,3,6-tetrahydropyridine-treated rhesus monkeys and patients with idiopathic Parkinson's disease. J. Neurochem. 1992; 58: 1997–2004.

Plata V, Duhne M, Pérez-Ortega JE, Barroso-Flores J, Galarraga E, Bargas J. Direct evaluation of L-DOPA actions on neuronal activity of Parkinsonian tissue in vitro. BioMed Res. Int. 2013; 2013: 519184.

Polito M, Guiot E, Gangarossa G, Longueville S, Doulazmi M, Valjent E, et al. Selective Effects of PDE10A Inhibitors on Striatopallidal Neurons Require Phosphatase Inhibition by DARPP-32. eNeuro 2015; 2

Quiroz C, Gomes C, Pak AC, Ribeiro JA, Goldberg SR, Hope BT, et al. Blockade of adenosine A2A receptors prevents protein phosphorylation in the striatum induced by cortical stimulation. J. Neurosci. Off. J. Soc. Neurosci. 2006; 26: 10808–10812.

Quiroz C, Luján R, Uchigashima M, Simoes AP, Lerner TN, Borycz J, et al. Key modulatory role of presynaptic adenosine A2A receptors in cortical neurotransmission to the striatal direct pathway. ScientificWorldJournal 2009; 9: 1321–1344.

Redgrave P, Rodriguez M, Smith Y, Rodriguez-Oroz MC, Lehericy S, Bergman H, et al. Goal-directed and habitual control in the basal ganglia: implications for Parkinson's disease. Nat. Rev. Neurosci. 2010; 11: 760–772.

Ruiz-DeDiego I, Naranjo JR, Hervé D, Moratalla R. Dopaminergic regulation of olfactory type G-protein α subunit expression in the striatum. Mov. Disord. Off. J. Mov. Disord. Soc. 2015; 30: 1039–1049.

Rylander D, Recchia A, Mela F, Dekundy A, Danysz W, Cenci MA. Pharmacological modulation of glutamate transmission in a rat model of L-DOPA-induced dyskinesia: effects on motor behavior and striatal nuclear signaling. J. Pharmacol. Exp. Ther. 2009; 330: 227–235.

Santini E, Alcacer C, Cacciatore S, Heiman M, Hervé D, Greengard P, et al. L-DOPA activates ERK signaling and phosphorylates histone H3 in the striatonigral medium spiny neurons of hemiparkinsonian mice. J. Neurochem. 2009; 108: 621–633.

Santini E, Valjent E, Usiello A, Carta M, Borgkvist A, Girault J-A, et al. Critical involvement of cAMP/DARPP-32 and extracellular signal-regulated protein kinase signaling in L-DOPA-induced dyskinesia. J. Neurosci. Off. J. Soc. Neurosci. 2007; 27: 6995–7005.

Savasta M, Dubois A, Benavidès J, Scatton B. Different plasticity changes in D1 and D2 receptors in rat striatal subregions following impairment of dopaminergic transmission. Neurosci. Lett. 1988; 85: 119–124.

Sgambato-Faure V, Cenci MA. Glutamatergic mechanisms in the dyskinesias induced by pharmacological dopamine replacement and deep brain stimulation for the treatment of Parkinson's disease. Prog. Neurobiol. 2012; 96: 69–86.

Sgambato V, Pagès C, Rogard M, Besson MJ, Caboche J. Extracellular signal-regulated kinase (ERK) controls immediate early gene induction on corticostriatal stimulation. J. Neurosci. Off. J. Soc. Neurosci. 1998; 18: 8814–8825.

Silverdale MA, Kobylecki C, Hallett PJ, Li Q, Dunah AW, Ravenscroft P, et al. Synaptic recruitment of AMPA glutamate receptor subunits in levodopa-induced dyskinesia in the MPTP-lesioned nonhuman primate. Synap. N. Y. N 2010; 64: 177–180.

Singh A, Jenkins MA, Burke KJ, Beck G, Jenkins A, Scimemi A, et al. Glutamatergic Tuning of Hyperactive Striatal Projection Neurons Controls the Motor Response to Dopamine Replacement in Parkinsonian Primates. Cell Rep. 2018; 22: 941–952.

Taverna S, Ilijic E, Surmeier DJ. Recurrent collateral connections of striatal medium spiny neurons are disrupted in models of Parkinson's disease. J. Neurosci. Off. J. Soc. Neurosci. 2008; 28: 5504–5512.

Tecuapetla F, Carrillo-Reid L, Guzmán JN, Galarraga E, Bargas J. Different inhibitory inputs onto neostriatal projection neurons as revealed by field stimulation. J. Neurophysiol. 2005; 93: 1119–1126.

Tomida T, Oda S, Takekawa M, Iino Y, Saito H. The temporal pattern of stimulation determines the extent and duration of MAPK activation in a Caenorhabditis elegans sensory neuron. Sci. Signal. 2012; 5: ra76.

Tong J, Fitzmaurice PS, Ang LC, Furukawa Y, Guttman M, Kish SJ. Brain dopamine-stimulated adenylyl cyclase activity in Parkinson's disease, multiple system atrophy, and progressive supranuclear palsy. Ann. Neurol. 2004; 55: 125–129.

Tricoire L, Lambolez B. Neuronal network imaging in acute slices using Ca2+ sensitive bioluminescent reporter. Methods Mol. Biol. Clifton NJ 2014; 1098: 33–45.

Valjent E, Corvol JC, Pages C, Besson MJ, Maldonado R, Caboche J. Involvement of the extracellular signal-regulated kinase cascade for cocaine-rewarding properties. J. Neurosci. Off. J. Soc. Neurosci. 2000; 20: 8701–8709.

Vanhoutte P, Barnier JV, Guibert B, Pagès C, Besson MJ, Hipskind RA, et al. Glutamate induces phosphorylation of Elk-1 and CREB, along with c-fos activation, via an extracellular signal-regulated kinase-dependent pathway in brain slices. Mol. Cell. Biol. 1999; 19: 136–146.

Visel A, Alvarez-Bolado G, Thaller C, Eichele G. Comprehensive analysis of the expression patterns of the adenylate cyclase gene family in the developing and adult mouse brain. J. Comp. Neurol. 2006; 496: 684–697.

Westin JE, Vercammen L, Strome EM, Konradi C, Cenci MA. Spatiotemporal pattern of striatal ERK1/2 phosphorylation in a rat model of L-DOPA-induced dyskinesia and the role of dopamine D1 receptors. Biol. Psychiatry 2007; 62: 800–810.

Yapo C, Nair AG, Clement L, Castro LR, Hellgren Kotaleski J, Vincent P. Detection of phasic dopamine by D1 and D2 striatal medium spiny neurons. J. Physiol. 2017; 595: 7451–7475.

Zhai S, Ark ED, Parra-Bueno P, Yasuda R. Long-distance integration of nuclear ERK signaling triggered by activation of a few dendritic spines. Science 2013; 342: 1107–1111.

Zhuang X, Belluscio L, Hen R. G(olf)alpha mediates dopamine D1 receptor signaling. J. Neurosci. Off. J. Soc. Neurosci. 2000; 20: RC91.

Figure legends

Figure 1. Quantitative real-time analysis of ERK activity dynamics with single cell resolution in neurons in culture and brain slices.

(A) EKARcyto, EKAR2G1 or EKAR-EV biosensors are transfected into striatal neurons in culture (DIV 7) using lipofectamine. Comparison of ERK responses in striatal neurons after application of brain-derived neurotrophic factor (BDNF) (10 ng/mL) for 5 min. Representative examples (left), time courses (middle) and maximal responses (ΔR/R0 in %, right) of FRET emission ratio. EKAR-EV shows a higher FRET signal increase than EKARcyto or EKAR2G1. **(B)** EKAR-EV biosensor is transduced in striatal slice preparations from neonatal mice (P8-P12) using a recombinant Sindbis virus. Examples (left) and time course of response to KCl 25 mM, 30s (middle). In right panel, maximal responses induced by AMPA (5 µM, 30s) and KCl (25 mM, 30s) are compared. In (**C-E**), EKAR-EV biosensor was expressed in striatal neurons of adult mice using a recombinant AAV microinjected into the striatum. Examples **(C)**, time courses **(D)** and maximal amplitudes **(E)** of FRET signal responses to sequential application of SKF (10 µM, 30 s) and KCl (25 mM, 30 s) as well as their blocade by U0126 (5 µM), a selective inhibitor of MEK1/2.

Figure 2. ERK responses are increased after dopamine depletion induced by 6-OHDA lesion

(A) General experimental set up. 4-6 week-old mice were injected with a solution containing the biosensor-expressing AAV with or without 6-OHDA in the right striatum. After 3 to 5 weeks recovery, multiphoton imaging is performed on parahorizontal acute corticostriatal slices. At the end of each experiment, striata are extracted for TH quantification by western blot (right upper pannel). In a few mice, loss of DA terminals is checked by TH immunofluorescence (middle upper panel). Maximal responses (ΔR/R0) of FRET emission ratio (**B**) and percentages of responsive cells (**D**) after 30 s-applications of AMPA (5 µM), SKF81297 (10 µM) or both in 6-OHDA-lesioned and control striata. Maximal responses (ΔR/R0) of FRET emission ratio (**C**) and percentages of responsive cells (**D**) after applications of ACSF (30 s) or KCl (25 mM, 30 s) in 6-OHDA-lesioned and control striata. Maximal ERK responses induced by SKF81297 or the combination of AMPA and SKF81297 are increased after DA-depletion **(B)**. The number of cells that respond to co-application of SKF81297 and AMPA is also increased after DA depletion **(D).**

Figure 3. PKA responses to D1R stimulation are increased in dSPN after 6-OHDA lesion in the striatum

Imaging of PKA activation with AKAR3 biosensor as the FRET emission ratio in living striatal neurons with two-photon microscopy (**A and B**). Stimulation of the slices with agonists of D1R (SKF81297, 10µM) and $A2_AR$ (CGS21680, 10 µM) differentiate two populations of neurons expressing either $A2_AR$ (**B**, upper panel) or D1R (**B,** lower panel). Forskolin (FSK, 10 µM) directly activates adenylyl cyclase in both types of neurons. Maximal responses of FRET emission ratio (**C**), percentage of responsive cells (**D**) and response rise time (10-90%) (**E**) after application of either SKF81297, CGS21680 or FSK in DA-intact striatum. Comparison of maximal responses of FRET emission ratio **(F)** and percentage of responsive cells **(G)** after application of SKF81297, CGS21680 or FSK in 6-OHDA-lesioned and control striata.

Figure 4. Role of $G\alpha_{olf}$ and PDEs in the upregulation of PKA response to D1R agonist in the 6-OHDA-lesioned striatum

PKA activation is evaluated with AKAR3 FRET emission after stimulation with CGS21680 **(A)**, SKF81297 **(B)** and FSK **(C)** in *Gnal* heterozygous mice ($Gnal^{+/-}$) with and without 6-OHDA lesion. The responses are compared to those observed in the unlesioned striatum of control littermates ($Gnal^{+/+}$) (**A-C**). Green dashed line in A, B and C indicate the levels of responses observed in the 6-OHDA-lesioned striatum of wild type animals as shown in Fig. 3. In the $Gnal^{+/-}$ mice (expressing 50% of the normal $G\alpha_{olf}$ levels), the PKA responses to CGS21680 or SKF81297, but not those to FSK, are reduced as compared to wild type littermates. Comparison of 6-OHDA-lesioned and control striata in $Gnal^{+/-}$ mice indicates that DA-depletion increases the SKF81297-induced response but not that induced by CGS2168. However, in the lesioned striata, the SKF81297-induced response remains lower in $Gnal^{+/-}$ mice than in wild type animals (green dashed line). **(D)** Increase of AKAR3 FRET signal by various concentrations of the broad-spectrum inhibitor of phosphodiesterases (PDEs), 3-isobutyl-1-methylxanthine (IBMX), in the intact striatum. Effects of partial PDE inhibition by IBMX (30 µM) on maximal responses of FRET emission ratio to CGS21680 (10 µM) **(E)** and SKF81297 (10 µM) **(F)** in 6-OHDA-lesioned and control striata. Effects of IBMX on FSK-induced responses in CGS-responsive cells (presumably iSPNs) **(G)** and SKF-

responsive cells (presumably dSPNs **(H)** in 6-OHDA-lesioned and control striata. IBMX enhances the PKA responses to CGS21680, SKF81297 and FSK in both types of SPNs in the intact striatum wheareas it only increase responses to CGS21680 and FSK in the 6-OHDA-lesioned striatum.

Figure 5. Spontaneous Ca^{2+} transients are increased in D1R-expressing neurons of 6-OHDA-lesioned striatum

In **(A)**, examples of transient increases in intracellular Ca^{2+} levels detected by the normalized fluorescence ratio (ΔF/F0) of GCaMP6S biosensor in spontaneously active neurons. These neurons are selected because signal amplitude increases over 3 standard deviations (SD) during baseline recording. **(B)** C57BL/6 mice receive AAV expressing GCaMP6S in all neurons (left). *D1*Cre (right) and *A2A*cre (middle) mice are injected with a Cre-dependent AAV (AAV-flex-GCaMP6s) to produce GCaMP6S expression in D1R and $A2_AR$-expressing SPNs, respectively. Comparison between non lesioned (NL) and 6-OHDA-lesion striata of percentages of spontaneously active neurons in the global neuronal population (left) or in the SPN types expressing $A2_AR$ (middle, presumably iSPNs) or D1R (right, presumably dSPNs). This percentage of spontaneously active neurons is increased in the global population of neurons and in dSPNs, but not in iSPNs.

Figure 6. Specific upregulation of AMPA-induced intracellular Ca^{2+} dynamics in $A2_AR$-expressing neurons in 6-OHDA-lesioned striatum

(A) GCaMP6S is expressed in all types of striatal neurons. GCaMP6S is selectively expressed in D1R- **(B)** or $A2_AR$- **(C)** expressing SPNs by injecting a Cre-dependent AAV in the striatum of *D1*Cre and *A2A*cre mice, respectively. **Left panels**: Ca^{2+} imaging in a field taken in non lesioned (NL) and 6-OHDA-lesioned striata, in basal condition and after sequential application of AMPA (5 µM, 30 s) and KCl (25 mM, 30 s). **Middle panels**: Time courses of intracellular Ca^{2+} levels evaluated by the normalized fluorescence ratio (ΔF/F0) in response to AMPA (5 µM, 30 s) in non lesioned (NL) and 6-OHDA-lesioned striata. Percentage of responsive cells (**Right upper panels**) and Area Under the Curves (AUCs, **Right lower panels**) of Ca^{2+} responses in striatal neurons after application of AMPA (0.5 µM, 30s) in non-lesioned (NL) and 6-OHDA lesioned (6-OHDA) mice.

Figure 1.

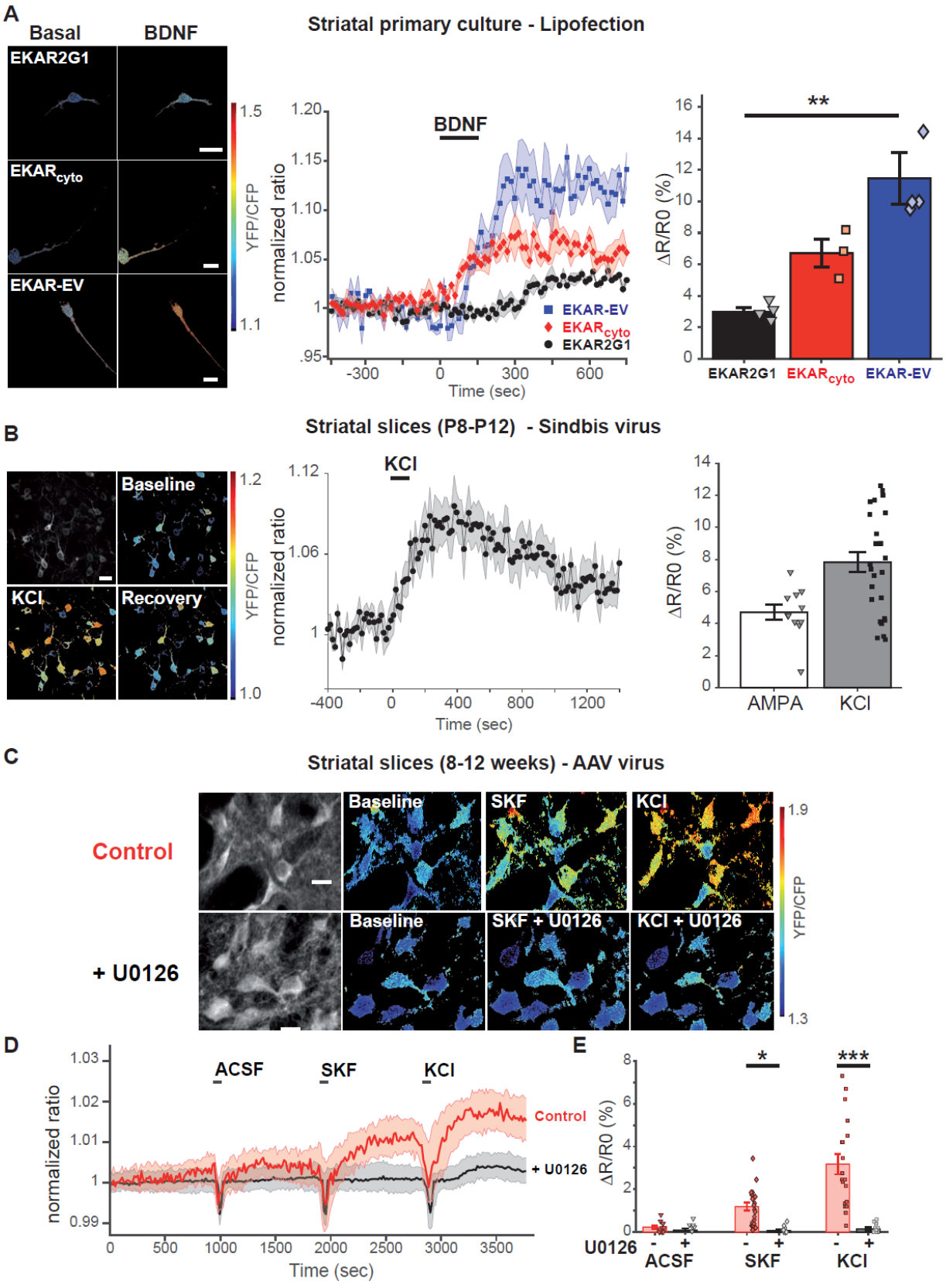
A
Basal
BDNF
EKAR2G1
EKAR$_{cyto}$
EKAR-EV
1.5
YFP/CFP
1.1
Striatal primary culture - Lipofection
BDNF
normalized ratio
1.20
1.15
1.10
1.05
1
.95
-300
0
300
600
Time (sec)
EKAR-EV
EKAR$_{cyto}$
EKAR2G1
**
ΔR/R0 (%)
16
14
12
10
8
6
4
2
0
EKAR2G1
EKAR$_{cyto}$
EKAR-EV
B
Striatal slices (P8-P12) - Sindbis virus
Baseline
KCl
Recovery
1.2
YFP/CFP
1.0
KCl
normalized ratio
1.12
1.06
1
-400
0
400
800
1200
Time (sec)
ΔR/R0 (%)
14
12
10
8
6
4
2
0
AMPA
KCl
C
Striatal slices (8-12 weeks) - AAV virus
Control
+ U0126
Baseline
SKF
KCl
SKF + U0126
KCl + U0126
1.9
YFP/CFP
1.3
D
ACSF
SKF
KCl
normalized ratio
1.03
1.02
1.01
1
0.99
0
500
1000
1500
2000
2500
3000
3500
Time (sec)
Control
+ U0126
E
*
***
ΔR/R0 (%)
8
6
4
2
0
U0126
- + - + - +
ACSF
SKF
KCl

Figure 2.

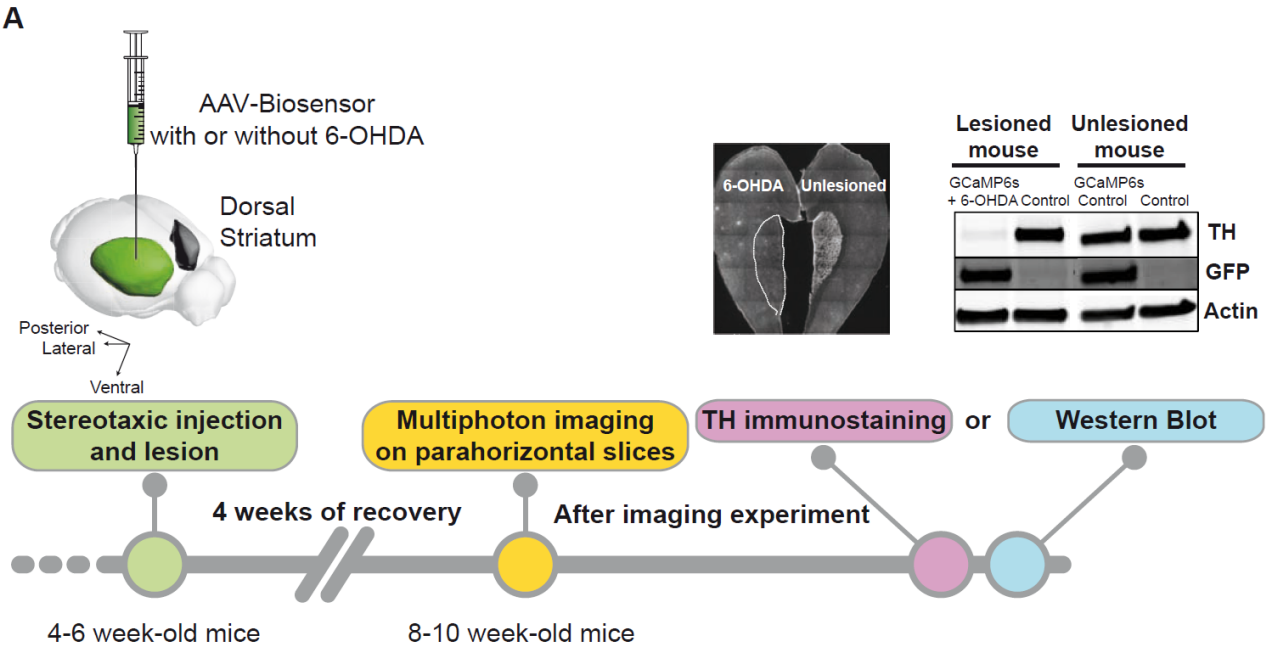
A
AAV-Biosensor
with or without 6-OHDA
Dorsal
Striatum
Posterior
Lateral
Ventral
6-OHDA
Unlesioned
Lesioned mouse
Unlesioned mouse
GCaMP6s
+ 6-OHDA
Control
GCaMP6s
Control
Control
TH
GFP
Actin
Stereotaxic injection and lesion
Multiphoton imaging on parahorizontal slices
TH immunostaining
or
Western Blot
4 weeks of recovery
After imaging experiment
4-6 week-old mice
8-10 week-old mice

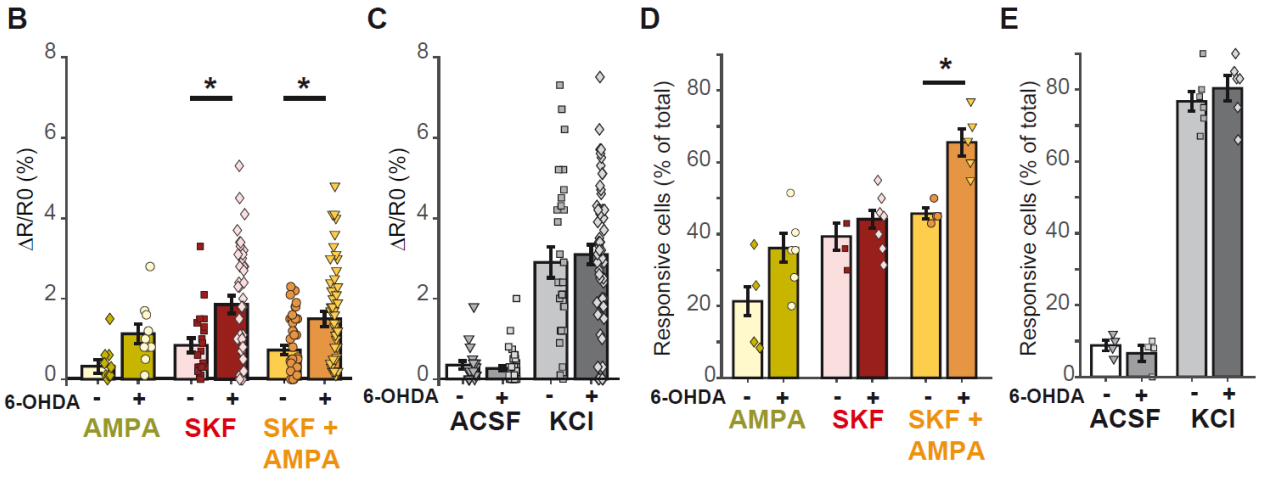
B
ΔR/R0 (%)
6-OHDA
AMPA
SKF
SKF + AMPA
C
ΔR/R0 (%)
6-OHDA
ACSF
KCl
D
Responsive cells (% of total)
6-OHDA
AMPA
SKF
SKF + AMPA
E
Responsive cells (% of total)
6-OHDA
ACSF
KCl

Figure 3.

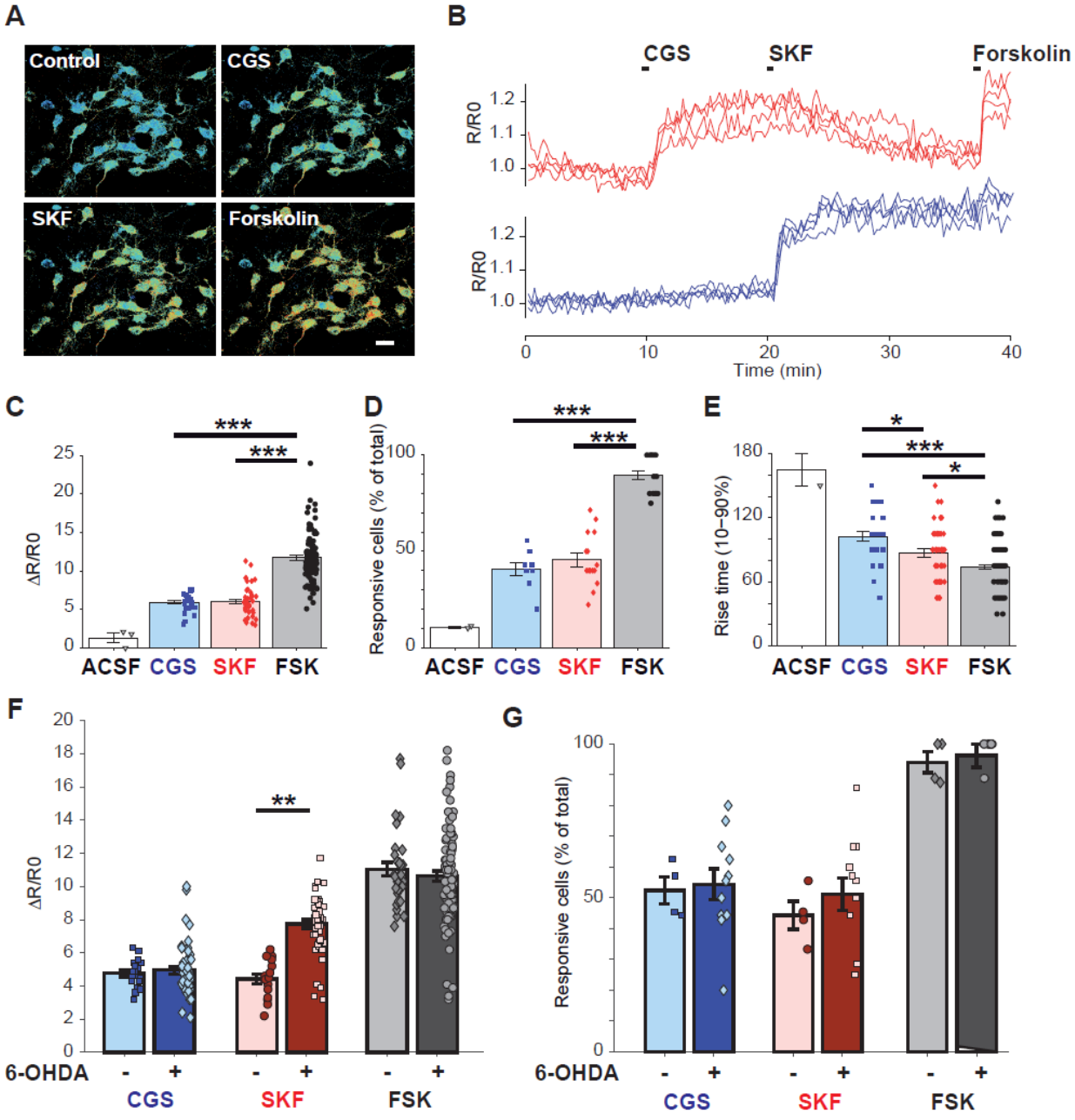
A
Control
CGS
SKF
Forskolin
B
CGS
SKF
Forskolin
R/R0
1.2
1.1
1.0
0
10
20
30
40
Time (min)
C
ΔR/R0
***
***
ACSF CGS SKF FSK
D
Responsive cells (% of total)
***
***
ACSF CGS SKF FSK
E
Rise time (10–90%)
*
***
*
ACSF CGS SKF FSK
F
ΔR/R0
**
6-OHDA
CGS SKF FSK
G
Responsive cells (% of total)
6-OHDA
CGS SKF FSK

Figure 4.

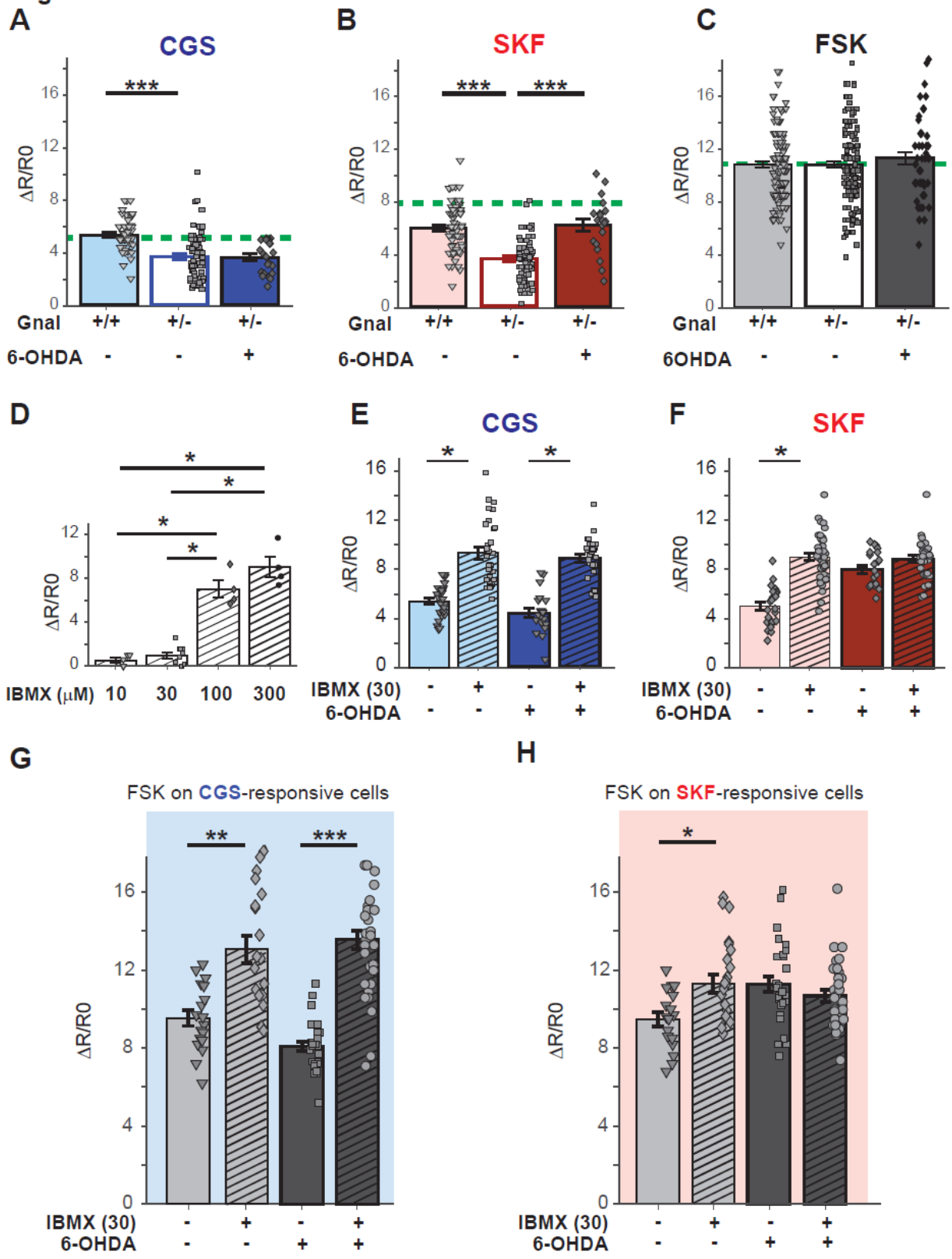
A
CGS
B
SKF
C
FSK
ΔR/R0
Gnal +/+ +/- +/-
6-OHDA - - +
6OHDA - - +
D
IBMX (μM) 10 30 100 300
E
CGS
IBMX (30) - + - +
6-OHDA - - + +
F
SKF
G
FSK on CGS-responsive cells
H
FSK on SKF-responsive cells

Figure 5

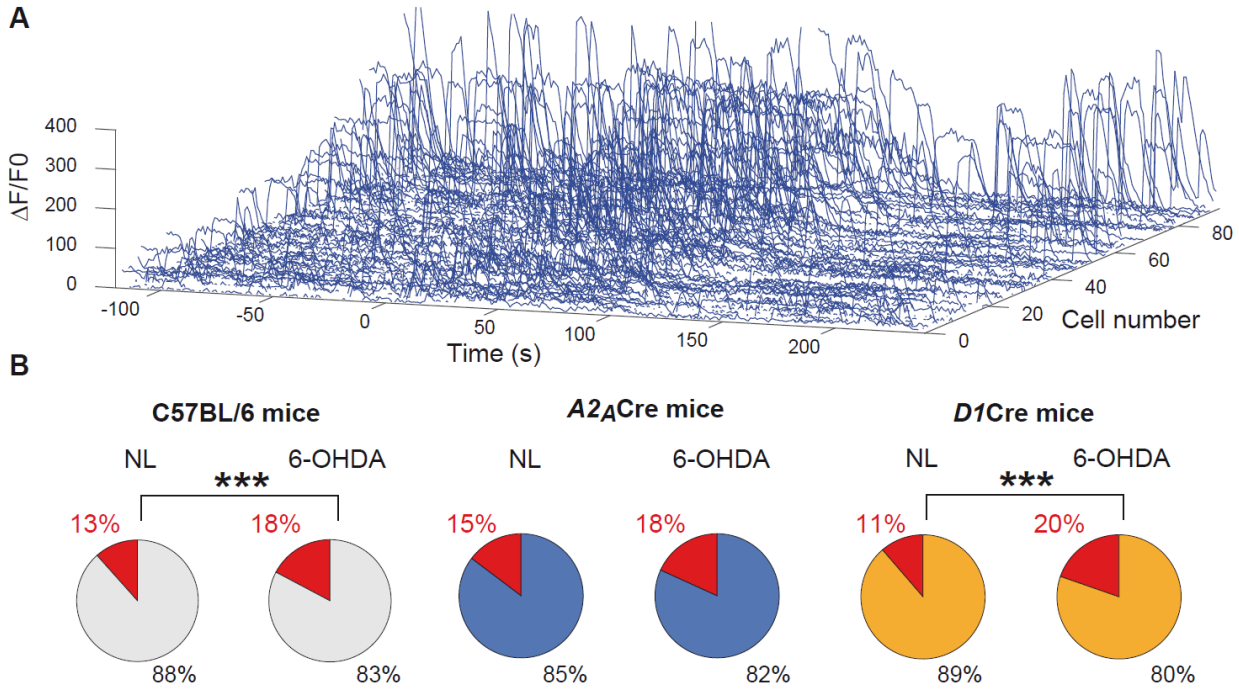
A
ΔF/F0
400
300
200
100
0
-100
-50
0
50
100
150
200
Time (s)
0
20
40
60
80
Cell number
B
C57BL/6 mice
NL
6-OHDA
***
13%
18%
88%
83%
A2ACre mice
NL
6-OHDA
15%
18%
85%
82%
D1Cre mice
NL
6-OHDA
***
11%
20%
89%
80%

Figure 6.

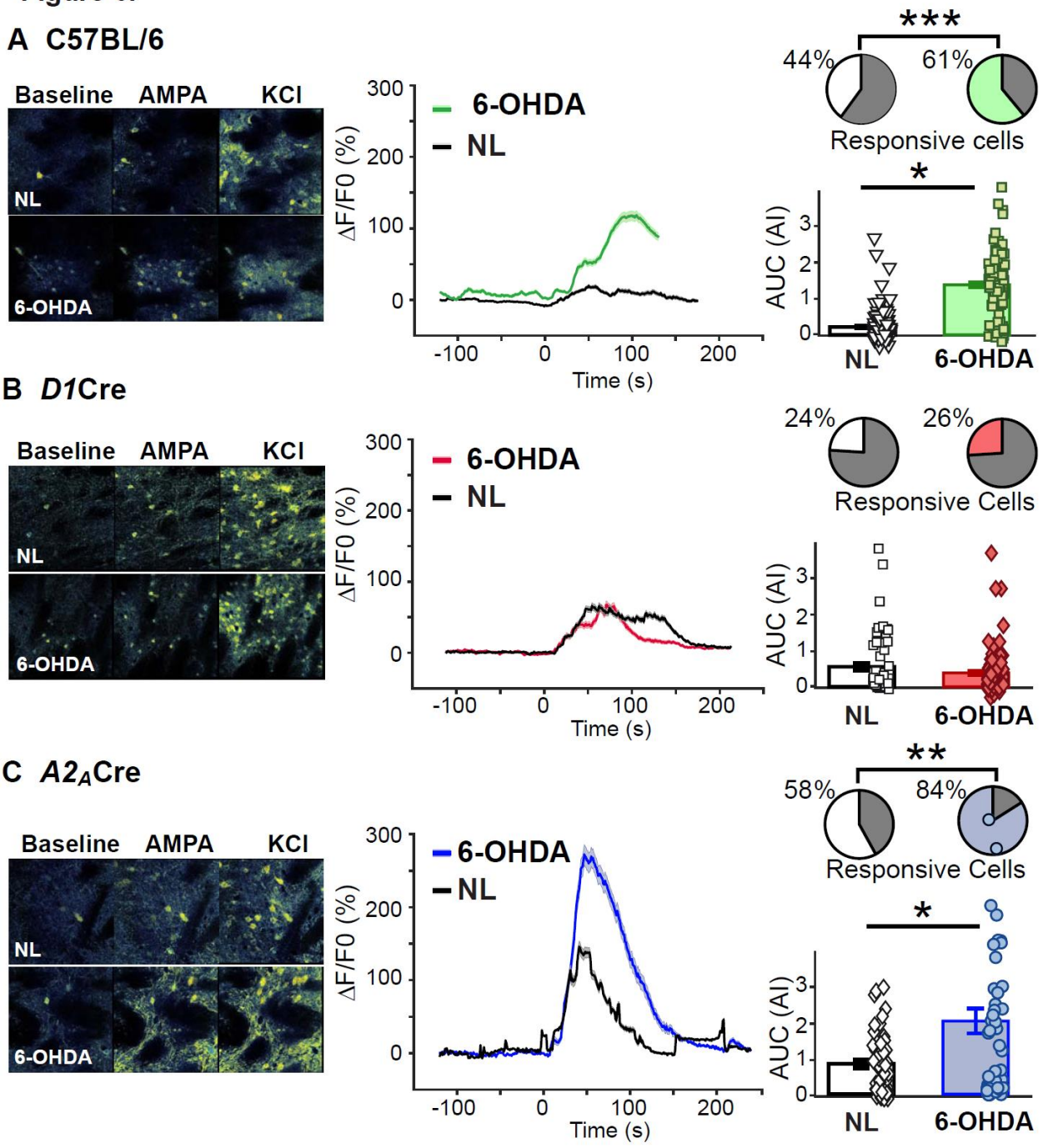
A C57BL/6
Baseline
AMPA
KCl
NL
6-OHDA
ΔF/F0 (%)
Time (s)
6-OHDA
NL
***
44%
61%
Responsive cells
*
AUC (AI)
B D1Cre
24%
26%
Responsive Cells
C A2ACre
**
58%
84%

2- Setting up the experimental protocol (Additional results I)

2.1. Slicing protocol, slice preparation for imaging and pharmacological applications in brain slices

Although brain slices have been used extensively, studies on the striatum are usually done in slices of young mice before puberty. Less damage appears to occur on neurons and neuronal processes of slices of young animals (2 to 7 weeks old) possibly because of the relative lack of connective tissue and myelination in the brain of these animals (Sakmann and Stuart, 1995).

One of the first difficulties was to set up viable corticostriatal slices from adult mice, since I was working on the 6-OHDA rodent model of PD. Indeed, swelling of the slices during imaging, poor spontaneous activity or drug- or KCl-induced reactivity, increased visible debris at the surface, change in the aspects of SPNs (smaller/shrinked) during imaging were clues to improve and adapt the protocol to obtain slices of better quality (e.g. with more living cells).

Various parameters were tested and changed among which:

2.1.1. Before and during slicing:

- Changing the sacrifice method from simple decapitation to cardiac perfusion with ice cold choline-aCSF, which allowed deeper and faster penetration of choline-aCSF in the brain for slicing. Cooling of the tissue is particularly important presumably as it minimizes damages from anoxia and improves the texture for slicing (Sakmann and Stuart, 1995). Especially in bigger animals were sometimes more time is required for dissecting the brain.
- Changing the angle of slicing to improve the corticostriatal connectivity remaining in the slices. For slicing, we switched from coronal plane, where bundles are mainly cut orthogonally (**Figure R.7.A**), to parahorizontal plane at an angle between 30° and 45 (**Figure R.7.B and C**), allowing to obtain more horizontal bundles and increased corticostriatal connectivity, as previously reported by others (Kawaguchi *et al.*, 1989; Kita, 1996; Wickens *et al.*, 1998; Fino *et al.*, 2005; Smeal *et al.*, 2007).
- Changing the temperature and composition of the recovery solution from aCSF low $CaCl_2$ concentration (0.5 mM) for 10 min at 30°C and then aCSF $CaCl_2$ (1 mM) for 1 h at room temperature to Choline-aCSF for 1 h at 34°C to recover a pH/metabolic equilibrium and changing the bath to avoid accumulation of toxic components released by the periphery of the slices.
- Changing the standard chamber for a custom-made interface chamber in which slices are kept on a net at the interface between aCSF and a humidified 95% O_2/5% CO_2 rich environment.

2.1.2. during imaging:

- We designed a specific recording chamber with top and bottom perfusion to optimize the oxygenation on both sides of the slice. The slice is lying on a nylon mesh that supports the slice and prevents it from touching the slide below, allowing the aCSF to flow above and under it. Compared with other types of chamber, where the slice is directly laying on a glass cover slip, this chamber reduces neuronal death in the bottom part of the slice, improves viability, and reduces slice movements due to the swelling of the slice.
- For a quick control of the global viability and responsiveness of the cells, we applied KCl at a high concentration (25 mM) in slices in which GCaMP6S was expressed in SPNs and we estimated

how many cells could respond to a massive depolarization. In the same way, in slices in which AKAR was expressed in SPNs, applying forskolin (10 µM) allowed controlling if cells were viable and responsive.

- Another difficulty was to improve the kinetics of drug delivery for the short drug applications that lasted up to 30 s. We initially used uniform bath applications for all drugs but high drug concentrations were needed to obtain any effect and high variability in the responses was observed. We kept bath applications for long drug applications of several minutes, where equilibrium is obtained. For fast delivery, we locally applied the various agents with a glass pipet linked to a pump with different channels for each compound/drug. To make sure we improved the kinetics, we monitored with fluorescein the time needed for filling up the recording chamber, first when fluorescein was applied in the bath and then through glass pipet. We observed the second method improved filling up the chamber.

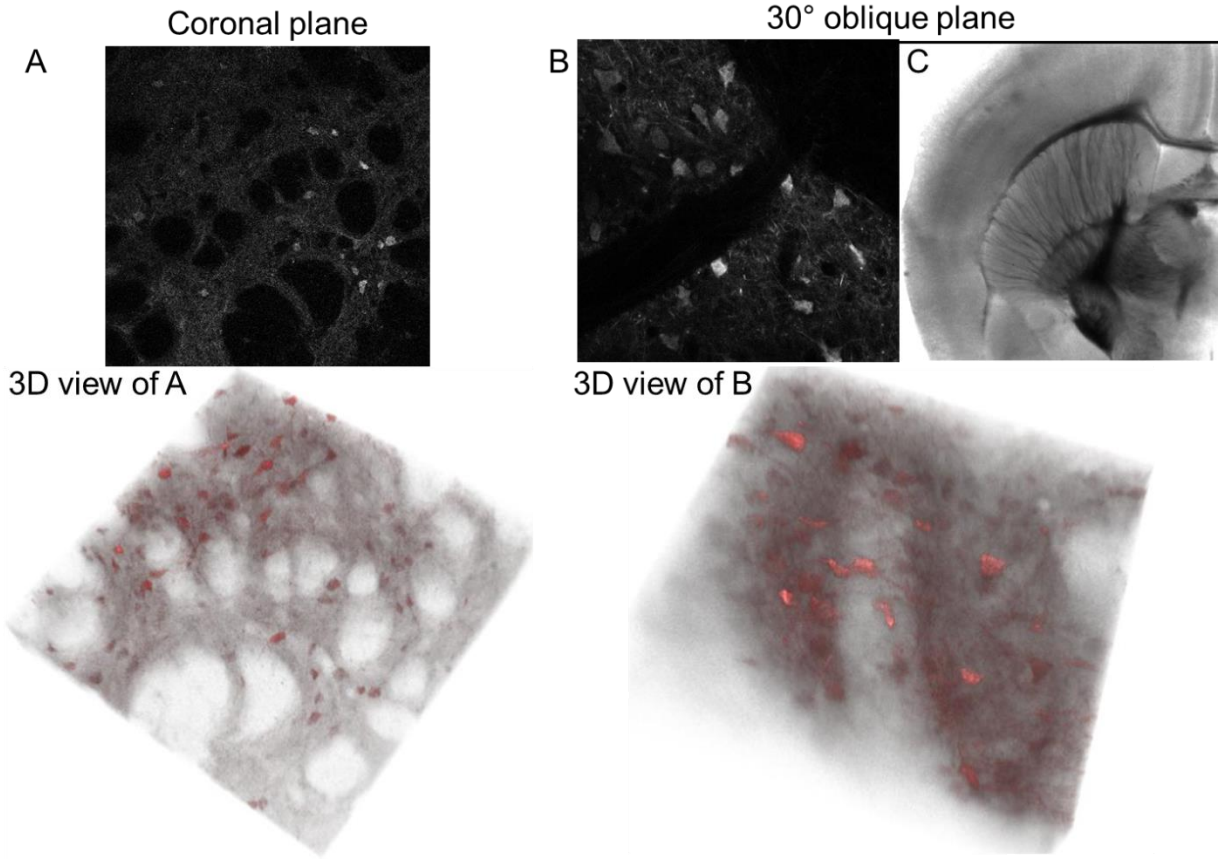

[Figure R.7. ***Different slicing angles.***
*2P-imaging of a corticostriatal slice in a coronal plane section (**A**) and in a 30° parahorizontal oblique plane section (**B**) and their respective 3D views of the corresponding image stack for better visualization of the bundles orientation.* ***C:*** *A light micrograph of a typical parahorizontal slice preparation with uncut bundles visible through the striatum.*]

2.2. Expression of the probes via viral vectors

We tested a Sindbis virus to express the PKA FRET sensor AKAR3, in adult brain slices in culture, as Sindbis viruses were already successfully used to follow other signaling pathways in acute slices of immature mice (Gervasi *et al.*, 2007; Hepp *et al.*, 2007; Castro *et al.*, 2013; Tricoire and Lambolez, 2014; Luczak *et al.*, 2017). The downside of Sindbis viruses is that they are toxic to the cells and have to be used on slices kept in culture and imaged the next day. In addition, we observed no infection in brain slices of P19 mice. The labelling was significantly sparser at the surface when we used P15 mice as compared to that obtained after an AAV infection in an 8.5 week-old mouse (**Figure R.8**). Because the 6-OHDA model needs at least 3 week delay after injection, it was clear that imaging should be performed in adult mice. Unfortunately, sindbis viruses do not allow effective neuronal infection of adult striatal slices. Hence the approach using AAV viral vectors was chosen.

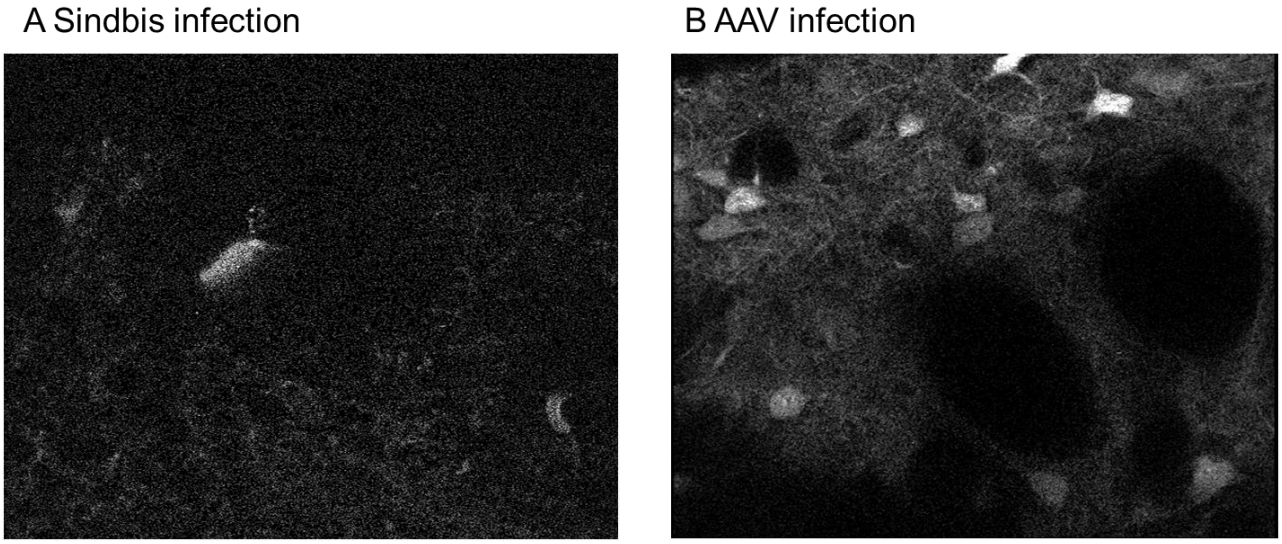

*[**Figure R.8. Comparison of AKAR3 expression in the striatum using Sindbis virus and AAV**:*
***2.9 WPRE AKAR3 expression in the striatum with Sindbis virus (A)** after 24h in a slice in culture of a P15 mouse **or AAV virus (B)** 3 weeks after intra-striatal injection and acute slicing of a mouse aged 8.5 weeks**.**]*

2.3. Combined intrastriatal microinjection of biosensor-expressing AAV and 6-OHDA

After setting up the acute slices in adult mice, we had to check that lesions could be correctly performed when the 6-OHDA toxin was co-injected intra-striatally with the AAV expressing the probes. Striatal denervation and 6-OHDA lesions were verified by immunoblotting or immunofluorescence. In lesioned animals, TH was measured either by immunostaining the slices which were directly dipped in PFA at the end of the recording session (**Figure R.9 A**) or by immunoblotting of striata dissected from the corticostriatal slices and frozen at -80°C at the end of the recording session (**Figure R.9 B**). As compared to controls, TH immunoreactivity is deeply decreased after 6-OHDA lesion, only on the side injected and this does not disturb the expression of the biosensor (**Figure R.9 B**). The presence of 6-OHDA did not prevent the good infection by the virus nor the expression of the probes. For instance, we co-injected 6-OHDA and an AAV expressing GCaMP6S in the striatum. Three weeks later, a good expression was seen in fluorescence microscopy (**Figure R.9. A**) and 2P-imaging. Donut-shaped SPNs and labelling in the neuropil (**Figure R.9 B**) and dendritic shaft and spines (**Figure R.9 C**) could be seen. The expressions of EKAR and AKAR probes by AAVs were not disturbed either by the co-injection with the 6-OHDA toxin.

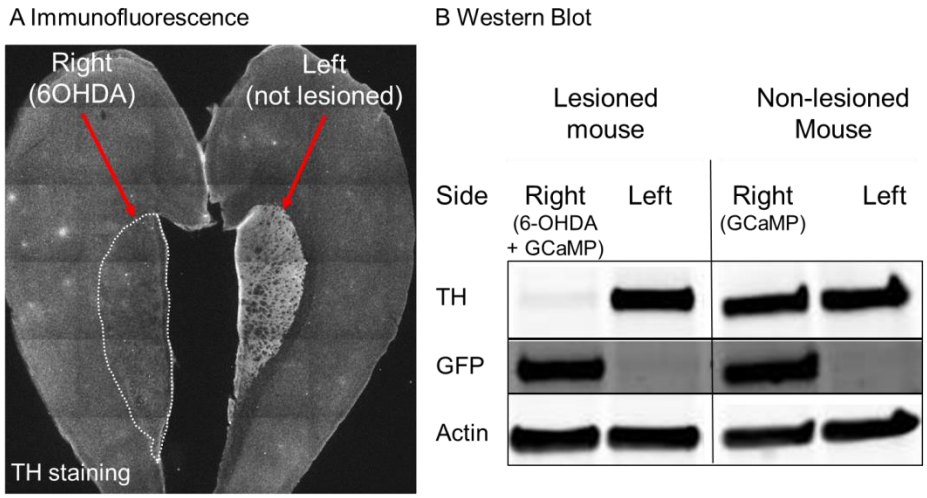

[***Figure R.9. Lesion and AAV infection checking***

A: TH immunostaining of right and left corticostriatal slices in a parahorizontal plane.

The right side shows virtually no TH positive fibers remaining in the striatum (delimited by dotted line) after 6-OHDA injection into the right hemisphere, whereas the left side is still completely innervated.

B: Immunoblot comparing TH and GFP levels in the right and left striata (Right R and Left L) in a lesioned mouse which received in the right side both GCaMP6S-expressing AAV and 6-OHDA, and a non-lesioned mouse only receiving GCaMP6S-expressing AAV. *TH is present in the same quantity in the right and left striata of the non-lesioned animal and in the left striatum of the lesioned animal, but virtually absent in the right striatum of the lesioned animal. The GFP antibody, which recognizes the GcAMP6S, is a control to show in which hemisphere GCaMP6S was injected (right striata). Actin is a control for protein loading.]*

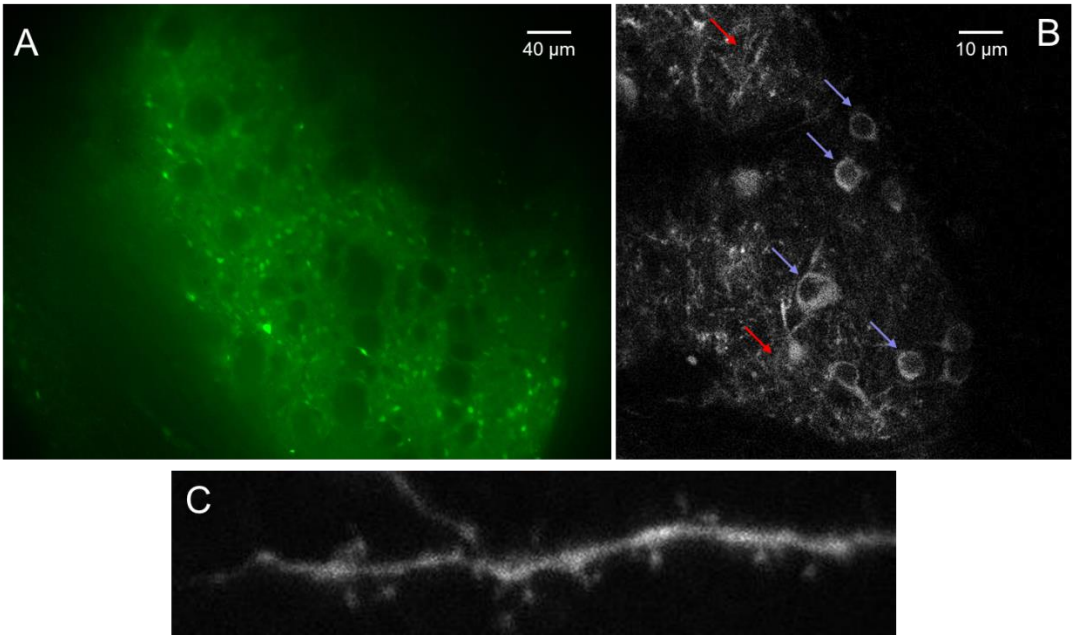

[***Figure R.10. GCaMP6S expression driven by AAV in the striatum*** *is visible as intense fluorescence signal in fluroescence microscopy (**A**), and 2P-imaging **(B, C)**. See labelling in SPNs (donut shaped pointed by **blue arrows in B**) neuropil (**red arrow** in **B**), dendrite shaft and spines (**C**)]*

2.4. Activation of ERK by a D1 DA agonist in acute brain slices

Before using new imaging tools like 2P-imaging and FRET probes to monitor ERK activity, or other signaling pathways, we had to make sure that ERK could be activated in these acute slices. To verify this point, we sectioned brains of lesioned animals and we treated the slices in the same set up (chamber, drug application) as for 2P-imaging (except no recording). The D1R agonist (SKF 81297) was bath-applied for 20 min at 10 µM, and the slices were directly dipped in paraformaldehyde (PFA) at the end of the application. Then, we performed phospho-ERK (pERK) immunostaining and confocal imaging of slices (**Figure R.11**). Virtually no cells were pERK-positive under basal conditions when aCSF was applied on slices (**see Figure R.11.A blue arrows** pointing at cell shadows in black). In contrast, many cells were pERK-positive following D1 agonist application (**see Figure R.11.B red arrows** pointing at pERK positive cells), the number of pERK-positive neurons being higher in the 6-OHDA-lesioned striatum than in the intact striatum (**Figure R.11C and D**). The results are consistent with those observed in experiments in which a D1 agonist was administered in vivo (see for instance Gerfen et al, 2002). These preliminary experiments clearly showed that our 2P-imaging set-up and application protocol were suitable to observe ERK activation in living brain slices.

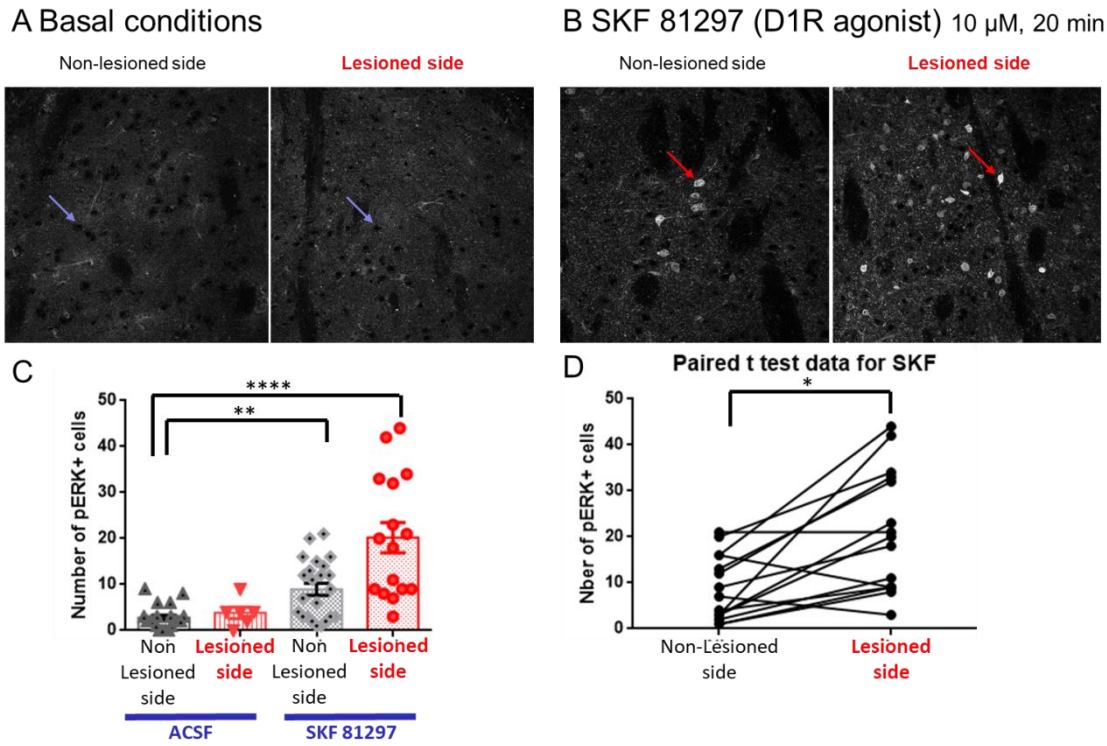

*[**Figure R.11. ERK activation by stimulation of D1 DA receptors**. Phospho-ERK immunostaining in striata of 6-OHDA lesioned animals under basal conditions (i.e. in the presence of aCSF, **A**) and after bath-application of the D1R agonist SKF81297, at 10 µM for 20 min **(B)**. SKF81297 application increases the number of pERK-positive cells in the striatum and the response is higher in the lesioned striatum than in the intact one. **C and D** Quantifications of the number of pERK positive cells per frame. In C, Kruskall Wallis followed by Dunn's multiple comparisons test shows significant differences in pERK positive cells after treatment by the D1 agonist as compared to controls treated by ACSF. In D, 2-tailed paired t test, shows significant increase in pERK positive cells on the lesioned side as compared to the non-lesioned side in slices treated by the D1 agonist. Analysis of 3 to 5 stacks per mice, in 2 to 5 mice per group. *p=0.01; **p<0.01; ****p<0.0001]*

2.5. Activation of biosensors in acute brain slices

The probe reactivity to various stimuli was tested. We examined the GcAMP response to electrical and pharmacological treatments and the response of AKAR3 to forskolin. Electrical stimulation was performed in the striatum, corpus callosum, and cortex. We tested the reactivity of the probe to various frequencies of trains of stimulation (5 to 100 Hz) and numbers of pulses per train of stimulation (2 to 10 pulses). The Ca^{2+} response was measured as normalized fluorescence ratio (ΔF/F0) expressed as a percentage of baseline before stimulation. The peak of the Ca^{2+} response (ΔFmax/F0; maximum of normalized fluorescence ratio (ΔF/F0)) increased with the number of pulses per train (**Figure R.12 B and C**) and the frequency of trains of stimulation (**Figure R.12 D**) applied. This showed the probe could react quantitatively to depolarization, but this approach allowed monitoring only a few cells near the electrode. We then used KCl (25 mM), AMPA (2.5 µM) **(Figure R.13)** and NMDA (10 µM in the absence of Mg^{2+}) as sources of massive depolarization. These chemical and pharmacological stimulations resulted in the possibility of monitoring the Ca^{2+} response in the SPNs and quantifying the response in individual cells but also the global striatal response. In our experimental conditions, applying DA or glutamate did not elicit any visible response.

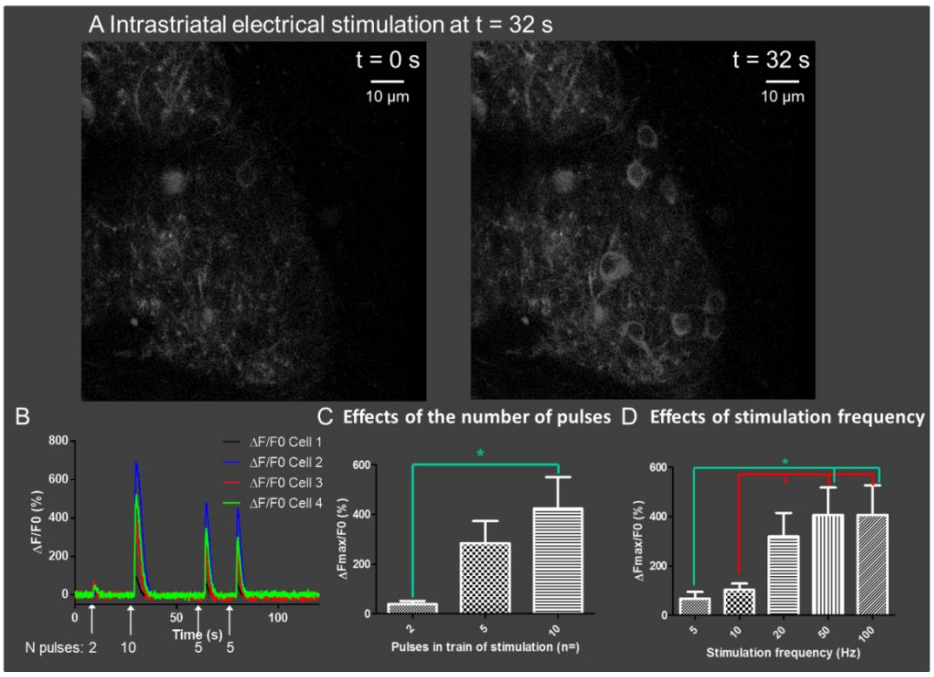

*[**Figure R.12. Ca^{2+} responses after local electrical stimulation in the striatum of mice injected with GcAMP6S-expressing AAV. A.** Stimulation by 1 train of 10 pulses (0.1 ms, 50 Hz, 0.3 mA). Images at 0 s and 32 s after the stimulation. An increase in the fluorescence in SPNs reflects Ca^{2+} increase in their cytoplasm. **B.** Monitoring of individual cells for Ca^{2+} response to trains of electrical stimulations (20 Hz each) with different number of pulses per train (2 to 10), as an expression of the fluorescence over time with normalized fluorescence ratio (ΔF/F0) expressed as a percentage of baseline before stimulation (ΔF(t)/F0). **C.** The peak of the response (ΔFmax/F0) increases with the number of pulses in the train of stimulation (each delivered at a frequency of 20Hz). **D.** The peak of the response (ΔFmax/F0) increases with the frequency at which each train of stimulation (of 5 pulses each) was delivered.*

** p<0.05 by 1 way ANOVA adjusted by Bonferroni's Multiple Comparison Test]*

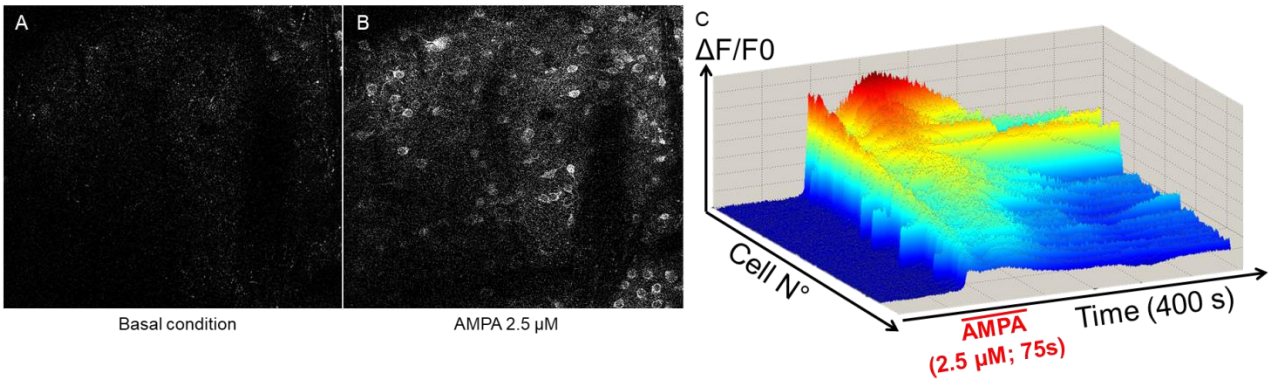

*[**Figure R. 13. Ca^{2+} responses after AMPA application**.*
***A.** GCaMP6S fluorescence under basal conditions and **B.** One minute after the beginning of AMPA application. After stimulation by AMPA (2.5 µM, 75 s), a strong increase in fluorescence linked to intracellular Ca^{2+} increase is observed. **C.** Monitoring of the Ca^{2+} response (ΔF(t)/F0), induced by AMPA application over time. Each line represents an individual cell. Note the variability of the response time courses between cells].*

2.6. Dose-dependence of Ca^{2+} responses to NMDA or AMPA application

During the period setting up the experimental protocol, we performed dose-response curves using various concentrations of glutamate ionotropic receptors agonists, NMDA and AMPA. At this initial period, the protocol included an immerged recovery phase for the slices (and not interface), no cardiac perfusion and bath application of the drugs. In these conditions, the slices showed low or no spontaneous cell activity.

NMDA proved to be very hard to explore because of a very steep dose-response curve and a large variability in the responses (**Figure R.14 A**). In an Mg^{2+}-free aCSF, preventing Mg^{2+} block of NMDARs, as expected, responses where greatly increased as compared to those in the presence of 2 mM Mg^{2+} (**Figure R.14 B**). The dose-response curve with AMPA appeared more gradual than those with NMDA (**Figure R.15 A and B**). When we analyzed the percent of responsive cells or the fluorescence changes (mean ΔFmax/F0), the curve indicated an EC50 close to 0.5 µM (0.55 µM). These initial setting up experiments led us to use AMPA rather than NMDA because of the more reliable responses. The EC50 measures for AMPA, helped us to decide which dose to apply on the slices with the local application system.

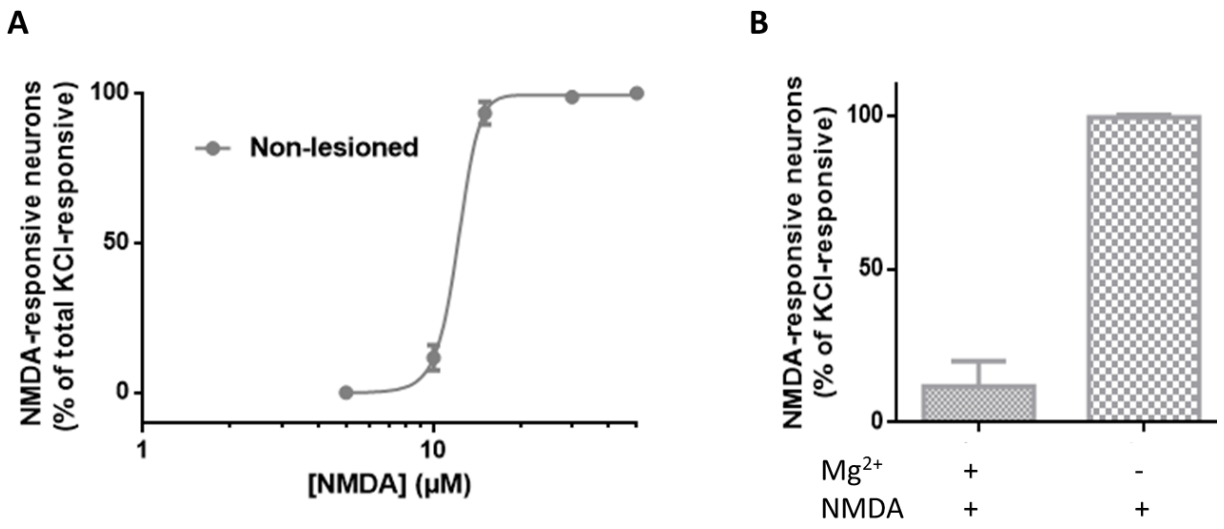

[Figure R.14. Effects of NMDA on Ca^{2+} monitored by GcAMP6s.

A. Dose-response curves of Ca^{2+} responses in the presence of 2 mM Mg^{2+}. The percentages of responsive cells are plotted as a function of drug concentration (plotted as the log of drug concentration). The non-lesioned mice (1-3 animals per drug concentration, 1-4 slices per drug concentration, 64 [11-102] cells per slice) appear in grey.

B. Ca^{2+} responses induced by 10 µM NMDA in the presence or absence of Mg^{2+}. Responses are normalized to the maximal response in the absence of Mg^{2+}. The non-lesioned mice group (2 mM Mg^{2+}, n = 3 animals, 4 slices, 85 [49-123] cells per slice and 0 mM Mg^{2+}, n = 2 animals, 2 slices, 51 [26-76] cells per slice) appear in grey.]

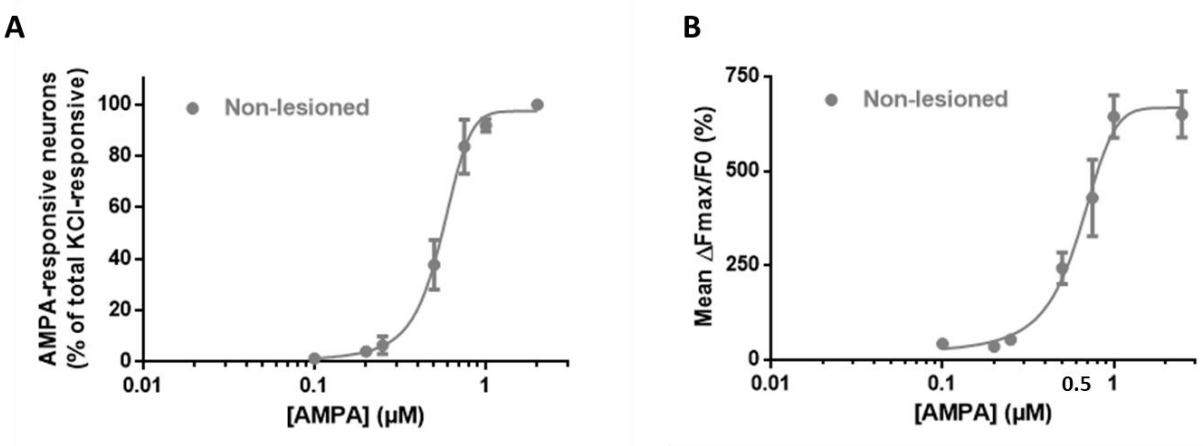

[Figure R.15 Effects of AMPA on Ca^{2+} monitored by GcAMP6s.

A. The percentage of responsive cells and **B.** the mean ΔFmax/F0 are plotted as a function of the log of drug concentration. The EC50 is close to 0.6 µM in both groups (Non-lesioned: EC50 = 0.55 µM for % of responsive cells; EC50 = 0.62 µM for ΔFmax/F0). The non-lesioned mice group (2-4 animals per drug concentration, 3-4 slices per drug concentration, 78 [20-148] cells per slice) appears in grey.]

3- Upregulation of ERK activation and Ca^{2+} responses to glutamate receptors stimulations in SPNs after dopamine depletion by 6-OHDA lesion (Additional results II)

We first tested ionotropic AMPAR implication in ERK activation and Ca^{2+} signaling. Results regarding AMPAR signaling upregulation are shown in the manuscript in preparation. We also tested the implication of metabotropic glutamate receptors. Indeed, group I mGluR and in particular mGluR5 have been implicated in the regulation of D1R signaling, activation of ERK and genesis of LID (Rylander *et al.*, 2009; Ouattara *et al.*, 2011; Fieblinger *et al.*, 2014b; Lin *et al.*, 2017; Sebastianutto and Cenci, 2018).

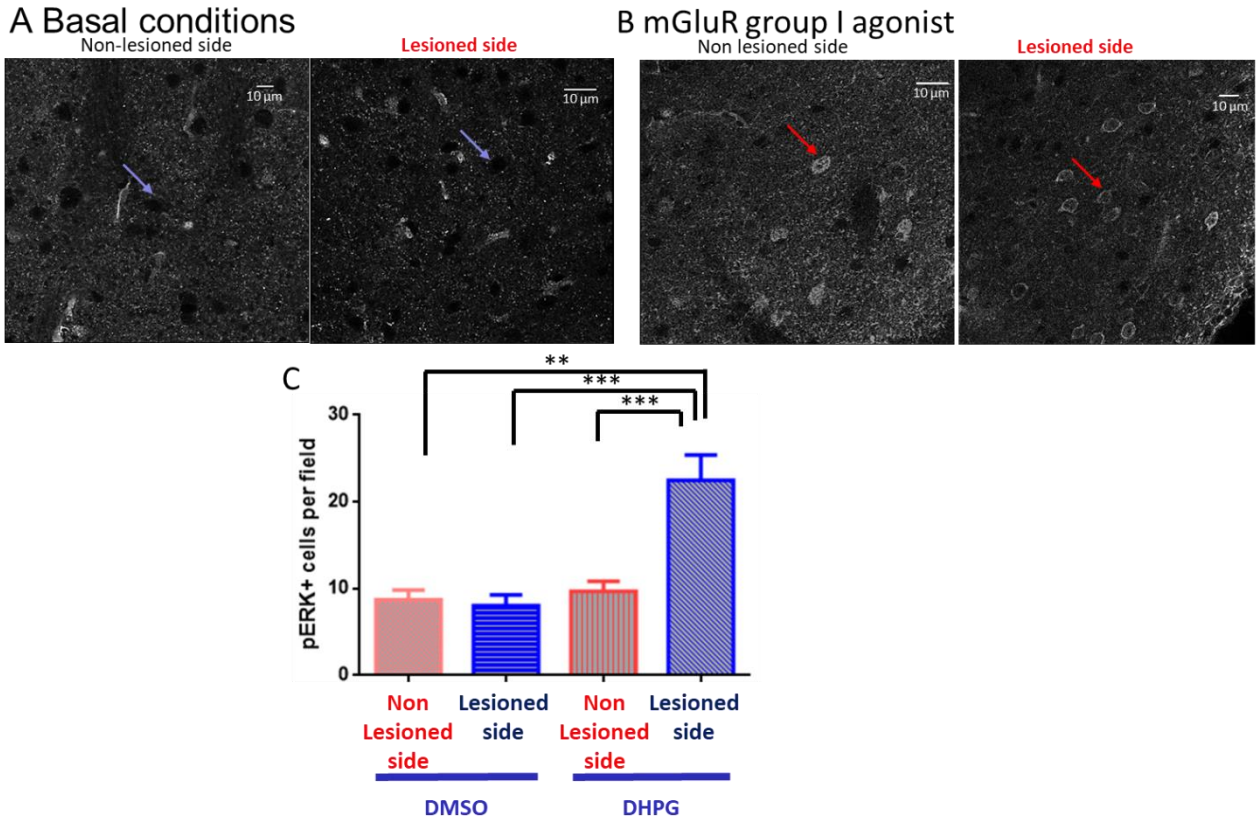

*[**Figure R.16. Effects of Group I mGluR stimulation on phospho-ERK immunostaining in the striatum following 6-OHDA lesion.** Phospho-ERK (pERK) immunostaining in striata of 6-OHDA-lesioned mice under basal conditions with DMSO (6 brain slices, 6 mice) **(A)** and after 20 min bath application of the mGluR goup I agonist (RS)-3,5-DHPG (100 µM) (11 brain slices, 8 mice) **(B). C** Quantification of pERK-positive cells in the various conditions. A significant increase in pERK-positive cells is seen after DHPG (B) as compared to basal conditions (A)**.** pERK immunofluorescence in confocal microscopy. Red arrows point at pERK-positive cells, blue arrows point at cell pERK-negative cells in black. Kruskal-Wallis test with Dunn's multiple comparisons test; **p<0.01; ***p < 0.001]*

First, in a preliminary experiment in immunofluorescence and bath application of drugs, we tested whether ERK could be activated after application of a group I mGluR agonist, in corticostriatal slices of adult mice (**Figure R.16. A-C**). We found that DHPG induced an activation of ERK in striatal neurons (**Figure I R.16**). As shown in the previous results (section III.A), the D1R agonist SKF81297 also

activated ERK (**Figure III.C.1C**). Together, these preliminary observations were in line with previous reports and suggested group I mGluR could be implicated in the activation of ERK and modulation of D1R signaling leading to ERK activation after 6-OHDA lesion.

As previously reported, Ca^{2+} signaling has been implicated in ERK activation in many models such as C Elegans (Tomida *et al.*, 2012), in CA1 pyramidal neurons of rodents (Zhai *et al.*, 2013) and in SPNs in dopamine depleted models (Fieblinger *et al.*, 2014b). Group I mGluRs are involved in Ca^{2+} signaling through various pathways including activation of PLC, leading to the activation of PKC, the regulation of CICR, and modulation of L-type VGCCs. We therefore monitored with GCaMP6S the Ca^{2+} responses after group I mGluR stimulation in 6-OHDA lesioned animals (**Figure R.17**). Ca^{2+} responses to local application of DHPG (30 s, 20 µM) were increased after DA depletion by 6-OHDA as shown by the increased percentage of responsive SPNs (Non-lesioned (NL): 33.1%, 168/508 neurons, 10 slices, 7 animals; 6-OHDA: 48.5%, 172/355 neurons, 8 slices, 4 animals; Fisher's exact test; $p<0.0001$, **Figure R.17.B**) and the increased amplitude of response (AUC mean ± SEM: NL, 2659 ± 256, n=168; 6-OHDA, 4832 ± 416, n = 172; unpaired t test, $p<0.0001$; **Figure R.17. A and C**) in the 6-OHDA-lesioned mice. As explained in the Manuscript in preparation, the spontaneously active cells were excluded of this analysis and analyzed separately. To test whether D1R were involved in the changes observed in lesioned animals, we repeated this experiment in D1 KO mice. Analysis of Ca^{2+}-responsive cells to DHPG in SPNs of 6-OHDA-lesioned D1KO mice revealed a significant decrease of percentage of responsive cells as compared to 6-OHDA-lesioned WT mice, back to levels similar to those of non-lesioned WT animals (WT-NL: 33.1%, n = 168/508 SPNs, 10 slices, 7 animals; WT-6-OHDA: 48.5%, n = 172/355 SPNs, 8 slices, 4 animals; D1KO-6-OHDA: 30.3%, 47/155 SPNs, 4 slices, 3 animals; Chi-square, $p<0.0001$, **Figure R.17.B**). Among the remaining responsive cells, the amplitude of the response to group I mGluR agonist was still increased in the 6-OHDA-lesioned D1KO mice as compared to non-lesioned WT animals (AUC Mean ± SEM: WT-NL, 2659 ± 256, n=168; WT-6-OHDA, 4832 ± 416, n=172; D1KO-6-OHDA = 4421 ± 888, n=47, one-way ANOVA, p<0,0001; **Figure R.17.A and C**).

Together, these results show there is an upregulation of Ca^{2+} responses to group I mGluR stimulations in SPNs after 6-OHDA lesions. The results in D1KO mice suggest that group I mGluR signaling and Ca^{2+} responses are mostly upregulated in D1-dSPNs. Indeed, in the absence of D1R, Ca^{2+} responses are inhibited in a subpopulation of SPNs, probably dSPNs. But group I mGluR-induced Ca^{2+} responses are also increased in some remaining responsive cells, probably iSPNs, since the amplitude of the Ca^{2+} responses triggered by DHPG in the remaining responsive cells remained increased in the 6-OHDA-lesioned D1KO mice. It showed that group I mGluR-dependent signaling is still functional and increase in some of the non-D1R SPNs. These data are too preliminary to affirm which mGluR is involved. Further experiments are required to explore the involvement in particular of mGluR5 since this receptor has previously been implicated in LIDs and ERK activation in SPN. Experiments in D1-cre and A2A-Cre mice would also help to confirm the subpopulations of SPN in which this upregulation takes place.

Together with the data that we reported regarding AMPA-induced Ca^{2+} responses, these results show that Ca^{2+} responses induced by glutamate, either by ionotropic or metabotropic receptors activation, are upregulated after 6-OHDA lesions.

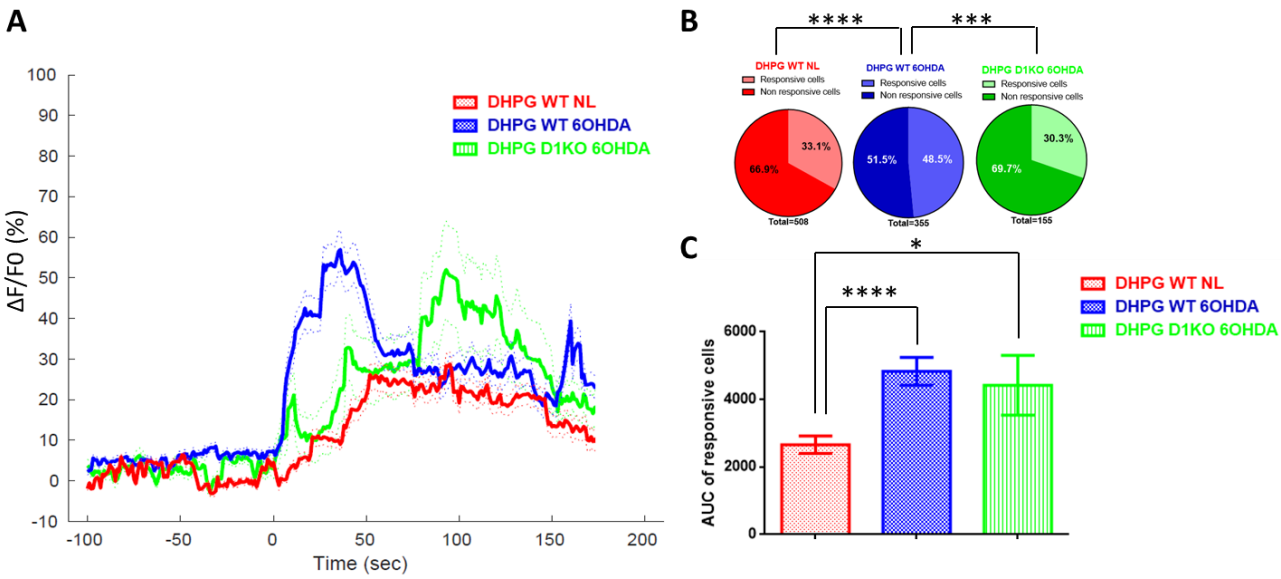

*[**Figure R.17. Ca^{2+} responses induced by the group I mGluR agonist DHPG are increased after 6-OHDA lesion.***
A. *Time course, in responsive cells, of Ca^{2+} responses induced by DHPG (30 s, 20 µM) in non-lesioned wild type (red curve), 6-OHDA-lesioned wild type (blue curve) and 6-OHDA-lesioned D1KO mice (green curve). Data are means +/- SEM (thin dashed lines) for 47 to 172 cells, 4 to 10 slices and 3 to 7 mice per condition.* ***B.*** *Percentage of responsive cells (light colors) versus non-responsive cells (dark colors) in these three groups.* ***C.*** *Mean area under the curve (AUC) of responsive cells in each group of mice after DHPG application (between T0 and T150). *p<0.05; ***p = 0.0001; **** p<0.0001]*

4- Upregulation of Ca^{2+} responses to D1-type receptor stimulation occurs in iSPNs after DA depletion possibly via a $A2_AR$-dependent pathway (Additional results III)

4.1. Ca^{2+} responses induced by the D1 receptor agonist SKF81297 are increased in SPNs after 6-OHDA lesion

Dopamine signaling via D1R being a major actor of ERK upregulation in dSPNs after 6-OHDA lesion and in LID (Gerfen *et al.*, 2002; Santini *et al.*, 2007; Westin *et al.*, 2007), we examined if Ca^{2+} responses after activation of D1R were also upregulated in SPNs after 6-OHDA lesions.

We first monitored Ca^{2+} responses to a D1R agonist, SKF81297, in SPNs of non-lesioned and 6-OHDA-lesioned striata (**Figure R.18.A-C**). Ca^{2+} responses to local application of SKF81297 (30 s, 10 µM) were increased after DA depletion, as shown by the increased percentage of responsive SPNs (NL: 29.1%, n = 199/685 SPNs, 15 slices, 8 animals; 6-OHDA: 46.4%, n= 407/878 SPNs, 23 slices, 10 animals; Chi-square; p<0.0001, **Figure R.18.B**) and increased amplitude of response (AUC Mean ± SEM: -NL, 1094 ± 322; 6-OHDA, 2964 ± 210; Mann-Whitney t test, p<0.0001; **Figure R.18.A and C**) in the 6-OHDA-lesioned mice. As above, the spontaneously active cells were excluded of this analysis and are analyzed separately as explained in the manuscript in preparation. These results show that as PKA activity, Ca^{2+} response is upregulated after D1R stimulation in 6-OHDA-lesioned mice. We then wanted to identify the subtype of SPNs in which this upregulation occurred.

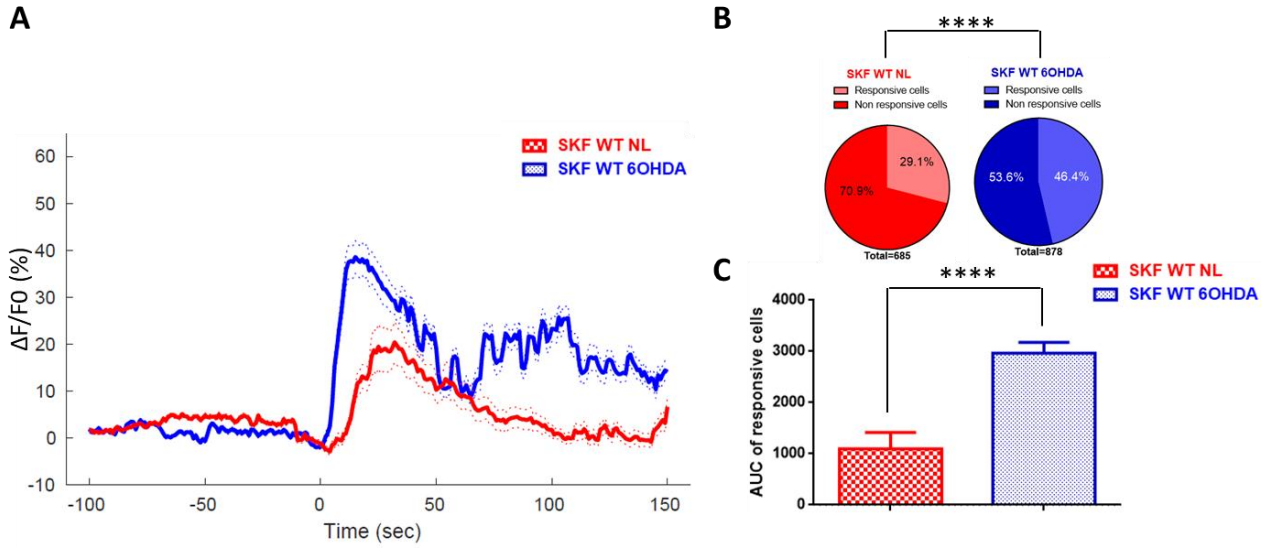

*[**Figure R.18. Ca^{2+} responses induced by the D1 receptor agonist SKF81297 are increased in SPNs after 6-OHDA-lesion.***

***A.** Time course, in responsive cells, of Ca^{2+} responses induced by the D1 receptor agonist SKF81297 (SKF, 30 s, 10 µM) in non-lesioned (red curve) and 6-OHDA-lesioned (blue curve) mice. Data are means +/- SEM (thin dashed lines) for 199 and 407 cells, 15 and 23 slices, 8 and 10 mice per condition. **B.** Percentage of responsive cells (light colors) and non-responsive cells (dark colors) in these two groups. **C.** Mean area under the curve (AUC) of responsive cells in each group of mice after SKF application (between 0 and 170 s). **** p<0.0001]*

4.2. Ca^{2+} responses induced by the D1 receptor agonist SKF81297 in dSPNs after 6-OHDA lesion

We first studied the implication of D1R-expressing dSPNs and the involvement of D1R signaling. To do so, we monitored Ca^{2+} responses induced by the D1R agonist SKF81297 (30 s, 10 µM) selectively in dSPNs (**Figure R.19**). In this aim, we injected a Flex-type AAV Cre-dependently expressing GCaMP6S into the striatum of D1Cre mice (**Figure R.19.A**). Unexpectedly, the percentage of responsive dSPNs (NL: 16.1%, n= 31/193 SPNs, 3 slices, 2 animals; 6-OHDA: 17.7%, n= 58/328 SPNs, 5 slices, 4 animals; Fisher's exact test; p=0.72, **Figure III.R.19.A**) and the amplitude of the responses in the responsive cells (AUC Mean ± SEM: NL, 2909 ± 1763; 6-OHDA, 3454 ± 398; unpaired t test, p=0.76; **Figure R.19.A**) did not differ between non-lesioned and 6-OHDA-lesioned mice. The important variability in the AUC of the responsive cells is due to the fact that with less responsive cells comes more variability. In particular, at the end of acquisition time, 3 cells started to respond with great amplitude. So, maybe the AUC results could in fact not reflect the overall amplitude of Ca^{2+} response that may still be increased in the D1dSPN responsive cells after 6-OHDA lesion. Although very preliminary, and needing to be repeated, these first results suggested that the increased Ca^{2+} response, first globally seen when all subtypes of SPNs were analyzed, did not occur in the dSPN.

We then tested whether the increased response was dependent on D1R by using D1RKO mice. In these mice, the percentage of responsive cells (NL: 13.5%, n = 24/178 SPNs, 6 slices, 5 animals; 6-OHDA: 49.4%, n = 160/324 SPNs, 8 slices, 5 animals; Fisher's exact test; p<0.0001, **Figure R.19.B**) remained greatly increased in the 6-OHDA-lesioned animals. Amplitude of responses did not seem increased (AUC Mean ± SEM: D1KO-NL= 2917 ± 556 vs D1KO-6-OHDA = 2250 ± 328; Mann Whitney test, p<0.05, **Figure R.19.B**). This may be due to the profile of responses in the responsive cells. First, many responsive cells had a low amplitude in the 6-OHDA group. Second, some responsive cells showed an important initial response and then decrease importantly under the baseline. Still, the important increase in percentage of responsive cells suggests an action of SKF81297 on non-D1R-SPNs, maybe iSPNs, upregulated after 6-OHDA-lesion, maybe through a D1R-dependent or D1R-independent pathway.

Since SKF81297 is a D1R agonist but also a D5R agonist, we then analyzed in D1RKO mice Ca^{2+} responses to SKF81297 in the presence of SCH23390 (10 µM), a D1R and D5R antagonist (Ki = 0.2 and 0.3 nM for D1R and D5R, respectively; (Bourne, 2001)). SCH23390 was bath-applied for 2 to 5 min prior to local application of SKF81297 (**Figure III.R.19.C**). We were surprised to still detect a response. Thus, SKF81297 induced some Ca^{2+} responses that were not antagonized by SCH23390 showing that these responses were not mediated by neither D1R nor D5R. Interestingly, the percentage of responsive cells (D1KO-NL SKF+SCH: 15.3%, n = 15/98 SPNs, 3 slices, 3 animals; D1KO-6-OHDA SKF+SCH: 22.4%, n = 47/210 SPNs, 4 slices, 4 animals; Fisher's exact test; p = 0.17, **Figure R.19.C**) and amplitude of the responses (SKF+SCH AUC, mean ± SEM: D1KO-NL, 1142 ± 589; D1KO-6-OHDA = 1998 ± 354; Mann Whitney test, p=0.21, **Figure R.19.C**) were not significantly different in lesioned animals compared to unlesioned, suggesting that the component of SKF81297 responses, independent of D1R or D5R, were not majorly affected by DA depletion. In these conditions, in both intact and 6-OHDA-lesioned striata, the percentages of responsive cells and response amplitude were low and comparable to those observed after SKF81297 alone in non-lesioned D1KO mice (percentage of responsive cells: D1KO-NL SKF alone, 13.5%; D1KO-NL SKF+SCH, 15.3%; D1KO-6-OHDA SKF+SCH = 22.4%, Chi-square, p=0.06. For AUC: D1KO-NL SKF alone, 2917 ± 556; D1KO-NL SKF+SCH, 1142 ± 589; D1KO-6-OHDA SKF+SCH, 1998 ± 354). These

data are clearly preliminary and should be taken with caution. Nevertheless they are intriguing and would be interesting to further investigate in the future. As they are, they suggest that the upregulated Ca^{2+} responses to SKF81297 observed globally in SPNs after 6-OHDA lesion do not specifically occur in dSPN. In addition, SKF81297 triggers low Ca^{2+} responses via an unidentified D1R- and D5R-independent mechanism which is not affected by DA depletion.

To further specify the source of Ca^{2+} increase that was observed, we applied SKF81297 in the presence of cadmium ion (Cd^{2+}), a broad VGCC blocker. Blockade of VGCCs with Cd^{2+} (100 µM) prevented Ca^{2+} entry induced by SKF81297 stimulation in SPNs and dramatically decreased the number of cells with KCl-induced Ca^{2+} responses (4 slices, 4 animals). Thus, SKF81297 induced Ca^{2+} entry depended on VGCCs and was caused by membrane depolarization affecting the cell bodies.

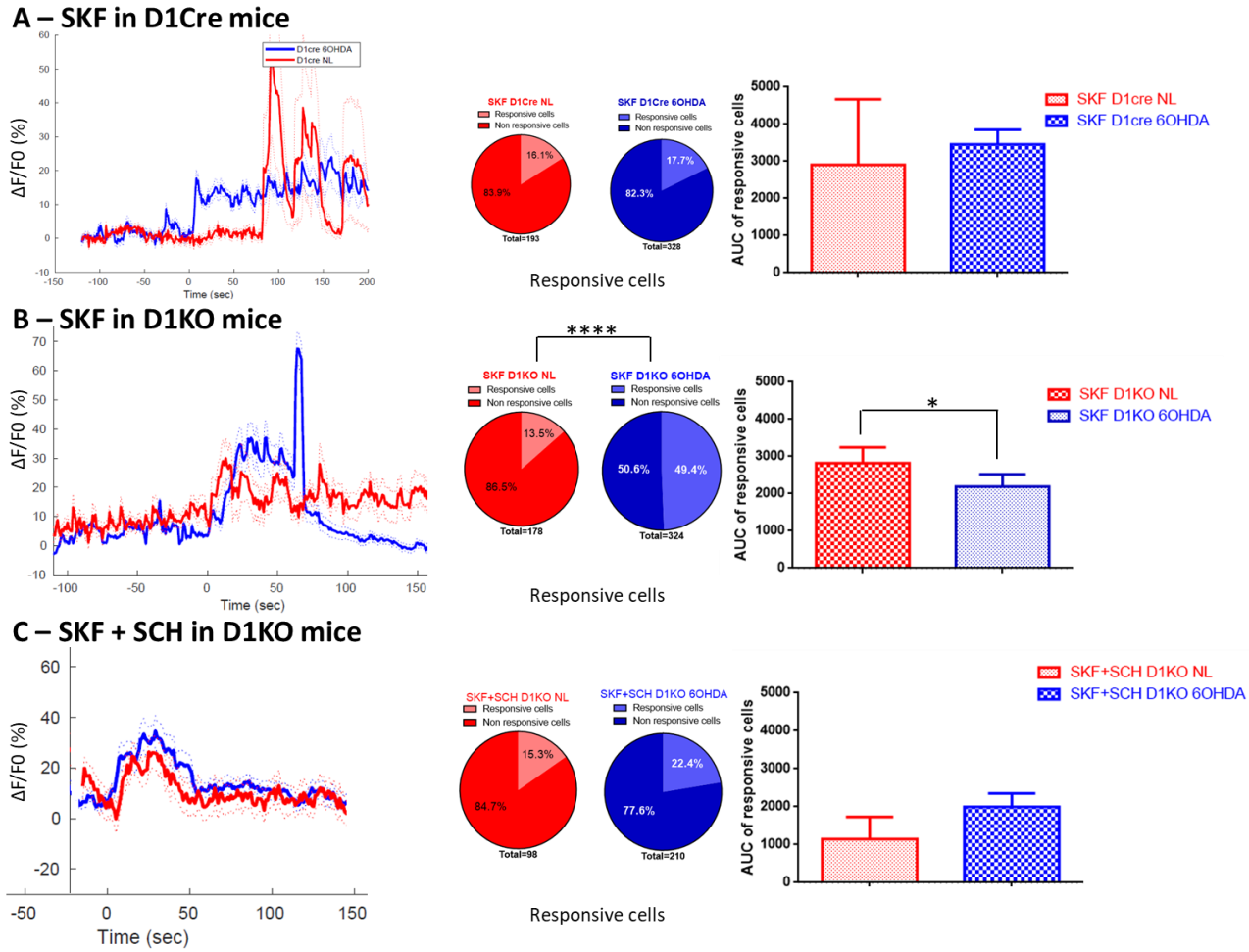

*[**Figure R.19. Ca^{2+} responses induced by SKF81297 are not increased in dSPN and are only partially D1R-dependent.** **A.** Time course of Ca^{2+} responses in responsive cells, percentage and area under the curve (AUC, between 0 and 170 s) of responsive cells after application of SKF81297 (SKF) (30s, 10 µM) in non-lesioned D1Cre (red) and 6-OHDA-lesioned D1Cre (blue) mice. (In the time course graph, 3 cells showed extreme variability after time 90 s). **B.** Time course of Ca^{2+} responses in responsive cells, percentage and AUC (between 0 and 170 s) of responsive cells after application of SKF (30 s, 10 µM) in non-lesioned D1KO (red) and 6-OHDA-lesioned D1KO (blue) mice. **C.** Time course of Ca^{2+} responses in responsive cells, percentage and AUC (between 0 and 110 s) of responsive*

*cells after application of SKF (30 s, 10 µM) with the D1-like receptor antagonist SCH23390 (SCH, 10 µM) bath applied for 5 min prior to SKF application, in non-lesioned D1KO (red) and 6-OHDA-lesioned D1KO (blue) mice. Unpaired t test and Mann Whitney test were used to compare AUCs, Chi-square and Fisher's exact test were used to compare percentage of cells,*p<0.05; **** p<0.0001]*

4.3. Ca^{2+} responses induced by the D1 receptor agonist SKF81297 are upregulated in iSPNs after 6-OHDA lesion

The SKF81297-induced Ca^{2+} responses were increased after 6-OHDA lesion when we considered all types of SPNs (experiments with wild type and D1KO mice), but not when we only analyzed dSPNs (experiments with D1Cre mice). These data suggested these Ca^{2+} responses were increased in iSPNs. To test this hypothesis, we selectively expressed GCaMP6S in the iSPNs by injecting into the striatum of $A2_A$Cre mice an AAV able to Cre-dependently express GCaMP6S. We then monitored Ca^{2+} responses induced by SKF81297 (30 s, 10 µM, **Figure R.20.A**). Both the percentage of responsive cells (NL: 28.3%, n = 91/322 SPNs, 9 slices, 4 animals; 6-OHDA: 39.4%, n = 84/213 SPNs, 7 slices, 4 animals; Fisher's exact test; p<0.01, **Figure R.20.A**) and amplitude of responses (AUC, Mean ± SEM: NL, 3123 ± 543; 6-OHDA, 5393 ± 958; unpaired t test, p<0.05, **Figure R.20.A**) were significantly increased after 6-OHDA lesion. These data suggested that the Ca^{2+} responses to SKF81297 are upregulated in iSPNs after DA depletion.

To test whether the increase was dependent on the release of adenosine on $A2_AR$ or not, we monitored the Ca^{2+} responses to SKF81297 in wild type animals in the presence of the $A2_AR$ antagonist, KW6002, also known as istradefylline, a compound shown to reduce parkinsonism and dyskinesia (Zhu *et al.*, 2014). In the presence of KW6002, the percentage of SKF81297-responsive cells (NL: 26.0%, n= 54/208 SPNs, 4 slices, 3 animals; 6-OHDA: 9.6%, n=11/114 SPNs, 5 slices, 4 animals; Fisher's exact test; p<0.001, **Figure R.20.B**) decreased in 6-OHDA-lesioned animals as compared to non-lesioned animals. In the presence of the $A2_AR$ antagonist KW6002, no significant response could be detected following SKF81297 treatment (**Figure R.20.B**). **These results show the SKF-81297-induced Ca^{2+} responses are mediated through mechanisms involving $A2_AR$ stimulation and are increased in iSPN in the DA-depleted striatum.**

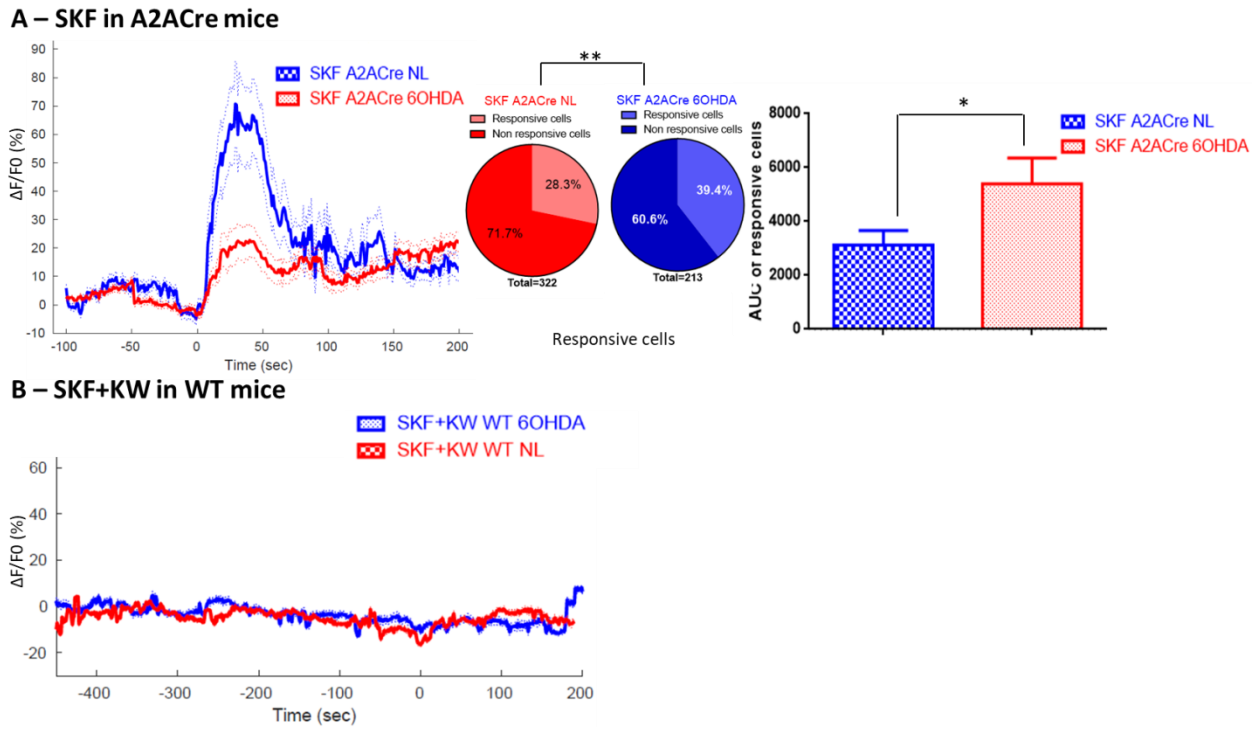

[Figure R.20. Ca^{2+} responses induced by SKF81297 are increased in iSPN in an $A2_AR$-dependent manner after dopamine depletion. A. *Time course of Ca^{2+} responses in responsive cells, percentage and area under the curve (AUC, between 0 and 210 s) of responsive cells after application of SKF81297 (SKF, 30 s, 10 µM) in non-lesioned $A2_ACre$ (red) and 6-OHDA-lesioned $A2_ACre$ (blue) mice.* ***B.*** *Time course of Ca^{2+} responses of all non-spontaneously active cells after application of SKF (30 s, 10 µM) with the $A2_A$ receptor antagonist KW6002 (KW). Bath application of KW6002 started 5 min prior to SKF application, in non-lesioned WT (red curve) and 6-OHDA-lesioned WT (blue curve) mice. KW6002 prevents the Ca^{2+} responses induced by SKF. The absence of detectable response prevents the specific analysis of the responsive cells.*

*Unpaired t test was used to compare AUCs, Fisher's exact test was used to compare percentage of cells, *p<0.05; ** p<0.01**]***

We tested whether these increased responses observed in iSPN were due to the appearance of D1R and D2R co-expression in these neurons. To do so, we used mice carrying both *drd1a*::tdTomato and *drd2*::L10-EFGP transgenes and quantified the number of cells expressing both D1R and D2R in the striata ipsilateral and contralateral to a unilateral 6-OHDA injection (**Figure R.21**). The percentage of cells co-expressing D1R and D2R over the total number of cells was similar on the non-lesioned side and the 6-OHDA-lesioned side (Mean ± SEM [Range]: NL side, 4.0‰ ± 0.6 [2.3-6.0]; 6-OHDA-lesioned side = 3.6‰ ± 0.4 [2.1-4.9]; Wilcoxon match-paired test; p = 0.81; 5 animals, 15 slices per side). This results using the expression of fluorescent proteins as a proxy suggests that the activity of the drd1 and drd2 promoters is not changed by the DA depletion induced by 6-OHDA lesion, and therefore that the number of SPN co-expressing D1R and D2R is unlikely to be modified by the lesion, in agreement with previous reports (Gagnon *et al.*, 2017).

Together these preliminary results show that the SKF81297-induced Ca^{2+} responses are increased in SPNs after 6-OHDA lesion. Unexpectedly, this increase appears to occur in iSPN rather than in dSPN.

This upregulation of Ca^{2+} responses in iSPN could occur through an indirect mechanism maybe implicating other receptors such as $A2_AR$ stimulation.

A

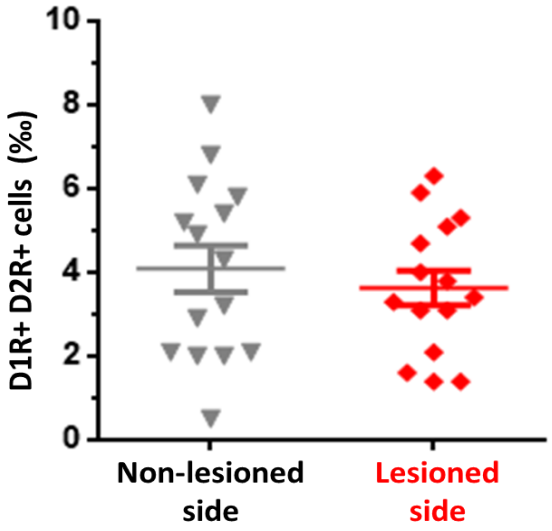

B

	Number of double green and red (D1R+ D2R+) cells	Total number of cells (DAPI +)	Ratio D1+D2R+/DAPI+ (‰)
Non-lesioned side	7.7 ± 1.0	2034 ± 159	4.0 ± 0.6
Lesioned side	6.8 ± 0.8	1948 ± 166	3.6 ± 0.4

[Figure R.21. Quantification of cells potentially co-expressing D1R and D2R in the striata of 6-OHDA-lesioned animals. *In this experiment, the expression of tomato or L10a-GFP under the control of the D1 and D2 promoters in BACs was taken as an indication of the expression of the corresponding endogenous receptors.*

A. *In 6-OHDA-lesioned* drd1a::*tdTomato x* drd2::*-L10-EFGP mice, the ratios of the number of cells co-expressing tdTomato (D1R-expressing cells) and L10-EGFP (D2R-expressing cells) over the total number of cells determined by DAPI staining were compared. Means and SEM are indicated. Statistics, Wilcoxon match-paired test; p = 0.81 not significant.*

B. *Absolute numbers of cells with co-expression of tdTomato (D1R-expressing cells) and L10-EGFP (D2R-expressing cells), absolute numbers of all cells stained with DAPI and ratios of co-expressing cellsover the total number of cells are detailed for lesioned and non-lesioned sides. Data are expressed as Means and SEM**]***

Discussion

Discussion

The results of my PhD have allowed better characterizing the upregulation of several signaling pathways after DA-depletion. The use of various biosensors and their genetic targeting helped understanding the specific differences occurring in distinct subpopulations of SPNs. These results are in keeping with the previous results of the literature showing a supersentivie D1R- $G\alpha_{olf}$-PKA pathway and increased glutamate signaling leading to the upregulation of ERK phosphorylation. I believe these results give new clues and new threads to follow by further research experiments. They will help better understanding the chain of events leading to the occurrence of LIDs in PD and find new strategies to prevent their onset.

1- Methodology discussion

An important part of this work was setting up a reliable experimental model. As we were using new tools to investigate signaling pathways in adult corticostriatal slices, we had to make several tests before performing the investigations per se. All the more that imaging with EKAR-EV had never been performed in the striatum of adult mice.

As ERK activation had been observed successfully using more "classical" western blot and immunofluorescence (IF) techniques in striatal slices (Vanhoutte *et al.*, 1999), in *in vivo* models of drug of abuse (Valjent *et al.*, 2000, 2004; Bertran-Gonzalez *et al.*, 2008; Besnard *et al.*, 2011; Pascoli *et al.*, 2011a) or DA-depletion by 6-OHDA (Santini *et al.*, 2007, 2009; Alcacer *et al.*, 2012), we first verified and confirmed in our experimental conditions that this activation of ERK was observed using the same classical IF techniques. The interest of our biosensor approach as opposed to these "static" assessments of ERK activation in fixed tissue was the possibility of monitoring the dynamics of this activation in living cells. More importantly, our assessment of ERK and PKA activations did not depend on antibody penetration in the slice since the cells were expressing the probe thoughout the striatum injected. The drawback of our approach was the impossibility to identify specific subpopulations of SPN involved during our imaging of ERK dynamics. Indeed, with the IF techniques using specific primary and fluorescent secondary antibodies, with confocal microscope imaging, only one wavelength is used for detecting ERK phosphorylation and allows using other wavelengths for identifying distinct subpopulations of SPNs that are tagged by fluorescent proteins in specific mouse strains (Bertran-Gonzalez *et al.*, 2008, 2009, 2010; Matamales *et al.*, 2009). In our approach, because the assessment of FRET emission ratios uses a pair of fluorophores and needs two wavelengths simultaneously, and because of emission spectrum overlaps, it is not possible to use mouse strains in which fluorescent protein expression is driven by cell-specific promoters. One possible solution could be to induce cell-specific expression by using Flex-type AAVs in Cre-lines as we did for GCaMP imaging but Flex-type AAVs for EKAR- and AKAR-type biosensors were not available to us at the time of this study. In addition we did not have access to specific mouse lines expressing those biosensors in specific subpopulations of SPNs. Goto et al (2015) performed an *in vivo* study using two lines of mutant mice with floxed transgenes (floxed-AKAR3EV and floxed-EKAREV). Crossing of the two lines with D1-Cre and D2-Cre BAC transgenic mice generated four species of transgenic mice, expressing either AKAR3EV or EKAREV in dSPNs or iSPNs

(Goto *et al.*, 2015). These mice could be very useful to monitor *in vivo* ERK and PKA activation in specific SPN types of 6-OHDA-lesioned mice treated or not with L-DOPA. However, such approaches are currently fairly invasive with limited resolution and could not have allowed detailed and extensive signaling studies that were possible in slices.

We know that ERK activation, but also behavioral motor impairments, morphological and synaptic plasticity alterations, depend on the degree of lesion (Florio *et al.*, 1993; Zaja-Milatovic *et al.*, 2005; Paillé *et al.*, 2010; Suárez *et al.*, 2014). To take into account this factor, we simply tested the degree of 6-OHDA lesion achieved by TH quantification in the striata that were imaged. A drawback of this approach is regarding the generation of LIDs because we could not know which mice would have develop LIDs and wo could not do behavioral correlations. One possibility would be to perform these experiments in mice previously treated subchronically by L-DOPA and already dyskinetic. But then, our findings would characterize more the abnormal signaling associated with LIDs, than the aberrant signaling leading to subsequent onset of LIDs. Another possibility would be to perform imaging *in vivo* and assess which mice will subsequently develop LIDs. This would allow specific correlations between the abnormal signaling observed and the ones leading to the onset of LIDs.

An advantage of *in vivo* imaging would be the assessment of molecular pathways in SPNs inside a full network with all the inputs and outputs. We tried our best to maintain as many inputs as possible by adapting our slicing protocol. First, ours slices contained cortex and thalamus. And secondly, we adapted the angle of slicing to increase corticostriatal and thalamostriatal connectivity on the basis of several previous reports by others (Kawaguchi et al., 1989; Kita, 1996; Wickens et al., 1998; Fino et al., 2005; Smeal et al., 2007). But obviously, the observations in our study are from a partially preserved network.

2- Cell-specific up-regulation of signaling pathways in the dopamine-depleted striatum (Manuscript in preparation)

Altogether our data show cell-specific up-regulation of various signaling pathways after DA-depletion.

- ERK activation by dopamine and glutamate is increased.
- D1R- $G\alpha_{olf}$-PKA pathway is upregulated in dSPNs and PDEs are down-regulated in dSPNs
- Differences in D1R-PKA signaling in SPNs of young and adult mice
- Intracellular Ca^{2+} transients in response to AMPAR stimulation are increased specifically in iSPN
- Spontaneous Ca^{2+} transients in SPN are increased.

2.1. ERK phosphorylation is upregulated after 6-OHDA lesion

In keeping with the literature, we confirmed that ERK activity is upregulated after 6-OHDA lesion, in particular after D1R stimulation as previously shown by several groups (Gerfen *et al.*, 2002; Pavón *et al.*, 2006; Santini *et al.*, 2007, 2009; Westin *et al.*, 2007; Nicholas *et al.*, 2008; Darmopil *et al.*, 2009; Alcacer *et al.*, 2014). The increased amplitude of ERK activity that we found is consistent with a supersensitive D1R pathway. The number of responsive cells to the D1 agonist was not significantly increased and, in our very sensitive experimental conditions, it corresponded to 40% of KCl-responsive cells in non-lesioned and 44% in lesioned animals. Indeed, this is probably close to the maximum of potentially responsive neurons since D1-dSPNs correspond to about 50% of SPNs in the dorsal striatum (Bertran-

Gonzalez *et al.*, 2010). Our data indicate that, in the DA-depleted striatum, the increase in ERK responses to D1R stimulation is attributable to greater activation in the vast majority of SPNs, but not to the emergence of a new cell population in which ERK responses to D1R stimulation is exacerbated. A low ERK activation is achieved in the majority of dSPNs in normal conditions and this activation appeared to be highly increased in most dSPNs in the 6-OHDA-lesioned striatum.

We also showed that pharmacological glutamate receptor stimulation, mimicking cortico/thalamo-striatal glutamatergic inputs, can activate ERK in SPNs. Indeed, previous works have shown that corticostriatal stimulation alone, in non-lesioned and lesioned animals, can induce ERK activation in SPNs (Sgambato *et al.*, 1998; Gerfen *et al.*, 2002; Quiroz *et al.*, 2009). We chose to use AMPA since ERK activation does not seem to be NMDAR-dependent after 6-OHDA lesion (Gerfen *et al.*, 2002; Rylander *et al.*, 2009), as opposed to findings in models of drug of abuse (Valjent *et al.*, 2000; Pascoli *et al.*, 2011a). AMPAR-mediated activation of ERK has also been previously reported in SPNs (Perkinton *et al.*, 1999; Mao *et al.*, 2004). Moreover administration of an AMPA agonist has the ability to induce LIDs, whereas blockade of AMPAR reduces LIDs (Konitsiotis *et al.*, 2000; Bibbiani *et al.*, 2005; Kobylecki *et al.*, 2010).

Interestingly, in our study, after glutamate AMPAR stimulation (alone or with a D1R agonist) a trend to an increase in the number of cells showing ERK activation was observed, reaching up to 67% of all SPNs when AMPA was co-administered with a D1R agonist. These results suggest that glutamate-induced ERK activation could be happening in another subtype of SPN, such as iSPNs. This is in line with previous findings by Gerfen et al. (2002) who found that after DA-depletion, corticostriatal stimulation alone or with co-administration of a D1R agonist could elicit ERK activation in iSPN, identified by histochemical localization of enkephalin mRNA (Gerfen *et al.*, 2002). Corticostriatal involvement in the activation of ERK preferentially in iSPN has also been reported (Ferguson and Robinson, 2004) maybe through adenosine release since it is prevented by $A2_AR$ blockade (Quiroz *et al.*, 2006). Westin et al. (2007) also showed ERK upregulation after DA-depletion could be elicited in iSPN in dyskinetic animals, identified with enkephalin markers (Westin *et al.*, 2007). Interestingly, Santini et al (2009) showed that L-DOPA-induced ERK activation in animals with LIDs was D1R-dependent and occurred only in dSPN, using *Drd1*-GFP and *Drd2*-GFP mice (Santini *et al.*, 2009). These findings suggest that, after DA-depletion, ERK activation induced by AMPAR and D1R stimulation arises in different SPN types , a process that may be similar to that proposed for ERK activation induced by drugs of abuse based on the coincident synergy of glutamate and DA inputs in dSPN (Girault *et al.*, 2007; Pascoli *et al.*, 2011a), except that in the case of corticostriatal or AMPAR stimulation in the DA-depleted striatum, DA may be replaced by endogenous adenosine.

Another interesting point is the kinetics of ERK activation following pharmacological stimulation (see Figure 1). Our approach allowed seeing ERK activation occurring within individual cells seconds after the pharmacological stimulation of different receptors, and reaching a plateau after approximately 6 to 10 minutes and did not return to baseline during our experiments. No specific differences in the kinetics of ERK activation were seen between the non-lesioned and lesioned animals (data not shown). These findings are quite in agreement with previous works using less sensitive approaches, with fixed tissue at specific time points, where maximal ERK signal was found at 10 to 20 min; and then slowly declined from 30 to 45 min and returned to basal levels at 60 min in the intact striatum and at least 120 min in the

lesioned striatum (Sgambato *et al.*, 1998; Vanhoutte *et al.*, 1999; Gerfen *et al.*, 2002; Pavón *et al.*, 2006; Westin *et al.*, 2007).

2.2. D1R-Gαolf-PKA pathway is upregulated in dSPNs after 6-OHDA lesion

We further investigated the dynamical changes in the upstream signaling pathways leading to ERK activation. We found that, as expected, PKA response was specifically amplified in SPN responsive to D1R agonist after DA depletion. Since no modification of PKA signaling was observed after $A2_AR$ stimulation, these results suggest the upregulation of PKA signaling occurs in dSPN after DA-depletion and D1R supersensitivity is related to an upregulation of the PKA pathway. This is in agreement with previous studies in which an acute administration of L-DOPA increased the phosphorylation of the PKA targets, DARPP-32 at Thr34 and GluA1 at Ser845 (Santini *et al.*, 2007). This pathway seems to be implicated, at least in part, in ERK upregulation and LIDs intensity. Indeed, PKA signaling appears to be necessary for the intensity of LIDs. Pharmacological intrastriatal inhibition of PKA partially reduces LIDs (Lebel *et al.*, 2010). LIDs and ERK phosphorylation were partially decreased in DARPP-32-KO mice (Santini *et al.*, 2007) and a robust decrease in LIDs was observed in 6-OHDA-lesioned mice with a targeted invalidation of DARPP-32 in dSPNs (Bateup *et al.*, 2010). In keeping with this view, in homozygous Golf-/- mice ERK activation was blocked following treatment by a drug of abuse (Corvol *et al.*, 2007), but ERK upregulation and LIDs were not decreased in heterozygous Golf+/- 6-OHDA lesioned mice (Alcacer *et al.*, 2012). This suggests that PKA is necessary for ERK activation but that its upregulation is not the major mechanism of ERK pathway upregulation.

We further investigated the mechanisms underlying this upregulation of PKA signaling specifically observed in dSPN of DA-depleted mice. The supersensitivity of D1R-PKA pathway is not linked to an increase of D1R as their levels were found to be unchanged or lowered following DA denervation in animal models (Savasta *et al.*, 1988; Herve *et al.*, 1989; Missale *et al.*, 1989; Gerfen *et al.*, 1990; Hervé *et al.*, 1992; Pavón *et al.*, 2006; Hervé, 2011). Analysis in PD patients revealed no significant alteration in D1R expression in the striatum (Nikolaus *et al.*, 2009) but an increase in activation of AC by DA in the striatum (Pifl *et al.*, 1992; Tong *et al.*, 2004). In contrast, we observed increased Gαolf levels after lesion of DA neurons in rats and mice as well as in PD patients. Levels of Gαolf were increased in PD patients and rodents after DA depletion (Hervé *et al.*, 1993; Marcotte *et al.*, 1994; Penit-Soria *et al.*, 1997; Corvol *et al.*, 2004; Alcacer *et al.*, 2012; Ruiz-DeDiego *et al.*, 2015; Morigaki *et al.*, 2017). Therefore, we took advantage of heterozygous *Gnal*+/- mice, which develop and breed normally, and provide a very interesting model because they display a decrease of ≈50% in Gαolf protein levels (Alcacer *et al.*, 2012). We found that DA-depletion in *Gnal*+/- mice reversed the decreased PKA activity specifically in dSPN. Our results suggest that an increase in Gαolf protein levels after DA-depletion contributes to increased PKA activity.

In line with a preponderant role of Gαolf-dependent pathways, chemogenetic stimulation of dSPNs mimicked, while stimulation of iSPNs abolished, the therapeutic action of L-DOPA in PD mice; with much stronger effects of DREADD activating Gs-type protein than Gq-type (Alcacer *et al.*, 2017). The homeostatic regulation of Gαolf levels is thought to occur through post-translational mechanisms in the striatum, where the altered expression of the Gαolf protein depends directly on its usage rate (Hervé, 2011). The agonist-induced activation of D1R or $A2_AR$ might lead to the degradation of Gαolf protein in striatal SPNs through this usage-dependent mechanism (Hervé *et al.*, 2001; Corvol *et al.*, 2004; Alcacer *et*

al., 2012; Ruiz-DeDiego *et al.*, 2015). In PD, because of DA-depletion, decreased usage of Gαolf could lead to its accumulation. In support of this hypothesis, in D1R KO and $A2_AR$ KO mice a significant increase of Gαolf protein levels was observed without any change in its mRNAs (Hervé *et al.*, 2001). These studies and our results indicate that one of the main factors leading to sensitized D1R-AC-PKA responses to D1R stimulation is the increase of Gαolf levels in dSPNs.

We investigated another key component of PKA regulation, PDEs. Our results suggest that PDE activity was down-regulated specifically in dSPN after DA depletion. Down-regulation in the expression of PDE in the striatum has been reported after DA-depletion in animal models and PD patients (Giorgi *et al.*, 2011; Niccolini *et al.*, 2015, 2017; Heckman *et al.*, 2018). This down-regulation is, consistent with the absence of efficacy of IBMX when co-applied with D1R agonist or FSK in the DA-depleted striatum that can be interpreted as an "occlusion" effect. We suggest that the decrease of PDE associated with an increase in cAMP production is likely to account for the enhanced PKA activity in response to DA or to direct AC stimulation in DA-depleted dSPNs. Preferential activity of specific PDEs remaining active in specific SPN subpopulations, such as PDE10 in iSPN (Nishi *et al.*, 2008), could also participate in this imbalance. Further investigations about which specific PDE subtype(s) could be down-regulated are needed.

2.3 Differences in D1R-PKA signaling in SPNs of young and adult mice

In our hands, PKA activity was reduced in both types of SPNs of non-lesioned adult heterozygous *Gnal*$^{+/-}$ animals. This was expected since these animals show a decrease of ≈50% in Gαolf protein levels leading to decreased cAMP production and decreased activation of PKA targets in both types of SPNs (Corvol *et al.*, 2001; Alcacer *et al.*, 2012). In contrast, a previous study assessing PKA activity using the AKAR3 biosensor in the striatum failed to find any difference between PKA activity in SPNs of *Gnal*$^{+/-}$ mice and their *Gnal*$^{+/+}$ littermates (Castro *et al.*, 2013). This apparent discrepancy is certainly due to differences in the age of the animals used. Indeed, Castro et al (2013) monitored PKA activity in striatal slices from young P8-P12 mice. We have found marked differences between PKA signaling in young and adult mice, since PKA activity is reduced in adult mice compared to young mice (**Figure D.1**). These differences could be due to the strong PDE activity that we have observed in adult mice (**Figure R.4.D**). Indeed, cAMP is tonically produced in striatal slices and PDEs contribute significantly to its degradation. Castro et al also found a basal PDE activity regulating PKA (Castro *et al.*, 2010; Polito *et al.*, 2015). But the PDE activity in adults could be stronger than in young mice. Indeed, we found that IBMX could further increase the response to FSK in SPNs of adult mice (**Figure R.4.G and H**). Castro et al found cAMP production in response to FSK was only increased by IBMX application in the cortex but not in the striatum of young mice (Castro *et al.*, 2013). This would mean that PDEs in the striatum of young mice are not sufficient to counteract the cAMP production elicited by forskolin.

Another point is the changes of expression of other actors of PKA signaling over development. Indeed, changes in expression of G-protein and AC occur during the postnatal to adult period (Iwamoto *et al.*, 2004). For instance, AC5, an AC inhibited by Ca^{2+}, predominates in the P56 adult brain and AC1, an AC stimulated by Ca^{2+}, has an expression restricted to scattered subset of cells in adults, whereas it is widely distributed in P7 young mice (Visel *et al.*, 2006). AC5 provides around 80% of basal AC activity in the adult striatum (Lee *et al.*, 2002b; Iwamoto *et al.*, 2003). This underlines the importance of working

with adult animals when studying adult disorders, to avoid the different changes in signalling pathways occurring during development.

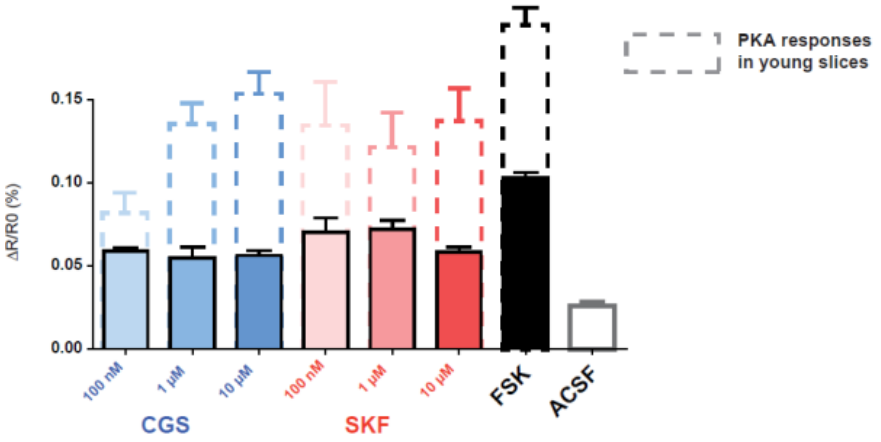

[***Figure D.1: PKA activity is reduced in both types of SPNs in adult wild-type mice compared to young mice***.]

3- Upregulation of ERK activation and Ca^{2+} signaling after glutamate receptors stimulations in SPNs in the dopamine-depleted striatum (Manuscript in preparation and Additional Results II)

Our findings of an activation of ERK after AMPAR stimulation have been discussed above (see section 2.1 of the Discussion). Our very preliminary results of a possible activation of ERK following mGluR group I stimulation (further quantifications and experiments using EKAR will be ultimately performed) are also in accordance to previous reports. Indeed, group I mGluR and in particular mGluR5 have been implicated in the regulation of D1R signaling, activation of ERK and genesis of LID (Rylander *et al.*, 2009; Ouattara *et al.*, 2011; Fieblinger *et al.*, 2014b; Lin *et al.*, 2017; Sebastianutto and Cenci, 2018). Both findings are in line with the fact that corticostriatal glutamatergic stimulation of SPN leads to ERK activation (Sgambato *et al.*, 1998; Quiroz *et al.*, 2009).

Intracellular Ca^{2+} dynamics have been implicated in ERK activation in many models including C. elegans (Tomida *et al.*, 2012), CA1 pyramidal neurons (Zhai *et al.*, 2013) and DA-depleted SPNs in rodents (Fieblinger *et al.*, 2014b). Since we found that stimulation of glutamate receptors of both ionotropic and metabotropic type activated ERK in SPNs after 6-OHDA-induced lesion, we investigated if Ca^{2+} dynamics were modified in SPNs. We observed an increase in intracellular Ca^{2+} in the DA-depleted striatum after glutamate receptors stimulation, in response to ionotropic or metabotropic receptor activation. These findings indicate an increased SPN reactivity to corticostriatal activity. Ca^{2+} imaging was previously shown to reflect SPNs firing after electrical or glutamatergic stimulation in corticostriatal slices (Carrillo-Reid *et al.*, 2008). Decrease in the threshold current required to evoke responses to cortical stimulation has been reported in SPNs after 6-OHDA-induced lesion and interpreted as an overall hyperexcitability of SPNs to cortical inputs (Nisenbaum and Berger, 1992; Florio *et al.*, 1993). This excitability seems to be decreased by AMPAR antagonists as they reduced 50% of SPN activity in MPTP-lesioned monkeys (Singh *et al.*, 2018). Others have demonstrated that this increased responsiveness only affects iSPNs (Mallet *et*

al., 2006; Flores-Barrera *et al.*, 2010). Conversely, dSPN responsiveness to cortical stimulation was found to be decreased by 10-fold, whereas iSPNs responsiveness was increased and correlated with motor deficit in mice with extensive striatal DA depletion (Escande *et al.*, 2016). Increased AMPAR signaling could be due to increased synaptic expression and altered trafficking of AMPAR (Mangiavacchi and Wolf, 2004; Silverdale *et al.*, 2010). An increased synaptic expression of AMPAR in LID was also suggested by the upregulation of Narp, a secreted protein that clusters AMPAR (Charbonnier-Beaupel *et al.*, 2015). Chronically L-DOPA-treated dyskinetic monkeys showed a marked enrichment of the GluA2/3 subunit (and a trend for the GluA1), in a post-synaptic membrane fraction relative to a cytoplasmic vesicular fraction (Silverdale *et al.*, 2010). This GluA2 enrichement at post-synaptic membranes could more specifically affect the GluA2-flip splice variant as suggested by Kobylecki et al. (2013). Increased expression of this specific splice variant of the GluA2 subunit may suggest slower desensitization and larger amplitude of AMPA-mediated synaptic currents (Kobylecki *et al.*, 2013). A possible mechanism for increased AMPAR signaling is through its phosphorylation by PKA since serine phosphorylation of GluA1 enhances channel opening and conductance (Banke *et al.*, 2000; Mangiavacchi and Wolf, 2004). This is however unlikely to explain our observations in iSPNs since cAMP pathway hypersensitivity preferentially happens in D1R-expressing dSPNs after D1R stimulation.

AMPAR-mediated activation of ERK has been previously reported in SPNs through a Ca^{2+}-dependent pathway,possibly via a direct entry through Ca^{2+}-permeable AMPAR (Perkinton *et al.*, 1999; Mao *et al.*, 2004). A functional population of GluA2-lacking Ca^{2+}-permeable receptors in SPNs has been demonstrated (Carter and Sabatini, 2004). Interestingly, in PD, an increased proportion of GluA2-lacking Ca^{2+}-permeable AMPARs at synaptic level was found in lesioned animals after either treatment by L-DOPA or high dose of the D2-agonist pramipexole (Bagetta *et al.*, 2012). These results are in line with those of Kobylecki et al. reporting that administration of an antagonist of Ca^{2+}-permeable AMPAR, IEM 1460, reduced LIDs (Kobylecki *et al.*, 2010). Increased insertion of GluA2-lacking receptors could trigger "abnormal" cellular Ca^{2+} dynamics, increase in related downstream pathways, and eventually pathological synaptic plasticity. Interestingly, dSPN express higher levels of GluA2 protein than iSPNs (Deng *et al.*, 2007). Hence, the increase in GluA2-lacking AMPAR could preferentially occur in iSPNs and be more visible in this subtype of neurons.

Group I mGluRs are involved in Ca^{2+} signaling through various pathways. Their activation induces mobilization of intracellular Ca^{2+} stores and activation of PLC (Conn *et al.*, 2005). mGluR5 also modulates L-type VGCC in a PLC/PKC dependent way (Fieblinger *et al.*, 2014b). We found that the number of responsive cells was decreased in the DA-depleted striatum of D1R KO mice as compared to wild type lesioned mice. This suggests that the Ca^{2+} dynamics after group I mGluR stimulation is partly dependent on D1R and increased in dSPNs. However in D1R KO lesioned mice, amplitude of the response was still increased in the remaining responsive cells, suggesting that this population of responsive cells also showed an upregulated response. Hence, our data suggest that Ca^{2+} dynamics are upregulated in both types of SPNs in response to Group I mGluR stimulation. In iSPN, mGluR5 antagonist in dyskinetic animals regulated the signaling modifications observed in iSPNs. It normalized changes in D2 receptors, signaling proteins (ERK1/2 and Akt/GSK3β levels) and neuropeptides (preproenkephalin but also preprodynorphin) and decreased LID (Morin *et al.*, 2014, 2016). Another possible level of interaction could be through mGluR5 interaction with D2R and $A2_AR$ as heteromers in iSPNs. In dSPN, it is possible that these upregulated Ca^{2+} responses participate in LIDs via ERK and PKC activation as suggested by findings DA-

depleted rodents (Fieblinger *et al.*, 2014b; Lin *et al.*, 2017). Further experiments are needed to better characterize the type of mGluR involved (mGluR1 or mGluR5), the type of SPNs in which these Ca^{2+} responses are upregulated (dSPN or iSPN) and the source of increased Ca^{2+} (intracellular stores, extracellular through VGCC,…).

4- Up-regulation of dopamine-induced Ca^{2+} signaling in the dopamine-depleted striatum (Additional Results III)

Additionally, to the study of ERK and PKA signaling in SPNs after D1R-like receptor stimulation, we explored Ca^{2+} dynamics following DA denervation and D1R-stimulation. Indeed, D1-like receptor-activation of ERK in lesioned animals has been previously shown to be Ca^{2+}-dependent (Fieblinger *et al.*, 2014b). Our preliminary results are in line with these findings since we show that Ca^{2+} dynamics induced by D1R-stimulation are upregulated in the DA-denervated striatum.

Very surprinsingly, this upregulation seems to occur in iSPNs rather than in dSPNs. Activation of iSPN after the use of D1R-agonists was previously reported. Indeed, ERK phosphorylation appears to increase in a small subpopulation of iSPN following the use of D1R agonist in DA-depleted striatum (Gerfen *et al.*, 2002; Westin *et al.*, 2007) which was D1R-dependent, as a D1R antagonist prevented this activation of ERK in iSPN (Westin *et al.*, 2007). A recent study has also shown effects in iSPNs via D1R-dependent mechanism. DA drives decreased Gαolf levels in iSPNs maybe through a D1R-dependent mechanism (Morigaki *et al.*, 2017) or an increased usage of Gαolf (Hervé *et al.*, 2001). Both Westin et al (2007) and Morigaki et al (2017) have hypothesized a multisynaptic chain of events leading to modifications in iSPN after D1R stimulation on dSPN, involving glutamate and adenosine signaling. Interestingly, decortication preferentially prevents ERK activation in iSPN (Ferguson and Robinson, 2004). Moreover, glutamate can evoke an increase in adenosine levels (Harvey and Lacey, 1997; Delaney *et al.*, 1998; Nash and Brotchie, 2000). And blockade of A2R prevents cAMP-PKA pathway activation and ERK phosphorylation in iSPN after corticostriatal stimulation (Quiroz *et al.*, 2006). In striatal neurons in culture, D1R-agonist induced an increase of ATP-induced intracellular Ca^{2+} rise (Rubini *et al.*, 2008). In the DA-depleted striatum with D1R hypersensitivity, the pulsatile activation of D1Rs, could facilitate the glutamate-evoked increase of extracellular adenosine levels and lead to the activation of $A2_ARs$. Our preliminary findings indicate that there is an increase in both D1 agonist- and AMPA-induced Ca^{2+} dynamics occuring in iSPN of DA-depleted striatum that is abolished after application of the $A2_A$ antagonist KW6002. These findings are compatible with the same hypothesis of a D1R-dependent activation of glutamate and adenosine transmissions on iSPNs leading to increased Ca^{2+} signaling but need further investigations.

Another point that should be kept in mind is the limited specificity of pharmacological agents. Indeed, the D1R-like agonist, SKF81297, that we used could perfectly well induce a stimulation of D5R located for instance on interneurons, but is also partial agonist of the D1/D2 heteromers if they exist in the dosal striatum (Rashid *et al.*, 2007). These potential pathways should not be ruled out. Further investigations will be needed to test the possible respective involvements of adenosine, glutamate and other DA receptors such as D2 and D5 in this very intriguing upregulation of Ca^{2+} signaling in iSPN in response to D1-like agonist application in DA-depleted mice.

5. Increased spontaneous intracellular Ca^{2+} transients in SPNs in the dopamine-depleted striatum (Aditional Results IV)

During our Ca^{2+} dynamics experiments we observed that some SPNs are spontaneously active and show transient increases in intracellular Ca^{2+} before any drug application. The same kind of spontaneous activity has been reported by others during Ca^{2+} imaging of SPNs in corticostriatal slices (Jáidar *et al.*, 2010; Carrillo-Reid *et al.*, 2011). We found that these spontaneous intracellular Ca^{2+} transients were increased in the DA-depleted striatum, similarly to previous findings by others (Jáidar *et al.*, 2010). This could be reflecting that, SPNs are more excitable after DA-depletion (Fino *et al.*, 2007). Our preliminary analysis shows that these increased spontaneous Ca^{2+} transients seem to affect more dSPN than iSPN after DA-depletion. Assuming that they reflect an increased intrinsic excitability of SPNs, our results would be compatible with previous electrophysiological results in specific subpopulations of SPN showing that dSPN intrinsic excitability was elevated in a PD model without neuronal scaling of the strength of corticostriatal synapses (Fieblinger *et al.*, 2014a).

Interestingly, Jaidar et al. and Carillo-Reid et al. found that DA deprivation enhances cell assemblies activation, showing activation of a specific network of neurons, engaging into a dominant network state (Carrillo-Reid *et al.*, 2008; Jáidar *et al.*, 2010). This effect could be related to reduced mutual inhibition between SPNs because DA depletion is known to greatly decrease the local axon collaterals of SPNs (Tecuapetla *et al.*, 2005; Taverna *et al.*, 2008). However the concept of network activation in the striatum, mostly comprised of inhibitory neurons remains to be clarified. Increased spontaneous Ca^{2+} transients could reflect corticostriatal hyperactivity as inhibition of NMDAR or AMPAR reduced the number of active cells and synchrony. However, some neurons remained active even in the presence of both glutamatergic antagonists (Jáidar *et al.*, 2010). This could reflect an increased intrinsic excitability or reactivity to other neurotransmitter modulations in those neurons.

The modulation of these putative striatal networks by DA has been explored and it was reported that activation of either D1R or D2R increased the correlated activity and synchrony of microcircuits in the DA-intact striatum (Carrillo-Reid *et al.*, 2011). After the application of a DA D1R agonist, the non-lesioned striatal network remained hyperactive. Peaks of synchronous activity continued to appear (Jáidar *et al.*, 2010), whereas L-DOPA significantly reduced the enhanced pathological activity of the DA-depleted circuit (Plata *et al.*, 2013). The mechanisms underlying these observations need to be further explored. As the dynamics and correlations of these spontaneously active cells are still unresolved, our plan is to further analyze by crosscorrelations the spontaneously active cells. We will then look into there behaviors after specific DA or glutamate pharmacological stimulations to determine if the DA-depleted network has a different organization and excitability.

Concluding remarks

This thesis has contributed insights into several aspects of Parkinson's disease and dyskinesias induced by L-DOPA. My work focused mainly on dysregulation of signaling pathways in striatal projection neurons that are produced by the loss of DA afferents. To address this question I developed an efficient experimental model combining 6-OHDA lesions in adult mice with virally transduced fluorescent biosensors for 2-photon imaging in corticostriatal slices.

Because of the proposed role of ERK signaling pathway in the generation of LIDs, we first examined the dynamics of ERK activation in the DA-depleted dorsal striatum. Our findings confirmed the upregulation of ERK signaling in response to the stimulation of either DA D1R or glutamate receptors. Since both cAMP and Ca^{2+} signaling are known to be able to activate ERK, we examined their regulation in our conditions. We first showed an increased responsiveness of PKA to D1R stimulation and provided evidence that the combination of an up-regulation of Gαolf and down-regulation of PDE activity could account for this hypersensitivity in D1 SPNs. It will remain to determine whether these alterations of cAMP and ERK pathways in dSPNs can account for the increase in spontaneous intracellular Ca^{2+} transients that we observed in these neurons in the absence of DA.

Importantly, in addition to these alterations in dSPNs, we showed that, in the absence of DA, Ca^{2+} signaling was upregulated in iSPNs following stimulation of ionotropic AMPA receptors. This finding is in agreement with previous reports using electrophysiological approaches, which suggested an hyperexcitability of iSPNs. This may account for the lesion-induced hyperactivation of ERK in iSPNs, reported following electrical stimulation of the corticostriatal pathway, and that was likely to occur in our experiments with AMPA treatment.

Our study of the DA- and glutamate-dependent pathways suggests different mechanisms of ERK in the two main populations of SPNs. Increased ERK activation following D1R activation can be explained, at least in part, by the selective upregulation of PKA signaling in dSPNs. In contrast, glutamate released from corticostriatal terminals may contribute to the upregulation of ERK signaling in iSPN since Ca^{2+} entry induced by AMPAR stimulation was only increased in this population. Hence DA/D1R and glutamate/AMPAR signaling pathways seem to be affected differentially in the two populations of SPNs rather than being jointly modified to enhance ERK activation in the same population.

Further experiments will be needed to determine whether chronic L-DOPA is able to normalize some of these abnormalities of intracellular signaling in dSPNs and iSPNs or whether it amplifies them. In fact, cAMP and ERK, the signaling pathways sensitized in the absence of DA, are those which are normally key positive modulators of synaptic plasticity in many brain regions including the striatum. We suggest that the strong and non-physiological variations of DA levels during the pharmacological replacement therapy will trigger exaggerated and inappropriate synaptic plasticity and thereby lead to the appearance of adverse consequences such as dyskinesia in PD patients.

Thus, our work combining the live imaging of multiple signaling pathways in adult striatal neurons in the presence and absence of DA, provides important clues about the mechanisms leading to the long-term complications of dopatherapy in PD and suggests hypotheses that will have to be tested directly in the future.

References

References

Abercrombie ED, Bonatz AE, Zigmond MJ. Effects of L-dopa on extracellular dopamine in striatum of normal and 6-hydroxydopamine-treated rats. Brain Res. 1990; 525: 36–44.

Adams SR, Harootunian AT, Buechler YJ, Taylor SS, Tsien RY. Fluorescence ratio imaging of cyclic AMP in single cells. Nature 1991; 349: 694–697.

Ade KK, Wan Y, Chen M, Gloss B, Calakos N. An Improved BAC Transgenic Fluorescent Reporter Line for Sensitive and Specific Identification of Striatonigral Medium Spiny Neurons. Front. Syst. Neurosci. 2011; 5: 32.

Ahlskog JE, Muenter MD. Frequency of levodopa-related dyskinesias and motor fluctuations as estimated from the cumulative literature. Mov. Disord. Off. J. Mov. Disord. Soc. 2001; 16: 448–458.

Ahmed I, Bose SK, Pavese N, Ramlackhansingh A, Turkheimer F, Hotton G, et al. Glutamate NMDA receptor dysregulation in Parkinson's disease with dyskinesias. Brain J. Neurol. 2011; 134: 979–986.

Akerboom J, Carreras Calderón N, Tian L, Wabnig S, Prigge M, Tolö J, et al. Genetically encoded calcium indicators for multi-color neural activity imaging and combination with optogenetics. Front. Mol. Neurosci. 2013; 6: 2.

Akerboom J, Chen T-W, Wardill TJ, Tian L, Marvin JS, Mutlu S, et al. Optimization of a GCaMP calcium indicator for neural activity imaging. J. Neurosci. Off. J. Soc. Neurosci. 2012; 32: 13819–13840.

Akerboom J, Rivera JDV, Guilbe MMR, Malavé ECA, Hernandez HH, Tian L, et al. Crystal structures of the GCaMP calcium sensor reveal the mechanism of fluorescence signal change and aid rational design. J. Biol. Chem. 2009; 284: 6455–6464.

Albin RL, Young AB, Penney JB. The functional anatomy of basal ganglia disorders. Trends Neurosci. 1989; 12: 366–375.

Alcacer C, Andreoli L, Sebastianutto I, Jakobsson J, Fieblinger T, Cenci MA. Chemogenetic stimulation of striatal projection neurons modulates responses to Parkinson's disease therapy. J. Clin. Invest. 2017; 127: 720–734.

Alcacer C, Charbonnier-Beaupel F, Corvol J-C, Girault J-A, Hervé D. Mitogen- and stress-activated protein kinase 1 is required for specific signaling responses in dopamine-denervated mouse striatum, but is not necessary for L-DOPA-induced dyskinesia. Neurosci. Lett. 2014; 583: 76–80.

Alcacer C, Santini E, Valjent E, Gaven F, Girault J-A, Hervé D. Gα(olf) mutation allows parsing the role of cAMP-dependent and extracellular signal-regulated kinase-dependent signaling in L-3,4-dihydroxyphenylalanine-induced dyskinesia. J. Neurosci. Off. J. Soc. Neurosci. 2012; 32: 5900–5910.

Alexander GE, Crutcher MD. Functional architecture of basal ganglia circuits: neural substrates of parallel processing. Trends Neurosci. 1990; 13: 266–271.

Alexander GE, DeLong MR, Strick PL. Parallel organization of functionally segregated circuits linking basal ganglia and cortex. Annu. Rev. Neurosci. 1986; 9: 357–381.

Allen MD, Zhang J. Subcellular dynamics of protein kinase A activity visualized by FRET-based reporters. Biochem. Biophys. Res. Commun. 2006; 348: 716–721.

Andersen PH, Gingrich JA, Bates MD, Dearry A, Falardeau P, Senogles SE, et al. Dopamine receptor subtypes: beyond the D1/D2 classification. Trends Pharmacol. Sci. 1990; 11: 231–236.

André VM, Cepeda C, Cummings DM, Jocoy EL, Fisher YE, William Yang X, et al. Dopamine modulation of excitatory currents in the striatum is dictated by the expression of D1 or D2 receptors and modified by endocannabinoids. Eur. J. Neurosci. 2010; 31: 14–28.

Antonini A, Jenner P. Apomorphine infusion in advanced Parkinson disease. Nat. Rev. Neurol. 2018

Arbuthnott GW, Wickens J. Space, time and dopamine. Trends Neurosci. 2007; 30: 62–69.

Assous M, Tepper JM. Excitatory extrinsic afferents to striatal interneurons and interactions with striatal microcircuitry. Eur. J. Neurosci. 2018

Aubert I, Guigoni C, Håkansson K, Li Q, Dovero S, Barthe N, et al. Increased D1 dopamine receptor signaling in levodopa-induced dyskinesia. Ann. Neurol. 2005; 57: 17–26.

Bacskai BJ, Hochner B, Mahaut-Smith M, Adams SR, Kaang BK, Kandel ER, et al. Spatially resolved dynamics of cAMP and protein kinase A subunits in Aplysia sensory neurons. Science 1993; 260: 222–226.

Bading H. Nuclear calcium signalling in the regulation of brain function. Nat. Rev. Neurosci. 2013; 14: 593–608.

Bagetta V, Picconi B, Marinucci S, Sgobio C, Pendolino V, Ghiglieri V, et al. Dopamine-dependent long-term depression is expressed in striatal spiny neurons of both direct and indirect pathways: implications for Parkinson's disease. J. Neurosci. Off. J. Soc. Neurosci. 2011; 31: 12513–12522.

Bagetta V, Sgobio C, Pendolino V, Del Papa G, Tozzi A, Ghiglieri V, et al. Rebalance of striatal NMDA/AMPA receptor ratio underlies the reduced emergence of dyskinesia during D2-like dopamine agonist treatment in experimental Parkinson's disease. J. Neurosci. Off. J. Soc. Neurosci. 2012; 32: 17921–17931.

Baird GS, Zacharias DA, Tsien RY. Circular permutation and receptor insertion within green fluorescent proteins. Proc. Natl. Acad. Sci. U. S. A. 1999; 96: 11241–11246.

Ballarín M, Fredholm BB, Ambrosio S, Mahy N. Extracellular levels of adenosine and its metabolites in the striatum of awake rats: inhibition of uptake and metabolism. Acta Physiol. Scand. 1991; 142: 97–103.

Ballarin M, Herrera-Marschitz M, Casas M, Ungerstedt U. Striatal adenosine levels measured 'in vivo' by microdialysis in rats with unilateral dopamine denervation. Neurosci. Lett. 1987; 83: 338–344.

Ballarin M, Reiriz J, Ambrosio S, Mahy N. Effect of locally infused 2-chloroadenosine, an A1 receptor agonist, on spontaneous and evoked dopamine release in rat neostriatum. Neurosci. Lett. 1995; 185: 29–32.

Balleine BW, Liljeholm M, Ostlund SB. The integrative function of the basal ganglia in instrumental conditioning. Behav. Brain Res. 2009; 199: 43–52.

Bamford NS, Zhang H, Schmitz Y, Wu N-P, Cepeda C, Levine MS, et al. Heterosynaptic dopamine neurotransmission selects sets of corticostriatal terminals. Neuron 2004; 42: 653–663.

Banke TG, Bowie D, Lee H, Huganir RL, Schousboe A, Traynelis SF. Control of GluR1 AMPA receptor function by cAMP-dependent protein kinase. J. Neurosci. Off. J. Soc. Neurosci. 2000; 20: 89–102.

Baquet ZC, Bickford PC, Jones KR. Brain-derived neurotrophic factor is required for the establishment of the proper number of dopaminergic neurons in the substantia nigra pars compacta. J. Neurosci. Off. J. Soc. Neurosci. 2005; 25: 6251–6259.

Bara-Jimenez W, Sherzai A, Dimitrova T, Favit A, Bibbiani F, Gillespie M, et al. Adenosine A(2A) receptor antagonist treatment of Parkinson's disease. Neurology 2003; 61: 293–296.

Bastiaens PI, Pepperkok R. Observing proteins in their natural habitat: the living cell. Trends Biochem. Sci. 2000; 25: 631–637.

Bastide MF, Dovero S, Charron G, Porras G, Gross CE, Fernagut P-O, et al. Immediate-early gene expression in structures outside the basal ganglia is associated to l-DOPA-induced dyskinesia. Neurobiol. Dis. 2014; 62: 179–192.

Bastide MF, Meissner WG, Picconi B, Fasano S, Fernagut P-O, Feyder M, et al. Pathophysiology of L-dopa-induced motor and non-motor complications in Parkinson's disease. Prog. Neurobiol. 2015; 132: 96–168.

Bateup HS, Santini E, Shen W, Birnbaum S, Valjent E, Surmeier DJ, et al. Distinct subclasses of medium spiny neurons differentially regulate striatal motor behaviors. Proc. Natl. Acad. Sci. U. S. A. 2010; 107: 14845–14850.

Bateup HS, Svenningsson P, Kuroiwa M, Gong S, Nishi A, Heintz N, et al. Cell type-specific regulation of DARPP-32 phosphorylation by psychostimulant and antipsychotic drugs. Nat. Neurosci. 2008; 11: 932–939.

Beaulieu J-M, Gainetdinov RR. The physiology, signaling, and pharmacology of dopamine receptors. Pharmacol. Rev. 2011; 63: 182–217.

Beck G, Maehara S, Chang PL, Papa SM. A Selective Phosphodiesterase 10A Inhibitor Reduces L-Dopa-Induced Dyskinesias in Parkinsonian Monkeys. Mov. Disord. Off. J. Mov. Disord. Soc. 2018a; 33: 805–814.

Beck G, Singh A, Papa SM. Dysregulation of striatal projection neurons in Parkinson's disease. J. Neural Transm. Vienna Austria 1996 2018b; 125: 449–460.

Beggiato S, Tomasini MC, Borelli AC, Borroto-Escuela DO, Fuxe K, Antonelli T, et al. Functional role of striatal A2A, D2, and mGlu5 receptor interactions in regulating striatopallidal GABA neuronal transmission. J. Neurochem. 2016; 138: 254–264.

Belin D, Jonkman S, Dickinson A, Robbins TW, Everitt BJ. Parallel and interactive learning processes within the basal ganglia: relevance for the understanding of addiction. Behav. Brain Res. 2009; 199: 89–102.

Belluscio L, Gold GH, Nemes A, Axel R. Mice deficient in G(olf) are anosmic. Neuron 1998; 20: 69–81.

Bender AT, Beavo JA. Cyclic nucleotide phosphodiesterases: molecular regulation to clinical use. Pharmacol. Rev. 2006; 58: 488–520.

Berendse HW, Groenewegen HJ. Organization of the thalamostriatal projections in the rat, with special emphasis on the ventral striatum. J. Comp. Neurol. 1990; 299: 187–228.

Berg J, Hung YP, Yellen G. A genetically encoded fluorescent reporter of ATP:ADP ratio. Nat. Methods 2009; 6: 161–166.

Bergman H, Wichmann T, DeLong MR. Reversal of experimental parkinsonism by lesions of the subthalamic nucleus. Science 1990; 249: 1436–1438.

Berke JD, Paletzki RF, Aronson GJ, Hyman SE, Gerfen CR. A complex program of striatal gene expression induced by dopaminergic stimulation. J. Neurosci. Off. J. Soc. Neurosci. 1998; 18: 5301–5310.

Bernard V, Bolam JP. Subcellular and subsynaptic distribution of the NR1 subunit of the NMDA receptor in the neostriatum and globus pallidus of the rat: co-localization at synapses with the GluR2/3 subunit of the AMPA receptor. Eur. J. Neurosci. 1998; 10: 3721–3736.

Bernard V, Somogyi P, Bolam JP. Cellular, subcellular, and subsynaptic distribution of AMPA-type glutamate receptor subunits in the neostriatum of the rat. J. Neurosci. Off. J. Soc. Neurosci. 1997; 17: 819–833.

Bernheimer H, Birkmayer W, Hornykiewicz O, Jellinger K, Seitelberger F. Brain dopamine and the syndromes of Parkinson and Huntington. Clinical, morphological and neurochemical correlations. J. Neurol. Sci. 1973; 20: 415–455.

Berridge MJ. Neuronal calcium signaling. Neuron 1998; 21: 13–26.

Berthet A, Porras G, Doudnikoff E, Stark H, Cador M, Bezard E, et al. Pharmacological analysis demonstrates dramatic alteration of D1 dopamine receptor neuronal distribution in the rat analog of L-DOPA-induced dyskinesia. J. Neurosci. Off. J. Soc. Neurosci. 2009; 29: 4829–4835.

Bertran-Gonzalez J, Bosch C, Maroteaux M, Matamales M, Hervé D, Valjent E, et al. Opposing patterns of signaling activation in dopamine D1 and D2 receptor-expressing striatal neurons in response to cocaine and haloperidol. J. Neurosci. Off. J. Soc. Neurosci. 2008; 28: 5671–5685.

Bertran-Gonzalez J, Håkansson K, Borgkvist A, Irinopoulou T, Brami-Cherrier K, Usiello A, et al. Histone H3 phosphorylation is under the opposite tonic control of dopamine D2 and adenosine A2A receptors in striatopallidal neurons. Neuropsychopharmacol. Off. Publ. Am. Coll. Neuropsychopharmacol. 2009; 34: 1710–1720.

Bertran-Gonzalez J, Hervé D, Girault J-A, Valjent E. What is the Degree of Segregation between Striatonigral and Striatopallidal Projections? Front. Neuroanat. 2010; 4

Besnard A, Bouveyron N, Kappes V, Pascoli V, Pagès C, Heck N, et al. Alterations of molecular and behavioral responses to cocaine by selective inhibition of Elk-1 phosphorylation. J. Neurosci. Off. J. Soc. Neurosci. 2011; 31: 14296–14307.

Betarbet R, Porter RH, Greenamyre JT. GluR1 glutamate receptor subunit is regulated differentially in the primate basal ganglia following nigrostriatal dopamine denervation. J. Neurochem. 2000; 74: 1166–1174.

Bibbiani F, Oh JD, Kielaite A, Collins MA, Smith C, Chase TN. Combined blockade of AMPA and NMDA glutamate receptors reduces levodopa-induced motor complications in animal models of PD. Exp. Neurol. 2005; 196: 422–429.

Bibbiani F, Oh JD, Petzer JP, Castagnoli N, Chen J-F, Schwarzschild MA, et al. A2A antagonist prevents dopamine agonist-induced motor complications in animal models of Parkinson's disease. Exp. Neurol. 2003; 184: 285–294.

Bibb JA, Snyder GL, Nishi A, Yan Z, Meijer L, Fienberg AA, et al. Phosphorylation of DARPP-32 by Cdk5 modulates dopamine signalling in neurons. Nature 1999; 402: 669–671.

Björklund A, Dunnett SB. Dopamine neuron systems in the brain: an update. Trends Neurosci. 2007; 30: 194–202.

Blackwell KT, Czubayko U, Plenz D. Quantitative estimate of synaptic inputs to striatal neurons during up and down states in vitro. J. Neurosci. Off. J. Soc. Neurosci. 2003; 23: 9123–9132.

Bleickardt CJ, Kazdoba TM, Jones NT, Hunter JC, Hodgson RA. Antagonism of the adenosine A2A receptor attenuates akathisia-like behavior induced with MP-10 or aripiprazole in a novel non-human primate model. Pharmacol. Biochem. Behav. 2014; 118: 36–45.

Blum Y, Fritz RD, Ryu H, Pertz O. Measuring ERK Activity Dynamics in Single Living Cells Using FRET Biosensors. Methods Mol. Biol. Clifton NJ 2017; 1487: 203–221.

Bogenpohl JW, Ritter SL, Hall RA, Smith Y. Adenosine A2A receptor in the monkey basal ganglia: ultrastructural localization and colocalization with the metabotropic glutamate receptor 5 in the striatum. J. Comp. Neurol. 2012; 520: 570–589.

Bolam JP, Hanley JJ, Booth PA, Bevan MD. Synaptic organisation of the basal ganglia. J. Anat. 2000; 196 (Pt 4): 527–542.

Bonaventura J, Navarro G, Casadó-Anguera V, Azdad K, Rea W, Moreno E, et al. Allosteric interactions between agonists and antagonists within the adenosine A2A receptor-dopamine D2 receptor heterotetramer. Proc. Natl. Acad. Sci. U. S. A. 2015; 112: E3609–3618.

Bootman MD, Rietdorf K, Collins T, Walker S, Sanderson M. Ca2+-sensitive fluorescent dyes and intracellular Ca2+ imaging. Cold Spring Harb. Protoc. 2013; 2013: 83–99.

Borroto-Escuela DO, Romero-Fernandez W, Tarakanov AO, Ciruela F, Agnati LF, Fuxe K. On the existence of a possible A2A-D2-β-Arrestin2 complex: A2A agonist modulation of D2 agonist-induced β-arrestin2 recruitment. J. Mol. Biol. 2011; 406: 687–699.

Bourne JA. SCH 23390: the first selective dopamine D1-like receptor antagonist. CNS Drug Rev. 2001; 7: 399–414.

Braithwaite SP, Adkisson M, Leung J, Nava A, Masterson B, Urfer R, et al. Regulation of NMDA receptor trafficking and function by striatal-enriched tyrosine phosphatase (STEP). Eur. J. Neurosci. 2006; 23: 2847–2856.

Brami-Cherrier K, Lavaur J, Pagès C, Arthur JSC, Caboche J. Glutamate induces histone H3 phosphorylation but not acetylation in striatal neurons: role of mitogen- and stress-activated kinase-1. J. Neurochem. 2007; 101: 697–708.

Brami-Cherrier K, Valjent E, Hervé D, Darragh J, Corvol J-C, Pages C, et al. Parsing molecular and behavioral effects of cocaine in mitogen- and stress-activated protein kinase-1-deficient mice. J. Neurosci. Off. J. Soc. Neurosci. 2005; 25: 11444–11454.

Brog JS, Salyapongse A, Deutch AY, Zahm DS. The patterns of afferent innervation of the core and shell in the 'accumbens' part of the rat ventral striatum: immunohistochemical detection of retrogradely transported fluoro-gold. J. Comp. Neurol. 1993; 338: 255–278.

Brown AM, Deutch AY, Colbran RJ. Dopamine depletion alters phosphorylation of striatal proteins in a model of Parkinsonism. Eur. J. Neurosci. 2005; 22: 247–256.

Cabello N, Gandía J, Bertarelli DCG, Watanabe M, Lluís C, Franco R, et al. Metabotropic glutamate type 5, dopamine D2 and adenosine A2a receptors form higher-order oligomers in living cells. J. Neurochem. 2009; 109: 1497–1507.

Calabresi P, Di Filippo M, Ghiglieri V, Picconi B. Molecular mechanisms underlying levodopa-induced dyskinesia. Mov. Disord. Off. J. Mov. Disord. Soc. 2008; 23 Suppl 3: S570–579.

Calabresi P, Maj R, Pisani A, Mercuri NB, Bernardi G. Long-term synaptic depression in the striatum: physiological and pharmacological characterization. J. Neurosci. Off. J. Soc. Neurosci. 1992; 12: 4224–4233.

Calabresi P, Mercuri NB, De Murtas M, Bernardi G. Involvement of GABA systems in feedback regulation of glutamate-and GABA-mediated synaptic potentials in rat neostriatum. J. Physiol. 1991; 440: 581–599.

Calabresi P, Mercuri NB, Sancesario G, Bernardi G. Electrophysiology of dopamine-denervated striatal neurons. Implications for Parkinson's disease. Brain J. Neurol. 1993; 116 (Pt 2): 433–452.

Calabresi P, Picconi B, Tozzi A, Di Filippo M. Dopamine-mediated regulation of corticostriatal synaptic plasticity. Trends Neurosci. 2007; 30: 211–219.

Callier S, Snapyan M, Le Crom S, Prou D, Vincent J-D, Vernier P. Evolution and cell biology of dopamine receptors in vertebrates. Biol. Cell 2003; 95: 489–502.

Calon F, Dridi M, Hornykiewicz O, Bédard PJ, Rajput AH, Di Paolo T. Increased adenosine A2A receptors in the brain of Parkinson's disease patients with dyskinesias. Brain J. Neurol. 2004; 127: 1075–1084.

Calon F, Morissette M, Ghribi O, Goulet M, Grondin R, Blanchet PJ, et al. Alteration of glutamate receptors in the striatum of dyskinetic 1-methyl-4-phenyl-1,2,3,6-tetrahydropyridine-treated monkeys following dopamine agonist treatment. Prog. Neuropsychopharmacol. Biol. Psychiatry 2002; 26: 127–138.

Calon F, Rajput AH, Hornykiewicz O, Bédard PJ, Di Paolo T. Levodopa-induced motor complications are associated with alterations of glutamate receptors in Parkinson's disease. Neurobiol. Dis. 2003; 14: 404–416.

Carriba P, Ortiz O, Patkar K, Justinova Z, Stroik J, Themann A, et al. Striatal adenosine A2A and cannabinoid CB1 receptors form functional heteromeric complexes that mediate the motor effects of cannabinoids. Neuropsychopharmacol. Off. Publ. Am. Coll. Neuropsychopharmacol. 2007; 32: 2249–2259.

Carrillo-Reid L, Hernández-López S, Tapia D, Galarraga E, Bargas J. Dopaminergic modulation of the striatal microcircuit: receptor-specific configuration of cell assemblies. J. Neurosci. Off. J. Soc. Neurosci. 2011; 31: 14972–14983.

Carrillo-Reid L, Tecuapetla F, Tapia D, Hernández-Cruz A, Galarraga E, Drucker-Colin R, et al. Encoding network states by striatal cell assemblies. J. Neurophysiol. 2008; 99: 1435–1450.

Carta M, Carlsson T, Kirik D, Björklund A. Dopamine released from 5-HT terminals is the cause of L-DOPA-induced dyskinesia in parkinsonian rats. Brain J. Neurol. 2007; 130: 1819–1833.

Carta M, Lindgren HS, Lundblad M, Stancampiano R, Fadda F, Cenci MA. Role of striatal L-DOPA in the production of dyskinesia in 6-hydroxydopamine lesioned rats. J. Neurochem. 2006; 96: 1718–1727.

Carter AG, Sabatini BL. State-dependent calcium signaling in dendritic spines of striatal medium spiny neurons. Neuron 2004; 44: 483–493.

Carter AG, Soler-Llavina GJ, Sabatini BL. Timing and location of synaptic inputs determine modes of subthreshold integration in striatal medium spiny neurons. J. Neurosci. Off. J. Soc. Neurosci. 2007; 27: 8967–8977.

Castro LRV, Brito M, Guiot E, Polito M, Korn CW, Hervé D, et al. Striatal neurones have a specific ability to respond to phasic dopamine release. J. Physiol. 2013; 591: 3197–3214.

Castro LRV, Gervasi N, Guiot E, Cavellini L, Nikolaev VO, Paupardin-Tritsch D, et al. Type 4 phosphodiesterase plays different integrating roles in different cellular domains in pyramidal cortical neurons. J. Neurosci. Off. J. Soc. Neurosci. 2010; 30: 6143–6151.

Castro L, Yapo C, Vincent P. [Physiopathology of cAMP/PKA signaling in neurons]. Biol. Aujourdhui 2016; 210: 191–203.

Cenci MA. Dopamine dysregulation of movement control in L-DOPA-induced dyskinesia. Trends Neurosci. 2007; 30: 236–243.

Cenci MA. Presynaptic Mechanisms of l-DOPA-Induced Dyskinesia: The Findings, the Debate, and the Therapeutic Implications. Front. Neurol. 2014; 5: 242.

Cenci MA, Crossman AR. Animal models of l-dopa-induced dyskinesia in Parkinson's disease. Mov. Disord. Off. J. Mov. Disord. Soc. 2018; 33: 889–899.

Cenci MA, Jörntell H, Petersson P. On the neuronal circuitry mediating L-DOPA-induced dyskinesia. J. Neural Transm. Vienna Austria 1996 2018; 125: 1157–1169.

Cenci MA, Konradi C. Maladaptive striatal plasticity in L-DOPA-induced dyskinesia. Prog. Brain Res. 2010; 183: 209–233.

Cenci MA, Lundblad M. Post- versus presynaptic plasticity in L-DOPA-induced dyskinesia. J. Neurochem. 2006; 99: 381–392.

Cenci MA, Tranberg A, Andersson M, Hilbertson A. Changes in the regional and compartmental distribution of FosB- and JunB-like immunoreactivity induced in the dopamine-denervated rat striatum by acute or chronic L-dopa treatment. Neuroscience 1999; 94: 515–527.

Cepeda C, André VM, Yamazaki I, Wu N, Kleiman-Weiner M, Levine MS. Differential electrophysiological properties of dopamine D1 and D2 receptor-containing striatal medium-sized spiny neurons. Eur. J. Neurosci. 2008; 27: 671–682.

Cepeda C, Buchwald NA, Levine MS. Neuromodulatory actions of dopamine in the neostriatum are dependent upon the excitatory amino acid receptor subtypes activated. Proc. Natl. Acad. Sci. U. S. A. 1993; 90: 9576–9580.

Cepeda C, Levine MS. Dopamine and N-methyl-D-aspartate receptor interactions in the neostriatum. Dev. Neurosci. 1998; 20: 1–18.

Cerovic M, Bagetta V, Pendolino V, Ghiglieri V, Fasano S, Morella I, et al. Derangement of Ras-guanine nucleotide-releasing factor 1 (Ras-GRF1) and extracellular signal-regulated kinase (ERK) dependent striatal plasticity in L-DOPA-induced dyskinesia. Biol. Psychiatry 2015; 77: 106–115.

Chao SZ, Ariano MA, Peterson DA, Wolf ME. D1 dopamine receptor stimulation increases GluR1 surface expression in nucleus accumbens neurons. J. Neurochem. 2002; 83: 704–712.

Charbonnier-Beaupel F, Malerbi M, Alcacer C, Tahiri K, Carpentier W, Wang C, et al. Gene expression analyses identify Narp contribution in the development of L-DOPA-induced dyskinesia. J. Neurosci. Off. J. Soc. Neurosci. 2015; 35: 96–111.

Chase TN, Bibbiani F, Bara-Jimenez W, Dimitrova T, Oh-Lee JD. Translating A2A antagonist KW6002 from animal models to parkinsonian patients. Neurology 2003; 61: S107–111.

Chen B-S, Roche KW. Regulation of NMDA receptors by phosphorylation. Neuropharmacology 2007; 53: 362–368.

Cheng HW, Rafols JA, Goshgarian HG, Anavi Y, Tong J, McNeill TH. Differential spine loss and regrowth of striatal neurons following multiple forms of deafferentation: a Golgi study. Exp. Neurol. 1997; 147: 287–298.

Chen J-F, Fredduzzi S, Bastia E, Yu L, Moratalla R, Ongini E, et al. Adenosine A2A receptors in neuroadaptation to repeated dopaminergic stimulation: implications for the treatment of dyskinesias in Parkinson's disease. Neurology 2003; 61: S74–81.

Chen J-F, Lee C, Chern Y. Adenosine receptor neurobiology: overview. Int. Rev. Neurobiol. 2014; 119: 1–49.

Chen MT, Morales M, Woodward DJ, Hoffer BJ, Janak PH. In vivo extracellular recording of striatal neurons in the awake rat following unilateral 6-hydroxydopamine lesions. Exp. Neurol. 2001; 171: 72–83.

Chen T-W, Wardill TJ, Sun Y, Pulver SR, Renninger SL, Baohan A, et al. Ultrasensitive fluorescent proteins for imaging neuronal activity. Nature 2013; 499: 295–300.

Chevalier G, Deniau JM. Disinhibition as a basic process in the expression of striatal functions. Trends Neurosci. 1990; 13: 277–280.

Chevalier G, Vacher S, Deniau JM, Desban M. Disinhibition as a basic process in the expression of striatal functions. I. The striato-nigral influence on tecto-spinal/tecto-diencephalic neurons. Brain Res. 1985; 334: 215–226.

Chisholm KI, Khovanov N, Lopes DM, La Russa F, McMahon SB. Large Scale In Vivo Recording of Sensory Neuron Activity with GCaMP6. eNeuro 2018; 5

Chou JJ, Li S, Klee CB, Bax A. Solution structure of Ca(2+)-calmodulin reveals flexible hand-like properties of its domains. Nat. Struct. Biol. 2001; 8: 990–997.

Chuhma N, Tanaka KF, Hen R, Rayport S. Functional connectome of the striatal medium spiny neuron. J. Neurosci. Off. J. Soc. Neurosci. 2011; 31: 1183–1192.

Chwang WB, Arthur JS, Schumacher A, Sweatt JD. The nuclear kinase mitogen- and stress-activated protein kinase 1 regulates hippocampal chromatin remodeling in memory formation. J. Neurosci. Off. J. Soc. Neurosci. 2007; 27: 12732–12742.

Ciruela F, Casadó V, Rodrigues RJ, Luján R, Burgueño J, Canals M, et al. Presynaptic control of striatal glutamatergic neurotransmission by adenosine A1-A2A receptor heteromers. J. Neurosci. Off. J. Soc. Neurosci. 2006; 26: 2080–2087.

Clapham DE. Calcium signaling. Cell 2007; 131: 1047–1058.

Coccurello R, Breysse N, Amalric M. Simultaneous blockade of adenosine A2A and metabotropic glutamate mGlu5 receptors increase their efficacy in reversing Parkinsonian deficits in rats. Neuropsychopharmacol. Off. Publ. Am. Coll. Neuropsychopharmacol. 2004; 29: 1451–1461.

Conn PJ, Battaglia G, Marino MJ, Nicoletti F. Metabotropic glutamate receptors in the basal ganglia motor circuit. Nat. Rev. Neurosci. 2005; 6: 787–798.

Conti M, Beavo J. Biochemistry and physiology of cyclic nucleotide phosphodiesterases: essential components in cyclic nucleotide signaling. Annu. Rev. Biochem. 2007; 76: 481–511.

Conti M, Richter W, Mehats C, Livera G, Park J-Y, Jin C. Cyclic AMP-specific PDE4 phosphodiesterases as critical components of cyclic AMP signaling. J. Biol. Chem. 2003; 278: 5493–5496.

Corvol J-C, Muriel M-P, Valjent E, Féger J, Hanoun N, Girault J-A, et al. Persistent increase in olfactory type G-protein alpha subunit levels may underlie D1 receptor functional hypersensitivity in Parkinson disease. J. Neurosci. Off. J. Soc. Neurosci. 2004; 24: 7007–7014.

Corvol JC, Studler JM, Schonn JS, Girault JA, Hervé D. Galpha(olf) is necessary for coupling D1 and A2a receptors to adenylyl cyclase in the striatum. J. Neurochem. 2001; 76: 1585–1588.

Corvol J-C, Valjent E, Pascoli V, Robin A, Stipanovich A, Luedtke RR, et al. Quantitative changes in Galphaolf protein levels, but not D1 receptor, alter specifically acute responses to psychostimulants. Neuropsychopharmacol. Off. Publ. Am. Coll. Neuropsychopharmacol. 2007; 32: 1109–1121.

Coskran TM, Morton D, Menniti FS, Adamowicz WO, Kleiman RJ, Ryan AM, et al. Immunohistochemical localization of phosphodiesterase 10A in multiple mammalian species. J. Histochem. Cytochem. Off. J. Histochem. Soc. 2006; 54: 1205–1213.

Cotzias GC, Van Woert MH, Schiffer LM. Aromatic amino acids and modification of parkinsonism. N. Engl. J. Med. 1967; 276: 374–379.

Crittenden JR, Graybiel AM. Basal Ganglia disorders associated with imbalances in the striatal striosome and matrix compartments. Front. Neuroanat. 2011; 5: 59.

Crivici A, Ikura M. Molecular and structural basis of target recognition by calmodulin. Annu. Rev. Biophys. Biomol. Struct. 1995; 24: 85–116.

Crutcher MD, DeLong MR. Single cell studies of the primate putamen. II. Relations to direction of movement and pattern of muscular activity. Exp. Brain Res. 1984; 53: 244–258.

Cui G, Jun SB, Jin X, Pham MD, Vogel SS, Lovinger DM, et al. Concurrent activation of striatal direct and indirect pathways during action initiation. Nature 2013; 494: 238–242.

Damier P, Hirsch EC, Agid Y, Graybiel AM. The substantia nigra of the human brain. II. Patterns of loss of dopamine-containing neurons in Parkinson's disease. Brain J. Neurol. 1999; 122 (Pt 8): 1437–1448.

Darmopil S, Martín AB, De Diego IR, Ares S, Moratalla R. Genetic inactivation of dopamine D1 but not D2 receptors inhibits L-DOPA-induced dyskinesia and histone activation. Biol. Psychiatry 2009; 66: 603–613.

Dauer W, Przedborski S. Parkinson's disease: mechanisms and models. Neuron 2003; 39: 889–909.

David HN, Ansseau M, Abraini JH. Dopamine-glutamate reciprocal modulation of release and motor responses in the rat caudate-putamen and nucleus accumbens of 'intact' animals. Brain Res. Brain Res. Rev. 2005; 50: 336–360.

Day M, Wang Z, Ding J, An X, Ingham CA, Shering AF, et al. Selective elimination of glutamatergic synapses on striatopallidal neurons in Parkinson disease models. Nat. Neurosci. 2006; 9: 251–259.

Day M, Wokosin D, Plotkin JL, Tian X, Surmeier DJ. Differential excitability and modulation of striatal medium spiny neuron dendrites. J. Neurosci. Off. J. Soc. Neurosci. 2008; 28: 11603–11614.

Delaney SM, Shepel PN, Geiger JD. Levels of endogenous adenosine in rat striatum. I. Regulation by ionotropic glutamate receptors, nitric oxide and free radicals. J. Pharmacol. Exp. Ther. 1998; 285: 561–567.

DeLong MR. Primate models of movement disorders of basal ganglia origin. Trends Neurosci. 1990; 13: 281–285.

De Mei C, Ramos M, Iitaka C, Borrelli E. Getting specialized: presynaptic and postsynaptic dopamine D2 receptors. Curr. Opin. Pharmacol. 2009; 9: 53–58.

Deng Y-P, Shelby E, Reiner AJ. Immunohistochemical localization of AMPA-type glutamate receptor subunits in the striatum of rhesus monkey. Brain Res. 2010; 1344: 104–123.

Deng YP, Xie JP, Wang HB, Lei WL, Chen Q, Reiner A. Differential localization of the GluR1 and GluR2 subunits of the AMPA-type glutamate receptor among striatal neuron types in rats. J. Chem. Neuroanat. 2007; 33: 167–192.

Deniau JM, Chevalier G. Disinhibition as a basic process in the expression of striatal functions. II. The striato-nigral influence on thalamocortical cells of the ventromedial thalamic nucleus. Brain Res. 1985; 334: 227–233.

Depry C, Allen MD, Zhang J. Visualization of PKA activity in plasma membrane microdomains. Mol. Biosyst. 2011; 7: 52–58.

Deutch AY, Colbran RJ, Winder DJ. Striatal plasticity and medium spiny neuron dendritic remodeling in parkinsonism. Parkinsonism Relat. Disord. 2007; 13 Suppl 3: S251–258.

Díaz-Cabiale Z, Hurd Y, Guidolin D, Finnman UB, Zoli M, Agnati LF, et al. Adenosine A2A agonist CGS 21680 decreases the affinity of dopamine D2 receptors for dopamine in human striatum. Neuroreport 2001; 12: 1831–1834.

Díaz-Cabiale Z, Vivó M, Del Arco A, O'Connor WT, Harte MK, Müller CE, et al. Metabotropic glutamate mGlu5 receptor-mediated modulation of the ventral striopallidal GABA pathway in rats. Interactions with adenosine A(2A) and dopamine D(2) receptors. Neurosci. Lett. 2002; 324: 154–158.

Dingledine R, Borges K, Bowie D, Traynelis SF. The glutamate receptor ion channels. Pharmacol. Rev. 1999; 51: 7–61.

Ding Y, Won L, Britt JP, Lim SAO, McGehee DS, Kang UJ. Enhanced striatal cholinergic neuronal activity mediates L-DOPA-induced dyskinesia in parkinsonian mice. Proc. Natl. Acad. Sci. U. S. A. 2011; 108: 840–845.

DiPilato LM, Cheng X, Zhang J. Fluorescent indicators of cAMP and Epac activation reveal differential dynamics of cAMP signaling within discrete subcellular compartments. Proc. Natl. Acad. Sci. U. S. A. 2004; 101: 16513–16518.

Dixon AK, Gubitz AK, Sirinathsinghji DJ, Richardson PJ, Freeman TC. Tissue distribution of adenosine receptor mRNAs in the rat. Br. J. Pharmacol. 1996; 118: 1461–1468.

Doig NM, Moss J, Bolam JP. Cortical and thalamic innervation of direct and indirect pathway medium-sized spiny neurons in mouse striatum. J. Neurosci. Off. J. Soc. Neurosci. 2010; 30: 14610–14618.

Domenici MR, Pepponi R, Martire A, Tebano MT, Potenza RL, Popoli P. Permissive role of adenosine A2A receptors on metabotropic glutamate receptor 5 (mGluR5)-mediated effects in the striatum. J. Neurochem. 2004; 90: 1276–1279.

Doyle JP, Dougherty JD, Heiman M, Schmidt EF, Stevens TR, Ma G, et al. Application of a translational profiling approach for the comparative analysis of CNS cell types. Cell 2008; 135: 749–762.

Drago J, Gerfen CR, Lachowicz JE, Steiner H, Hollon TR, Love PE, et al. Altered striatal function in a mutant mouse lacking D1A dopamine receptors. Proc. Natl. Acad. Sci. U. S. A. 1994; 91: 12564–12568.

Dulla C, Tani H, Okumoto S, Frommer WB, Reimer RJ, Huguenard JR. Imaging of glutamate in brain slices using FRET sensors. J. Neurosci. Methods 2008; 168: 306–319.

Dumartin B, Doudnikoff E, Gonon F, Bloch B. Differences in ultrastructural localization of dopaminergic D1 receptors between dorsal striatum and nucleus accumbens in the rat. Neurosci. Lett. 2007; 419: 273–277.

Dunah AW, Sirianni AC, Fienberg AA, Bastia E, Schwarzschild MA, Standaert DG. Dopamine D1-dependent trafficking of striatal N-methyl-D-aspartate glutamate receptors requires Fyn protein tyrosine kinase but not DARPP-32. Mol. Pharmacol. 2004; 65: 121–129.

Dunah AW, Wang Y, Yasuda RP, Kameyama K, Huganir RL, Wolfe BB, et al. Alterations in subunit expression, composition, and phosphorylation of striatal N-methyl-D-aspartate glutamate receptors in a rat 6-hydroxydopamine model of Parkinson's disease. Mol. Pharmacol. 2000; 57: 342–352.

Dunn TA, Wang C-T, Colicos MA, Zaccolo M, DiPilato LM, Zhang J, et al. Imaging of cAMP levels and protein kinase A activity reveals that retinal waves drive oscillations in second-messenger cascades. J. Neurosci. Off. J. Soc. Neurosci. 2006; 26: 12807–12815.

Dunwiddie TV, Masino SA. The role and regulation of adenosine in the central nervous system. Annu. Rev. Neurosci. 2001; 24: 31–55.

Durieux PF, Bearzatto B, Guiducci S, Buch T, Waisman A, Zoli M, et al. D2R striatopallidal neurons inhibit both locomotor and drug reward processes. Nat. Neurosci. 2009; 12: 393–395.

Durieux PF, Schiffmann SN, de Kerchove d'Exaerde A. Targeting neuronal populations of the striatum. Front. Neuroanat. 2011; 5: 40.

Durieux PF, Schiffmann SN, de Kerchove d'Exaerde A. Differential regulation of motor control and response to dopaminergic drugs by D1R and D2R neurons in distinct dorsal striatum subregions. EMBO J. 2012; 31: 640–653.

El Atifi-Borel M, Buggia-Prevot V, Platet N, Benabid A-L, Berger F, Sgambato-Faure V. De novo and long-term l-Dopa induce both common and distinct striatal gene profiles in the hemiparkinsonian rat. Neurobiol. Dis. 2009; 34: 340–350.

Erard M, Fredj A, Pasquier H, Beltolngar D-B, Bousmah Y, Derrien V, et al. Minimum set of mutations needed to optimize cyan fluorescent proteins for live cell imaging. Mol. Biosyst. 2013; 9: 258–267.

Escande MV, Taravini IRE, Zold CL, Belforte JE, Murer MG. Loss of Homeostasis in the Direct Pathway in a Mouse Model of Asymptomatic Parkinson's Disease. J. Neurosci. Off. J. Soc. Neurosci. 2016; 36: 5686–5698.

Faas GC, Raghavachari S, Lisman JE, Mody I. Calmodulin as a direct detector of Ca2+ signals. Nat. Neurosci. 2011; 14: 301–304.

Fahn S. The medical treatment of Parkinson disease from James Parkinson to George Cotzias. Mov. Disord. Off. J. Mov. Disord. Soc. 2015; 30: 4–18.

Fahn S. The 200-year journey of Parkinson disease: Reflecting on the past and looking towards the future. Parkinsonism Relat. Disord. 2018; 46 Suppl 1: S1–S5.

Fahn S, Oakes D, Shoulson I, Kieburtz K, Rudolph A, Lang A, et al. Levodopa and the progression of Parkinson's disease. N. Engl. J. Med. 2004; 351: 2498–2508.

Fasano S, Bezard E, D'Antoni A, Francardo V, Indrigo M, Qin L, et al. Inhibition of Ras-guanine nucleotide-releasing factor 1 (Ras-GRF1) signaling in the striatum reverts motor symptoms associated with L-dopa-induced dyskinesia. Proc. Natl. Acad. Sci. U. S. A. 2010; 107: 21824–21829.

Fasano S, Brambilla R. Ras-ERK Signaling in Behavior: Old Questions and New Perspectives. Front. Behav. Neurosci. 2011; 5: 79.

Fasano S, D'Antoni A, Orban PC, Valjent E, Putignano E, Vara H, et al. Ras-guanine nucleotide-releasing factor 1 (Ras-GRF1) controls activation of extracellular signal-regulated kinase (ERK) signaling in the striatum and long-term behavioral responses to cocaine. Biol. Psychiatry 2009; 66: 758–768.

Ferguson SM, Robinson TE. Amphetamine-evoked gene expression in striatopallidal neurons: regulation by corticostriatal afferents and the ERK/MAPK signaling cascade. J. Neurochem. 2004; 91: 337–348.

Fernández-Dueñas V, Gómez-Soler M, Morató X, Núñez F, Das A, Kumar TS, et al. Dopamine D(2) receptor-mediated modulation of adenosine A(2A) receptor agonist binding within the A(2A)R/D(2)R oligomer framework. Neurochem. Int. 2013; 63: 42–46.

Fernández-Dueñas V, Taura JJ, Cottet M, Gómez-Soler M, López-Cano M, Ledent C, et al. Untangling dopamine-adenosine receptor-receptor assembly in experimental parkinsonism in rats. Dis. Model. Mech. 2015; 8: 57–63.

Fernandez HH, Greeley DR, Zweig RM, Wojcieszek J, Mori A, Sussman NM, et al. Istradefylline as monotherapy for Parkinson disease: results of the 6002-US-051 trial. Parkinsonism Relat. Disord. 2010; 16: 16–20.

Ferraguti F, Shigemoto R. Metabotropic glutamate receptors. Cell Tissue Res. 2006; 326: 483–504.

Ferré S, Bonaventura J, Tomasi D, Navarro G, Moreno E, Cortés A, et al. Allosteric mechanisms within the adenosine A2A-dopamine D2 receptor heterotetramer. Neuropharmacology 2016; 104: 154–160.

Ferré S, Karcz-Kubicha M, Hope BT, Popoli P, Burgueño J, Gutiérrez MA, et al. Synergistic interaction between adenosine A2A and glutamate mGlu5 receptors: implications for striatal neuronal function. Proc. Natl. Acad. Sci. U. S. A. 2002; 99: 11940–11945.

Ferré S, Popoli P, Rimondini R, Reggio R, Kehr J, Fuxe K. Adenosine A2A and group I metabotropic glutamate receptors synergistically modulate the binding characteristics of dopamine D2 receptors in the rat striatum. Neuropharmacology 1999; 38: 129–140.

Ferré S, Quiroz C, Orru M, Guitart X, Navarro G, Cortés A, et al. Adenosine A(2A) Receptors and A(2A) Receptor Heteromers as Key Players in Striatal Function. Front. Neuroanat. 2011; 5: 36.

Fieblinger T, Cenci MA. Zooming in on the small: the plasticity of striatal dendritic spines in L-DOPA-induced dyskinesia. Mov. Disord. Off. J. Mov. Disord. Soc. 2015; 30: 484–493.

Fieblinger T, Graves SM, Sebel LE, Alcacer C, Plotkin JL, Gertler TS, et al. Cell type-specific plasticity of striatal projection neurons in parkinsonism and L-DOPA-induced dyskinesia. Nat. Commun. 2014a; 5: 5316.

Fieblinger T, Sebastianutto I, Alcacer C, Bimpisidis Z, Maslava N, Sandberg S, et al. Mechanisms of dopamine D1 receptor-mediated ERK1/2 activation in the parkinsonian striatum and their modulation by metabotropic glutamate receptor type 5. J. Neurosci. Off. J. Soc. Neurosci. 2014b; 34: 4728–4740.

Fienberg AA, Hiroi N, Mermelstein PG, Song W, Snyder GL, Nishi A, et al. DARPP-32: regulator of the efficacy of dopaminergic neurotransmission. Science 1998; 281: 838–842.

Filion M, Tremblay L. Abnormal spontaneous activity of globus pallidus neurons in monkeys with MPTP-induced parkinsonism. Brain Res. 1991; 547: 142–151.

Fink JS, Weaver DR, Rivkees SA, Peterfreund RA, Pollack AE, Adler EM, et al. Molecular cloning of the rat A2 adenosine receptor: selective co-expression with D2 dopamine receptors in rat striatum. Brain Res. Mol. Brain Res. 1992; 14: 186–195.

Fino E, Glowinski J, Venance L. Bidirectional activity-dependent plasticity at corticostriatal synapses. J. Neurosci. Off. J. Soc. Neurosci. 2005; 25: 11279–11287.

Fino E, Glowinski J, Venance L. Effects of acute dopamine depletion on the electrophysiological properties of striatal neurons. Neurosci. Res. 2007; 58: 305–316.

Fiorentini C, Gardoni F, Spano P, Di Luca M, Missale C. Regulation of dopamine D1 receptor trafficking and desensitization by oligomerization with glutamate N-methyl-D-aspartate receptors. J. Biol. Chem. 2003; 278: 20196–20202.

Fiorentini C, Mattanza C, Collo G, Savoia P, Spano P, Missale C. The tyrosine phosphatase Shp-2 interacts with the dopamine D(1) receptor and triggers D(1) -mediated Erk signaling in striatal neurons. J. Neurochem. 2011; 117: 253–263.

Fiorentini C, Rizzetti MC, Busi C, Bontempi S, Collo G, Spano P, et al. Loss of synaptic D1 dopamine/N-methyl-D-aspartate glutamate receptor complexes in L-DOPA-induced dyskinesia in the rat. Mol. Pharmacol. 2006; 69: 805–812.

Fiorentini C, Savoia P, Savoldi D, Barbon A, Missale C. Persistent activation of the D1R/Shp-2/Erk1/2 pathway in l-DOPA-induced dyskinesia in the 6-hydroxy-dopamine rat model of Parkinson's disease. Neurobiol. Dis. 2013; 54: 339–348.

Fiorillo CD, Tobler PN, Schultz W. Discrete coding of reward probability and uncertainty by dopamine neurons. Science 2003; 299: 1898–1902.

Flajolet M, Wang Z, Futter M, Shen W, Nuangchamnong N, Bendor J, et al. FGF acts as a co-transmitter through adenosine A(2A) receptor to regulate synaptic plasticity. Nat. Neurosci. 2008; 11: 1402–1409.

Flores-Barrera E, Vizcarra-Chacón BJ, Tapia D, Bargas J, Galarraga E. Different corticostriatal integration in spiny projection neurons from direct and indirect pathways. Front. Syst. Neurosci. 2010; 4: 15.

Flores-Hernández J, Cepeda C, Hernández-Echeagaray E, Calvert CR, Jokel ES, Fienberg AA, et al. Dopamine enhancement of NMDA currents in dissociated medium-sized striatal neurons: role of D1 receptors and DARPP-32. J. Neurophysiol. 2002; 88: 3010–3020.

Flores-Hernandez J, Hernandez S, Snyder GL, Yan Z, Fienberg AA, Moss SJ, et al. D(1) dopamine receptor activation reduces GABA(A) receptor currents in neostriatal neurons through a PKA/DARPP-32/PP1 signaling cascade. J. Neurophysiol. 2000; 83: 2996–3004.

Florio T, Di Loreto S, Cerrito F, Scarnati E. Influence of prelimbic and sensorimotor cortices on striatal neurons in the rat: electrophysiological evidence for converging inputs and the effects of 6-OHDA-induced degeneration of the substantia nigra. Brain Res. 1993; 619: 180–188.

Forster Y, Haas E. Preparation and characterization of three fluorescent labels for proteins, suitable for structural studies. Anal. Biochem. 1993; 209: 9–14.

Fosque BF, Sun Y, Dana H, Yang C-T, Ohyama T, Tadross MR, et al. Neural circuits. Labeling of active neural circuits in vivo with designed calcium integrators. Science 2015; 347: 755–760.

Fox SH, Katzenschlager R, Lim S-Y, Barton B, de Bie RMA, Seppi K, et al. International Parkinson and movement disorder society evidence-based medicine review: Update on treatments for the motor symptoms of Parkinson's disease. Mov. Disord. Off. J. Mov. Disord. Soc. 2018; 33: 1248–1266.

Fredduzzi S, Moratalla R, Monopoli A, Cuellar B, Xu K, Ongini E, et al. Persistent behavioral sensitization to chronic L-DOPA requires A2A adenosine receptors. J. Neurosci. Off. J. Soc. Neurosci. 2002; 22: 1054–1062.

Fredholm BB. Adenosine receptors as drug targets. Exp. Cell Res. 2010; 316: 1284–1288.

Fredholm BB, Irenius E, Kull B, Schulte G. Comparison of the potency of adenosine as an agonist at human adenosine receptors expressed in Chinese hamster ovary cells. Biochem. Pharmacol. 2001; 61: 443–448.

Fritz RD, Letzelter M, Reimann A, Martin K, Fusco L, Ritsma L, et al. A versatile toolkit to produce sensitive FRET biosensors to visualize signaling in time and space. Sci. Signal. 2013; 6: rs12.

Fujishige K, Kotera J, Omori K. Striatum- and testis-specific phosphodiesterase PDE10A isolation and characterization of a rat PDE10A. Eur. J. Biochem. 1999; 266: 1118–1127.

Fujiyama F, Kuramoto E, Okamoto K, Hioki H, Furuta T, Zhou L, et al. Presynaptic localization of an AMPA-type glutamate receptor in corticostriatal and thalamostriatal axon terminals. Eur. J. Neurosci. 2004; 20: 3322–3330.

Fujiyama F, Unzai T, Nakamura K, Nomura S, Kaneko T. Difference in organization of corticostriatal and thalamostriatal synapses between patch and matrix compartments of rat neostriatum. Eur. J. Neurosci. 2006; 24: 2813–2824.

Fuxe K, Agnati LF, Jacobsen K, Hillion J, Canals M, Torvinen M, et al. Receptor heteromerization in adenosine A2A receptor signaling: relevance for striatal function and Parkinson's disease. Neurology 2003; 61: S19–23.

Fuxe K, Ferré S, Canals M, Torvinen M, Terasmaa A, Marcellino D, et al. Adenosine A2A and dopamine D2 heteromeric receptor complexes and their function. J. Mol. Neurosci. MN 2005; 26: 209–220.

Fuxe K, Ferré S, Genedani S, Franco R, Agnati LF. Adenosine receptor-dopamine receptor interactions in the basal ganglia and their relevance for brain function. Physiol. Behav. 2007; 92: 210–217.

Gagnon D, Petryszyn S, Sanchez MG, Bories C, Beaulieu JM, De Koninck Y, et al. Striatal Neurons Expressing D1 and D2 Receptors are Morphologically Distinct and Differently Affected by Dopamine Denervation in Mice. Sci. Rep. 2017; 7: 41432.

Galarraga E, Bargas J, Martínez-Fong D, Aceves J. Spontaneous synaptic potentials in dopamine-denervated neostriatal neurons. Neurosci. Lett. 1987; 81: 351–355.

Galarraga E, Hernández-López S, Reyes A, Barral J, Bargas J. Dopamine facilitates striatal EPSPs through an L-type Ca2+ conductance. Neuroreport 1997; 8: 2183–2186.

Gangarossa G, Espallergues J, de Kerchove d'Exaerde A, El Mestikawy S, Gerfen CR, Hervé D, et al. Distribution and compartmental organization of GABAergic medium-sized spiny neurons in the mouse nucleus accumbens. Front. Neural Circuits 2013a; 7: 22.

Gangarossa G, Espallergues J, Mailly P, De Bundel D, de Kerchove d'Exaerde A, Hervé D, et al. Spatial distribution of D1R- and D2R-expressing medium-sized spiny neurons differs along the rostro-caudal axis of the mouse dorsal striatum. Front. Neural Circuits 2013b; 7: 124.

Gan J, Qi C, Mao L-M, Liu Z. Changes in surface expression of N-methyl-D-aspartate receptors in the striatum in a rat model of Parkinson's disease. Drug Des. Devel. Ther. 2014; 8: 165–173.

Garcia BG, Neely MD, Deutch AY. Cortical regulation of striatal medium spiny neuron dendritic remodeling in parkinsonism: modulation of glutamate release reverses dopamine depletion-induced dendritic spine loss. Cereb. Cortex N. Y. N 1991 2010; 20: 2423–2432.

Gardoni F, Bellone C. Modulation of the glutamatergic transmission by Dopamine: a focus on Parkinson, Huntington and Addiction diseases. Front. Cell. Neurosci. 2015; 9: 25.

Gardoni F, Picconi B, Ghiglieri V, Polli F, Bagetta V, Bernardi G, et al. A critical interaction between NR2B and MAGUK in L-DOPA induced dyskinesia. J. Neurosci. Off. J. Soc. Neurosci. 2006; 26: 2914–2922.

Gardoni F, Sgobio C, Pendolino V, Calabresi P, Di Luca M, Picconi B. Targeting NR2A-containing NMDA receptors reduces L-DOPA-induced dyskinesias. Neurobiol. Aging 2012; 33: 2138–2144.

Gardoni F, Zianni E, Eramo A, Canonico PL, Di Luca M. Effect of rasagiline on the molecular composition of the excitatory postsynaptic density. Eur. J. Pharmacol. 2011; 670: 458–463.

Gasparini F, Di Paolo T, Gomez-Mancilla B. Metabotropic glutamate receptors for Parkinson's disease therapy. Park. Dis. 2013; 2013: 196028.

Gerfen CR. The neostriatal mosaic: multiple levels of compartmental organization in the basal ganglia. Annu. Rev. Neurosci. 1992; 15: 285–320.

Gerfen CR, Engber TM, Mahan LC, Susel Z, Chase TN, Monsma FJ, et al. D1 and D2 dopamine receptor-regulated gene expression of striatonigral and striatopallidal neurons. Science 1990; 250: 1429–1432.

Gerfen CR, Keefe KA, Gauda EB. D1 and D2 dopamine receptor function in the striatum: coactivation of D1- and D2-dopamine receptors on separate populations of neurons results in potentiated immediate early gene response in D1-containing neurons. J. Neurosci. Off. J. Soc. Neurosci. 1995; 15: 8167–8176.

Gerfen CR, Miyachi S, Paletzki R, Brown P. D1 dopamine receptor supersensitivity in the dopamine-depleted striatum results from a switch in the regulation of ERK1/2/MAP kinase. J. Neurosci. Off. J. Soc. Neurosci. 2002; 22: 5042–5054.

Gerfen CR, Paletzki R, Worley P. Differences between dorsal and ventral striatum in Drd1a dopamine receptor coupling of dopamine- and cAMP-regulated phosphoprotein-32 to activation of extracellular signal-regulated kinase. J. Neurosci. Off. J. Soc. Neurosci. 2008; 28: 7113–7120.

Gerfen CR, Surmeier DJ. Modulation of striatal projection systems by dopamine. Annu. Rev. Neurosci. 2011a; 34: 441–466.

Gerfen CR, Surmeier DJ. Modulation of striatal projection systems by dopamine. Annu. Rev. Neurosci. 2011b; 34: 441–466.

German DC, Manaye KF. Midbrain dopaminergic neurons (nuclei A8, A9, and A10): three-dimensional reconstruction in the rat. J. Comp. Neurol. 1993; 331: 297–309.

Gertler TS, Chan CS, Surmeier DJ. Dichotomous anatomical properties of adult striatal medium spiny neurons. J. Neurosci. Off. J. Soc. Neurosci. 2008; 28: 10814–10824.

Gervasi N, Hepp R, Tricoire L, Zhang J, Lambolez B, Paupardin-Tritsch D, et al. Dynamics of protein kinase A signaling at the membrane, in the cytosol, and in the nucleus of neurons in mouse brain slices. J. Neurosci. Off. J. Soc. Neurosci. 2007; 27: 2744–2750.

Gervasi N, Tchénio P, Preat T. PKA dynamics in a Drosophila learning center: coincidence detection by rutabaga adenylyl cyclase and spatial regulation by dunce phosphodiesterase. Neuron 2010; 65: 516–529.

Ginés S, Hillion J, Torvinen M, Le Crom S, Casadó V, Canela EI, et al. Dopamine D1 and adenosine A1 receptors form functionally interacting heteromeric complexes. Proc. Natl. Acad. Sci. U. S. A. 2000; 97: 8606–8611.

Gingrich JA, Caron MG. Recent advances in the molecular biology of dopamine receptors. Annu. Rev. Neurosci. 1993; 16: 299–321.

Giorgi C, Danese A, Missiroli S, Patergnani S, Pinton P. Calcium Dynamics as a Machine for Decoding Signals. Trends Cell Biol. 2018; 28: 258–273.

Giorgi M, D'Angelo V, Esposito Z, Nuccetelli V, Sorge R, Martorana A, et al. Lowered cAMP and cGMP signalling in the brain during levodopa-induced dyskinesias in hemiparkinsonian rats: new aspects in the pathogenetic mechanisms. Eur. J. Neurosci. 2008; 28: 941–950.

Giorgi M, Melchiorri G, Nuccetelli V, D'Angelo V, Martorana A, Sorge R, et al. PDE10A and PDE10A-dependent cAMP catabolism are dysregulated oppositely in striatum and nucleus accumbens after lesion of midbrain dopamine neurons in rat: a key step in parkinsonism physiopathology. Neurobiol. Dis. 2011; 43: 293–303.

Girasole AE, Lum MY, Nathaniel D, Bair-Marshall CJ, Guenthner CJ, Luo L, et al. A Subpopulation of Striatal Neurons Mediates Levodopa-Induced Dyskinesia. Neuron 2018; 97: 787–795.e6.

Girault J-A. Signaling in striatal neurons: the phosphoproteins of reward, addiction, and dyskinesia. Prog. Mol. Biol. Transl. Sci. 2012; 106: 33–62.

Girault JA, Hemmings HC, Zorn SH, Gustafson EL, Greengard P. Characterization in mammalian brain of a DARPP-32 serine kinase identical to casein kinase II. J. Neurochem. 1990; 55: 1772–1783.

Girault J-A, Valjent E, Caboche J, Hervé D. ERK2: a logical AND gate critical for drug-induced plasticity? Curr. Opin. Pharmacol. 2007; 7: 77–85.

Giros B, Martres MP, Pilon C, Sokoloff P, Schwartz JC. Shorter variants of the D3 dopamine receptor produced through various patterns of alternative splicing. Biochem. Biophys. Res. Commun. 1991; 176: 1584–1592.

Gittis AH, Kreitzer AC. Striatal microcircuitry and movement disorders. Trends Neurosci. 2012; 35: 557–564.

Gloerich M, Bos JL. Epac: defining a new mechanism for cAMP action. Annu. Rev. Pharmacol. Toxicol. 2010; 50: 355–375.

Goaillard JM, Vincent PV, Fischmeister R. Simultaneous measurements of intracellular cAMP and L-type Ca2+ current in single frog ventricular myocytes. J. Physiol. 2001; 530: 79–91.

Goldman PS, Nauta WJ. An intricately patterned prefronto-caudate projection in the rhesus monkey. J. Comp. Neurol. 1977; 72: 369–386.

Gong S, Doughty M, Harbaugh CR, Cummins A, Hatten ME, Heintz N, et al. Targeting Cre recombinase to specific neuron populations with bacterial artificial chromosome constructs. J. Neurosci. Off. J. Soc. Neurosci. 2007; 27: 9817–9823.

Gorbunova YV, Spitzer NC. Dynamic interactions of cyclic AMP transients and spontaneous Ca(2+) spikes. Nature 2002; 418: 93–96.

Goto A, Nakahara I, Yamaguchi T, Kamioka Y, Sumiyama K, Matsuda M, et al. Circuit-dependent striatal PKA and ERK signaling underlies rapid behavioral shift in mating reaction of male mice. Proc. Natl. Acad. Sci. U. S. A. 2015; 112: 6718–6723.

Grauer SM, Pulito VL, Navarra RL, Kelly MP, Kelley C, Graf R, et al. Phosphodiesterase 10A inhibitor activity in preclinical models of the positive, cognitive, and negative symptoms of schizophrenia. J. Pharmacol. Exp. Ther. 2009; 331: 574–590.

Graybiel AM, Aosaki T, Flaherty AW, Kimura M. The basal ganglia and adaptive motor control. Science 1994; 265: 1826–1831.

Greengard P, Allen PB, Nairn AC. Beyond the dopamine receptor: the DARPP-32/protein phosphatase-1 cascade. Neuron 1999; 23: 435–447.

Greer PL, Greenberg ME. From synapse to nucleus: calcium-dependent gene transcription in the control of synapse development and function. Neuron 2008; 59: 846–860.

Grillner S, Hellgren J, Ménard A, Saitoh K, Wikström MA. Mechanisms for selection of basic motor programs--roles for the striatum and pallidum. Trends Neurosci. 2005; 28: 364–370.

Groves PM, Linder JC, Young SJ. 5-hydroxydopamine-labeled dopaminergic axons: three-dimensional reconstructions of axons, synapses and postsynaptic targets in rat neostriatum. Neuroscience 1994; 58: 593–604.

Gruber AJ, McDonald RJ. Context, emotion, and the strategic pursuit of goals: interactions among multiple brain systems controlling motivated behavior. Front. Behav. Neurosci. 2012; 6: 50.

Grynkiewicz G, Poenie M, Tsien RY. A new generation of Ca2+ indicators with greatly improved fluorescence properties. J. Biol. Chem. 1985; 260: 3440–3450.

Gubellini P, Picconi B, Bari M, Battista N, Calabresi P, Centonze D, et al. Experimental parkinsonism alters endocannabinoid degradation: implications for striatal glutamatergic transmission. J. Neurosci. Off. J. Soc. Neurosci. 2002; 22: 6900–6907.

Guigoni C, Doudnikoff E, Li Q, Bloch B, Bezard E. Altered D(1) dopamine receptor trafficking in parkinsonian and dyskinetic non-human primates. Neurobiol. Dis. 2007; 26: 452–463.

Guzman JN, Sánchez-Padilla J, Chan CS, Surmeier DJ. Robust pacemaking in substantia nigra dopaminergic neurons. J. Neurosci. Off. J. Soc. Neurosci. 2009; 29: 11011–11019.

Håkansson K, Galdi S, Hendrick J, Snyder G, Greengard P, Fisone G. Regulation of phosphorylation of the GluR1 AMPA receptor by dopamine D2 receptors. J. Neurochem. 2006; 96: 482–488.

Hallett PJ, Dunah AW, Ravenscroft P, Zhou S, Bezard E, Crossman AR, et al. Alterations of striatal NMDA receptor subunits associated with the development of dyskinesia in the MPTP-lesioned primate model of Parkinson's disease. Neuropharmacology 2005; 48: 503–516.

Hallett PJ, Spoelgen R, Hyman BT, Standaert DG, Dunah AW. Dopamine D1 activation potentiates striatal NMDA receptors by tyrosine phosphorylation-dependent subunit trafficking. J. Neurosci. Off. J. Soc. Neurosci. 2006; 26: 4690–4700.

Hamasaki R, Shirasaki T, Soeda F, Takahama K. Tipepidine activates VTA dopamine neuron via inhibiting dopamine D_2 receptor-mediated inward rectifying K^+ current. Neuroscience 2013; 252: 24–34.

Hammond C, Bergman H, Brown P. Pathological synchronization in Parkinson's disease: networks, models and treatments. Trends Neurosci. 2007; 30: 357–364.

Hanley JJ, Bolam JP. Synaptology of the nigrostriatal projection in relation to the compartmental organization of the neostriatum in the rat. Neuroscience 1997; 81: 353–370.

Hanoune J, Defer N. Regulation and role of adenylyl cyclase isoforms. Annu. Rev. Pharmacol. Toxicol. 2001; 41: 145–174.

Hara Y, Pickel VM. Overlapping intracellular and differential synaptic distributions of dopamine D1 and glutamate N-methyl-D-aspartate receptors in rat nucleus accumbens. J. Comp. Neurol. 2005; 492: 442–455.

Harvey CD, Ehrhardt AG, Cellurale C, Zhong H, Yasuda R, Davis RJ, et al. A genetically encoded fluorescent sensor of ERK activity. Proc. Natl. Acad. Sci. U. S. A. 2008; 105: 19264–19269.

Harvey J, Lacey MG. A postsynaptic interaction between dopamine D1 and NMDA receptors promotes presynaptic inhibition in the rat nucleus accumbens via adenosine release. J. Neurosci. Off. J. Soc. Neurosci. 1997; 17: 5271–5280.

Hasbi A, Fan T, Alijaniaram M, Nguyen T, Perreault ML, O'Dowd BF, et al. Calcium signaling cascade links dopamine D1-D2 receptor heteromer to striatal BDNF production and neuronal growth. Proc. Natl. Acad. Sci. U. S. A. 2009; 106: 21377–21382.

Hauser RA, Cantillon M, Pourcher E, Micheli F, Mok V, Onofrj M, et al. Preladenant in patients with Parkinson's disease and motor fluctuations: a phase 2, double-blind, randomised trial. Lancet Neurol. 2011; 10: 221–229.

Hauser RA, Shulman LM, Trugman JM, Roberts JW, Mori A, Ballerini R, et al. Study of istradefylline in patients with Parkinson's disease on levodopa with motor fluctuations. Mov. Disord. Off. J. Mov. Disord. Soc. 2008; 23: 2177–2185.

Hayashi T, Huganir RL. Tyrosine phosphorylation and regulation of the AMPA receptor by SRC family tyrosine kinases. J. Neurosci. Off. J. Soc. Neurosci. 2004; 24: 6152–6160.

Heckman PRA, Blokland A, Bollen EPP, Prickaerts J. Phosphodiesterase inhibition and modulation of corticostriatal and hippocampal circuits: Clinical overview and translational considerations. Neurosci. Biobehav. Rev. 2018; 87: 233–254.

Heiman M, Heilbut A, Francardo V, Kulicke R, Fenster RJ, Kolaczyk ED, et al. Molecular adaptations of striatal spiny projection neurons during levodopa-induced dyskinesia. Proc. Natl. Acad. Sci. U. S. A. 2014a; 111: 4578–4583.

Heiman M, Kulicke R, Fenster RJ, Greengard P, Heintz N. Cell type-specific mRNA purification by translating ribosome affinity purification (TRAP). Nat. Protoc. 2014b; 9: 1282–1291.

Heiman M, Schaefer A, Gong S, Peterson JD, Day M, Ramsey KE, et al. A translational profiling approach for the molecular characterization of CNS cell types. Cell 2008; 135: 738–748.

Heim N, Griesbeck O. Genetically encoded indicators of cellular calcium dynamics based on troponin C and green fluorescent protein. J. Biol. Chem. 2004; 279: 14280–14286.

Hely MA, Morris JG, Traficante R, Reid WG, O'Sullivan DJ, Williamson PM. The sydney multicentre study of Parkinson's disease: progression and mortality at 10 years. J. Neurol. Neurosurg. Psychiatry 1999; 67: 300–307.

Hempel CM, Vincent P, Adams SR, Tsien RY, Selverston AI. Spatio-temporal dynamics of cyclic AMP signals in an intact neural circuitm. Nature 1996; 384: 166–169.

Henry B, Duty S, Fox SH, Crossman AR, Brotchie JM. Increased striatal pre-proenkephalin B expression is associated with dyskinesia in Parkinson's disease. Exp. Neurol. 2003; 183: 458–468.

Hepp R, Tricoire L, Hu E, Gervasi N, Paupardin-Tritsch D, Lambolez B, et al. Phosphodiesterase type 2 and the homeostasis of cyclic GMP in living thalamic neurons. J. Neurochem. 2007; 102: 1875–1886.

Hernández-Echeagaray E, Starling AJ, Cepeda C, Levine MS. Modulation of AMPA currents by D2 dopamine receptors in striatal medium-sized spiny neurons: are dendrites necessary? Eur. J. Neurosci. 2004; 19: 2455–2463.

Hernandez-Lopez S, Tkatch T, Perez-Garci E, Galarraga E, Bargas J, Hamm H, et al. D2 dopamine receptors in striatal medium spiny neurons reduce L-type Ca2+ currents and excitability via a novel PLC[beta]1-IP3-calcineurin-signaling cascade. J. Neurosci. Off. J. Soc. Neurosci. 2000; 20: 8987–8995.

Herrera-Marschitz M, Luthman J, Ferré S. Unilateral neonatal intracerebroventricular 6-hydroxydopamine administration in rats: II. Effects on extracellular monoamine, acetylcholine and adenosine levels monitored with in vivo microdialysis. Psychopharmacology (Berl.) 1994; 116: 451–456.

Hervé D. Identification of a specific assembly of the g protein golf as a critical and regulated module of dopamine and adenosine-activated cAMP pathways in the striatum. Front. Neuroanat. 2011; 5: 48.

Hervé D, Le Moine C, Corvol JC, Belluscio L, Ledent C, Fienberg AA, et al. Galpha(olf) levels are regulated by receptor usage and control dopamine and adenosine action in the striatum. J. Neurosci. Off. J. Soc. Neurosci. 2001; 21: 4390–4399.

Hervé D, Lévi-Strauss M, Marey-Semper I, Verney C, Tassin JP, Glowinski J, et al. G(olf) and Gs in rat basal ganglia: possible involvement of G(olf) in the coupling of dopamine D1 receptor with adenylyl cyclase. J. Neurosci. Off. J. Soc. Neurosci. 1993; 13: 2237–2248.

Hervé D, Trovero F, Blanc G, Glowinski J, Tassin JP. Autoradiographic identification of D1 dopamine receptors labelled with [3H]dopamine: distribution, regulation and relationship to coupling. Neuroscience 1992; 46: 687–700.

Herve D, Trovero F, Blanc G, Thierry AM, Glowinski J, Tassin JP. Nondopaminergic prefrontocortical efferent fibers modulate D1 receptor denervation supersensitivity in specific regions of the rat striatum. J. Neurosci. Off. J. Soc. Neurosci. 1989; 9: 3699–3708.

Hettinger BD, Lee A, Linden J, Rosin DL. Ultrastructural localization of adenosine A2A receptors suggests multiple cellular sites for modulation of GABAergic neurons in rat striatum. J. Comp. Neurol. 2001; 431: 331–346.

Higley MJ, Sabatini BL. Calcium signaling in dendrites and spines: practical and functional considerations. Neuron 2008; 59: 902–913.

Higley MJ, Sabatini BL. Competitive regulation of synaptic Ca2+ influx by D2 dopamine and A2A adenosine receptors. Nat. Neurosci. 2010; 13: 958–966.

Hikosaka O, Takikawa Y, Kawagoe R. Role of the basal ganglia in the control of purposive saccadic eye movements. Physiol. Rev. 2000; 80: 953–978.

Hillion J, Canals M, Torvinen M, Casado V, Scott R, Terasmaa A, et al. Coaggregation, cointernalization, and codesensitization of adenosine A2A receptors and dopamine D2 receptors. J. Biol. Chem. 2002; 277: 18091–18097.

Hoffmann R, Baillie GS, MacKenzie SJ, Yarwood SJ, Houslay MD. The MAP kinase ERK2 inhibits the cyclic AMP-specific phosphodiesterase HSPDE4D3 by phosphorylating it at Ser579. EMBO J. 1999; 18: 893–903.

Honda A, Adams SR, Sawyer CL, Lev-Ram V, Tsien RY, Dostmann WR. Spatiotemporal dynamics of guanosine 3',5'-cyclic monophosphate revealed by a genetically encoded, fluorescent indicator. Proc. Natl. Acad. Sci. U. S. A. 2001; 98: 2437–2442.

Hong KP, Spitzer NC, Nicol X. Improved molecular toolkit for cAMP studies in live cells. BMC Res. Notes 2011; 4: 241.

Horikawa K, Yamada Y, Matsuda T, Kobayashi K, Hashimoto M, Matsu-ura T, et al. Spontaneous network activity visualized by ultrasensitive Ca(2+) indicators, yellow Cameleon-Nano. Nat. Methods 2010; 7: 729–732.

Hornykiewicz O. Dopamine (3-hydroxytyramine) and brain function. Pharmacol. Rev. 1966; 18: 925–964.

Hornykiewicz O. Chemical neuroanatomy of the basal ganglia--normal and in Parkinson's disease. J. Chem. Neuroanat. 2001; 22: 3–12.

Howard CD, Li H, Geddes CE, Jin X. Dynamic Nigrostriatal Dopamine Biases Action Selection. Neuron 2017; 93: 1436–1450.e8.

Hsu Y-T, Liao G, Bi X, Oka T, Tamura S, Baudry M. The PDE10A inhibitor, papaverine, differentially activates ERK in male and female rat striatal slices. Neuropharmacology 2011; 61: 1275–1281.

Huang Q, Zhou D, Chase K, Gusella JF, Aronin N, DiFiglia M. Immunohistochemical localization of the D1 dopamine receptor in rat brain reveals its axonal transport, pre- and postsynaptic localization, and prevalence in the basal ganglia, limbic system, and thalamic reticular nucleus. Proc. Natl. Acad. Sci. U. S. A. 1992; 89: 11988–11992.

Huang Y-X, Luo W-F, Li D, Hu W-D, Liu C-F. CSC counteracts l-DOPA-induced overactivity of the corticostriatal synaptic ultrastructure and function in 6-OHDA-lesioned rats. Brain Res. 2011; 1376: 113–121.

Huerta-Ocampo I, Mena-Segovia J, Bolam JP. Convergence of cortical and thalamic input to direct and indirect pathway medium spiny neurons in the striatum. Brain Struct. Funct. 2014; 219: 1787–1800.

Hughes AJ, Daniel SE, Kilford L, Lees AJ. Accuracy of clinical diagnosis of idiopathic Parkinson's disease: a clinico-pathological study of 100 cases. J. Neurol. Neurosurg. Psychiatry 1992; 55: 181–184.

Hunnicutt BJ, Jongbloets BC, Birdsong WT, Gertz KJ, Zhong H, Mao T. A comprehensive excitatory input map of the striatum reveals novel functional organization. eLife 2016; 5

Hurley MJ, Dexter DT. Voltage-gated calcium channels and Parkinson's disease. Pharmacol. Ther. 2012; 133: 324–333.

Hurley MJ, Jackson MJ, Smith LA, Rose S, Jenner P. Immunoautoradiographic analysis of NMDA receptor subunits and associated postsynaptic density proteins in the brain of dyskinetic MPTP-treated common marmosets. Eur. J. Neurosci. 2005; 21: 3240–3250.

Ibáñez-Sandoval O, Tecuapetla F, Unal B, Shah F, Koós T, Tepper JM. A novel functionally distinct subtype of striatal neuropeptide Y interneuron. J. Neurosci. Off. J. Soc. Neurosci. 2011; 31: 16757–16769.

Ibraheem A, Yap H, Ding Y, Campbell RE. A bacteria colony-based screen for optimal linker combinations in genetically encoded biosensors. BMC Biotechnol. 2011; 11: 105.

Ince E, Ciliax BJ, Levey AI. Differential expression of D1 and D2 dopamine and m4 muscarinic acetylcholine receptor proteins in identified striatonigral neurons. Synap. N. Y. N 1997; 27: 357–366.

Ingham CA, Hood SH, Arbuthnott GW. Spine density on neostriatal neurones changes with 6-hydroxydopamine lesions and with age. Brain Res. 1989; 503: 334–338.

Ingham CA, Hood SH, Taggart P, Arbuthnott GW. Plasticity of synapses in the rat neostriatum after unilateral lesion of the nigrostriatal dopaminergic pathway. J. Neurosci. Off. J. Soc. Neurosci. 1998; 18: 4732–4743.

Iravani MM, Jenner P. Mechanisms underlying the onset and expression of levodopa-induced dyskinesia and their pharmacological manipulation. J. Neural Transm. Vienna Austria 1996 2011; 118: 1661–1690.

Iravani MM, McCreary AC, Jenner P. Striatal plasticity in Parkinson's disease and L-dopa induced dyskinesia. Parkinsonism Relat. Disord. 2012; 18 Suppl 1: S123–125.

Iwamoto T, Iwatsubo K, Okumura S, Hashimoto Y, Tsunematsu T, Toya Y, et al. Disruption of type 5 adenylyl cyclase negates the developmental increase in Galphaolf expression in the striatum. FEBS Lett. 2004; 564: 153–156.

Iwamoto T, Okumura S, Iwatsubo K, Kawabe J-I, Ohtsu K, Sakai I, et al. Motor dysfunction in type 5 adenylyl cyclase-null mice. J. Biol. Chem. 2003; 278: 16936–16940.

Jáidar O, Carrillo-Reid L, Hernández A, Drucker-Colín R, Bargas J, Hernández-Cruz A. Dynamics of the Parkinsonian striatal microcircuit: entrainment into a dominant network state. J. Neurosci. Off. J. Soc. Neurosci. 2010; 30: 11326–11336.

Jares-Erijman EA, Jovin TM. FRET imaging. Nat. Biotechnol. 2003; 21: 1387–1395.

Jenner P. Molecular mechanisms of L-DOPA-induced dyskinesia. Nat. Rev. Neurosci. 2008; 9: 665–677.

Jocoy EL, André VM, Cummings DM, Rao SP, Wu N, Ramsey AJ, et al. Dissecting the contribution of individual receptor subunits to the enhancement of N-methyl-d-aspartate currents by dopamine D1 receptor activation in striatum. Front. Syst. Neurosci. 2011; 5: 28.

Joel D, Weiner I. The organization of the basal ganglia-thalamocortical circuits: open interconnected rather than closed segregated. Neuroscience 1994; 63: 363–379.

Joel D, Weiner I. The connections of the dopaminergic system with the striatum in rats and primates: an analysis with respect to the functional and compartmental organization of the striatum. Neuroscience 2000; 96: 451–474.

Johnson JW, Ascher P. Glycine potentiates the NMDA response in cultured mouse brain neurons. Nature 1987; 325: 529–531.

Jones DT, Reed RR. Golf: an olfactory neuron specific-G protein involved in odorant signal transduction. Science 1989; 244: 790–795.

Jourdain VA, Morin N, Grégoire L, Morissette M, Di Paolo T. Changes in glutamate receptors in dyskinetic parkinsonian monkeys after unilateral subthalamotomy. J. Neurosurg. 2015; 123: 1383–1393.

Kachroo A, Orlando LR, Grandy DK, Chen J-F, Young AB, Schwarzschild MA. Interactions between metabotropic glutamate 5 and adenosine A2A receptors in normal and parkinsonian mice. J. Neurosci. Off. J. Soc. Neurosci. 2005; 25: 10414–10419.

Kase H, Aoyama S, Ichimura M, Ikeda K, Ishii A, Kanda T, et al. Progress in pursuit of therapeutic A2A antagonists: the adenosine A2A receptor selective antagonist KW6002: research and development toward a novel nondopaminergic therapy for Parkinson's disease. Neurology 2003; 61: S97–100.

Kawaguchi Y. Physiological, morphological, and histochemical characterization of three classes of interneurons in rat neostriatum. J. Neurosci. Off. J. Soc. Neurosci. 1993; 13: 4908–4923.

Kawaguchi Y. Neostriatal cell subtypes and their functional roles. Neurosci. Res. 1997; 27: 1–8.

Kawaguchi Y, Wilson CJ, Augood SJ, Emson PC. Striatal interneurones: chemical, physiological and morphological characterization. Trends Neurosci. 1995; 18: 527–535.

Kawaguchi Y, Wilson CJ, Emson PC. Intracellular recording of identified neostriatal patch and matrix spiny cells in a slice preparation preserving cortical inputs. J. Neurophysiol. 1989; 62: 1052–1068.

Kebabian JW, Calne DB. Multiple receptors for dopamine. Nature 1979; 277: 93–96.

Kelsey JE, Langelier NA, Oriel BS, Reedy C. The effects of systemic, intrastriatal, and intrapallidal injections of caffeine and systemic injections of A2A and A1 antagonists on forepaw stepping in the unilateral 6-OHDA-lesioned rat. Psychopharmacology (Berl.) 2009; 201: 529–539.

Kemp JM, Powell TP. The termination of fibres from the cerebral cortex and thalamus upon dendritic spines in the caudate nucleus: a study with the Golgi method. Philos. Trans. R. Soc. Lond. B. Biol. Sci. 1971; 262: 429–439.

Kerr JND, Plenz D. Action potential timing determines dendritic calcium during striatal up-states. J. Neurosci. Off. J. Soc. Neurosci. 2004; 24: 877–885.

Kheirbek MA, Britt JP, Beeler JA, Ishikawa Y, McGehee DS, Zhuang X. Adenylyl cyclase type 5 contributes to corticostriatal plasticity and striatum-dependent learning. J. Neurosci. Off. J. Soc. Neurosci. 2009; 29: 12115–12124.

Kim B, Hawes SL, Gillani F, Wallace LJ, Blackwell KT. Signaling pathways involved in striatal synaptic plasticity are sensitive to temporal pattern and exhibit spatial specificity. PLoS Comput. Biol. 2013; 9: e1002953.

Kimura M, Aosaki T, Hu Y, Ishida A, Watanabe K. Activity of primate putamen neurons is selective to the mode of voluntary movement: visually guided, self-initiated or memory-guided. Exp. Brain Res. 1992; 89: 473–477.

Kincaid AE, Zheng T, Wilson CJ. Connectivity and convergence of single corticostriatal axons. J. Neurosci. Off. J. Soc. Neurosci. 1998; 18: 4722–4731.

King AE, Ackley MA, Cass CE, Young JD, Baldwin SA. Nucleoside transporters: from scavengers to novel therapeutic targets. Trends Pharmacol. Sci. 2006; 27: 416–425.

Kish LJ, Palmer MR, Gerhardt GA. Multiple single-unit recordings in the striatum of freely moving animals: effects of apomorphine and D-amphetamine in normal and unilateral 6-hydroxydopamine-lesioned rats. Brain Res. 1999; 833: 58–70.

Kita H. GABAergic circuits of the striatum. Prog. Brain Res. 1993; 99: 51–72.

Kita H. Glutamatergic and GABAergic postsynaptic responses of striatal spiny neurons to intrastriatal and cortical stimulation recorded in slice preparations. Neuroscience 1996; 70: 925–940.

Kita H, Kita T. Role of Striatum in the Pause and Burst Generation in the Globus Pallidus of 6-OHDA-Treated Rats. Front. Syst. Neurosci. 2011; 5: 42.

Kleckner NW, Dingledine R. Requirement for glycine in activation of NMDA-receptors expressed in Xenopus oocytes. Science 1988; 241: 835–837.

Klug JR, Mathur BN, Kash TL, Wang H-D, Matthews RT, Robison AJ, et al. Genetic inhibition of CaMKII in dorsal striatal medium spiny neurons reduces functional excitatory synapses and enhances intrinsic excitability. PloS One 2012; 7: e45323.

Kobylecki C, Cenci MA, Crossman AR, Ravenscroft P. Calcium-permeable AMPA receptors are involved in the induction and expression of l-DOPA-induced dyskinesia in Parkinson's disease. J. Neurochem. 2010; 114: 499–511.

Kobylecki C, Crossman AR, Ravenscroft P. Alternative splicing of AMPA receptor subunits in the 6-OHDA-lesioned rat model of Parkinson's disease and L-DOPA-induced dyskinesia. Exp. Neurol. 2013; 247: 476–484.

Koga K, Kurokawa M, Ochi M, Nakamura J, Kuwana Y. Adenosine A(2A) receptor antagonists KF17837 and KW-6002 potentiate rotation induced by dopaminergic drugs in hemi-Parkinsonian rats. Eur. J. Pharmacol. 2000; 408: 249–255.

Komatsu N, Aoki K, Yamada M, Yukinaga H, Fujita Y, Kamioka Y, et al. Development of an optimized backbone of FRET biosensors for kinases and GTPases. Mol. Biol. Cell 2011; 22: 4647–4656.

Konitsiotis S, Blanchet PJ, Verhagen L, Lamers E, Chase TN. AMPA receptor blockade improves levodopa-induced dyskinesia in MPTP monkeys. Neurology 2000; 54: 1589–1595.

Konradi C, Macías W, Dudman JT, Carlson RR. Striatal proenkephalin gene induction: coordinated regulation by cyclic AMP and calcium pathways. Brain Res. Mol. Brain Res. 2003; 115: 157–161.

Konradi C, Westin JE, Carta M, Eaton ME, Kuter K, Dekundy A, et al. Transcriptome analysis in a rat model of L-DOPA-induced dyskinesia. Neurobiol. Dis. 2004; 17: 219–236.

Koos T, Tepper JM, Wilson CJ. Comparison of IPSCs evoked by spiny and fast-spiking neurons in the neostriatum. J. Neurosci. Off. J. Soc. Neurosci. 2004; 24: 7916–7922.

Kostic V, Przedborski S, Flaster E, Sternic N. Early development of levodopa-induced dyskinesias and response fluctuations in young-onset Parkinson's disease. Neurology 1991; 41: 202–205.

Kotecha SA, Oak JN, Jackson MF, Perez Y, Orser BA, Van Tol HHM, et al. A D2 class dopamine receptor transactivates a receptor tyrosine kinase to inhibit NMDA receptor transmission. Neuron 2002; 35: 1111–1122.

Kramer PF, Williams JT. Calcium Release from Stores Inhibits GIRK. Cell Rep. 2016; 17: 3246–3255.

Krapivinsky G, Krapivinsky L, Manasian Y, Ivanov A, Tyzio R, Pellegrino C, et al. The NMDA receptor is coupled to the ERK pathway by a direct interaction between NR2B and RasGRF1. Neuron 2003; 40: 775–784.

Kravitz AV, Freeze BS, Parker PRL, Kay K, Thwin MT, Deisseroth K, et al. Regulation of parkinsonian motor behaviours by optogenetic control of basal ganglia circuitry. Nature 2010; 466: 622–626.

Kreitzer AC. Physiology and pharmacology of striatal neurons. Annu. Rev. Neurosci. 2009; 32: 127–147.

Kreitzer AC, Malenka RC. Endocannabinoid-mediated rescue of striatal LTD and motor deficits in Parkinson's disease models. Nature 2007; 445: 643–647.

Kress GJ, Yamawaki N, Wokosin DL, Wickersham IR, Shepherd GMG, Surmeier DJ. Convergent cortical innervation of striatal projection neurons. Nat. Neurosci. 2013; 16: 665–667.

van der Krogt GNM, Ogink J, Ponsioen B, Jalink K. A comparison of donor-acceptor pairs for genetically encoded FRET sensors: application to the Epac cAMP sensor as an example. PloS One 2008; 3: e1916.

Kruusmägi M, Kumar S, Zelenin S, Brismar H, Aperia A, Scott L. Functional differences between D(1) and D(5) revealed by high resolution imaging on live neurons. Neuroscience 2009; 164: 463–469.

Kull B, Svenningsson P, Fredholm BB. Adenosine A(2A) receptors are colocalized with and activate g(olf) in rat striatum. Mol. Pharmacol. 2000; 58: 771–777.

Künzle H. Bilateral projections from precentral motor cortex to the putamen and other parts of the basal ganglia. An autoradiographic study in Macaca fascicularis. Brain Res. 1975; 88: 195–209.

Ladepeche L, Dupuis JP, Bouchet D, Doudnikoff E, Yang L, Campagne Y, et al. Single-molecule imaging of the functional crosstalk between surface NMDA and dopamine D1 receptors. Proc. Natl. Acad. Sci. U. S. A. 2013; 110: 18005–18010.

Lakics V, Karran EH, Boess FG. Quantitative comparison of phosphodiesterase mRNA distribution in human brain and peripheral tissues. Neuropharmacology 2010; 59: 367–374.

Landry P, Wilson CJ, Kitai ST. Morphological and electrophysiological characteristics of pyramidal tract neurons in the rat. Exp. Brain Res. 1984; 57: 177–190.

Latini S, Pedata F. Adenosine in the central nervous system: release mechanisms and extracellular concentrations. J. Neurochem. 2001; 79: 463–484.

Laube B, Hirai H, Sturgess M, Betz H, Kuhse J. Molecular determinants of agonist discrimination by NMDA receptor subunits: analysis of the glutamate binding site on the NR2B subunit. Neuron 1997; 18: 493–503.

Lavaur J, Bernard F, Trifilieff P, Pascoli V, Kappes V, Pagès C, et al. A TAT-DEF-Elk-1 peptide regulates the cytonuclear trafficking of Elk-1 and controls cytoskeleton dynamics. J. Neurosci. Off. J. Soc. Neurosci. 2007; 27: 14448–14458.

La Via L, Bonini D, Russo I, Orlandi C, Barlati S, Barbon A. Modulation of dendritic AMPA receptor mRNA trafficking by RNA splicing and editing. Nucleic Acids Res. 2013; 41: 617–631.

Lavine N, Ethier N, Oak JN, Pei L, Liu F, Trieu P, et al. G protein-coupled receptors form stable complexes with inwardly rectifying potassium channels and adenylyl cyclase. J. Biol. Chem. 2002; 277: 46010–46019.

Lebel M, Chagniel L, Bureau G, Cyr M. Striatal inhibition of PKA prevents levodopa-induced behavioural and molecular changes in the hemiparkinsonian rat. Neurobiol. Dis. 2010; 38: 59–67.

Ledent C, Vaugeois JM, Schiffmann SN, Pedrazzini T, El Yacoubi M, Vanderhaeghen JJ, et al. Aggressiveness, hypoalgesia and high blood pressure in mice lacking the adenosine A2a receptor. Nature 1997; 388: 674–678.

Lee FJS, Xue S, Pei L, Vukusic B, Chéry N, Wang Y, et al. Dual regulation of NMDA receptor functions by direct protein-protein interactions with the dopamine D1 receptor. Cell 2002a; 111: 219–230.

Lee K-W, Hong J-H, Choi IY, Che Y, Lee J-K, Yang S-D, et al. Impaired D2 dopamine receptor function in mice lacking type 5 adenylyl cyclase. J. Neurosci. Off. J. Soc. Neurosci. 2002b; 22: 7931–7940.

Lees AJ, Tolosa E, Olanow CW. Four pioneers of L-dopa treatment: Arvid Carlsson, Oleh Hornykiewicz, George Cotzias, and Melvin Yahr. Mov. Disord. Off. J. Mov. Disord. Soc. 2015; 30: 19–36.

Lei W, Deng Y, Liu B, Mu S, Guley NM, Wong T, et al. Confocal laser scanning microscopy and ultrastructural study of VGLUT2 thalamic input to striatal projection neurons in rats. J. Comp. Neurol. 2013; 521: 1354–1377.

Le Moine C, Bloch B. D1 and D2 dopamine receptor gene expression in the rat striatum: sensitive cRNA probes demonstrate prominent segregation of D1 and D2 mRNAs in distinct neuronal populations of the dorsal and ventral striatum. J. Comp. Neurol. 1995; 355: 418–426.

Le Moine C, Bloch B. Expression of the D3 dopamine receptor in peptidergic neurons of the nucleus accumbens: comparison with the D1 and D2 dopamine receptors. Neuroscience 1996; 73: 131–143.

Lesser RP, Fahn S, Snider SR, Cote LJ, Isgreen WP, Barrett RE. Analysis of the clinical problems in parkinsonism and the complications of long-term levodopa therapy. Neurology 1979; 29: 1253–1260.

Levandis G, Bazzini E, Armentero M-T, Nappi G, Blandini F. Systemic administration of an mGluR5 antagonist, but not unilateral subthalamic lesion, counteracts l-DOPA-induced dyskinesias in a rodent model of Parkinson's disease. Neurobiol. Dis. 2008; 29: 161–168.

LeWitt PA, Guttman M, Tetrud JW, Tuite PJ, Mori A, Chaikin P, et al. Adenosine A2A receptor antagonist istradefylline (KW-6002) reduces 'off' time in Parkinson's disease: a double-blind, randomized, multicenter clinical trial (6002-US-005). Ann. Neurol. 2008; 63: 295–302.

Liang L, DeLong MR, Papa SM. Inversion of dopamine responses in striatal medium spiny neurons and involuntary movements. J. Neurosci. Off. J. Soc. Neurosci. 2008; 28: 7537–7547.

Liles SL, Updyke BV. Projection of the digit and wrist area of precentral gyrus to the putamen: relation between topography and physiological properties of neurons in the putamen. Brain Res. 1985; 339: 245–255.

Li L, Gervasi N, Girault J-A. Dendritic geometry shapes neuronal cAMP signalling to the nucleus. Nat. Commun. 2015; 6: 6319.

Lindgren HS, Andersson DR, Lagerkvist S, Nissbrandt H, Cenci MA. L-DOPA-induced dopamine efflux in the striatum and the substantia nigra in a rat model of Parkinson's disease: temporal and quantitative relationship to the expression of dyskinesia. J. Neurochem. 2010; 112: 1465–1476.

Lindgren HS, Ohlin KE, Cenci MA. Differential involvement of D1 and D2 dopamine receptors in L-DOPA-induced angiogenic activity in a rat model of Parkinson's disease. Neuropsychopharmacol. Off. Publ. Am. Coll. Neuropsychopharmacol. 2009; 34: 2477–2488.

Lindgren HS, Rylander D, Iderberg H, Andersson M, O'Sullivan SS, Williams DR, et al. Putaminal upregulation of FosB/ΔFosB-like immunoreactivity in Parkinson's disease patients with dyskinesia. J. Park. Dis. 2011; 1: 347–357.

Lindgren HS, Rylander D, Ohlin KE, Lundblad M, Cenci MA. The 'motor complication syndrome' in rats with 6-OHDA lesions treated chronically with L-DOPA: relation to dose and route of administration. Behav. Brain Res. 2007; 177: 150–159.

Lin J-Y, Liu Z-G, Xie C-L, Song L, Yan A-J. Antidyskinetic Treatment with MTEP Affects Multiple Molecular Pathways in the Parkinsonian Striatum. Park. Dis. 2017; 2017: 5798734.

Lissandron V, Terrin A, Collini M, D'alfonso L, Chirico G, Pantano S, et al. Improvement of a FRET-based indicator for cAMP by linker design and stabilization of donor-acceptor interaction. J. Mol. Biol. 2005; 354: 546–555.

Litim N, Morissette M, Di Paolo T. Metabotropic glutamate receptors as therapeutic targets in Parkinson's disease: An update from the last 5 years of research. Neuropharmacology 2017; 115: 166–179.

Liu X-Y, Chu X-P, Mao L-M, Wang M, Lan H-X, Li M-H, et al. Modulation of D2R-NR2B interactions in response to cocaine. Neuron 2006; 52: 897–909.

Lobo MK, Karsten SL, Gray M, Geschwind DH, Yang XW. FACS-array profiling of striatal projection neuron subtypes in juvenile and adult mouse brains. Nat. Neurosci. 2006; 9: 443–452.

Logue JS, Scott JD. Organizing signal transduction through A-kinase anchoring proteins (AKAPs). FEBS J. 2010; 277: 4370–4375.

Lortet S, Lacombe E, Boulanger N, Rihet P, Nguyen C, Kerkerian-Le Goff L, et al. Striatal molecular signature of subchronic subthalamic nucleus high frequency stimulation in parkinsonian rat. PloS One 2013; 8: e60447.

Lovinger DM, Tyler E. Synaptic transmission and modulation in the neostriatum. Int. Rev. Neurobiol. 1996; 39: 77–111.

Luczak V, Blackwell KT, Abel T, Girault J-A, Gervasi N. Dendritic diameter influences the rate and magnitude of hippocampal cAMP and PKA transients during β-adrenergic receptor activation. Neurobiol. Learn. Mem. 2017; 138: 10–20.

Luttrell LM. Minireview: More than just a hammer: ligand 'bias' and pharmaceutical discovery. Mol. Endocrinol. Baltim. Md 2014; 28: 281–294.

Luttrell LM, Wang J, Plouffe B, Smith JS, Yamani L, Kaur S, et al. Manifold roles of β-arrestins in GPCR signaling elucidated with siRNA and CRISPR/Cas9. Sci. Signal. 2018; 11

Mahan LC, McVittie LD, Smyk-Randall EM, Nakata H, Monsma FJ, Gerfen CR, et al. Cloning and expression of an A1 adenosine receptor from rat brain. Mol. Pharmacol. 1991; 40: 1–7.

Mallet N, Ballion B, Le Moine C, Gonon F. Cortical inputs and GABA interneurons imbalance projection neurons in the striatum of parkinsonian rats. J. Neurosci. Off. J. Soc. Neurosci. 2006; 26: 3875–3884.

Mangiavacchi S, Wolf ME. D1 dopamine receptor stimulation increases the rate of AMPA receptor insertion onto the surface of cultured nucleus accumbens neurons through a pathway dependent on protein kinase A. J. Neurochem. 2004; 88: 1261–1271.

Manson A, Stirpe P, Schrag A. Levodopa-induced-dyskinesias clinical features, incidence, risk factors, management and impact on quality of life. J. Park. Dis. 2012; 2: 189–198.

Manzoni OJ, Manabe T, Nicoll RA. Release of adenosine by activation of NMDA receptors in the hippocampus. Science 1994; 265: 2098–2101.

Mao L, Tang Q, Samdani S, Liu Z, Wang JQ. Regulation of MAPK/ERK phosphorylation via ionotropic glutamate receptors in cultured rat striatal neurons. Eur. J. Neurosci. 2004; 19: 1207–1216.

Marchi S, Pinton P. The mitochondrial calcium uniporter complex: molecular components, structure and physiopathological implications. J. Physiol. 2014; 592: 829–839.

Marcotte ER, Sullivan RM, Mishra RK. Striatal G-proteins: effects of unilateral 6-hydroxydopamine lesions. Neurosci. Lett. 1994; 169: 195–198.

Marshall JF, Navarrete R, Joyce JN. Decreased striatal D1 binding density following mesotelencephalic 6-hydroxydopamine injections: an autoradiographic analysis. Brain Res. 1989; 493: 247–257.

Martinez-Mir MI, Probst A, Palacios JM. Adenosine A2 receptors: selective localization in the human basal ganglia and alterations with disease. Neuroscience 1991; 42: 697–706.

Marvin JS, Borghuis BG, Tian L, Cichon J, Harnett MT, Akerboom J, et al. An optimized fluorescent probe for visualizing glutamate neurotransmission. Nat. Methods 2013; 10: 162–170.

Matamales M, Bertran-Gonzalez J, Salomon L, Degos B, Deniau J-M, Valjent E, et al. Striatal medium-sized spiny neurons: identification by nuclear staining and study of neuronal subpopulations in BAC transgenic mice. PloS One 2009; 4: e4770.

Matsuda W, Furuta T, Nakamura KC, Hioki H, Fujiyama F, Arai R, et al. Single nigrostriatal dopaminergic neurons form widely spread and highly dense axonal arborizations in the neostriatum. J. Neurosci. Off. J. Soc. Neurosci. 2009; 29: 444–453.

Mayer ML, Westbrook GL, Guthrie PB. Voltage-dependent block by Mg2+ of NMDA responses in spinal cord neurones. Nature 1984; 309: 261–263.

Mazzella L, Yahr MD, Marinelli L, Huang N, Moshier E, Di Rocco A. Dyskinesias predict the onset of motor response fluctuations in patients with Parkinson's disease on L-dopa monotherapy. Parkinsonism Relat. Disord. 2005; 11: 151–155.

McCombs JE, Palmer AE. Measuring calcium dynamics in living cells with genetically encodable calcium indicators. Methods San Diego Calif 2008; 46: 152–159.

McGeorge AJ, Faull RL. The organization of the projection from the cerebral cortex to the striatum in the rat. Neuroscience 1989; 29: 503–537.

McNeill TH, Brown SA, Hogg E, Cheng H-W, Meshul CK. Synapse replacement in the striatum of the adult rat following unilateral cortex ablation. J. Comp. Neurol. 2003; 467: 32–43.

McNeill TH, Brown SA, Rafols JA, Shoulson I. Atrophy of medium spiny I striatal dendrites in advanced Parkinson's disease. Brain Res. 1988; 455: 148–152.

Meissner W, Ravenscroft P, Reese R, Harnack D, Morgenstern R, Kupsch A, et al. Increased slow oscillatory activity in substantia nigra pars reticulata triggers abnormal involuntary movements in the 6-OHDA-lesioned rat in the presence of excessive extracellular striatal dopamine. Neurobiol. Dis. 2006; 22: 586–598.

Mellone M, Gardoni F. Modulation of NMDA receptor at the synapse: promising therapeutic interventions in disorders of the nervous system. Eur. J. Pharmacol. 2013; 719: 75–83.

Menegas W, Bergan JF, Ogawa SK, Isogai Y, Umadevi Venkataraju K, Osten P, et al. Dopamine neurons projecting to the posterior striatum form an anatomically distinct subclass. eLife 2015; 4: e10032.

Menegoz M, Lau LF, Hervé D, Huganir RL, Girault JA. Tyrosine phosphorylation of NMDA receptor in rat striatum: effects of 6-OH-dopamine lesions. Neuroreport 1995; 7: 125–128.

Menniti FS, Faraci WS, Schmidt CJ. Phosphodiesterases in the CNS: targets for drug development. Nat. Rev. Drug Discov. 2006; 5: 660–670.

Meshul CK, Allen C. Haloperidol reverses the changes in striatal glutamatergic immunolabeling following a 6-OHDA lesion. Synap. N. Y. N 2000; 36: 129–142.

Meshul CK, Emre N, Nakamura CM, Allen C, Donohue MK, Buckman JF. Time-dependent changes in striatal glutamate synapses following a 6-hydroxydopamine lesion. Neuroscience 1999; 88: 1–16.

Mink JW. The basal ganglia: focused selection and inhibition of competing motor programs. Prog. Neurobiol. 1996; 50: 381–425.

Mink JW. The Basal Ganglia and involuntary movements: impaired inhibition of competing motor patterns. Arch. Neurol. 2003; 60: 1365–1368.

Miró X, Pérez-Torres S, Palacios JM, Puigdomènech P, Mengod G. Differential distribution of cAMP-specific phosphodiesterase 7A mRNA in rat brain and peripheral organs. Synap. N. Y. N 2001; 40: 201–214.

Mishina M, Ishii K, Kimura Y, Suzuki M, Kitamura S, Ishibashi K, et al. Adenosine A1 receptors measured with 11 C-MPDX PET in early Parkinson's disease. Synap. N. Y. N 2017; 71

Mishina M, Ishiwata K, Naganawa M, Kimura Y, Kitamura S, Suzuki M, et al. Adenosine A(2A) receptors measured with [C]TMSX PET in the striata of Parkinson's disease patients. PloS One 2011; 6: e17338.

Missale C, Nisoli E, Liberini P, Rizzonelli P, Memo M, Buonamici M, et al. Repeated reserpine administration up-regulates the transduction mechanisms of D1 receptors without changing the density of [3H]SCH 23390 binding. Brain Res. 1989; 483: 117–122.

Miyawaki A. Visualization of the spatial and temporal dynamics of intracellular signaling. Dev. Cell 2003a; 4: 295–305.

Miyawaki A. Fluorescence imaging of physiological activity in complex systems using GFP-based probes. Curr. Opin. Neurobiol. 2003b; 13: 591–596.

Miyawaki A, Griesbeck O, Heim R, Tsien RY. Dynamic and quantitative Ca2+ measurements using improved cameleons. Proc. Natl. Acad. Sci. U. S. A. 1999; 96: 2135–2140.

Miyawaki A, Llopis J, Heim R, McCaffery JM, Adams JA, Ikura M, et al. Fluorescent indicators for Ca2+ based on green fluorescent proteins and calmodulin. Nature 1997; 388: 882–887.

Mizuno Y, Kondo T, Japanese Istradefylline Study Group. Adenosine A2A receptor antagonist istradefylline reduces daily OFF time in Parkinson's disease. Mov. Disord. Off. J. Mov. Disord. Soc. 2013; 28: 1138–1141.

Moeyaert B, Holt G, Madangopal R, Perez-Alvarez A, Fearey BC, Trojanowski NF, et al. Improved methods for marking active neuron populations. Nat. Commun. 2018; 9: 4440.

Moore ED, Becker PL, Fogarty KE, Williams DA, Fay FS. Ca2+ imaging in single living cells: theoretical and practical issues. Cell Calcium 1990; 11: 157–179.

Morales-Garcia JA, Aguilar-Morante D, Hernandez-Encinas E, Alonso-Gil S, Gil C, Martinez A, et al. Silencing phosphodiesterase 7B gene by lentiviral-shRNA interference attenuates neurodegeneration and motor deficits in hemiparkinsonian mice. Neurobiol. Aging 2015; 36: 1160–1173.

Morales-Garcia JA, Redondo M, Alonso-Gil S, Gil C, Perez C, Martinez A, et al. Phosphodiesterase 7 inhibition preserves dopaminergic neurons in cellular and rodent models of Parkinson disease. PloS One 2011; 6: e17240.

Morelli M, Di Paolo T, Wardas J, Calon F, Xiao D, Schwarzschild MA. Role of adenosine A2A receptors in parkinsonian motor impairment and l-DOPA-induced motor complications. Prog. Neurobiol. 2007; 83: 293–309.

Morelli M, Fenu S, Pinna A, Di Chiara G. Adenosine A2 receptors interact negatively with dopamine D1 and D2 receptors in unilaterally 6-hydroxydopamine-lesioned rats. Eur. J. Pharmacol. 1994; 251: 21–25.

Moreno CM, Dixon RE, Tajada S, Yuan C, Opitz-Araya X, Binder MD, et al. Ca(2+) entry into neurons is facilitated by cooperative gating of clustered CaV1.3 channels. eLife 2016; 5

Moreno E, Chiarlone A, Medrano M, Puigdellívol M, Bibic L, Howell LA, et al. Singular Location and Signaling Profile of Adenosine A2A-Cannabinoid CB1 Receptor Heteromers in the Dorsal Striatum. Neuropsychopharmacol. Off. Publ. Am. Coll. Neuropsychopharmacol. 2018; 43: 964–977.

Morgane PJ, Galler JR, Mokler DJ. A review of systems and networks of the limbic forebrain/limbic midbrain. Prog. Neurobiol. 2005; 75: 143–160.

Morgante F, Espay AJ, Gunraj C, Lang AE, Chen R. Motor cortex plasticity in Parkinson's disease and levodopa-induced dyskinesias. Brain J. Neurol. 2006; 129: 1059–1069.

Mori A, Shindou T. Modulation of GABAergic transmission in the striatopallidal system by adenosine A2A receptors: a potential mechanism for the antiparkinsonian effects of A2A antagonists. Neurology 2003; 61: S44–48.

Morigaki R, Okita S, Goto S. Dopamine-Induced Changes in Gαolf Protein Levels in Striatonigral and Striatopallidal Medium Spiny Neurons Underlie the Genesis of l-DOPA-Induced Dyskinesia in Parkinsonian Mice. Front. Cell. Neurosci. 2017; 11: 26.

Morin N, Jourdain VA, Morissette M, Grégoire L, Di Paolo T. Long-term treatment with l-DOPA and an mGlu5 receptor antagonist prevents changes in brain basal ganglia dopamine receptors, their associated signaling proteins and neuropeptides in parkinsonian monkeys. Neuropharmacology 2014; 79: 688–706.

Morin N, Morissette M, Grégoire L, Di Paolo T. mGlu5, Dopamine D2 and Adenosine A2A Receptors in L-DOPA-induced Dyskinesias. Curr. Neuropharmacol. 2016; 14: 481–493.

Morissette M, Dridi M, Calon F, Hadj Tahar A, Meltzer LT, Bédard PJ, et al. Prevention of dyskinesia by an NMDA receptor antagonist in MPTP monkeys: effect on adenosine A2A receptors. Synap. N. Y. N 2006; 60: 239–250.

Morissette M, Goulet M, Soghomonian JJ, Blanchet PJ, Calon F, Bédard PJ, et al. Preproenkephalin mRNA expression in the caudate-putamen of MPTP monkeys after chronic treatment with the D2 agonist U91356A in continuous or intermittent mode of administration: comparison with L-DOPA therapy. Brain Res. Mol. Brain Res. 1997; 49: 55–62.

Moss J, Bolam JP. A dopaminergic axon lattice in the striatum and its relationship with cortical and thalamic terminals. J. Neurosci. Off. J. Soc. Neurosci. 2008; 28: 11221–11230.

Mothet JP, Parent AT, Wolosker H, Brady RO, Linden DJ, Ferris CD, et al. D-serine is an endogenous ligand for the glycine site of the N-methyl-D-aspartate receptor. Proc. Natl. Acad. Sci. U. S. A. 2000; 97: 4926–4931.

Musante V, Neri E, Feligioni M, Puliti A, Pedrazzi M, Conti V, et al. Presynaptic mGlu1 and mGlu5 autoreceptors facilitate glutamate exocytosis from mouse cortical nerve endings. Neuropharmacology 2008; 55: 474–482.

Muto A, Ohkura M, Kotani T, Higashijima S, Nakai J, Kawakami K. Genetic visualization with an improved GCaMP calcium indicator reveals spatiotemporal activation of the spinal motor neurons in zebrafish. Proc. Natl. Acad. Sci. U. S. A. 2011; 108: 5425–5430.

Nagai T, Nakamuta S, Kuroda K, Nakauchi S, Nishioka T, Takano T, et al. Phosphoproteomics of the Dopamine Pathway Enables Discovery of Rap1 Activation as a Reward Signal In Vivo. Neuron 2016a; 89: 550–565.

Nagai T, Yamada S, Tominaga T, Ichikawa M, Miyawaki A. Expanded dynamic range of fluorescent indicators for Ca(2+) by circularly permuted yellow fluorescent proteins. Proc. Natl. Acad. Sci. U. S. A. 2004; 101: 10554–10559.

Nagai T, Yoshimoto J, Kannon T, Kuroda K, Kaibuchi K. Phosphorylation Signals in Striatal Medium Spiny Neurons. Trends Pharmacol. Sci. 2016b; 37: 858–871.

Nakai J, Ohkura M, Imoto K. A high signal-to-noise Ca(2+) probe composed of a single green fluorescent protein. Nat. Biotechnol. 2001; 19: 137–141.

Nakazawa T, Komai S, Tezuka T, Hisatsune C, Umemori H, Semba K, et al. Characterization of Fyn-mediated tyrosine phosphorylation sites on GluR epsilon 2 (NR2B) subunit of the N-methyl-D-aspartate receptor. J. Biol. Chem. 2001; 276: 693–699.

Nambu A. Seven problems on the basal ganglia. Curr. Opin. Neurobiol. 2008; 18: 595–604.

Nash JE, Brotchie JM. A common signaling pathway for striatal NMDA and adenosine A2a receptors: implications for the treatment of Parkinson's disease. J. Neurosci. Off. J. Soc. Neurosci. 2000; 20: 7782–7789.

Nash JE, Ravenscroft P, McGuire S, Crossman AR, Menniti FS, Brotchie JM. The NR2B-selective NMDA receptor antagonist CP-101,606 exacerbates L-DOPA-induced dyskinesia and provides mild potentiation of anti-parkinsonian effects of L-DOPA in the MPTP-lesioned marmoset model of Parkinson's disease. Exp. Neurol. 2004; 188: 471–479.

Navarro G, Cordomí A, Brugarolas M, Moreno E, Aguinaga D, Pérez-Benito L, et al. Cross-communication between Gi and Gs in a G-protein-coupled receptor heterotetramer guided by a receptor C-terminal domain. BMC Biol. 2018a; 16: 24.

Navarro G, Cordomí A, Casadó-Anguera V, Moreno E, Cai N-S, Cortés A, et al. Evidence for functional pre-coupled complexes of receptor heteromers and adenylyl cyclase. Nat. Commun. 2018b; 9: 1242.

Neely MD, Schmidt DE, Deutch AY. Cortical regulation of dopamine depletion-induced dendritic spine loss in striatal medium spiny neurons. Neuroscience 2007; 149: 457–464.

Neve KA, Seamans JK, Trantham-Davidson H. Dopamine receptor signaling. J. Recept. Signal Transduct. Res. 2004; 24: 165–205.

Neves SR, Tsokas P, Sarkar A, Grace EA, Rangamani P, Taubenfeld SM, et al. Cell shape and negative links in regulatory motifs together control spatial information flow in signaling networks. Cell 2008; 133: 666–680.

Nevian T, Sakmann B. Single spine Ca2+ signals evoked by coincident EPSPs and backpropagating action potentials in spiny stellate cells of layer 4 in the juvenile rat somatosensory barrel cortex. J. Neurosci. Off. J. Soc. Neurosci. 2004; 24: 1689–1699.

Niccolini F, Foltynie T, Reis Marques T, Muhlert N, Tziortzi AC, Searle GE, et al. Loss of phosphodiesterase 10A expression is associated with progression and severity in Parkinson's disease. Brain J. Neurol. 2015; 138: 3003–3015.

Niccolini F, Wilson H, Pagano G, Coello C, Mehta MA, Searle GE, et al. Loss of phosphodiesterase 4 in Parkinson disease: Relevance to cognitive deficits. Neurology 2017; 89: 586–593.

Nicholas AP, Lubin FD, Hallett PJ, Vattem P, Ravenscroft P, Bezard E, et al. Striatal histone modifications in models of levodopa-induced dyskinesia. J. Neurochem. 2008; 106: 486–494.

Nicola SM. The nucleus accumbens as part of a basal ganglia action selection circuit. Psychopharmacology (Berl.) 2007; 191: 521–550.

Nicoletti F, Bockaert J, Collingridge GL, Conn PJ, Ferraguti F, Schoepp DD, et al. Metabotropic glutamate receptors: from the workbench to the bedside. Neuropharmacology 2011; 60: 1017–1041.

Nikolaev VO, Bünemann M, Hein L, Hannawacker A, Lohse MJ. Novel single chain cAMP sensors for receptor-induced signal propagation. J. Biol. Chem. 2004; 279: 37215–37218.

Nikolaus S, Antke C, Müller H-W. In vivo imaging of synaptic function in the central nervous system: I. Movement disorders and dementia. Behav. Brain Res. 2009; 204: 1–31.

Ni Q, Titov DV, Zhang J. Analyzing protein kinase dynamics in living cells with FRET reporters. Methods San Diego Calif 2006; 40: 279–286.

Nisenbaum ES, Berger TW. Functionally distinct subpopulations of striatal neurons are differentially regulated by GABAergic and dopaminergic inputs--I. In vivo analysis. Neuroscience 1992; 48: 561–578.

Nishi A, Kuroiwa M, Miller DB, O'Callaghan JP, Bateup HS, Shuto T, et al. Distinct roles of PDE4 and PDE10A in the regulation of cAMP/PKA signaling in the striatum. J. Neurosci. Off. J. Soc. Neurosci. 2008; 28: 10460–10471.

Nishi A, Kuroiwa M, Shuto T. Mechanisms for the modulation of dopamine d(1) receptor signaling in striatal neurons. Front. Neuroanat. 2011; 5: 43.

Nishi A, Liu F, Matsuyama S, Hamada M, Higashi H, Nairn AC, et al. Metabotropic mGlu5 receptors regulate adenosine A2A receptor signaling. Proc. Natl. Acad. Sci. U. S. A. 2003; 100: 1322–1327.

Nishi A, Snyder GL. Advanced research on dopamine signaling to develop drugs for the treatment of mental disorders: biochemical and behavioral profiles of phosphodiesterase inhibition in dopaminergic neurotransmission. J. Pharmacol. Sci. 2010; 114: 6–16.

Nishi A, Snyder GL, Greengard P. Bidirectional regulation of DARPP-32 phosphorylation by dopamine. J. Neurosci. Off. J. Soc. Neurosci. 1997; 17: 8147–8155.

Nishi A, Snyder GL, Nairn AC, Greengard P. Role of calcineurin and protein phosphatase-2A in the regulation of DARPP-32 dephosphorylation in neostriatal neurons. J. Neurochem. 1999; 72: 2015–2021.

Nishijima H, Suzuki S, Kon T, Funamizu Y, Ueno T, Haga R, et al. Morphologic changes of dendritic spines of striatal neurons in the levodopa-induced dyskinesia model. Mov. Disord. Off. J. Mov. Disord. Soc. 2014; 29: 336–343.

Niswender CM, Conn PJ. Metabotropic glutamate receptors: physiology, pharmacology, and disease. Annu. Rev. Pharmacol. Toxicol. 2010; 50: 295–322.

Nomoto M, Kaseda S, Iwata S, Shimizu T, Fukuda T, Nakagawa S. The metabolic rate and vulnerability of dopaminergic neurons, and adenosine dynamics in the cerebral cortex, nucleus accumbens, caudate nucleus, and putamen of the common marmoset. J. Neurol. 2000; 247 Suppl 5: V16–22.

Nowak L, Bregestovski P, Ascher P, Herbet A, Prochiantz A. Magnesium gates glutamate-activated channels in mouse central neurones. Nature 1984; 307: 462–465.

Nthenge-Ngumbau DN, Mohanakumar KP. Can Cyclic Nucleotide Phosphodiesterase Inhibitors Be Drugs for Parkinson's Disease? Mol. Neurobiol. 2018; 55: 822–834.

Nutt JG, Gunzler SA, Kirchhoff T, Hogarth P, Weaver JL, Krams M, et al. Effects of a NR2B selective NMDA glutamate antagonist, CP-101,606, on dyskinesia and Parkinsonism. Mov. Disord. Off. J. Mov. Disord. Soc. 2008; 23: 1860–1866.

Obeso JA, Rodriguez-Oroz MC, Rodriguez M, Macias R, Alvarez L, Guridi J, et al. Pathophysiologic basis of surgery for Parkinson's disease. Neurology 2000; 55: S7–12.

Ochi M, Koga K, Kurokawa M, Kase H, Nakamura J, Kuwana Y. Systemic administration of adenosine A(2A) receptor antagonist reverses increased GABA release in the globus pallidus of unilateral 6-hydroxydopamine-lesioned rats: a microdialysis study. Neuroscience 2000; 100: 53–62.

O'Dell TJ, Kandel ER. Low-frequency stimulation erases LTP through an NMDA receptor-mediated activation of protein phosphatases. Learn. Mem. Cold Spring Harb. N 1994; 1: 129–139.

Oh JD, Russell DS, Vaughan CL, Chase TN, Russell D. Enhanced tyrosine phosphorylation of striatal NMDA receptor subunits: effect of dopaminergic denervation and L-DOPA administration. Brain Res. 1998; 813: 150–159.

Ohkura M, Matsuzaki M, Kasai H, Imoto K, Nakai J. Genetically encoded bright Ca2+ probe applicable for dynamic Ca2+ imaging of dendritic spines. Anal. Chem. 2005; 77: 5861–5869.

Ohkura M, Sasaki T, Kobayashi C, Ikegaya Y, Nakai J. An improved genetically encoded red fluorescent Ca2+ indicator for detecting optically evoked action potentials. PloS One 2012; 7: e39933.

Oh SW, Harris JA, Ng L, Winslow B, Cain N, Mihalas S, et al. A mesoscale connectome of the mouse brain. Nature 2014; 508: 207–214.

Okada M, Mizuno K, Kaneko S. Adenosine A1 and A2 receptors modulate extracellular dopamine levels in rat striatum. Neurosci. Lett. 1996; 212: 53–56.

Onn S-P, Fienberg AA, Grace AA. Dopamine modulation of membrane excitability in striatal spiny neurons is altered in DARPP-32 knockout mice. J. Pharmacol. Exp. Ther. 2003; 306: 870–879.

Ormö M, Cubitt AB, Kallio K, Gross LA, Tsien RY, Remington SJ. Crystal structure of the Aequorea victoria green fluorescent protein. Science 1996; 273: 1392–1395.

Ouattara B, Grégoire L, Morissette M, Gasparini F, Vranesic I, Bilbe G, et al. Metabotropic glutamate receptor type 5 in levodopa-induced motor complications. Neurobiol. Aging 2011; 32: 1286–1295.

Ouattara B, Hoyer D, Grégoire L, Morissette M, Gasparini F, Gomez-Mancilla B, et al. Changes of AMPA receptors in MPTP monkeys with levodopa-induced dyskinesias. Neuroscience 2010; 167: 1160–1167.

Pack TF, Orlen MI, Ray C, Peterson SM, Caron MG. The dopamine D2 receptor can directly recruit and activate GRK2 without G protein activation. J. Biol. Chem. 2018; 293: 6161–6171.

Padovan-Neto FE, West AR. Regulation of Striatal Neuron Activity by Cyclic Nucleotide Signaling and Phosphodiesterase Inhibition: Implications for the Treatment of Parkinson's Disease. Adv. Neurobiol. 2017; 17: 257–283.

Paillé V, Picconi B, Bagetta V, Ghiglieri V, Sgobio C, Di Filippo M, et al. Distinct levels of dopamine denervation differentially alter striatal synaptic plasticity and NMDA receptor subunit composition. J. Neurosci. Off. J. Soc. Neurosci. 2010; 30: 14182–14193.

Paoletti P, Bellone C, Zhou Q. NMDA receptor subunit diversity: impact on receptor properties, synaptic plasticity and disease. Nat. Rev. Neurosci. 2013; 14: 383–400.

Parent A, Hazrati LN. Functional anatomy of the basal ganglia. I. The cortico-basal ganglia-thalamo-cortical loop. Brain Res. Brain Res. Rev. 1995; 20: 91–127.

Parent M, Parent A. Single-axon tracing study of corticostriatal projections arising from primary motor cortex in primates. J. Comp. Neurol. 2006; 496: 202–213.

Park H-Y, Kang Y-M, Kang Y, Park T-S, Ryu Y-K, Hwang J-H, et al. Inhibition of adenylyl cyclase type 5 prevents L-DOPA-induced dyskinesia in an animal model of Parkinson's disease. J. Neurosci. Off. J. Soc. Neurosci. 2014; 34: 11744–11753.

Pascoli V, Besnard A, Hervé D, Pagès C, Heck N, Girault J-A, et al. Cyclic adenosine monophosphate-independent tyrosine phosphorylation of NR2B mediates cocaine-induced extracellular signal-regulated kinase activation. Biol. Psychiatry 2011a; 69: 218–227.

Pascoli V, Turiault M, Lüscher C. Reversal of cocaine-evoked synaptic potentiation resets drug-induced adaptive behaviour. Nature 2011b; 481: 71–75.

Patterson MA, Szatmari EM, Yasuda R. AMPA receptors are exocytosed in stimulated spines and adjacent dendrites in a Ras-ERK-dependent manner during long-term potentiation. Proc. Natl. Acad. Sci. U. S. A. 2010; 107: 15951–15956.

Pavón N, Martín AB, Mendialdua A, Moratalla R. ERK phosphorylation and FosB expression are associated with L-DOPA-induced dyskinesia in hemiparkinsonian mice. Biol. Psychiatry 2006; 59: 64–74.

Pedata F, Corsi C, Melani A, Bordoni F, Latini S. Adenosine extracellular brain concentrations and role of A2A receptors in ischemia. Ann. N. Y. Acad. Sci. 2001; 939: 74–84.

Pedata F, Pazzagli M, Pepeu G. Endogenous adenosine release from hippocampal slices: excitatory amino acid agonists stimulate release, antagonists reduce the electrically-evoked release. Naunyn. Schmiedebergs Arch. Pharmacol. 1991; 344: 538–543.

Penit-Soria J, Durand C, Besson MJ, Herve D. Levels of stimulatory G protein are increased in the rat striatum after neonatal lesion of dopamine neurons. Neuroreport 1997; 8: 829–833.

Penn AC, Balik A, Wozny C, Cais O, Greger IH. Activity-mediated AMPA receptor remodeling, driven by alternative splicing in the ligand-binding domain. Neuron 2012; 76: 503–510.

Pérez-Torres S, Miró X, Palacios JM, Cortés R, Puigdoménech P, Mengod G. Phosphodiesterase type 4 isozymes expression in human brain examined by in situ hybridization histochemistry and[3H]rolipram binding autoradiography. Comparison with monkey and rat brain. J. Chem. Neuroanat. 2000; 20: 349–374.

Perkinton MS, Sihra TS, Williams RJ. Ca(2+)-permeable AMPA receptors induce phosphorylation of cAMP response element-binding protein through a phosphatidylinositol 3-kinase-dependent stimulation of the mitogen-activated protein kinase signaling cascade in neurons. J. Neurosci. Off. J. Soc. Neurosci. 1999; 19: 5861–5874.

Perreault ML, Hasbi A, Alijaniaram M, Fan T, Varghese G, Fletcher PJ, et al. The dopamine D1-D2 receptor heteromer localizes in dynorphin/enkephalin neurons: increased high affinity state following amphetamine and in schizophrenia. J. Biol. Chem. 2010; 285: 36625–36634.

Perroy J, Raynaud F, Homburger V, Rousset M-C, Telley L, Bockaert J, et al. Direct interaction enables cross-talk between ionotropic and group I metabotropic glutamate receptors. J. Biol. Chem. 2008; 283: 6799–6805.

Peterson YK, Luttrell LM. The Diverse Roles of Arrestin Scaffolds in G Protein-Coupled Receptor Signaling. Pharmacol. Rev. 2017; 69: 256–297.

Picconi B, Bagetta V, Ghiglieri V, Paillè V, Di Filippo M, Pendolino V, et al. Inhibition of phosphodiesterases rescues striatal long-term depression and reduces levodopa-induced dyskinesia. Brain J. Neurol. 2011; 134: 375–387.

Picconi B, Centonze D, Håkansson K, Bernardi G, Greengard P, Fisone G, et al. Loss of bidirectional striatal synaptic plasticity in L-DOPA-induced dyskinesia. Nat. Neurosci. 2003; 6: 501–506.

Picconi B, Centonze D, Rossi S, Bernardi G, Calabresi P. Therapeutic doses of L-dopa reverse hypersensitivity of corticostriatal D2-dopamine receptors and glutamatergic overactivity in experimental parkinsonism. Brain J. Neurol. 2004a; 127: 1661–1669.

Picconi B, Gardoni F, Centonze D, Mauceri D, Cenci MA, Bernardi G, et al. Abnormal Ca2+-calmodulin-dependent protein kinase II function mediates synaptic and motor deficits in experimental parkinsonism. J. Neurosci. Off. J. Soc. Neurosci. 2004b; 24: 5283–5291.

Picconi B, Paillé V, Ghiglieri V, Bagetta V, Barone I, Lindgren HS, et al. l-DOPA dosage is critically involved in dyskinesia via loss of synaptic depotentiation. Neurobiol. Dis. 2008; 29: 327–335.

Picconi B, Piccoli G, Calabresi P. Synaptic dysfunction in Parkinson's disease. Adv. Exp. Med. Biol. 2012; 970: 553–572.

Pifl C, Nanoff C, Schingnitz G, Schütz W, Hornykiewicz O. Sensitization of dopamine-stimulated adenylyl cyclase in the striatum of 1-methyl-4-phenyl-1,2,3,6-tetrahydropyridine-treated rhesus monkeys and patients with idiopathic Parkinson's disease. J. Neurochem. 1992; 58: 1997–2004.

Pinna A, Corsi C, Carta AR, Valentini V, Pedata F, Morelli M. Modification of adenosine extracellular levels and adenosine A(2A) receptor mRNA by dopamine denervation. Eur. J. Pharmacol. 2002; 446: 75–82.

Pinna A, Wardas J, Simola N, Morelli M. New therapies for the treatment of Parkinson's disease: adenosine A2A receptor antagonists. Life Sci. 2005; 77: 3259–3267.

Pittaluga A. Presynaptic Release-Regulating mGlu1 Receptors in Central Nervous System. Front. Pharmacol. 2016; 7: 295.

Planert H, Szydlowski SN, Hjorth JJJ, Grillner S, Silberberg G. Dynamics of synaptic transmission between fast-spiking interneurons and striatal projection neurons of the direct and indirect pathways. J. Neurosci. Off. J. Soc. Neurosci. 2010; 30: 3499–3507.

Plata V, Duhne M, Pérez-Ortega JE, Barroso-Flores J, Galarraga E, Bargas J. Direct evaluation of L-DOPA actions on neuronal activity of Parkinsonian tissue in vitro. BioMed Res. Int. 2013; 2013: 519184.

Plenz D. When inhibition goes incognito: feedback interaction between spiny projection neurons in striatal function. Trends Neurosci. 2003; 26: 436–443.

Plotkin JL, Shen W, Rafalovich I, Sebel LE, Day M, Chan CS, et al. Regulation of dendritic calcium release in striatal spiny projection neurons. J. Neurophysiol. 2013; 110: 2325–2336.

Polito M, Guiot E, Gangarossa G, Longueville S, Doulazmi M, Valjent E, et al. Selective Effects of PDE10A Inhibitors on Striatopallidal Neurons Require Phosphatase Inhibition by DARPP-32. eNeuro 2015; 2

Polli JW, Kincaid RL. Expression of a calmodulin-dependent phosphodiesterase isoform (PDE1B1) correlates with brain regions having extensive dopaminergic innervation. J. Neurosci. Off. J. Soc. Neurosci. 1994; 14: 1251–1261.

Ponsioen B, Zhao J, Riedl J, Zwartkruis F, van der Krogt G, Zaccolo M, et al. Detecting cAMP-induced Epac activation by fluorescence resonance energy transfer: Epac as a novel cAMP indicator. EMBO Rep. 2004; 5: 1176–1180.

Popoli P, Pèzzola A, Torvinen M, Reggio R, Pintor A, Scarchilli L, et al. The selective mGlu(5) receptor agonist CHPG inhibits quinpirole-induced turning in 6-hydroxydopamine-lesioned rats and modulates the binding characteristics of dopamine D(2) receptors in the rat striatum: interactions with adenosine A(2a) receptors. Neuropsychopharmacol. Off. Publ. Am. Coll. Neuropsychopharmacol. 2001; 25: 505–513.

Pozzi L, Håkansson K, Usiello A, Borgkvist A, Lindskog M, Greengard P, et al. Opposite regulation by typical and atypical anti-psychotics of ERK1/2, CREB and Elk-1 phosphorylation in mouse dorsal striatum. J. Neurochem. 2003; 86: 451–459.

Prasher DC, Eckenrode VK, Ward WW, Prendergast FG, Cormier MJ. Primary structure of the Aequorea victoria green-fluorescent protein. Gene 1992; 111: 229–233.

Prensa L, Parent A. The nigrostriatal pathway in the rat: A single-axon study of the relationship between dorsal and ventral tier nigral neurons and the striosome/matrix striatal compartments. J. Neurosci. Off. J. Soc. Neurosci. 2001; 21: 7247–7260.

Preston Z, Lee K, Widdowson L, Freeman TC, Dixon AK, Richardson PJ. Adenosine receptor expression and function in rat striatal cholinergic interneurons. Br. J. Pharmacol. 2000; 130: 886–890.

Price KS, Farley IJ, Hornykiewicz O. Neurochemistry of Parkinson's disease: relation between striatal and limbic dopamine. Adv. Biochem. Psychopharmacol. 1978; 19: 293–300.

Pulido R, Zúñiga A, Ullrich A. PTP-SL and STEP protein tyrosine phosphatases regulate the activation of the extracellular signal-regulated kinases ERK1 and ERK2 by association through a kinase interaction motif. EMBO J. 1998; 17: 7337–7350.

Qian Y, Rancic V, Wu J, Ballanyi K, Campbell RE. A Bioluminescent Ca2+ Indicator Based on a Topological Variant of GCaMP6s. Chembiochem Eur. J. Chem. Biol. 2018

Quintana A, Melon C, Kerkerian-Le Goff L, Salin P, Savasta M, Sgambato-Faure V. Forelimb dyskinesia mediated by high-frequency stimulation of the subthalamic nucleus is linked to rapid activation of the NR2B subunit of N-methyl-D-aspartate receptors. Eur. J. Neurosci. 2010; 32: 423–434.

Quiroz C, Gomes C, Pak AC, Ribeiro JA, Goldberg SR, Hope BT, et al. Blockade of adenosine A2A receptors prevents protein phosphorylation in the striatum induced by cortical stimulation. J. Neurosci. Off. J. Soc. Neurosci. 2006; 26: 10808–10812.

Quiroz C, Luján R, Uchigashima M, Simoes AP, Lerner TN, Borycz J, et al. Key modulatory role of presynaptic adenosine A2A receptors in cortical neurotransmission to the striatal direct pathway. ScientificWorldJournal 2009; 9: 1321–1344.

Ragsdale CW, Graybiel AM. The fronto-striatal projection in the cat and monkey and its relationship to inhomogeneities established by acetylcholinesterase histochemistry. Brain Res. 1981; 208: 259–266.

Raju DV, Ahern TH, Shah DJ, Wright TM, Standaert DG, Hall RA, et al. Differential synaptic plasticity of the corticostriatal and thalamostriatal systems in an MPTP-treated monkey model of parkinsonism. Eur. J. Neurosci. 2008; 27: 1647–1658.

Raju DV, Shah DJ, Wright TM, Hall RA, Smith Y. Differential synaptology of vGluT2-containing thalamostriatal afferents between the patch and matrix compartments in rats. J. Comp. Neurol. 2006; 499: 231–243.

Ramirez AD, Smith SM. Regulation of dopamine signaling in the striatum by phosphodiesterase inhibitors: novel therapeutics to treat neurological and psychiatric disorders. Cent. Nerv. Syst. Agents Med. Chem. 2014; 14: 72–82.

Ramlackhansingh AF, Bose SK, Ahmed I, Turkheimer FE, Pavese N, Brooks DJ. Adenosine 2A receptor availability in dyskinetic and nondyskinetic patients with Parkinson disease. Neurology 2011; 76: 1811–1816.

Rangel-Barajas C, Silva I, Lopéz-Santiago LM, Aceves J, Erlij D, Florán B. L-DOPA-induced dyskinesia in hemiparkinsonian rats is associated with up-regulation of adenylyl cyclase type V/VI and increased GABA release in the substantia nigra reticulata. Neurobiol. Dis. 2011; 41: 51–61.

Rascol O, Brooks DJ, Korczyn AD, De Deyn PP, Clarke CE, Lang AE. A five-year study of the incidence of dyskinesia in patients with early Parkinson's disease who were treated with ropinirole or levodopa. N. Engl. J. Med. 2000; 342: 1484–1491.

Rascol O, Fox S, Gasparini F, Kenney C, Di Paolo T, Gomez-Mancilla B. Use of metabotropic glutamate 5-receptor antagonists for treatment of levodopa-induced dyskinesias. Parkinsonism Relat. Disord. 2014; 20: 947–956.

Rascol O, Lozano A, Stern M, Poewe W. Milestones in Parkinson's disease therapeutics. Mov. Disord. Off. J. Mov. Disord. Soc. 2011; 26: 1072–1082.

Rashid AJ, So CH, Kong MMC, Furtak T, El-Ghundi M, Cheng R, et al. D1-D2 dopamine receptor heterooligomers with unique pharmacology are coupled to rapid activation of Gq/11 in the striatum. Proc. Natl. Acad. Sci. U. S. A. 2007; 104: 654–659.

Raz A, Vaadia E, Bergman H. Firing patterns and correlations of spontaneous discharge of pallidal neurons in the normal and the tremulous 1-methyl-4-phenyl-1,2,3,6-tetrahydropyridine vervet model of parkinsonism. J. Neurosci. Off. J. Soc. Neurosci. 2000; 20: 8559–8571.

Rebola N, Canas PM, Oliveira CR, Cunha RA. Different synaptic and subsynaptic localization of adenosine A2A receptors in the hippocampus and striatum of the rat. Neuroscience 2005; 132: 893–903.

Redgrave P, Prescott TJ, Gurney K. The basal ganglia: a vertebrate solution to the selection problem? Neuroscience 1999; 89: 1009–1023.

Redgrave P, Rodriguez M, Smith Y, Rodriguez-Oroz MC, Lehericy S, Bergman H, et al. Goal-directed and habitual control in the basal ganglia: implications for Parkinson's disease. Nat. Rev. Neurosci. 2010; 11: 760–772.

Reed TM, Repaske DR, Snyder GL, Greengard P, Vorhees CV. Phosphodiesterase 1B knock-out mice exhibit exaggerated locomotor hyperactivity and DARPP-32 phosphorylation in response to dopamine agonists and display impaired spatial learning. J. Neurosci. Off. J. Soc. Neurosci. 2002; 22: 5188–5197.

Reiner A, Jiao Y, Del Mar N, Laverghetta AV, Lei WL. Differential morphology of pyramidal tract-type and intratelencephalically projecting-type corticostriatal neurons and their intrastriatal terminals in rats. J. Comp. Neurol. 2003; 457: 420–440.

Révy D, Jaouen F, Salin P, Melon C, Chabbert D, Tafi E, et al. Cellular and behavioral outcomes of dorsal striatonigral neuron ablation: new insights into striatal functions. Neuropsychopharmacol. Off. Publ. Am. Coll. Neuropsychopharmacol. 2014; 39: 2662–2672.

Reyes-Irisarri E, Pérez-Torres S, Mengod G. Neuronal expression of cAMP-specific phosphodiesterase 7B mRNA in the rat brain. Neuroscience 2005; 132: 1173–1185.

Ribeiro JA, Sebastião AM, de Mendonça A. Adenosine receptors in the nervous system: pathophysiological implications. Prog. Neurobiol. 2002; 68: 377–392.

Richfield EK, Penney JB, Young AB. Anatomical and affinity state comparisons between dopamine D1 and D2 receptors in the rat central nervous system. Neuroscience 1989; 30: 767–777.

Ridgway EB, Ashley CC. Calcium transients in single muscle fibers. Biochem. Biophys. Res. Commun. 1967; 29: 229–234.

Rivera A, Alberti I, Martín AB, Narváez JA, de la Calle A, Moratalla R. Molecular phenotype of rat striatal neurons expressing the dopamine D5 receptor subtype. Eur. J. Neurosci. 2002; 16: 2049–2058.

Robertson GS, Jian M. D1 and D2 dopamine receptors differentially increase Fos-like immunoreactivity in accumbal projections to the ventral pallidum and midbrain. Neuroscience 1995; 64: 1019–1034.

Robertson GS, Vincent SR, Fibiger HC. Striatonigral projection neurons contain D1 dopamine receptor-activated c-fos. Brain Res. 1990; 523: 288–290.

Roche KW, O'Brien RJ, Mammen AL, Bernhardt J, Huganir RL. Characterization of multiple phosphorylation sites on the AMPA receptor GluR1 subunit. Neuron 1996; 16: 1179–1188.

Rodrigues RJ, Alfaro TM, Rebola N, Oliveira CR, Cunha RA. Co-localization and functional interaction between adenosine A(2A) and metabotropic group 5 receptors in glutamatergic nerve terminals of the rat striatum. J. Neurochem. 2005; 92: 433–441.

Roe MW, Lemasters JJ, Herman B. Assessment of Fura-2 for measurements of cytosolic free calcium. Cell Calcium 1990; 11: 63–73.

Romoser VA, Hinkle PM, Persechini A. Detection in living cells of Ca2+-dependent changes in the fluorescence emission of an indicator composed of two green fluorescent protein variants linked by a calmodulin-binding sequence. A new class of fluorescent indicators. J. Biol. Chem. 1997; 272: 13270–13274.

Rose S, Ramsay Croft N, Jenner P. The novel adenosine A2a antagonist ST1535 potentiates the effects of a threshold dose of l-dopa in unilaterally 6-OHDA-lesioned rats. Brain Res. 2007; 1133: 110–114.

Rosin DL, Hettinger BD, Lee A, Linden J. Anatomy of adenosine A2A receptors in brain: morphological substrates for integration of striatal function. Neurology 2003; 61: S12–18.

Rubini P, Engelhardt J, Wirkner K, Illes P. Modulation by D1 and D2 dopamine receptors of ATP-induced release of intracellular Ca2+ in cultured rat striatal neurons. Neurochem. Int. 2008; 52: 113–118.

Ruiz-DeDiego I, Naranjo JR, Hervé D, Moratalla R. Dopaminergic regulation of olfactory type G-protein α subunit expression in the striatum. Mov. Disord. Off. J. Mov. Disord. Soc. 2015; 30: 1039–1049.

Russwurm C, Koesling D, Russwurm M. Phosphodiesterase 10A Is Tethered to a Synaptic Signaling Complex in Striatum. J. Biol. Chem. 2015; 290: 11936–11947.

Rylander D, Recchia A, Mela F, Dekundy A, Danysz W, Cenci MA. Pharmacological modulation of glutamate transmission in a rat model of L-DOPA-induced dyskinesia: effects on motor behavior and striatal nuclear signaling. J. Pharmacol. Exp. Ther. 2009; 330: 227–235.

Sakmann B, Stuart G. Patch-pipette Recording from the soma, dendrites and Axon of neurons in brain slices. In: Single-Channel Recording. Bert Sakmann, Erwin Neher; 1995. p. 199–212.

Salter MW, Dong Y, Kalia LV, Liu XJ, Pitcher G. Regulation of NMDA Receptors by Kinases and Phosphatases [Internet]. In: Van Dongen AM, editor(s). Biology of the NMDA Receptor. Boca Raton (FL): CRC Press/Taylor & Francis; 2009. Available from: http://www.ncbi.nlm.nih.gov/books/NBK5288/

Samadi P, Grégoire L, Morissette M, Calon F, Hadj Tahar A, Bélanger N, et al. Basal ganglia group II metabotropic glutamate receptors specific binding in non-human primate model of L-Dopa-induced dyskinesias. Neuropharmacology 2008; 54: 258–268.

Sancesario G, Giorgi M, D'Angelo V, Modica A, Martorana A, Morello M, et al. Down-regulation of nitrergic transmission in the rat striatum after chronic nigrostriatal deafferentation. Eur. J. Neurosci. 2004; 20: 989–1000.

Sancesario G, Morrone LA, D'Angelo V, Castelli V, Ferrazzoli D, Sica F, et al. Levodopa-induced dyskinesias are associated with transient down-regulation of cAMP and cGMP in the caudate-putamen of hemiparkinsonian rats: reduced synthesis or increased catabolism? Neurochem. Int. 2014; 79: 44–56.

Santini E, Alcacer C, Cacciatore S, Heiman M, Hervé D, Greengard P, et al. L-DOPA activates ERK signaling and phosphorylates histone H3 in the striatonigral medium spiny neurons of hemiparkinsonian mice. J. Neurochem. 2009; 108: 621–633.

Santini E, Sgambato-Faure V, Li Q, Savasta M, Dovero S, Fisone G, et al. Distinct changes in cAMP and extracellular signal-regulated protein kinase signalling in L-DOPA-induced dyskinesia. PloS One 2010; 5: e12322.

Santini E, Valjent E, Usiello A, Carta M, Borgkvist A, Girault J-A, et al. Critical involvement of cAMP/DARPP-32 and extracellular signal-regulated protein kinase signaling in L-DOPA-induced dyskinesia. J. Neurosci. Off. J. Soc. Neurosci. 2007; 27: 6995–7005.

Santulli G, Marks AR. Essential Roles of Intracellular Calcium Release Channels in Muscle, Brain, Metabolism, and Aging. Curr. Mol. Pharmacol. 2015; 8: 206–222.

Sasaki T, Kotera J, Omori K. Novel alternative splice variants of rat phosphodiesterase 7B showing unique tissue-specific expression and phosphorylation. Biochem. J. 2002; 361: 211–220.

Sasaki T, Omori K. Transcriptional activation of phosphodiesterase 7B1 by dopamine D1 receptor stimulation through the cyclic AMP/cyclic AMP-dependent protein kinase/cyclic AMP-response element binding protein pathway in primary striatal neurons. J. Neurochem. 2004; 89: 474–483.

Sato M, Ozawa T, Inukai K, Asano T, Umezawa Y. Fluorescent indicators for imaging protein phosphorylation in single living cells. Nat. Biotechnol. 2002; 20: 287–294.

Savasta M, Dubois A, Benavidès J, Scatton B. Different plasticity changes in D1 and D2 receptors in rat striatal subregions following impairment of dopaminergic transmission. Neurosci. Lett. 1988; 85: 119–124.

Schiffmann SN, Desdouits F, Menu R, Greengard P, Vincent JD, Vanderhaeghen JJ, et al. Modulation of the voltage-gated sodium current in rat striatal neurons by DARPP-32, an inhibitor of protein phosphatase. Eur. J. Neurosci. 1998; 10: 1312–1320.

Schiffmann SN, Libert F, Vassart G, Vanderhaeghen JJ. Distribution of adenosine A2 receptor mRNA in the human brain. Neurosci. Lett. 1991; 130: 177–181.

Schneggenburger R, Neher E. Presynaptic calcium and control of vesicle fusion. Curr. Opin. Neurobiol. 2005; 15: 266–274.

Schrag A, Dodel R, Spottke A, Bornschein B, Siebert U, Quinn NP. Rate of clinical progression in Parkinson's disease. A prospective study. Mov. Disord. Off. J. Mov. Disord. Soc. 2007; 22: 938–945.

Schrag A, Quinn N. Dyskinesias and motor fluctuations in Parkinson's disease. A community-based study. Brain J. Neurol. 2000; 123 (Pt 11): 2297–2305.

Schultz W. Multiple dopamine functions at different time courses. Annu. Rev. Neurosci. 2007a; 30: 259–288.

Schultz W. Behavioral dopamine signals. Trends Neurosci. 2007b; 30: 203–210.

Schultz W, Ungerstedt U. Short-term increase and long-term reversion of striatal cell activity after degeneration of the nigrostriatal dopamine system. Exp. Brain Res. 1978; 33: 159–171.

Schuster S, Doudnikoff E, Rylander D, Berthet A, Aubert I, Ittrich C, et al. Antagonizing L-type Ca2+ channel reduces development of abnormal involuntary movement in the rat model of L-3,4-dihydroxyphenylalanine-induced dyskinesia. Biol. Psychiatry 2009; 65: 518–526.

Schwindinger WF, Betz KS, Giger KE, Sabol A, Bronson SK, Robishaw JD. Loss of G protein gamma 7 alters behavior and reduces striatal alpha(olf) level and cAMP production. J. Biol. Chem. 2003; 278: 6575–6579.

Scott L, Zelenin S, Malmersjö S, Kowalewski JM, Markus EZ, Nairn AC, et al. Allosteric changes of the NMDA receptor trap diffusible dopamine 1 receptors in spines. Proc. Natl. Acad. Sci. U. S. A. 2006; 103: 762–767.

Sebastianutto I, Cenci MA. mGlu receptors in the treatment of Parkinson's disease and L-DOPA-induced dyskinesia. Curr. Opin. Pharmacol. 2018; 38: 81–89.

Seeburg PH, Hartner J. Regulation of ion channel/neurotransmitter receptor function by RNA editing. Curr. Opin. Neurobiol. 2003; 13: 279–283.

Seroogy KB, Lundgren KH, Tran TM, Guthrie KM, Isackson PJ, Gall CM. Dopaminergic neurons in rat ventral midbrain express brain-derived neurotrophic factor and neurotrophin-3 mRNAs. J. Comp. Neurol. 1994; 342: 321–334.

Sesack SR, Aoki C, Pickel VM. Ultrastructural localization of D2 receptor-like immunoreactivity in midbrain dopamine neurons and their striatal targets. J. Neurosci. Off. J. Soc. Neurosci. 1994; 14: 88–106.

Sgambato-Faure V, Cenci MA. Glutamatergic mechanisms in the dyskinesias induced by pharmacological dopamine replacement and deep brain stimulation for the treatment of Parkinson's disease. Prog. Neurobiol. 2012; 96: 69–86.

Sgambato V, Pagès C, Rogard M, Besson MJ, Caboche J. Extracellular signal-regulated kinase (ERK) controls immediate early gene induction on corticostriatal stimulation. J. Neurosci. Off. J. Soc. Neurosci. 1998; 18: 8814–8825.

Sharma S, Kumar K, Deshmukh R, Sharma PL. Phosphodiesterases: Regulators of cyclic nucleotide signals and novel molecular target for movement disorders. Eur. J. Pharmacol. 2013; 714: 486–497.

Sheintuch L, Rubin A, Brande-Eilat N, Geva N, Sadeh N, Pinchasof O, et al. Tracking the Same Neurons across Multiple Days in Ca2+ Imaging Data. Cell Rep. 2017; 21: 1102–1115.

Shen H-Y, Canas PM, Garcia-Sanz P, Lan J-Q, Boison D, Moratalla R, et al. Adenosine A_2A receptors in striatal glutamatergic terminals and GABAergic neurons oppositely modulate psychostimulant action and DARPP-32 phosphorylation. PloS One 2013; 8: e80902.

Shen W, Flajolet M, Greengard P, Surmeier DJ. Dichotomous dopaminergic control of striatal synaptic plasticity. Science 2008; 321: 848–851.

Shen W, Tian X, Day M, Ulrich S, Tkatch T, Nathanson NM, et al. Cholinergic modulation of Kir2 channels selectively elevates dendritic excitability in striatopallidal neurons. Nat. Neurosci. 2007; 10: 1458–1466.

Shepherd GMG. Corticostriatal connectivity and its role in disease. Nat. Rev. Neurosci. 2013; 14: 278–291.

Shepherd JD, Huganir RL. The cell biology of synaptic plasticity: AMPA receptor trafficking. Annu. Rev. Cell Dev. Biol. 2007; 23: 613–643.

Shimomura O. Discovery of green fluorescent protein (GFP) (Nobel Lecture). Angew. Chem. Int. Ed Engl. 2009; 48: 5590–5602.

Shimomura O, Johnson FH, Saiga Y. Extraction, purification and properties of aequorin, a bioluminescent protein from the luminous hydromedusan, Aequorea. J. Cell. Comp. Physiol. 1962; 59: 223–239.

Shindou T, Richardson PJ, Mori A, Kase H, Ichimura M. Adenosine modulates the striatal GABAergic inputs to the globus pallidus via adenosine A2A receptors in rats. Neurosci. Lett. 2003; 352: 167–170.

Shuen JA, Chen M, Gloss B, Calakos N. Drd1a-tdTomato BAC transgenic mice for simultaneous visualization of medium spiny neurons in the direct and indirect pathways of the basal ganglia. J. Neurosci. Off. J. Soc. Neurosci. 2008; 28: 2681–2685.

Sibley DR, Monsma FJ. Molecular biology of dopamine receptors. Trends Pharmacol. Sci. 1992; 13: 61–69.

Silverdale MA, Kobylecki C, Hallett PJ, Li Q, Dunah AW, Ravenscroft P, et al. Synaptic recruitment of AMPA glutamate receptor subunits in levodopa-induced dyskinesia in the MPTP-lesioned nonhuman primate. Synap. N. Y. N 2010; 64: 177–180.

Singh A, Jenkins MA, Burke KJ, Beck G, Jenkins A, Scimemi A, et al. Glutamatergic Tuning of Hyperactive Striatal Projection Neurons Controls the Motor Response to Dopamine Replacement in Parkinsonian Primates. Cell Rep. 2018; 22: 941–952.

Singh A, Mewes K, Gross RE, DeLong MR, Obeso JA, Papa SM. Human striatal recordings reveal abnormal discharge of projection neurons in Parkinson's disease. Proc. Natl. Acad. Sci. U. S. A. 2016; 113: 9629–9634.

Siuciak JA, McCarthy SA, Chapin DS, Fujiwara RA, James LC, Williams RD, et al. Genetic deletion of the striatum-enriched phosphodiesterase PDE10A: evidence for altered striatal function. Neuropharmacology 2006; 51: 374–385.

Skeberdis VA, Chevaleyre V, Lau CG, Goldberg JH, Pettit DL, Suadicani SO, et al. Protein kinase A regulates calcium permeability of NMDA receptors. Nat. Neurosci. 2006; 9: 501–510.

Smeal RM, Gaspar RC, Keefe KA, Wilcox KS. A rat brain slice preparation for characterizing both thalamostriatal and corticostriatal afferents. J. Neurosci. Methods 2007; 159: 224–235.

Smith AD, Bolam JP. The neural network of the basal ganglia as revealed by the study of synaptic connections of identified neurones. Trends Neurosci. 1990; 13: 259–265.

Smith Y, Bennett BD, Bolam JP, Parent A, Sadikot AF. Synaptic relationships between dopaminergic afferents and cortical or thalamic input in the sensorimotor territory of the striatum in monkey. J. Comp. Neurol. 1994; 344: 1–19.

Smith Y, Raju DV, Pare J-F, Sidibe M. The thalamostriatal system: a highly specific network of the basal ganglia circuitry. Trends Neurosci. 2004; 27: 520–527.

Smith Y, Surmeier DJ, Redgrave P, Kimura M. Thalamic contributions to Basal Ganglia-related behavioral switching and reinforcement. J. Neurosci. Off. J. Soc. Neurosci. 2011; 31: 16102–16106.

Smith Y, Villalba RM, Raju DV. Striatal spine plasticity in Parkinson's disease: pathological or not? Parkinsonism Relat. Disord. 2009; 15 Suppl 3: S156–161.

Snyder GL, Allen PB, Fienberg AA, Valle CG, Huganir RL, Nairn AC, et al. Regulation of phosphorylation of the GluR1 AMPA receptor in the neostriatum by dopamine and psychostimulants in vivo. J. Neurosci. Off. J. Soc. Neurosci. 2000; 20: 4480–4488.

Snyder GL, Fienberg AA, Huganir RL, Greengard P. A dopamine/D1 receptor/protein kinase A/dopamine- and cAMP-regulated phosphoprotein (Mr 32 kDa)/protein phosphatase-1 pathway regulates dephosphorylation of the NMDA receptor. J. Neurosci. Off. J. Soc. Neurosci. 1998; 18: 10297–10303.

Soderling TR. The Ca-calmodulin-dependent protein kinase cascade. Trends Biochem. Sci. 1999; 24: 232–236.

Soloaga A, Thomson S, Wiggin GR, Rampersaud N, Dyson MH, Hazzalin CA, et al. MSK2 and MSK1 mediate the mitogen- and stress-induced phosphorylation of histone H3 and HMG-14. EMBO J. 2003; 22: 2788–2797.

Song RS, Massenburg B, Wenderski W, Jayaraman V, Thompson L, Neves SR. ERK regulation of phosphodiesterase 4 enhances dopamine-stimulated AMPA receptor membrane insertion. Proc. Natl. Acad. Sci. U. S. A. 2013; 110: 15437–15442.

Song WJ, Tkatch T, Surmeier DJ. Adenosine receptor expression and modulation of Ca(2+) channels in rat striatal cholinergic interneurons. J. Neurophysiol. 2000; 83: 322–332.

Stathopulos PB, Ikura M. Structural aspects of calcium-release activated calcium channel function. Channels Austin Tex 2013; 7: 344–353.

Steiner H, Gerfen CR. Dynorphin regulates D1 dopamine receptor-mediated responses in the striatum: relative contributions of pre- and postsynaptic mechanisms in dorsal and ventral striatum demonstrated by altered immediate-early gene induction. J. Comp. Neurol. 1996; 376: 530–541.

Stephens B, Mueller AJ, Shering AF, Hood SH, Taggart P, Arbuthnott GW, et al. Evidence of a breakdown of corticostriatal connections in Parkinson's disease. Neuroscience 2005; 132: 741–754.

Stern EA, Kincaid AE, Wilson CJ. Spontaneous subthreshold membrane potential fluctuations and action potential variability of rat corticostriatal and striatal neurons in vivo. J. Neurophysiol. 1997; 77: 1697–1715.

Stigler J, Rief M. Calcium-dependent folding of single calmodulin molecules. Proc. Natl. Acad. Sci. U. S. A. 2012; 109: 17814–17819.

Stroebel D, Casado M, Paoletti P. Triheteromeric NMDA receptors: from structure to synaptic physiology. Curr. Opin. Physiol. 2018; 2: 1–12.

Suárez LM, Solís O, Caramés JM, Taravini IR, Solís JM, Murer MG, et al. L-DOPA treatment selectively restores spine density in dopamine receptor D2-expressing projection neurons in dyskinetic mice. Biol. Psychiatry 2014; 75: 711–722.

Sudhof TC. The synaptic vesicle cycle. Annu. Rev. Neurosci. 2004; 27: 509–547.

Surmeier DJ, Bargas J, Hemmings HC, Nairn AC, Greengard P. Modulation of calcium currents by a D1 dopaminergic protein kinase/phosphatase cascade in rat neostriatal neurons. Neuron 1995; 14: 385–397.

Surmeier DJ, Ding J, Day M, Wang Z, Shen W. D1 and D2 dopamine-receptor modulation of striatal glutamatergic signaling in striatal medium spiny neurons. Trends Neurosci. 2007; 30: 228–235.

Surmeier DJ, Shen W, Day M, Gertler T, Chan S, Tian X, et al. The role of dopamine in modulating the structure and function of striatal circuits. Prog. Brain Res. 2010; 183: 149–167.

Svenningsson P, Le Moine C, Aubert I, Burbaud P, Fredholm BB, Bloch B. Cellular distribution of adenosine A2A receptor mRNA in the primate striatum. J. Comp. Neurol. 1998; 399: 229–240.

Svenningsson P, Le Moine C, Fisone G, Fredholm BB. Distribution, biochemistry and function of striatal adenosine A2A receptors. Prog. Neurobiol. 1999; 59: 355–396.

Svenningsson P, Le Moine C, Kull B, Sunahara R, Bloch B, Fredholm BB. Cellular expression of adenosine A2A receptor messenger RNA in the rat central nervous system with special reference to dopamine innervated areas. Neuroscience 1997; 80: 1171–1185.

Sweatt JD. Mitogen-activated protein kinases in synaptic plasticity and memory. Curr. Opin. Neurobiol. 2004; 14: 311–317.

Swulius MT, Waxham MN. Ca(2+)/calmodulin-dependent protein kinases. Cell. Mol. Life Sci. CMLS 2008; 65: 2637–2657.

Taha SA, Nicola SM, Fields HL. Cue-evoked encoding of movement planning and execution in the rat nucleus accumbens. J. Physiol. 2007; 584: 801–818.

Takao K, Okamoto K-I, Nakagawa T, Neve RL, Nagai T, Miyawaki A, et al. Visualization of synaptic Ca2+ /calmodulin-dependent protein kinase II activity in living neurons. J. Neurosci. Off. J. Soc. Neurosci. 2005; 25: 3107–3112.

Tallaksen-Greene SJ, Albin RL. Localization of AMPA-selective excitatory amino acid receptor subunits in identified populations of striatal neurons. Neuroscience 1994; 61: 509–519.

Tallini YN, Ohkura M, Choi B-R, Ji G, Imoto K, Doran R, et al. Imaging cellular signals in the heart in vivo: Cardiac expression of the high-signal Ca2+ indicator GCaMP2. Proc. Natl. Acad. Sci. U. S. A. 2006; 103: 4753–4758.

Tang K, Low MJ, Grandy DK, Lovinger DM. Dopamine-dependent synaptic plasticity in striatum during in vivo development. Proc. Natl. Acad. Sci. U. S. A. 2001; 98: 1255–1260.

Tang S, Yasuda R. Imaging ERK and PKA Activation in Single Dendritic Spines during Structural Plasticity. Neuron 2017; 93: 1315–1324.e3.

Tanimura A, Nezu A, Morita T, Turner RJ, Tojyo Y. Fluorescent biosensor for quantitative real-time measurements of inositol 1,4,5-trisphosphate in single living cells. J. Biol. Chem. 2004; 279: 38095–38098.

Tarazi FI, Baldessarini RJ. Regional localization of dopamine and ionotropic glutamate receptor subtypes in striatolimbic brain regions. J. Neurosci. Res. 1999; 55: 401–410.

Tarazi FI, Campbell A, Yeghiayan SK, Baldessarini RJ. Localization of ionotropic glutamate receptors in caudate-putamen and nucleus accumbens septi of rat brain: comparison of NMDA, AMPA, and kainate receptors. Synap. N. Y. N 1998; 30: 227–235.

Taura J, Valle-León M, Sahlholm K, Watanabe M, Van Craenenbroeck K, Fernández-Dueñas V, et al. Behavioral control by striatal adenosine A2A -dopamine D2 receptor heteromers. Genes Brain Behav. 2018; 17: e12432.

Taussig R, Tang WJ, Hepler JR, Gilman AG. Distinct patterns of bidirectional regulation of mammalian adenylyl cyclases. J. Biol. Chem. 1994; 269: 6093–6100.

Taverna S, Canciani B, Pennartz CMA. Dopamine D1-receptors modulate lateral inhibition between principal cells of the nucleus accumbens. J. Neurophysiol. 2005; 93: 1816–1819.

Taverna S, van Dongen YC, Groenewegen HJ, Pennartz CMA. Direct physiological evidence for synaptic connectivity between medium-sized spiny neurons in rat nucleus accumbens in situ. J. Neurophysiol. 2004; 91: 1111–1121.

Taverna S, Ilijic E, Surmeier DJ. Recurrent collateral connections of striatal medium spiny neurons are disrupted in models of Parkinson's disease. J. Neurosci. Off. J. Soc. Neurosci. 2008; 28: 5504–5512.

Tecuapetla F, Carrillo-Reid L, Guzmán JN, Galarraga E, Bargas J. Different inhibitory inputs onto neostriatal projection neurons as revealed by field stimulation. J. Neurophysiol. 2005; 93: 1119–1126.

Tepper JM, Bolam JP. Functional diversity and specificity of neostriatal interneurons. Curr. Opin. Neurobiol. 2004; 14: 685–692.

Tepper JM, Koós T, Wilson CJ. GABAergic microcircuits in the neostriatum. Trends Neurosci. 2004; 27: 662–669.

Tepper JM, Tecuapetla F, Koós T, Ibáñez-Sandoval O. Heterogeneity and diversity of striatal GABAergic interneurons. Front. Neuroanat. 2010; 4: 150.

Tepper JM, Wilson CJ, Koós T. Feedforward and feedback inhibition in neostriatal GABAergic spiny neurons. Brain Res. Rev. 2008; 58: 272–281.

Thestrup T, Litzlbauer J, Bartholomäus I, Mues M, Russo L, Dana H, et al. Optimized ratiometric calcium sensors for functional in vivo imaging of neurons and T lymphocytes. Nat. Methods 2014; 11: 175–182.

Thiele SL, Chen B, Lo C, Gertler TS, Warre R, Surmeier JD, et al. Selective loss of bi-directional synaptic plasticity in the direct and indirect striatal output pathways accompanies generation of parkinsonism and l-DOPA induced dyskinesia in mouse models. Neurobiol. Dis. 2014; 71: 334–344.

Thomas GM, Huganir RL. MAPK cascade signalling and synaptic plasticity. Nat. Rev. Neurosci. 2004; 5: 173–183.

Thorn CA, Atallah H, Howe M, Graybiel AM. Differential dynamics of activity changes in dorsolateral and dorsomedial striatal loops during learning. Neuron 2010; 66: 781–795.

Tian L, Hires SA, Mao T, Huber D, Chiappe ME, Chalasani SH, et al. Imaging neural activity in worms, flies and mice with improved GCaMP calcium indicators. Nat. Methods 2009; 6: 875–881.

Tiberi M, Jarvie KR, Silvia C, Falardeau P, Gingrich JA, Godinot N, et al. Cloning, molecular characterization, and chromosomal assignment of a gene encoding a second D1 dopamine receptor subtype: differential expression pattern in rat brain compared with the D1A receptor. Proc. Natl. Acad. Sci. U. S. A. 1991; 88: 7491–7495.

Ting AY, Kain KH, Klemke RL, Tsien RY. Genetically encoded fluorescent reporters of protein tyrosine kinase activities in living cells. Proc. Natl. Acad. Sci. U. S. A. 2001; 98: 15003–15008.

Tomida T, Oda S, Takekawa M, Iino Y, Saito H. The temporal pattern of stimulation determines the extent and duration of MAPK activation in a Caenorhabditis elegans sensory neuron. Sci. Signal. 2012; 5: ra76.

Tomiyama M, Kimura T, Maeda T, Tanaka H, Kannari K, Baba M. Upregulation of striatal adenosine A2A receptor mRNA in 6-hydroxydopamine-lesioned rats intermittently treated with L-DOPA. Synap. N. Y. N 2004; 52: 218–222.

Tong H, Gibb AJ. Dopamine D1 receptor inhibition of NMDA receptor currents mediated by tyrosine kinase-dependent receptor trafficking in neonatal rat striatum. J. Physiol. 2008; 586: 4693–4707.

Tong J, Fitzmaurice PS, Ang LC, Furukawa Y, Guttman M, Kish SJ. Brain dopamine-stimulated adenylyl cyclase activity in Parkinson's disease, multiple system atrophy, and progressive supranuclear palsy. Ann. Neurol. 2004; 55: 125–129.

Torvinen M, Kozell LB, Neve KA, Agnati LF, Fuxe K. Biochemical identification of the dopamine D2 receptor domains interacting with the adenosine A2A receptor. J. Mol. Neurosci. MN 2004; 24: 173–180.

Torvinen M, Marcellino D, Canals M, Agnati LF, Lluis C, Franco R, et al. Adenosine A2A receptor and dopamine D3 receptor interactions: evidence of functional A2A/D3 heteromeric complexes. Mol. Pharmacol. 2005; 67: 400–407.

Traynelis SF, Wollmuth LP, McBain CJ, Menniti FS, Vance KM, Ogden KK, et al. Glutamate receptor ion channels: structure, regulation, and function. Pharmacol. Rev. 2010; 62: 405–496.

Tremblay M, Salin P, Soghomonian JJ. Effect of 6-OHDA lesions on striatal mRNA levels encoding for glutamate receptor subunits. Neuroreport 1995; 6: 2225–2229.

Tricoire L, Lambolez B. Neuronal network imaging in acute slices using Ca2+ sensitive bioluminescent reporter. Methods Mol. Biol. Clifton NJ 2014; 1098: 33–45.

Trifilieff P, Lavaur J, Pascoli V, Kappès V, Brami-Cherrier K, Pagès C, et al. Endocytosis controls glutamate-induced nuclear accumulation of ERK. Mol. Cell. Neurosci. 2009; 41: 325–336.

Trifilieff P, Rives M-L, Urizar E, Piskorowski RA, Vishwasrao HD, Castrillon J, et al. Detection of antigen interactions ex vivo by proximity ligation assay: endogenous dopamine D2-adenosine A2A receptor complexes in the striatum. BioTechniques 2011; 51: 111–118.

Tritsch NX, Sabatini BL. Dopaminergic modulation of synaptic transmission in cortex and striatum. Neuron 2012; 76: 33–50.

Tseng KY, Kasanetz F, Kargieman L, Riquelme LA, Murer MG. Cortical slow oscillatory activity is reflected in the membrane potential and spike trains of striatal neurons in rats with chronic nigrostriatal lesions. J. Neurosci. Off. J. Soc. Neurosci. 2001; 21: 6430–6439.

Tsien RY. The green fluorescent protein. Annu. Rev. Biochem. 1998; 67: 509–544.

Tunstall MJ, Oorschot DE, Kean A, Wickens JR. Inhibitory interactions between spiny projection neurons in the rat striatum. J. Neurophysiol. 2002; 88: 1263–1269.

Turrigiano G. Homeostatic synaptic plasticity: local and global mechanisms for stabilizing neuronal function. Cold Spring Harb. Perspect. Biol. 2012; 4: a005736.

Turrigiano GG. Homeostatic plasticity in neuronal networks: the more things change, the more they stay the same. Trends Neurosci. 1999; 22: 221–227.

Uchida S, Soshiroda K, Okita E, Kawai-Uchida M, Mori A, Jenner P, et al. The adenosine A2A receptor antagonist, istradefylline enhances the anti-parkinsonian activity of low doses of dopamine agonists in MPTP-treated common marmosets. Eur. J. Pharmacol. 2015; 747: 160–165.

Umezawa Y. Genetically encoded optical probes for imaging cellular signaling pathways. Biosens. Bioelectron. 2005; 20: 2504–2511.

Valjent E, Bertran-Gonzalez J, Hervé D, Fisone G, Girault J-A. Looking BAC at striatal signaling: cell-specific analysis in new transgenic mice. Trends Neurosci. 2009; 32: 538–547.

Valjent E, Corvol JC, Pages C, Besson MJ, Maldonado R, Caboche J. Involvement of the extracellular signal-regulated kinase cascade for cocaine-rewarding properties. J. Neurosci. Off. J. Soc. Neurosci. 2000; 20: 8701–8709.

Valjent E, Pagès C, Hervé D, Girault J-A, Caboche J. Addictive and non-addictive drugs induce distinct and specific patterns of ERK activation in mouse brain. Eur. J. Neurosci. 2004; 19: 1826–1836.

Valjent E, Pascoli V, Svenningsson P, Paul S, Enslen H, Corvol J-C, et al. Regulation of a protein phosphatase cascade allows convergent dopamine and glutamate signals to activate ERK in the striatum. Proc. Natl. Acad. Sci. U. S. A. 2005; 102: 491–496.

Vandecaetsbeek I, Vangheluwe P, Raeymaekers L, Wuytack F, Vanoevelen J. The Ca2+ pumps of the endoplasmic reticulum and Golgi apparatus. Cold Spring Harb. Perspect. Biol. 2011; 3

Vanhoutte P, Barnier JV, Guibert B, Pagès C, Besson MJ, Hipskind RA, et al. Glutamate induces phosphorylation of Elk-1 and CREB, along with c-fos activation, via an extracellular signal-regulated kinase-dependent pathway in brain slices. Mol. Cell. Biol. 1999; 19: 136–146.

Van Tol HH, Wu CM, Guan HC, Ohara K, Bunzow JR, Civelli O, et al. Multiple dopamine D4 receptor variants in the human population. Nature 1992; 358: 149–152.

Vastagh C, Gardoni F, Bagetta V, Stanic J, Zianni E, Giampà C, et al. N-methyl-D-aspartate (NMDA) receptor composition modulates dendritic spine morphology in striatal medium spiny neurons. J. Biol. Chem. 2012; 287: 18103–18114.

Vergassola M, Olivero G, Cisani F, Usai C, Bossi S, Puliti A, et al. Presynaptic mGlu1 Receptors Control GABAB Receptors in an Antagonist-Like Manner in Mouse Cortical GABAergic and Glutamatergic Nerve Endings. Front. Mol. Neurosci. 2018; 11: 324.

Verhagen Metman L, Del Dotto P, Blanchet PJ, van den Munckhof P, Chase TN. Blockade of glutamatergic transmission as treatment for dyskinesias and motor fluctuations in Parkinson's disease. Amino Acids 1998a; 14: 75–82.

Verhagen Metman L, Del Dotto P, van den Munckhof P, Fang J, Mouradian MM, Chase TN. Amantadine as treatment for dyskinesias and motor fluctuations in Parkinson's disease. Neurology 1998b; 50: 1323–1326.

Vidi P-A, Chen J, Irudayaraj JMK, Watts VJ. Adenosine A(2A) receptors assemble into higher-order oligomers at the plasma membrane. FEBS Lett. 2008; 582: 3985–3990.

Villalba RM, Lee H, Smith Y. Dopaminergic denervation and spine loss in the striatum of MPTP-treated monkeys. Exp. Neurol. 2009; 215: 220–227.

Villalba RM, Smith Y. Differential structural plasticity of corticostriatal and thalamostriatal axo-spinous synapses in MPTP-treated Parkinsonian monkeys. J. Comp. Neurol. 2011; 519: 989–1005.

Vincent P, Brusciano D. Cyclic AMP imaging in neurones in brain slice preparations. J. Neurosci. Methods 2001; 108: 189–198.

Visel A, Alvarez-Bolado G, Thaller C, Eichele G. Comprehensive analysis of the expression patterns of the adenylate cyclase gene family in the developing and adult mouse brain. J. Comp. Neurol. 2006; 496: 684–697.

Volicer L, Beal MF, Direnfeld LK, Marquis JK, Albert ML. CSF cyclic nucleotides and somatostatin in Parkinson's disease. Neurology 1986; 36: 89–92.

Volkow ND, Wang G-J, Fowler JS, Tomasi D, Telang F. Addiction: beyond dopamine reward circuitry. Proc. Natl. Acad. Sci. U. S. A. 2011; 108: 15037–15042.

Volkow ND, Wise RA, Baler R. The dopamine motive system: implications for drug and food addiction. Nat. Rev. Neurosci. 2017; 18: 741–752.

Walaas SI, Aswad DW, Greengard P. A dopamine- and cyclic AMP-regulated phosphoprotein enriched in dopamine-innervated brain regions. Nature 1983; 301: 69–71.

Wall NR, De La Parra M, Callaway EM, Kreitzer AC. Differential innervation of direct- and indirect-pathway striatal projection neurons. Neuron 2013; 79: 347–360.

Wallrabe H, Periasamy A. Imaging protein molecules using FRET and FLIM microscopy. Curr. Opin. Biotechnol. 2005; 16: 19–27.

Wang H, Pickel VM. Dopamine D2 receptors are present in prefrontal cortical afferents and their targets in patches of the rat caudate-putamen nucleus. J. Comp. Neurol. 2002; 442: 392–404.

Wang Q, Jolly JP, Surmeier JD, Mullah BM, Lidow MS, Bergson CM, et al. Differential dependence of the D1 and D5 dopamine receptors on the G protein gamma 7 subunit for activation of adenylylcyclase. J. Biol. Chem. 2001; 276: 39386–39393.

Wang Q, Shui B, Kotlikoff MI, Sondermann H. Structural basis for calcium sensing by GCaMP2. Struct. Lond. Engl. 1993 2008; 16: 1817–1827.

Wang Q, Yin P, Yu B, Zhao Z, Richter-Levin G, Yu L, et al. Down-regulation of dorsal striatal αCaMKII causes striatum-related cognitive and synaptic disorders. Exp. Neurol. 2017; 298: 112–121.

Wanneveich M, Moisan F, Jacqmin-Gadda H, Elbaz A, Joly P. Projections of prevalence, lifetime risk, and life expectancy of Parkinson's disease (2010-2030) in France. Mov. Disord. Off. J. Mov. Disord. Soc. 2018

Warren EB, Sillivan SE, Konradi C. Receptors and second messengers in the basal ganglia. In: Handbook of Basal Ganglia Structure and Function, 2nd ed. (Steiner H, Tseng KY, eds). 2017. p. 555–581.

Watabe-Uchida M, Zhu L, Ogawa SK, Vamanrao A, Uchida N. Whole-brain mapping of direct inputs to midbrain dopamine neurons. Neuron 2012; 74: 858–873.

Wei W, Ding S, Zhou F-M. Dopaminergic treatment weakens medium spiny neuron collateral inhibition in the parkinsonian striatum. J. Neurophysiol. 2017; 117: 987–999.

Wen W, Lin C-Y, Niu L. R/G editing in GluA2Rflop modulates the functional difference between GluA1 flip and flop variants in GluA1/2R heteromeric channels. Sci. Rep. 2017; 7: 13654.

Westin JE, Vercammen L, Strome EM, Konradi C, Cenci MA. Spatiotemporal pattern of striatal ERK1/2 phosphorylation in a rat model of L-DOPA-induced dyskinesia and the role of dopamine D1 receptors. Biol. Psychiatry 2007; 62: 800–810.

Wickens JR, Mckenzie D, Costanzo E, Arbuthnott GW. Effects of potassium channel blockers on synaptic plasticity in the corticostriatal pathway. Neuropharmacology 1998; 37: 523–533.

Wilson CJ. Morphology and synaptic connections of crossed corticostriatal neurons in the rat. J. Comp. Neurol. 1987; 263: 567–580.

Wilson CJ. The generation of natural firing patterns in neostriatal neurons. Prog. Brain Res. 1993; 99: 277–297.

Wilson CJ, Kawaguchi Y. The origins of two-state spontaneous membrane potential fluctuations of neostriatal spiny neurons. J. Neurosci. Off. J. Soc. Neurosci. 1996; 16: 2397–2410.

Wilson JM, Ogden AML, Loomis S, Gilmour G, Baucum AJ, Belecky-Adams TL, et al. Phosphodiesterase 10A inhibitor, MP-10 (PF-2545920), produces greater induction of c-Fos in dopamine D2 neurons than in D1 neurons in the neostriatum. Neuropharmacology 2015; 99: 379–386.

Wise RA. Roles for nigrostriatal--not just mesocorticolimbic--dopamine in reward and addiction. Trends Neurosci. 2009; 32: 517–524.

Won S, Incontro S, Nicoll RA, Roche KW. PSD-95 stabilizes NMDA receptors by inducing the degradation of STEP61. Proc. Natl. Acad. Sci. U. S. A. 2016; 113: E4736–4744.

Wouters FS, Bastiaens PI. Imaging protein-protein interactions by fluorescence resonance energy transfer (FRET) microscopy. Curr. Protoc. Protein Sci. 2001; Chapter 19: Unit19.5.

Wright A, Vissel B. The essential role of AMPA receptor GluR2 subunit RNA editing in the normal and diseased brain. Front. Mol. Neurosci. 2012; 5: 34.

Wu J, Prole DL, Shen Y, Lin Z, Gnanasekaran A, Liu Y, et al. Red fluorescent genetically encoded Ca2+ indicators for use in mitochondria and endoplasmic reticulum. Biochem. J. 2014; 464: 13–22.

Xiao D, Bastia E, Xu Y-H, Benn CL, Cha J-HJ, Peterson TS, et al. Forebrain adenosine A2A receptors contribute to L-3,4-dihydroxyphenylalanine-induced dyskinesia in hemiparkinsonian mice. J. Neurosci. Off. J. Soc. Neurosci. 2006; 26: 13548–13555.

Xiao D, Cassin JJ, Healy B, Burdett TC, Chen J-F, Fredholm BB, et al. Deletion of adenosine A_1 or $A(_2A)$ receptors reduces L-3,4-dihydroxyphenylalanine-induced dyskinesia in a model of Parkinson's disease. Brain Res. 2011; 1367: 310–318.

Xia Z, Storm DR. The role of calmodulin as a signal integrator for synaptic plasticity. Nat. Rev. Neurosci. 2005; 6: 267–276.

Xie Z, Adamowicz WO, Eldred WD, Jakowski AB, Kleiman RJ, Morton DG, et al. Cellular and subcellular localization of PDE10A, a striatum-enriched phosphodiesterase. Neuroscience 2006; 139: 597–607.

Yager LM, Garcia AF, Wunsch AM, Ferguson SM. The ins and outs of the striatum: role in drug addiction. Neuroscience 2015; 301: 529–541.

Yamashita N, Hayashi A, Baba J, Sawa A. Rolipram, a phosphodiesterase-4-selective inhibitor, promotes the survival of cultured rat dopaminergic neurons. Jpn. J. Pharmacol. 1997; 75: 155–159.

Yang J-N, Chen J-F, Fredholm BB. Physiological roles of A1 and A2A adenosine receptors in regulating heart rate, body temperature, and locomotion as revealed using knockout mice and caffeine. Am. J. Physiol. Heart Circ. Physiol. 2009; 296: H1141–1149.

Yang L, Calingasan NY, Lorenzo BJ, Beal MF. Attenuation of MPTP neurotoxicity by rolipram, a specific inhibitor of phosphodiesterase IV. Exp. Neurol. 2008; 211: 311–314.

Yang X, Wu N, Song L, Liu Z. Intrastriatal injections of KN-93 ameliorates levodopa-induced dyskinesia in a rat model of Parkinson's disease. Neuropsychiatr. Dis. Treat. 2013; 9: 1213–1220.

Yan Z, Hsieh-Wilson L, Feng J, Tomizawa K, Allen PB, Fienberg AA, et al. Protein phosphatase 1 modulation of neostriatal AMPA channels: regulation by DARPP-32 and spinophilin. Nat. Neurosci. 1999; 2: 13–17.

Yan Z, Surmeier DJ. D5 dopamine receptors enhance Zn2+-sensitive GABA(A) currents in striatal cholinergic interneurons through a PKA/PP1 cascade. Neuron 1997; 19: 1115–1126.

Yapo C, Nair AG, Clement L, Castro LR, Hellgren Kotaleski J, Vincent P. Detection of phasic dopamine by D1 and D2 striatal medium spiny neurons. J. Physiol. 2017; 595: 7451–7475.

Yasuda R. Imaging spatiotemporal dynamics of neuronal signaling using fluorescence resonance energy transfer and fluorescence lifetime imaging microscopy. Curr. Opin. Neurobiol. 2006; 16: 551–561.

Yetnikoff L, Lavezzi HN, Reichard RA, Zahm DS. An update on the connections of the ventral mesencephalic dopaminergic complex. Neuroscience 2014; 282: 23–48.

Yger M, Girault J-A. DARPP-32, Jack of All Trades… Master of Which? Front. Behav. Neurosci. 2011; 5: 56.

Yin HH, Knowlton BJ. The role of the basal ganglia in habit formation. Nat. Rev. Neurosci. 2006; 7: 464–476.

Yin HH, Lovinger DM. Frequency-specific and D2 receptor-mediated inhibition of glutamate release by retrograde endocannabinoid signaling. Proc. Natl. Acad. Sci. U. S. A. 2006; 103: 8251–8256.

You H, Mariani L-L, Mangone G, Le Febvre de Nailly D, Charbonnier-Beaupel F, Corvol J-C. Molecular basis of dopamine replacement therapy and its side effects in Parkinson's disease. Cell Tissue Res. 2018; 373: 111–135.

Yung KK, Bolam JP, Smith AD, Hersch SM, Ciliax BJ, Levey AI. Immunocytochemical localization of D1 and D2 dopamine receptors in the basal ganglia of the rat: light and electron microscopy. Neuroscience 1995; 65: 709–730.

Zaborszky L, Vadasz C. The midbrain dopaminergic system: anatomy and genetic variation in dopamine neuron number of inbred mouse strains. Behav. Genet. 2001; 31: 47–59.

Zaccolo M, De Giorgi F, Cho CY, Feng L, Knapp T, Negulescu PA, et al. A genetically encoded, fluorescent indicator for cyclic AMP in living cells. Nat. Cell Biol. 2000; 2: 25–29.

Zacharias DA, Violin JD, Newton AC, Tsien RY. Partitioning of lipid-modified monomeric GFPs into membrane microdomains of live cells. Science 2002; 296: 913–916.

Zaja-Milatovic S, Milatovic D, Schantz AM, Zhang J, Montine KS, Samii A, et al. Dendritic degeneration in neostriatal medium spiny neurons in Parkinson disease. Neurology 2005; 64: 545–547.

Zariwala HA, Borghuis BG, Hoogland TM, Madisen L, Tian L, De Zeeuw CI, et al. A Cre-dependent GCaMP3 reporter mouse for neuronal imaging in vivo. J. Neurosci. Off. J. Soc. Neurosci. 2012; 32: 3131–3141.

Zhai S, Ark ED, Parra-Bueno P, Yasuda R. Long-distance integration of nuclear ERK signaling triggered by activation of a few dendritic spines. Science 2013; 342: 1107–1111.

Zhang J, Campbell RE, Ting AY, Tsien RY. Creating new fluorescent probes for cell biology. Nat. Rev. Mol. Cell Biol. 2002; 3: 906–918.

Zhang J, Hupfeld CJ, Taylor SS, Olefsky JM, Tsien RY. Insulin disrupts beta-adrenergic signalling to protein kinase A in adipocytes. Nature 2005; 437: 569–573.

Zhang J, Ma Y, Taylor SS, Tsien RY. Genetically encoded reporters of protein kinase A activity reveal impact of substrate tethering. Proc. Natl. Acad. Sci. U. S. A. 2001; 98: 14997–15002.

Zhang J, Xu T-X, Hallett PJ, Watanabe M, Grant SGN, Isacson O, et al. PSD-95 uncouples dopamine-glutamate interaction in the D1/PSD-95/NMDA receptor complex. J. Neurosci. Off. J. Soc. Neurosci. 2009; 29: 2948–2960.

Zhang S, Xie C, Wang Q, Liu Z. Interactions of CaMKII with dopamine D2 receptors: roles in levodopa-induced dyskinesia in 6-hydroxydopamine lesioned Parkinson's rats. Sci. Rep. 2014; 4: 6811.

Zhang Y, Meredith GE, Mendoza-Elias N, Rademacher DJ, Tseng KY, Steece-Collier K. Aberrant restoration of spines and their synapses in L-DOPA-induced dyskinesia: involvement of corticostriatal but not thalamostriatal synapses. J. Neurosci. Off. J. Soc. Neurosci. 2013; 33: 11655–11667.

Zhao Y, Araki S, Wu J, Teramoto T, Chang Y-F, Nakano M, et al. An expanded palette of genetically encoded Ca^{2+} indicators. Science 2011; 333: 1888–1891.

Zhou X, Doorduin J, Elsinga PH, Dierckx R a. JO, de Vries EFJ, Casteels C. Altered adenosine 2A and dopamine D2 receptor availability in the 6-hydroxydopamine-treated rats with and without levodopa-induced dyskinesia. NeuroImage 2017; 157: 209–218.

Zhuang X, Belluscio L, Hen R. G(olf)alpha mediates dopamine D1 receptor signaling. J. Neurosci. Off. J. Soc. Neurosci. 2000; 20: RC91.

Zhu C, Wang G, Li J, Chen L, Wang C, Wang Y, et al. Adenosine A2A receptor antagonist istradefylline 20 versus 40 mg/day as augmentation for Parkinson's disease: a meta-analysis. Neurol. Res. 2014; 36: 1028–1034.

Zold CL, Escande MV, Pomata PE, Riquelme LA, Murer MG. Striatal NMDA receptors gate cortico-pallidal synchronization in a rat model of Parkinson's disease. Neurobiol. Dis. 2012; 47: 38–48.

Appendix

Appendix: Supplementary Methods

Animals

To tag dSPNs and iSPNs with tdTomato and EGFP respectively, drd1a-dtTomato mice [Tg(Drd1-tdTomato) (Shuen *et al.*, 2008)] were crossed with drd2-L10-EGFP mice [Tg(Drd2-EGFP/Rpl10a)CP101Htz, (Doyle *et al.*, 2008)] to obtain drd1a-tdTomato;drd2-L10-EFGP mice bearing both transgenes. Previous studies showed that tdTomato and L10-EGFP are selectively expressed in dSPN and iSPN respectively (Doyle *et al.*, 2008; Shuen *et al.*, 2008). The mice were genotyped by PCR analysis of genomic DNA using standard PCR protocols. The mice were kept in groups (maximum five per cage) on a 12 h light/dark cycle at a constant temperature of 22°C with access to food and water ad libitum.

Immunofluorescence

Immunofluorescence were performed as previously described (Alcacer *et al.*, 2012). For the experiment in drd1a-tdTomato;drd2-L10-EFGP mice, slices of 30µM were used. For phosphoERK experiments, slices of 250µM were used to be in the same experimental conditions as with the acute striatal slices used for 2-photon live imaging. The slices were incubated in chicken anti-TH (polyclonal, AVES, dilution 1:500), rabbit anti-p44/42MAPK (Erk1/2) Antibody (Cells signaling/ozyme #9102, dilution 1/200) and mouse anti GFP (polyclonal, Clontech) antibodies. Secondary antibodies (dilution 1/400) were A488 anti Mouse, A633 anti Chicken and Cy3 anti Rabbit. Sections were mounted in Vectashield (Vector Laboratories) for 30µm-thick slices and in Mowiol-Dabco for 250µm-thick slices.

Summary

Parkinson's disease (PD) is the second most common neurodegenerative disorder after Alzheimer's disease. There is currently no cure for PD. Symptomatic drug therapy essentially relies on dopamine (DA) replacement therapy. The spectacular antiparkinsonian effect of levodopa in PD is however hampered by long-term complications, motor fluctuations and dyskinesia in all patients at some time during the disease course. The mechanisms of the maladaptive striatal plasticity leading to dyskinesia are not well understood.

The aim of this project was to identify the dysregulations of signaling pathways in striatal projection neurons (SPN) in the absence of dopamine. We used a mouse model of lesion of DA neurons with 6-OHDA and virally transduced biosensors to monitor signaling pathways in live neurons with two-photon imaging of corticostriatal slices. We focused our attention on extracellular signal-regulated kinase (ERK), cAMP-dependent protein kinase (PKA) and Ca^{2+} which are known to be altered in the absence of DA.

We first set up a reliable experimental model in adult mice, successfully combining 6-OHDA and viral vector in the same unilateral stereotactic injection into the dorsal striatum. In some experiments we targeted the biosensor expression to specific neuronal populations using Cre-dependent "flexed" biosensors. We used mice expressing Cre under the control of the D1 DA receptor (D1R) promoter to target specifically striatal projection neurons of the direct pathway (dSPNs) or the adenosine $A2_A$ receptor ($A2_AR$) to target SPNs of the indirect pathway (iSPNs). We used fluorescence resonance energy transfer (FRET)-based biosensors EKAR-EV and AKAR-3 to monitor ERK and PKA activities, respectively. We also monitored cytosolic free Ca^{2+} with the genetically encoded calcium indicator GCaMP6S. We used pharmacological tools to modulate glutamate, DA, and adenosine receptors as well as phosphodiesterases (PDE) and kinases activities. We observed that the DA lesion increased ERK responsiveness to stimulation of D1R. Since ERK activation depends on both cAMP and Ca^{2+} signals, we then investigated these two pathways. We observed an increased activation of PKA in response to D1R but not $A2_AR$. We explored the mechanism of this increased sensitivity using mice deficient for Gαolf, the G protein that couples striatal receptors to adenylyl cyclase. We provided evidence that increased levels of Gαolf contributed to enhanced D1 responses after 6-OHDA lesions and identified a deficit in PDE activity in D1 neurons that was likely to amplify this effect. By monitoring Ca^{2+} signals we showed an increased spontaneous activity of D1 neurons in lesioned mice. However, unexpectedly the Ca^{2+} responses to stimulation of AMPA glutamate receptors were increased in iSPNs and not dSPNs.

In conclusion, our work using for the first time 2-photon biosensor imaging in the DA-depleted striatum of adult mice confirms and extends previous observations on signaling dysregulations in the absence of DA. It reveals distinct cell type-specific alterations of cAMP, Ca^{2+} and ERK responses in the two populations of SPNs and suggests possible mechanisms for these alterations.

Résumé

La maladie de Parkinson (MP) est la seconde maladie neurodégénérative la plus fréquente. Il n'y a pas de traitement curatif de la maladie. Les traitements symptomatiques s'appuient principalement sur le remplacement de la dopamine (DA). Le traitement par L-DOPA, particulièrement efficace initialement, se complique à long terme par des fluctuations et dyskinésies. Les mécanismes de la plasticité striatale anormale sous-tendant l'apparition de ces dyskinésies sont mal compris. Le but de ce projet était d'identifier les anomalies des voies de signalisation dans les neurones de projection du striatum en l'absence de DA.

Nous avons utilisé chez des souris avec lésion ou non des neurones DA par la 6-OHDA, des biosenseurs permettant l'étude de voies de signalisation en imagerie cellulaire multiphotonique de neurones vivants dans des tranches corticostriatales. Nous avons d'abord mis au point ce modèle combinant injection stéréotaxique de toxine et de vecteur viral chez des souris adultes. Dans certaines expériences nous avons étudié spécifiquement les réponses des neurones de projection striataux des voies directe (NPSd) ou indirecte (NPSi) en utilisant des biosenseurs activés par la recombinase Cre et des lignées transgéniques exprimant spécifiquement cette enzyme dans l'une ou l'autre population. Nous avons utilisé des biosenseurs FRET pour mesurer l'activité de la kinase dépendante de l'AMPc (PKA, sonde AKAR3) ou ERK (*extracellular signal-regulated kinase*, sonde EKAR-EV) et le senseur calcique GcAMP6S pour le Ca^{2+} libre cytosolique avec une bonne résolution spatiale et temporelle. Nous avons modulé pharmacologiquement les récepteurs de la DA, du glutamate et de l'adénosine, ainsi que les activités des kinases et phosphodiestérases. Nous avons observé que la lésion augmentait les réponses ERK à la stimulation des récepteurs D1 de la DA dans les NPSd. Nous avons montré une augmentation des réponses PKA dans ces neurones pouvant être liée à une augmentation de la protéine G stimulatrice d'adénylyle cyclase, Gαolf, ainsi qu'à une inhibition des phosphodiestérases. L'imagerie calcique a mis en évidence une augmentation de l'activité spontanée des NPSd et, de manière inattendue, de la sensibilité à la stimulation des récepteurs AMPA du glutamate des NPSi.

En conclusion notre travail utilise pour la première fois l'imagerie biphotonique par biosenseurs dans le striatum dépourvu de DA de souris adulte. Il met en évidence des déficits multiples et distincts de la signalisation dans les deux populations de neurones de projection du striatum et suggère des mécanismes possibles de ces altérations.